die talsperren österreichs

Large Dams in Austria/Volume 35

Arch Dams

Experiences – Problems – Developments

R. Widmann

Published by the **Austrian National Committee on Large Dams**
with the support of the Austrian Reservoir Commission (Staubeckenkommission).

die talsperren österreichs

Large Dams in Austria/Volume 35

Arch Dams

Experiences – Problems – Developments

R. Widmann

Salzburg, April 2005

Translation by Lingua-Team, Salzburg, Austria

The publishers accept no responsibility for the contents of this report, which represent the personal opinion of the author only.

Edited and Published by:

ÖSTERREICHISCHES NATIONALKOMITEE FÜR TALSPERREN
(AUSTRIAN NATIONAL COMMITEE ON LARGE DAMS – ATCOLD)
Elisabethstrasse 59/4
A-8010 Graz

Published with the support of the
Austrian Federal Ministry of Agriculture and Forestry, Environment and Water Management,
and The Austrian Water and Solid Waste Management Association

Printed with the support of the Austrian Society for Geomechanics

Cover photo: Schlegeis Arch Dam
Austrian Hydropower AG

Foreword of the editor

With the present paper the Austrian National Committee on Large Dams (ATCOLD) continues its series "Austrian dams" initiated in 1954, with new graphic design since 1999 and this second monograph in English.

This monograph is an extensive study, documenting the developments in the field of arch dam construction in Austria as well as beyond. Its author, Dipl.-Ing. Dr. techn. Richard WIDMANN will assuredly need no introduction to most of his readers and a brief summary of his professional background only should suffice :

R. Widmann began his employment at the Tauernkraftwerke AG in Salzburg; his professional career culminated in his appointment as director with responsibilities included planning, maintenance and supervision for all civil engineering tasks. R. Widmann's professional activities placed a major emphasis on the construction of dams, particularly arch dams. He was responsible for project design, construction and supervision of several large Austrian arch dams and has decisively influenced developments in this field. This is also manifested in his many years' participation in the Austrian Reservoir Commission and in several committees of the International Commission on Large Dams (ICOLD) as well as by his activities on four continents. On the merit of his work in the field of rock mechanics he was appointed president of the Austrian Society for Geomechanics (ÖGG), which he headed for 15 years; he also acted as vice-president for the International Society of Rock Mechanics (ISRM) for the duration of one term.

The present monograph is a summary of the author's many years of experience and observations in regard to the planning and supervision of arch dams, also prompting critical statements as well as valuable suggestions for future developments.

Since this paper is of common interest the Austrian National Committee on Large Dams decided to include it in its series, (Die Talsperren Österreichs, Vol. 33, Gewölbemauern - Erfahrungen, Probleme, Entwicklungen) as well as to publish a revised version in English. As chairman, I would like to especially thank the author, but also all others involved in this publication.

The Austrian Society for Geomechanics has contributed to the costs, for which I would like to express my gratitude to its president, director Dipl.-Ing. Dr. mont. G.M. Vavrovsky.

I hope this volume will meet with great interest, not least on the grounds that it will prove a valuable basis of discussions for future developments.

G. Heigerth

Gratefully dedicated

to my wife

TABLE OF CONTENT

REMARKS

The references list above all reports published several decades ago, in order to point out that the individual problems discussed in the present paper have been known for a long time. Over the past decades, valuable suggestions have been offered; but are rarely put into practice.

(Linsbauer 1985) Papers at the end of each chapter.

[77] Papers of the author see annex C.

[*56*] Papers of the author in English.

1. INTRODUCTION

Since the Club of Rome's first report (1972), if not earlier, the term 'spacecraft earth' has been widely used to highlight the fact that only limited space and resources are available to mankind and that, therefore, mankind's growth and demands as well as resource consumption must be limited. One essential requirement for human life is water which, though considered a renewable resource, is nonetheless available in limited quantities only. Life, in every conceivable dimension, from each single cell to the global cycle, depends on water. The mean natural water resources on our planet have remained practically constant throughout the period of human habitation and are independent of the population size. World population, however, tripled in the 20th century and is expected to rise by another 50% to approximately $9x10^9$ in the 21st century. One crucial problem in the future development of mankind will be to ensure a sufficient supply of water. It is the most essential of all elements - besides air and soil - without which life on our planet, whether plant, animal or human, would not be possible.

1.1 WATER RESOURCES

For six millennia mankind has struggled to adapt the natural, seasonally varying water resources to the actual demand. There is in fact almost 1,400 million km³ of water on our planet, but 97.5% of this is salt water stored in oceans or salt lakes and deep-seated groundwater. The remaining 2.5% (35 million km³) is freshwater, but, again, 69.6% of this is bound in polar and permafrost regions, another 30.1% is actually non-renewable groundwater.

For sustained development, man can use only the renewable part of the water cycle found on land. According to Fig. 1.1 (data in literature varies) approximately 110,000 km³ fall annually as precipitation over land. Depending on the region, however, the distribution can vary considerably: from nil (in deserts) to 8,000 mm/year (in tropical rain forests) and can have annual fluctuations within one region of ± 50%. Depending on the climate and with regional variations 70,000 km³ of this will again evaporate. Worldwide, therefore, only approximately 40,000 km³ of freshwater is available and will,

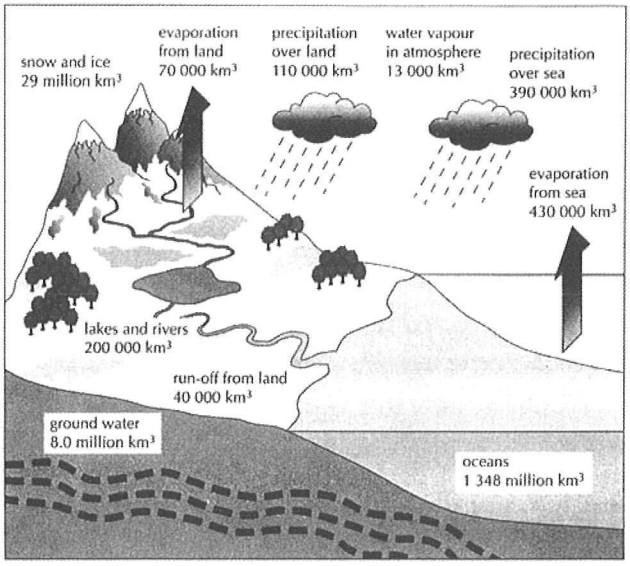

Fig. 1.1: Renewable water resources (Clarke 1993).

eventually, above or below the earth's surface flow into the sea.

A large part of this water flows off in flood waves (28,000 km³) or through very sparsely inhabited regions (5,000 km³), leaving mankind only approximately 7,000 km³ or 16% of the overall runoff without use of technical interventions (Meadows 1992).

Table 1.1: Renewable water resources of selected rivers, relative to the population in the catchment area (Shiklomanow 2003).

	Renewable Water Resources km³/ year	River	Area, $Km^2.10^6$	Population 10^6	Average Water Resources, $km^3.10^6$/year	Coefficient of Variation	Water Availability 10^3 m³/year,head
Highest		Mackenzie	1.78	0.35	325	0.12	929
		Amazon	6.92	14.3	6,920	0.08	484
		Lena	2.49	1.9	539	0.11	284
		Yenisei	2.58	4.8	642	0.08	134
Lowest		Danube	0.82	85.1	225	0.18	2.64
		Nile	2.87	89	161	0.16	1.81
		Don	0.42	17.5	26.9	0.36	1.54
		Indus	0.96	150	220	0.19	1.47
		Dnieper	0.50	36.6	55.3	0.25	1.46
		Huang He	0.75	82.0	66.7	0.38	0.81

To compensate seasonal variations or collect part of the flood waves, a number of dams have been constructed over the past decades, providing storage

facilities with a storage capacity of approximately 6,700 km³. Only half of these, however, can be used for annual runoff transfers from periods of high to periods of low runoff. Ecological considerations also set spatial and temporal limits to runoff transfers, if the species diversity that has evolved over the past is to be preserved both in regard to the number of species as well as to their individual representatives. To ensure sustained use, the amount of groundwater withdrawn must in the long run not exceed the amount that will be replaced by the natural cycle.

The global mean values of water resources therefore offer a general overview, but do not say anything about regional or even local problems. In addition, there is no correlation at all between regional population density and natural water resources.

1.2 WATER REQUIREMENTS

Since the evolution of Homo sapiens 3 – 400,000 years ago, man has lived predominantly as a hunter, his water requirements being limited largely to drinking water. About 10,000 years ago man began to cultivate the land and to domesticate animals and plants. This was of course possible only in regions where, at least during the growing periods, sufficient water was available. Therefore, the advanced civilizations of ancient times developed almost exclusively in river valleys such as between the Euphrates and Tigris rivers in Mesopotamia, the Nile in Egypt, the Indus in India and the Yellow River in China. As the concentration of people in confined areas increased, the problems of a consistent supply as well as disposal of water and food increased as well.

Today, particularly in industrialized countries, mankind influences the individual elements of the hydrologic cycle in a number of ways:

- Direct use of water.
- Changing land use.
- Anthropogenic climate changes.

In regard to the use of water, one can distinguish, basically, between two types of usage (Table 1.2):

- Consumptive usage, such as in nourishment, since farm yields depend directly (e.g. grain, vegetables, fruit, etc.) or indirectly (e.g. meat, milk, eggs, etc.) on sufficient watering. The consumed water is returned only indirectly to the natural water cycle, and then it is usually polluted to some degree.
- Non-consumptive usage, after which the water is directly returned to the natural cycle and is again available to other users. This includes:
  - Most municipal and industrial uses; the water returned to the natural cycle is, however, polluted.
  - Water required for power generation by hydroelectric power stations; the quantity and quality of the water remains unchanged.
  - Cooling water for thermal power stations, which is returned to the natural cycle in a more or less heated condition.

The principal share of overall usage but particularly of consumptive water use falls, therefore, to agriculture

Sector	Assessment					Forecast		
	1900	1940	1960	1980	1995	2000	2010	2025
Population 10^6	1,900	2,300	3,029	4,410	5,285	6,181	7,113	7,877
Municipal use	16	37	83	206	356	388	468	650
Consumption	(4)	(9)	(20)	(42)	(58)	(64)	(70)	(83)
Industry	38	127	334	686	714	748	862	1,105
Consumption	(3)	(9)	(24)	(58)	(77)	(82)	(101)	(135)
Agriculture	525	891	1,551	2,190	2,494	2,570	2,747	3,113
Consumption	(406)	(678)	(1,177)	(1,699)	(1,945)	(1,981)	(2,109)	(2,350)
Reservoirs	0,3	4	29	129	188	210	235	269
Total	579	1,066	1,997	3,212	3,752	3,917	4,314	5,139
Consumption	(415)	(704)	(1,251)	(1,928)	(2,268)	(2,336)	(2,514)	(2,836)

1st line ... total requirement
2nd line ... there from consumption

Table 1.2: Dynamics of world water use in km³/year (Shiklomanov 2003).

(Table 1.2), while the share of municipal and industrial uses is already relatively low and may be even further reduced in the future with appropriate engineering techniques. Just to provide the 2,800 calories per person/day needed for adequate nourishment requires an average of 1,000 m³ of water per person/year or 9,000 km³ of water for 9 billion people/year (WWDR 2003).

However, even this figure does not really indicate the actual requirement since the consumption of water hasn't risen in some regions simply because there wasn't any more water available.

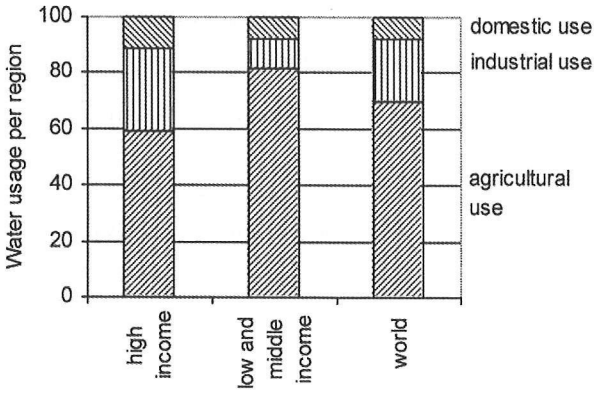

Fig. 1.2: Competing world water uses in %, (WWDR 2003).

The distribution of the almost 4,000 km³ of global water requirements (Table 1.1) around the year 2000 is illustrated in Fig. 1.2. Worldwide, agriculture requires an average of 70% of the available water resources, reaching 82% in low and medium-income countries and falling to as little as 30% in high-income countries.

1.3 DAMS

The history of dam construction goes back a long way. For 5,000 years man has tried to collect at least part of the flood flows both to prevent unwelcome flooding as well as to utilize this water in water-short periods. In Azerbaijan as well as on Java the remains of naturally low earth dams dating back to the 4th millennia B.C. have been discovered. These have been found to have provided the basic water requirements of towns with approximately 2,000 inhabitants.

Based on his experience with existing dams, man has built ever-higher dams (Table 1.3). However, with the present height of approximately 300 m a limit seems to have been reached, as the properties of fill material, concrete and bedrock cannot be increased at will to withstand the rising abutment forces.

The first low dams were constructed using uniform soils; later, a stone wall was supported by a shoulder or the space between two stone walls was filled with soil. This method was also used for the construction of the Chinese Wall. The present construction method for zoned dams (one sealing element upstream or inside the dam cross section, drainage zones and shoulders) makes high demands on design and construction. The transition from dams made of two walls with a filling in between to gravity dams came about gradually.

Table 1.3: Examples illustrating the increase in dam heights.

EMBANKMENT DAMS			CONCRETE DAMS		
2500 B.C.	Khabour (Syria)	12 m	300 B.C.	Kosheish (Egypt)	15 m
240 B.C .	Gukow (China)	30 m	1100 A.C.	Almonacid (Spain)	29 m
1128 A.C.	Daimonike (Japan)	32 m	1589	Tibi (Spain)	46 m
around 1500	Mudduck Masur (India)	33 m	1866	Gouffred'Enfer (F)	60 m
1675	St. Ferreol (F)	36 m	1904	Cheeseman (USA)	72 m
1867	Maday (India)	44 m	1905	New Croton (USA)	91 m
1892	San Leandro (USA)	47 m	1910	Shoshone (USA)	99 m
1909	Nexaca (Mexico)	56 m	1915	Arrowcrock (USA)	107 m
1924	Dix River (USA)	84 m	1924	Schräh (CH)	111 m
1931	Salt Springs (USA)	100 m	1929	Diablo (USA)	119 m
1939	San Gabriel (USA)	115 m	1932	Owyee (USA)	127 m
1948	Mud Mountains (USA)	130 m	1934	Chambon (F)	136 m
1950	Anderson Ranch (USA)	139 m	1936	Hoover (USA)	221 m
1958	Swift (USA)	156 m	1958	Mauvoisin (CH)	237 m
1962	Trinity (USA)	164 m	1961	Vajont (I)	262 m
1965	Rosella (Italy)	265 m	1962	Grande Dixence (Ch)	284 m
1978	Nurek (USSR)	300 m	1980	Inguri (USSR)	272 m

The first gravity dam constructed in accordance with modern concepts was probably the dam of Geoffre d'Enfer (F), which was 60 m high and built in 1866. The Baume dam in France, which is 12 m high and dates back to Roman times, is considered the oldest arch dam in the world. The two highest dams in the world are both situated in the former USSR and are embankment dams; the 335 m high Rogun dam and the 300 m high Nurek dam, followed by the Grande Dixence gravity dam (285 m, CH) and the Inguri (272 m, USSR) and Vajont (262 m, Italy) arch dams. Favourable topographic conditions for large reservoirs have become rare, particularly in Europe, as in most cases these have already been utilized long ago. In addition, the resistance among inhabitants against the manipulation of natural water flows is steadily growing, so that in the future fewer dams and reservoirs will be built than would be necessary or desirable in terms of economically effective water usage.

Table 1.3: Various data on the development of arch dams (Schnitter 1976).

Name	Country	Construction	Height	L/H	d_A/H
Baume	France	roman	12	1.5	0.32
Kurit	Iran	~1300	60	0.4	?
Elche	Spain	ab 1632	23	3.0	0.50
Zola	France	1847-54	43	1.5	0.34
Pathfinder	USA	1905-09	65	1.4	0.45
Buffalo Bill	USA	1905-10	99	0.6	0.33
Pacoima	USA	1926-29	117	1.72	0.27
Lumiei	Italy	1942-47	136	1.01	0.10
Ross	USA	1943-49	165	2.41	0.37
Tignes	France	1949-53	180	1.63	0.25
Mauvoisin	Switzerl.	1951-57	237	2.19	0.23
Vajoint	Italy	1957-60	261	0.73	0.09
Inguri	USSR	1964-81	272	2.80	0.31

L/H ..... crest length/height,
d_A/H ... max. thickness at the base/height

Since 1980 the construction of new dams has decreased dramatically (Fig. 1.3). This is more likely attributable to economic and ecological problems than to declining requirements or to the lack of technical possibilities. 75% of all dams serve both as a water supply and as flood protection, only 15% are used exclusively as hydroelectric power plants.

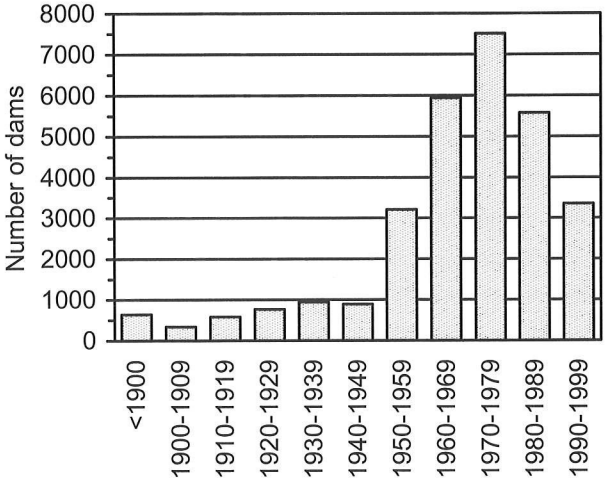

Fig. 1.3: Construction of new dams worldwide (ICOLD 2004).

The classification of dams according to type and height (ICOLD 1988) shows that with increasing dam height the share of embankment dams decreases from 88% of dams with a height below 30 m to 25% of dams with heights exceeding 200 m. Approximately 23% of all dams are concrete dams, only 5% are arch dams.
In the world dam register (ICOLD 2004) more than 33,000 dams with a height above 15 m are registered. Only 9% of these, however, are higher than 60 m.

1.4 RESERVOIRS AND ENVIRONMENT

When the economics of water usage so require, reservoirs will then be built as flood protection of the regions below or to adapt the natural water resources to the actual requirements. As with other human activities, the creation of reservoirs by the construction of dams also affects the environment. While the economic advantages of dams to the national economy have always been thoroughly examined and verified, the ecological examination of environmental relationships has in the past only rarely been carried out but will, without doubt, gain in importance in future. On the basis of a general water economy plan, comprehensive ecological reviews for the river region concerned – even across political borders - will have to be prepared, including realistic alternatives capable of serving the same purpose.
The influence of reservoirs on environmental changes (Fig. 1.4) increases with:
– The area requirement (Table 1.4); as the

The largest lakes of the world					
Natural lakes			Man-made lakes		
Upper lake	Canada	82,414	Akosombo	Ghana	8,482
Victoria lake	Uganda,	68,800	High Aswan	Egypt	5,900
Aral lake	USSR	62,000	Bratsk	USSR	5,470
Huron lake	USA	59,568	Kariba	Zimbabwe	5,100
Michigan lake	USA	57,994	Cabora Bassa	Mozambique	2,580

Table 1.4: Comparison of the surface areas (in km²) of the largest natural and man-made lakes.

retention of flood waves provides the best flood protection (Fig. 2.2). The area required for the retention in reservoirs must be offset by the advantages gained in reducing the risk of floods in agriculturally productive areas previously susceptible to flooding.

– The ratio of the active storage volume to the natural water volume at the site under consideration; therefore, the greatest changes will occur in the area immediately below the reservoir but will diminish with increasing distance. The extent of possible changes in the water flow can be estimated on the basis of the annual flow at the dam site (reservoir characteristic) or at the considered location (basin characteristic).

The construction of reservoirs inevitably leads to local changes, such as changing water level heights and flow rates in the reservoirs and changes in the annual runoff fluctuation below the reservoir [82a, b; 88], while the dam height as such is of consequence only in regard to its visual impact on the environment. In the reservoir area, water running usually in a relatively shallow and narrow river bed is turned into an almost stagnant, deep and broad lake, which inevitably causes limnological changes. Above the highest, normal reservoir water level the groundwater level varies only slightly. In the zone in which the reservoir water level varies, the groundwater level will follow these variations accordingly. Generally, the growth of vegetation in this area will not be possible. Changes in the natural groundwater level will affect the vegetation only, if the groundwater level lies above the deepest roots.

The rate of silting depends on the ratio of storage volume to catchment area as well as on the probable degree of erosion due to geological conditions.

The extent of the changes in the hydrologic balance below the reservoir is dependent on the water resource management, i.e. for which purpose the

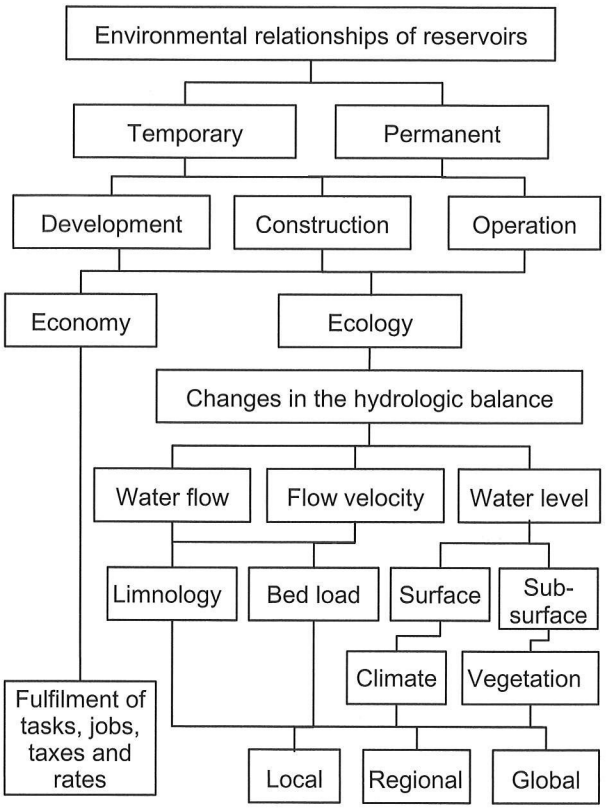

Fig. 1.4: Environmental relationships of reservoirs [88].

water and the entire plant are used. If the stored water is used for irrigating farmland, it will be lacking in the lower course. This may cause not only ecological but also international political problems as well. This happened for example in the case of the reservoirs built along the upper courses of the Euphrates and Tigris rivers to irrigate and thus increase the productiveness of farmland in Turkey, yet could however lead to water shortages in the countries along the river's lower course, namely Syria and Iraq.

Reservoirs of hydroelectric power plants, with the exception of the withdrawal sections of diversion power plants, return their water to the riverbed without changes in quality and quantity but possibly with some delay in time, so that the river usually carries

less water in water-rich periods and more water in water-short periods. Generally, this compensation is of advantage; potential negative consequences especially limnological changes may sometimes occur along the withdrawal sections, only rarely below the return point. Therefore, in these cases compensation measures, which must conform to existing environmental relationships, may be required to achieve a reasonable and stable ecological balance.

1.5 SUMMARY

Of the 1,400 million km³ of water on our planet only 2.5% is freshwater, 7,000 km³ of which are renewable resources for human usage. However, even these resources are distributed unevenly, regionally as well as seasonally. Cattle breeding, industry and domestic water requirements remain essentially the same during the whole year. Vegetation and agriculture, however, require considerably more water during growing periods than at other times, which in many regions does not conform to the local, climate-dependent annual precipitation. Only reservoirs can prevent or at least mitigate droughts in growing periods by transferring seasonal surpluses to water-short periods.

In agriculture it will be necessary as well to not only use water-saving irrigation methods, but also to develop environmentally friendly fertilizers for the prevention of groundwater pollution through seepage.

Due to the increasing population density (a threefold increase in the 20th century and probably another 50% increase in the 21st century) the exclusive ideology of strictly preserving nature will have to yield to that of forming nature to achieve new, reasonable and sustainable ecological conditions. The available land per head has decreased from 4.3 ha to 1.3 ha in the 20th century and is expected to fall to 0.9 ha in the 21st century. Therefore, creating retention volumes in reservoirs to protect settlements as well as farmland from flooding will increase in importance.

However, the highly developed pollution-free conversion of the mechanical power of water into electrical energy in hydroelectric power plants will also continue to be of importance. Storage power plants can be used at any time to make up for the unavoidable, natural production breaks that are to be expected when making direct use of solar (photovoltaic) and wind energy and will become even more important, at least until ecologically and economically acceptable storage facilities for large quantities of electrical energy have been developed. To date, developed countries are exploiting about 70% of their electricity potential, whereas in developing countries the figure is only 15% (WWDR 2003).

Water is one of the irreplaceable key requirements for life on our planet. To have sufficient water available constitutes, no doubt, one of mankind's natural rights. Guaranteeing an adequate water supply will be one of the 21st century's essential tasks.

The construction of reservoirs, and thus also of dams, will help to fulfil these tasks:

- The retention of flood waves, presently running off unused and causing damage, by creating retention volumes in reservoirs which will require the construction of dams.
- The already technically fully developed use of hydro power for the generation of electrical energy, of which as yet only 15% is being used in developing countries.

Effective compensation measures may, however be required to ensure a new, reasonable and stable ecological balance.

The following chapters focus, above all, on experiences with the no doubt most fascinating of all dam types, the arch dam.

REFERENCES

ATCOLD: Dams in Austria 1991

CLARKE R.: Water, the International Crisis. Earthscan Publications Ltd., London 1991.

ICOLD: World Register of Dams, Edition 1988, 1998.

MEADOWS D.: Beyond the Limits. Chelsea Green Publishing Co, Post Mills, Vermont, USA 1992

SHIKLOMANOV I. A., J. C. RODDA, Editors: World Water Resources at the Beginning of the 21st Century. Cambridge, University press, 2003

SCHNITTER N.: A short History of Dam Engineering. Water Power, April 1967.

SCHNITTER N,: The evolution of the arch dam. Water Power, Oct./Nov. 1976

SCHNITTER N.: Vorrömische Talsperren. SIA 1986/20.

WWI Report: The state of the world 1996. World Watch Institute.

WWDR: Water for People, Water for Life – UN World Water Development Report 2003.

2. SAFETY CONSIDERATIONS

2.1 GENERAL

At a time when there is a great deal of public concern about safety, particularly in technical structures, it is of course of central importance in dam construction to take safety aspects into consideration. As with all other large civil engineering structures of our times, the failure of dams can cause extensive damage and endanger the lives of many people. The first known dams were constructed in Mesopotamia 5,000 years ago. Since then there have always been disasters caused by dams, the extent of which depended not only on the reservoir volume but also on the population density below the dam.

As with all other structures, the safety of dams rests on three fundamental pillars:

– Design, for which the project engineer must have extensive basic knowledge not only in the field of static's but also in special subjects such as hydrology, geology, including soil and rock mechanics, concrete technology, etc.

– Construction, including geological site investigation and monitoring of the required quality during construction.

– Surveillance and maintenance, including local inspections and operating tests, as well as monitoring, including evaluation and interpretation of the measurement results during the dam's entire lifetime.

Fig. 2.1: The three fundamental pillars of safety.

To evaluate the safety of structures, usually two entirely different procedures are used:

– Statistical procedures which are based on the probability of a certain event or state, e.g.:

- Number of failures or defects of dams relative to the overall dam number, including all causes.
- The decisive strength determined by interpolation based on the test results.
- The decisive flood determined by extrapolation based on the incidents observed during a certain number of years.

Statistical procedures assume uniform conditions and establish the probability by which a certain incident will recur. However, they cannot predict whether or when such an incident will happen at a specific dam.

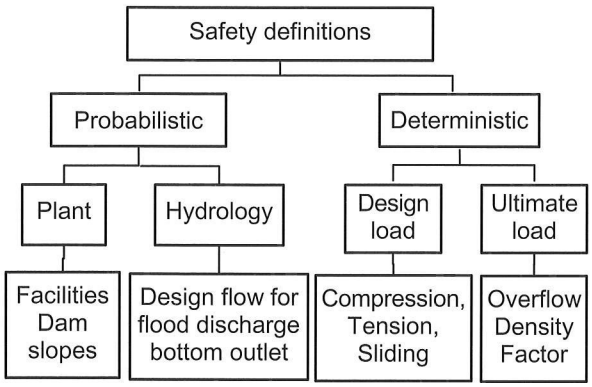

Fig. 2. 2 Safety definitions.

– Deterministic procedures based on the numerical determination of a safety factor, e.g. for:

- The decisive material strength and its permissible utilization or
- Design load or ultimate load.

Deterministic procedures only take known and quantifiable influences into consideration and are used in the design of structures.

Safety evaluation could however also be based on the more graphic concept of function fulfilment since all type of dams must be watertight (Fig. 2.3), with no flow over, through or under the dam.

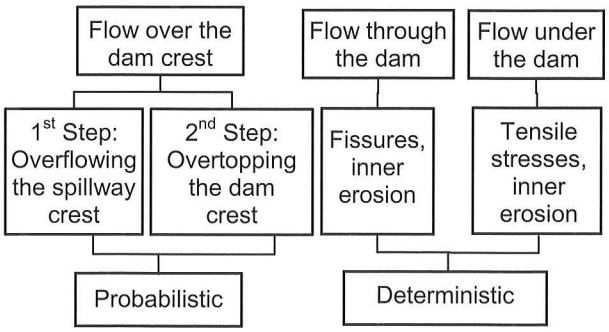

Fig. 2. 3: Proposal of a new safety definition [113].

With all dam types, the statistical safety against flow over the dam crest depends on the design flood and the operational reliability of the spillways.

This should be verified during operation (see chapter 7). The safety against flow through the dam is dependent on the water tightness and crack resistance of the concrete of concrete dams or the sealing zones of embankment dams. This in turn depends on the stress state and quality of the material.

With concrete dams, the safety factor against inadmissible flow under the dam (joint expansion due to inadmissible tensile stresses below the dam base) can already be determined upon first reservoir filling, based on the amount of seepage which in turn depends on the storage level (Chapter 7).

This type of safety definition largely includes the conventional definitions.

2.2 STATISTICAL SAFETY ANALYSIS

2.2.1 General

Statistically-oriented safety analysis evaluates all plants constructed in the past, taking into account not only the effects of design assumptions but also structural design, actual conditions and operational management.

2.2.2 Overall statistically-oriented evaluation (ICOLD 1983, 1994).

Dam failures.

An analysis of 165 dam failures outside China has shown that 67% of the failures occurred during construction or within the first 10 years of operation (Fig. 2.4). This indicates avoidable design and construction defects.

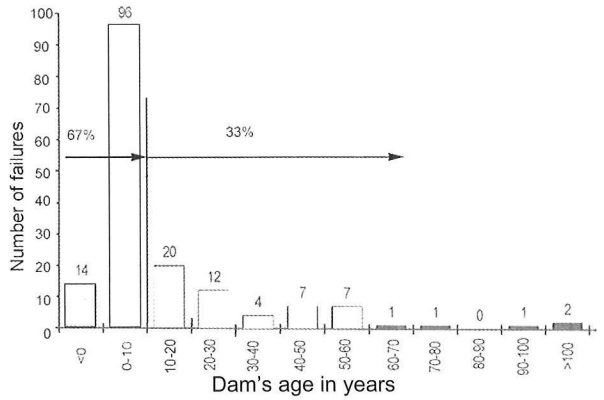

Fig. 2. 4: Dam failures, relative to dam age (ICOLD 1994).

The progress made in the field of dam design has been confirmed by a trend analysis [79] that revealed that the percentage of failures decreases decisively, the later the dam was constructed. Approximately 5% of the dams constructed before 1900, 2% of the dams constructed between 1901 and 1950 and 0.5% of the dams constructed between 1951 and 1986 have failed.

Damage to dams

In order to prevent further damages, an assessment of the causes is undoubtedly important for future technical developments. A study of the causes of damage according to frequency has shown that (Table 2.3):

– Approximately 30% can be attributed to appurtenant works, e.g. insufficient design flood, hydraulic design and insufficient operational reliability of spillways with mechanical gates. For Europe, however, this figure is much too high. A comparatively high number of dam ruptures caused by damage or insufficient dimensioning of spillways have occurred in countries where there are difficulties in estimating extreme flood levels for lack of long-term hydro-graphical documentation as well as in carrying out proper maintenance of spillways.

– 47% are caused by unexpected structural behaviour, including flow under the dam and increased uplift.

– 11% are due to insufficient construction material quality.

Table 2.3: Most frequent damage causes 1950 - 1975 (ICOLD 1983).

Dam types		Embankment	Concrete
Appurtenant works	Overtopping	19	7
	Others	91	37
Seepage		86	13
Material behaviour		31	27
Structural behaviour		114	36
Reservoir slopes		9	3
Others		29	24
TOTAL		379	147

The estimated number of unknown cases would probably be distributed evenly among all dam types and heights, but has doubtlessly decreased considerably in the last decades, even further emphasizing the tendency indicated by the above-mentioned trend analysis. It would be highly recommendable to update these statistics and evaluations in order to enable the development of specific strategies for the prevention of the most frequent problems.

2.3 APPURTENANT WORKS

For all dam types, safety considerations are similar in regard to appurtenant works such as intake structure, bottom outlets and spillway. Their operational reliability must be checked when first put into operation and periodically thereafter.

2.3.1 Bottom outlet

Most dams are constructed with bottom outlets which must fulfil two functions:

– The intake structure must be swept free of sedimentations. Previous experience has shown that due to the flow velocity required this can only be done efficiently, if the reservoir is more or less empty. Yet at the same time ecological considerations must be taken into account as well for the river below the dam.

– In case of unforeseen incidents, the reservoir level must be drawn down speedily to enable a quick load relief of the dam. This, however, cannot be achieved if reservoirs have very large inflows or storage volumes, due to the technically limited capacity of bottom outlets.

In case of unexpected incidents, dams can be relieved in various ways:

– Stepped-up operation, during which no energy is forfeited, but only the value difference between peak and standard energy production is lost.
– Bottom outlets which can be opened and closed again at any time.
– Outlet fitted with a bursting gate; which when opened, completely empties the reservoir as far as its inlet sill.

One example of static dam relief via bottom outlet is the Zillergründl dam (reservoir capacity 90 hm³) (Fig. 2.5). For this, all river intakes must be drawn off and the inflow to the reservoir is assumed to correspond to the mean annual value. The design flow of the bottom outlet corresponds approximately to a recurrence interval of ten years at the dam site. If the other discharge possibilities are also taken into consideration, the discharge periods shorten accordingly (Table 2.4).

Although the use of bottom outlets for safety reasons is rarely mentioned in technical literature, a comparatively large number of damage cases concerning bottom outlets have become known. Therefore, if reservoirs are to be fitted with bottom outlets, their structural, hydraulic and operational reliability must be ensured especially in regard to the neutralization of the harmful effects of the water's mechanical power.

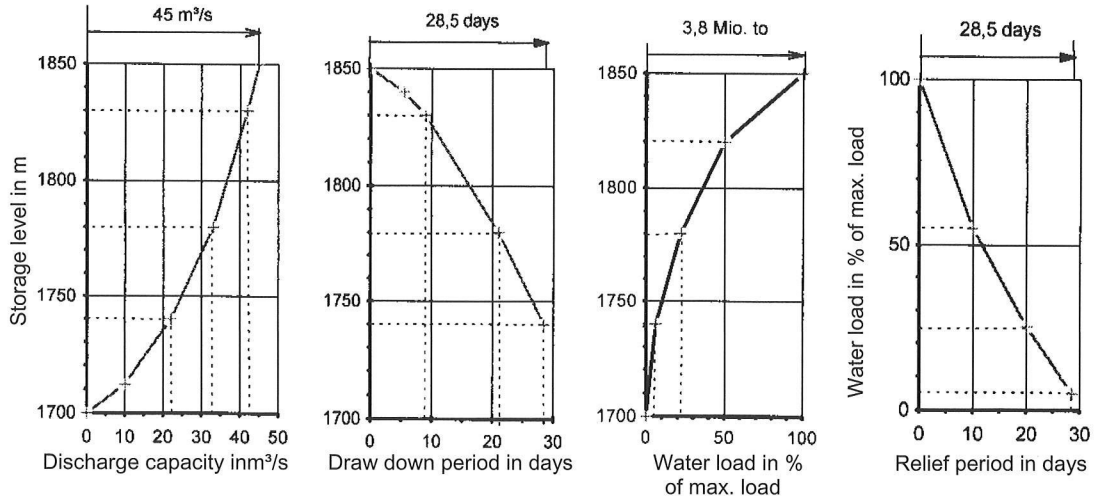

Fig. 2.5: Load relief of the Zillergründl arch dam using only bottom outlet.

Table 2.4: Water load relief of the Zillergründl reservoir.

		Max. discharge m³/s	Discharge to half the water load			Emptying of reservoir		
			individually	1 + 2	1 + 2 + 3	individually	1 + 2	1 + 2 + 3
			Days			Days		
1	Turbines	65	≈ 7			≈		
2	Bottom outlet	45	≈ 11	≈ 4.5	≈ 3.5	≈ 28.5	≈ 10.5	≈ 8
3	Bursting gate	40	≈ 12			≈	-	

2.3.2 Spillway

Spillways can be designed using two entirely different methods:

– Mechanical gates, with which the top water level is not exceeded; however, reliable maintenance is required to ensure their functional reliability. For the hydraulic design of these systems the peak inflow is decisive.

– Overflow with spillway crest. In this case the maximum reservoir level is then attained when the inflow equals the capacity of the overflow. With these systems, a natural retention volume is available corresponding in volume to the overflow height. Therefore, with relatively large reservoir surface areas, the hydraulic design must be based on the flood wave volume.

The standard definition of hydrological safety is based exclusively on the determined probability of the inflowing flood which comprises three steps:

a) Collection of primary data using all available possibilities.

b) Determination of the decisive inflowing flood.

c) Derivation of the decisive design flood for the hydraulic design of the spillway.

Ad b): All statistical prognoses assume that external conditions remain unchanged. The decisive inflow, in most cases with a recurrence interval of 5,000 or 10,000 years, is determined on the basis of the collected data using statistical analysis by extrapolation from the observed period of a few decades to a period that is at least one hundred times longer. Mathematically, such an extrapolation is inadmissible. In addition, it must be pointed out (Lenhardt 1996) that the probability of a 100-year event exceeding its recurrence interval can be determined on the basis of a Poisson distribution:

Table 2.5: Probabilities P of exceeding the flood during specified period Ta as function of recurrence interval Tb in %.

Probability of flood	Observation period		Working life	
	25 years	50 years	100 years	200 years
100 years	22	39	63	86
200 years	11	22	39	63
500 years	5	10	18	33
1000 years	2	5	10	18
5000 years	0.5	1	2	4

$$P = 100\ (1 - \exp^{(-Ta/Tb)}) \quad \text{or} \quad N = 100 - P$$

where

P = Probability of exceeding the flood volume in %
Ta = Considered period
Tb = Mean recurrence interval of incident
N = Probability of not exceeding the flood volume in %

An analysis of this relation (Tab. 2.5) reveals that e.g.:

– An incident with a recurrence interval of 100 years has a 22% probability of already recurring during an observation period of 25 years, which makes it all the more difficult to evaluate the observed data.

– An incident with a recurrence interval of 5,000 years can still be expected to exceed that extrapolation with a probability of 2% during a working life of 100 years.

The difference between the two extrapolation methods commonly used in Austria remains within acceptable limits up to100 years; the values according to Pearson exceed the values according to Gumbel by up to 9 ± 6% (Table 2.7). Curves that go beyond those periods can only be based on non-verifiable and, therefore, more or less arbitrary assumptions of great variance. The difference of an extrapolation to floods with a probability of 5,000 (10,000) years exceeds according to Pearson 160 ± 25% (181 ± 30%) the values according to Gumbel and is no longer acceptable.

Table 2.7: Comparison of the two extrapolation methods.

Probability of flood in years	PF				Design flood	
	1	10	100	1,000	5,000	10,000
Log Pearson III	0.21	0.55	1.09	1.75	2.46	3.08
Gumbel	0.15	0.60	1.00	1.37	1.60	1.71

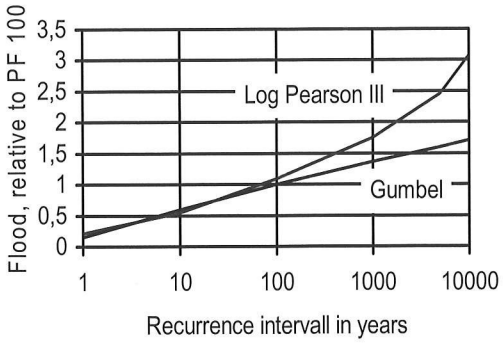

The above-mentioned qualifications are also apply when determining the flood with a recurrence interval of 100 years; the unavoidable error, however, is of less consequence due to the lower extrapolation.

Ad c) Determination of the design flood is generally based on the assumption that the flood wave enters a full reservoir and that all discharge facilities are out of operation. The reservoir retention capacity provided by the permanently available retention volume between the reservoir level at full storage level and the overflow height of an overflow with spillway crest is taken into consideration at the determined inflow wave. The reduction of the often only very short inflow peak depends, therefore, substantially on the ratio of this retention volume to the flood wave volume.

In general, reservoirs, particularly seasonal and year-to-year reservoirs, are only partially filled when the flood arrives. In most cases, the remaining storage capacity combined with standard operation will suffice to prevent discharge via the spillway. In any case this will effect an additional reduction of the discharge, which in turn will reduce the flood risk of the regions below the dam. Hence a distinction must be drawn between (Fig. 2.6):

– The 'assured' retention volume between the normal top water level and the maximum water level during flood discharge.

– The additional 'operational' retention volume between the reservoir level at the beginning of the flood wave and the normal top water level.

The optimal height of spillway crest, maximum reservoir level and dam crest relative to the normal top water level should be examined in detail.

The retention volume levels off and slows down the inflowing flood wave, whereas river training for flood protection of riverside residents, steepens and accelerates the flood wave by reducing the natural retention volume.

An empirical study of Austrian alpine seasonal reservoirs based on up to 50 observation years has shown (Fig. 2.7) that the probability of overflowing the spillway crest decreases with the

reservoir characteristic λ_R,

the storage capacity / mean annual inflow.

If this ratio remains above 0.6, overtopping is hardly to be expected and spillway operation will not be necessary [29a]. This empirical method is based on the overflows observed during their respective operating periods, actual operational management and the flood flows that have occurred. However, the storage capacity should be substituted by the actually used mean active storage volume. This examination method cannot be used to determine the far lower probability of overtopping the dam crest.

The small Margaritze reservoir with a reservoir characteristic below 0.03 shall serve as an example for a more precise method of determining the probability of overflowing after several years of operation (Fig. 2.8). The intersection of the curve (2) with the x-axis shows the probability of overflowing the spillway crest and that:

– The overflow is activated on the average of every 15 years.

– Only every 100 years does the volume of the overflowing discharge wave almost equal the volume of the former annual inflow wave.

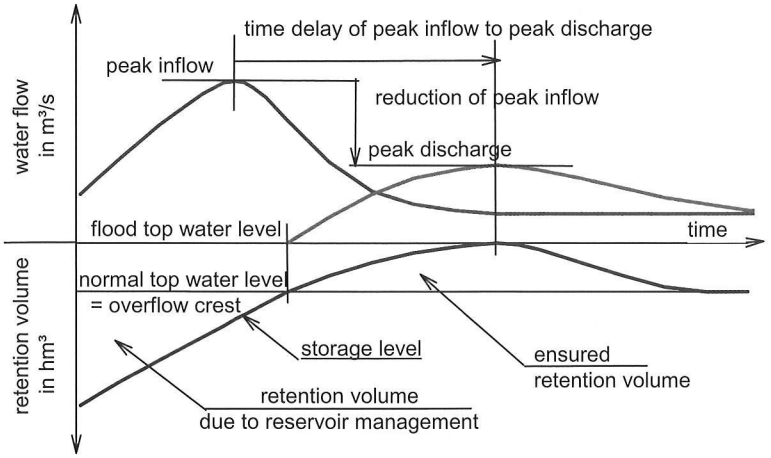

Fig. 2.6: Reduction of the inflowing flood wave by means of the retention volume.

No.	Name	Reservoir characteristic	Probability of overtopping
6	Spullersee *	0.68	0.20
43	Schlegeis	0.63	0.02
42	Durlassboden	0.55	0.06
46	Tauernmoos	0.50	0.07
13	Silvretta	0.48	0.06
26	Mooserboden	0.43	0.04
19	Wasserfallboden	0.36	0.03
40	Dießbach	0.19	0.22
37	Freibach	0.10	0.25

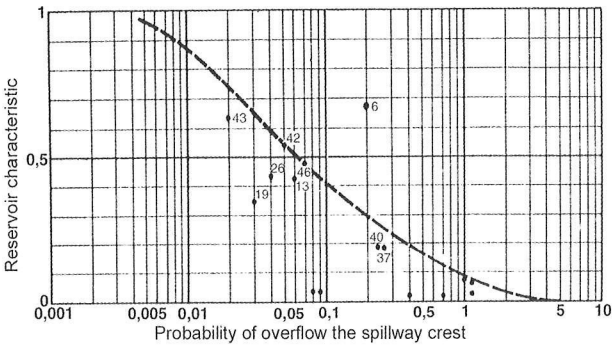

*Only a very small amount of the storage capacity is used during operation.

Fig. 2.7: Probability of overflowing the spillway crest as a function of the reservoir characteristic [66, *78*]

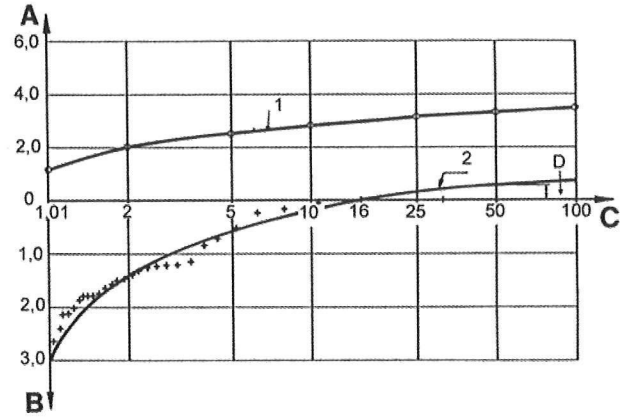

A ... Flood wave volume in hm³
B ... Retention volume in hm³
C ... Recurrence probability
D ... Overflow volume
1 .... Inflow volume in hm³
2 .... Volume of retention at the beginning of flood

Fig. 2.8: Determination of the probability of overflowing of the Margaritze reservoir spillway [34, 66].

The low probability of overflowing also depends on the fact that the highest floods in the Austrian alpine region only rarely occur during the season when the reservoir is full and no operational retention volume would be available. In addition, the plant managers utilize all possibilities to prevent water loss via overflows.

Naturally, the influence of the reservoir on reducing the flood risk of the regions below the dam decreases with increasing distance from the reservoir in proportion to the basin characteristic which is the ratio of reservoir inflow to overall inflow at the respective location λ_B.

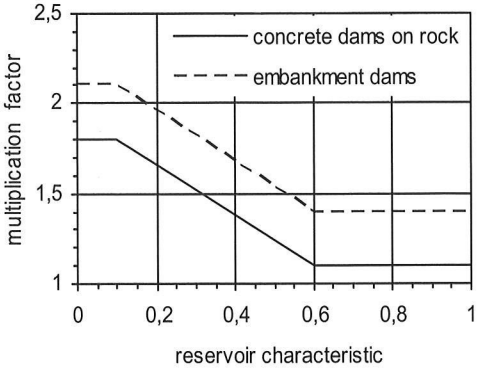

Fig. 2.9: Proposed multiplication factor.

For determination of the spillway's design flood a method shall be proposed which – similar to the determination of allowable stresses – is based on a theoretically still allowable extrapolation of observed data (PF_{100}) and a multiplication factor, which takes the local conditions into account (Fig. 2.9).

According to this proposal and in contrast to the method used up to now, the design flood will be increased for reservoirs with a reservoir characteristic of approximately ≤ 0.3 and decreased for reservoirs with a characteristic λ_R of ≥ 0.4. The proposed method leads to at least the same probability of overtopping as the former method, but is undoubtedly more descriptive and theoretically easier to justify than the present method based on an at least theoretically inadmissible extrapolation.

Recently, a probabilistic design procedure has been developed (Hable 2001) which stresses the total water level as the only quantity to be considered in assessing hydrologic dam safety by combining probable storage level with the flood extrapolated in the usual manner. This total water level is determined on the basis of three random quantities:

– The random height of the water level at flood begin.

– Coincident water level resulting from the retention of a given flood wave.
– Similarly coincidental corresponding wind-related freeboard.

2.4 DETERMINISTIC SAFETY ANALYSIS IN ARCH DAM DESIGN

2.4.1 General

All structures must be designed using deterministic safety factors. This method requires the definition of the decisive material strength β as well as of the decisive stress σ. Statically, the attainment of a critical state depends on:
– The degree of utilization of the decisive strength both in the structure and underground.
– The probability of the occurrence of stresses that are more unfavourable than assumed in the design.
Strictly speaking, deterministic methods are hybrid procedures since they combine statistically determined strength values and numerical safety factors. In addition it must be determined in advance whether the safety definition should be applied to:
– Cracking in the concrete or rock (exceeding of the tensile strength).
– Exceeding of the compressive strength or shear strength.
– Failure of the structure due to exceeding of the ultimate load.
Yet even then the use of different methods or definitions is still possible. In principle, each safety definition requires a specific safety factor, therefore a distinction must be drawn between:
– Safety under design load, which is defined by the ratio of maximum stress to respective strength. This forms the basis of most design calculations yet leads to different safety factors for compression, tension and shear.
– Safety under ultimate load, which is of course far higher for statically highly indeterminate systems than under the design load assumption, but is dependent on the definition of the load increase.
Areas of arch dams subject to tensile stresses due to external stresses and therefore susceptible to cracking are illustrated in Fig. 2.10.
For compressive stresses most countries require safety factors Sc between 3 and 4. However, since the compressive strength of concrete βc is determined according to different guidelines, it is not possible to directly compare the various safety factors specified in international literature.

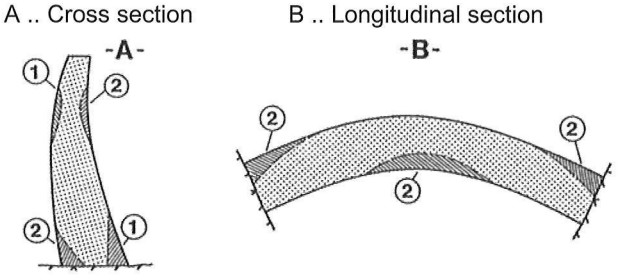

Fig. 2.10: Arch dam areas susceptible to cracking [80].

2.4.2 Design load method

Due to the relatively high compressive strength of concrete there is a large absolute distance between stress peak and failure state. In addition, local overstressing due to the curved working line of concrete in the failure area causes a certain stress transfer into adjoining areas before any damage can occur. Generally, therefore, local weak zones (e.g. nests) or stress peaks under compressive stress do not significantly affect the bearing capacity of mass concrete structures.
For areas under tensile stress, conditions are considerably more unfavourable, even if the same safety factor $S_t = S_C$ applies. As is commonly known, the "true" tensile strength β_t reaches approximately one tenth of the compressive strength, the absolute distance between stress peak and strength is there-fore less than one tenth of the absolute distance under compressive stress, i.e. for mass concrete ~2 N/mm². The disregard of 'secondary stresses' and the restraint stresses calculable only with relatively high uncertainty can exceed 1 N/mm².
In addition, even if the concrete tensile strength is exceeded only locally, cracking can occur. Its effects on the bearing capacity must be examined separately, particularly if the water pressure in the cracks increases with rising storage level (see 5.7.1).
In the last decade, cracking of various concrete dams was attributed to shear stresses (Lombardi 1985). It is known that these lead to inclined principal tensile stresses that must be taken into consideration in tensile strength verification.
It must be pointed out that the crack resistance of

This is especially true of arch dams, as the concrete strength under short-time stress, i.e. stress peaks during vibrations, is significantly higher than under long-time stress.

2.6 SAFETY EVALUATION DURING OPERATION

To evaluate dam safety during operation, any irregularities must be discovered early and assessed. The determination of a safety factor will only be possible in certain cases. Therefore, the dam must have an adequate monitoring system in continuous operation that records at least all behaviour data relevant for dam safety. The early discovery of optical changes which cannot as yet be recorded by measuring instruments make regular local inspections of particular importance (see chapter 7).

The most frequent indication of unexpected behaviour is leakage through the dam body or underground, which indicates cracking in the concrete or the opening of joints in the underground. The evaluation of these leakages in regard to the bearing capacity is described in section 8.7

2.7 SUMMARY

If carefully designed, executed and monitored, all dam types have the same static and structural safety, which are for the most part determined in the design phase.

Safety factors are only meaningful, if the determination method is specified as well. For ultimate load methods, the method of load increase must also be specified. The lowest calculated safety factor results, if only the specific weight of water is increased.

Determination of the design flood is of particular importance. However, this determination should not be based on an extreme, theoretically questionable extrapolation of discharge measurements during a relatively short observation period. The design flood should be determined by multiplying PF_{100} with a multiplication factor, which takes into consideration the dam's susceptibility to overflowing and the extent of damage to be expected in case of flooding.

Comparatively, the effect of earthquakes on dam stability is minimal. Experience has shown that earthquakes causing extensive damages to other structures have hardly affected dams.

Experience has also shown that the occurrence of sudden dam failures can largely be excluded. Expert and responsible surveillance of the dam, reservoir slopes and the functional reliability of the dam's appurtenant works during operation will ensure the early discovery of all unfavourable changes so that appropriate corrective measures can be carried out.

REFERENCES

Bellier, J.: Le Barrage de Malpasset. Travaux 1967

Bergmann H.: Hydrologisches Risiko und Sicherheit von Wasserbauten. Proceedings zum Symposium Sicherheit und Kontrolle von Wasserbauten, TU Wien 1987.

Goubet, A.: Risques associes aux barrages. La Houille Blanche, N° 8-1979.

Goubet, A.: La securite dans les barrages. Traveaux, Mars 1984.

Gumbel E.B.: Methodes graphiques pour l'analyse des debils de crues. Houille Blanche, 1956, n°5.

Hable,O.: Multidimensional probabilistic design concept for the estimation of the overtopping probability of dams. Schriftenreihe zur Wasserwirtschaft 37, Techn. Univ. Graz 2001.

Huber B., Linsbauer H. N.: Erdbebenschäden an Talsperren - selektive Beurteilung. Felsbau 1996, Heft 5.

ICOLD: Lessons from Dam Incidents, 1974.

ICOLD: Deterioration of Dams and Reservoirs, Dec. 1983.

ICOLD: World Register of Dams, 1984, 1988, 1998 und 2004.

ICOLD, Bulletin 99: Dam Failures, Statistical Analyses. 1994.

Lenhardt W.: Erdbebenkennwerte zur Berechnung der Talsperren Österreichs. Bericht an das BMfLF, Öst. Staubeckenkommission, 1996, unveröffentlicht.

Lenhardt W. A.: Zur Abschätzung von Erdbebenbelastungen. Felsbau 1996, Heft 5.

Lombardi G.: Querkraftbedingte Schäden an Betonsperren. Wasser-Energie-Luft 1988, Nr. 5/6.

Marazio A., Dolcetta M., Bavestrello F.: The peripheral Joints at Arch Dams. Design, Behaviour and Constructive Aspects. Felsbau 1991, Heft 2.

Schnitter, N.: Statistische Sicherheit von Talsperren. Wasser, Energie, Luft; 1976, Heft 5.

Serafim, J.L.: Safety of Dams Judged from Failures. Water Power 1981/12.

Yamazumi A.: Influence of the Hyogoken-Nanbu earthquake on Japanese dams. Felsbau 1996, Heft 5.

3. DESCRIPTION OF THE ROCK

3.1 GENERAL

Concrete dams make great demands on the bearing capacity and impermeability of the underground and may, therefore, only be constructed on rock. Not least the failure of the Malpasset arch dam (Bellier 1967) has shown that the determination of the behaviour of jointed rock in many cases requires the development of new methods based on a discontinuum – in contrast to the continuum that forms the basis of soil mechanics.

Rock mechanical calculations differ fundamentally from the usual design calculations in construction engineering, where the building materials are produced specifically for the intended structure, so that the properties of the building materials are largely known.

The fabric of the rock mass as well as the properties of the individual rock elements, however, have been predetermined by nature. They must still be ascertained and will vary according to the rock or fabric changes along the abutment. They can be improved upon only to a limited extent by using constructional measures such as injections and anchors.

The stresses acting upon the foundation are clearly predetermined by the dam body. More difficult is the assumption of the effective joint water pressures, particularly in the presence of seepage flow. For slopes, the stresses generated by the dead load and the possible seepage flow may be assumed with relative precision as well. For underground structures, however, the determination of the loads acting on the lining, is considered one of the most difficult tasks of all.

Rock mechanical calculations must be based on a geological site investigation in the area of the projected dam, taking into consideration the aspects listed below:

– Geometrical description of the rock mass structure, i.e. of the joints including their formation.

– Mechanical properties of the structural elements, based on rock types and joint fillings, such as strength, time-dependent deformability and the rock mass primary stress state.

– Hydrological conditions (groundwater level, water flows, springs, etc.) and the hydraulic properties of the flow paths, i.e. permeability and the pressure at which joints will form or propagate.

– Potential displacement zones, e.g. due to tectonics or seismicity.

In regard to joints a distinction must be drawn between:

– Closed joints (e.g. stratification, foliation) can represent weak zones and affect the cohesion.

– Complete interruptions of the mechanical continuity of the rock, i.e. tension or shear joints as well as slickensides, caused during rock formation and/or by tectonic overstressing of the material. Depending how the rock formed, open joints may also be filled with alluvial deposits (tension joints) or fractured material (shear joints).

The primary stress state may be of some consequence, especially at the foot of steep valley slopes and in regard to the excavation also at the dam site.

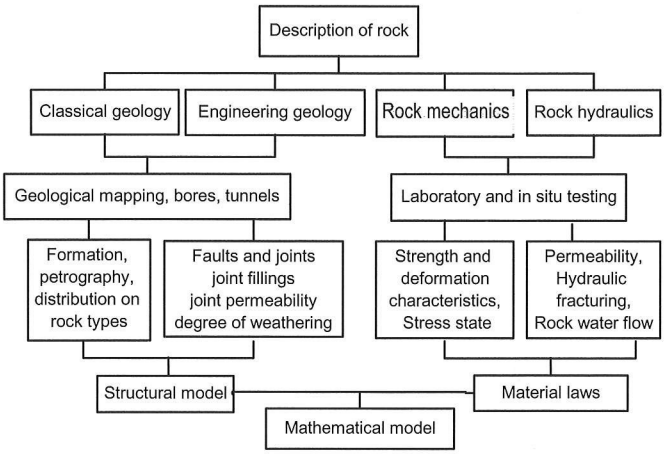

Fig. 3.1: Investigations to describe the rock ground.

The evaluation of rock mechanical problems in relation to the founding of concrete dams comprises basically three aspects which, though of course interrelated through the geological structure, must nonetheless be considered separately:

– Stability of the ground and reservoir slopes. Generally this is determined by the shear strength in the joints.

– Deformability of the dam body's foundation.

– Permeability of the underground.

3.2 GEOLOGICAL DESCRIPTION

Geological investigations of dam sites must cover a ground area corresponding upstream and in depth approximately to the height and downstream to double the height of the planned structure. Geologically

complex cases may require investigations of larger areas. Reservoir slopes as well may require at least general investigations of areas extending to a greater height.

Geodetic mapping of the dam site and reservoir, as detailed as possible, must be followed by the geological mapping of all geologic zones and joint locations visible on the surface. These are best depicted using the spherical projection (e.g. Reitmeier 1982) that also facilitates the graphical solution of some of the basic tasks of rock mechanics (John 1974, Londe 1965). This geological mapping serves as the basis for determining the bores to examine the geological conditions down to the required depth.

The probability of encountering unexpected geologic conditions during construction – resulting in longer construction periods and higher costs - or at the worst even requiring a new project design, can only be reduced by sufficiently extensive geological investigations.

A deterministic description of the rock or fault structure is not really capable of truly reflecting the in-situ conditions. During the last decade, therefore, statistical procedures were developed that come closer to describing the true conditions in nature (e.g. Brosch 1994). To describe jointed rock the aspects listed below must be determined in situ:

Location, opening widths, roughness.
Outcrop, track length, joint size.
Spacing, frequency, degree of fracturing.

Probabilistic descriptions showing a statistical distribution of the rock's characteristic data will only then prove their true worth when the probabilistic composition of the rock structure is taken into account by the rock mechanical calculations as well. Relevant procedures are presently being developed (e.g. Pöttler 2002).

Geophysical examination methods can facilitate the summing-up of individual results. Depending on the task, these can include:

– Electrical methods based on the fact that different ground layers also have different levels of electrical resistance.
– Seismic methods to measure the propagation velocity of artificially generated vibrations, e.g. between boreholes, as different layers also have different propagation velocities for sound waves.
– Gravimetric methods capable of deducing the location of the rock surface from among the varying underground densities even in the presence of high overlying strata.

All geophysical methods provide improved results, if they can be calibrated against several representative bores. In addition, it must also be taken into consideration that different groundwater conditions can lead to widely varying measurement results.

Recently, improved and also more expressive evaluation methods have been developed such as:

– Ultra-sound diagraphy; irregularities in the signal sequence indicate a change in layers.
– Ultra-sound tomography; a spatial network of repeatedly crisscrossing measurements of the wave propagation period indicates the sound velocities in the examined sections which are assumed to reflect the varying rock mass properties.

In addition, a geologically-oriented evaluation of rock resistance in regard to the influence of water on chemical or physical properties must be carried out.

Geological investigations must result in the preparation of a structure model of the dam site and reservoir area. Based on this the civil engineer has to determine the expected reactions of the underground to the construction and operation of the dam.

Finally, the seismicity of the reservoir, dam site and the surrounding area must also be examined, particularly in regard to three aspects:

– Active fault zones at the dam site in which tectonic or seismic activity can cause relative displacements along the faults, the length of which:

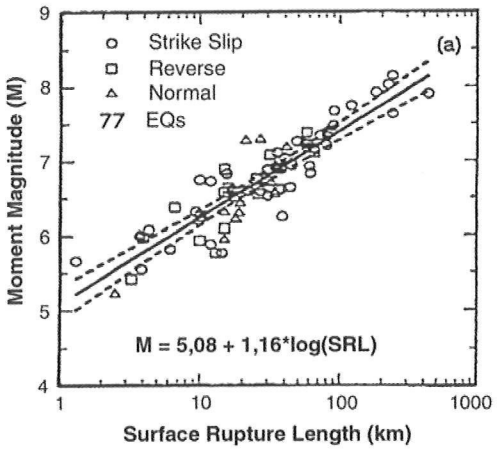

Fig. 3.2: Relation of fault zone length to earthquake magnitude (Wells 1994).

– Can be a measure of the expected earthquake intensity. Such active fault zones should be avoided, if they cross the abutment area (Fig. 3.2).
– The magnitude of any vibrations emanating from epicentres nearby or further away (see section 3.4).
– The possibility of induced earthquakes triggered by mining or by the filling of the reservoir must also be considered (see Annex B 2).

3.3 GEOMECHANICAL DESCRIPTION

Rock is one of those materials the behaviour of which under imposed loads or deformations is the most difficult to describe using quantitative material laws. Rock is a body irregularly traversed by joints, often in three directions approximately perpendicular to each other. How they were formed has the greatest influence on the properties of the rock mass. This may explain the particularly problematic nature of rock mass properties, since a distinction must be drawn between:
– Properties of the rock, i.e. of the intact rock body between joints. These can be determined similar to those of concrete by using small rock samples.
– Properties of the joints, particularly their fillings.
– Properties of the rock mass, i.e. of the rock body traversed by joints.
The characteristic data are determined in laboratory tests using more or less homogenous small test specimens. These tests are comparatively cheap and can therefore be performed in high numbers. The large deviation of laboratory tests can be reduced to the standard testing deviation by classifying specimens according to geologically comparable fracture areas. However, laboratory testing cannot determine the in many cases decisive influence of discontinuities on the behaviour of the entire rock mass.
In-situ testing is justified, if the tested rock volume corresponds approximately to the REV (Representative Elementary Volume, the smallest rock volume with properties reflecting those of a much larger area), which can be different for each property. Otherwise, also in-situ testing will ultimately produce only mean characteristic parameters for the deformation behaviour of the rock mass in the test area under the test stress level.

The more pronounced the joint structure, the more difficult it becomes to transpose intact rock properties into rock mass properties decisive for the structure. As in other technical fields, index procedures have been developed to deduce the rock mass properties from the rock properties. Thereby, data derived from simplified methods is corrected by geometrically determined coefficients. (Barton 1994, Beniawsky 1994).
All the indexes or coefficients of these methods are ultimately based on statistically determined correlations between parameters. These are valid only, if the system on which the empirical assessment is based reflects the true conditions. In some cases, using the RMR (Rock Mass Rating) parameters, a correlation could be empirically established between the deformation moduli of compact rock and the parameters of the rock mass derived from measurements (Fig. 3.3).

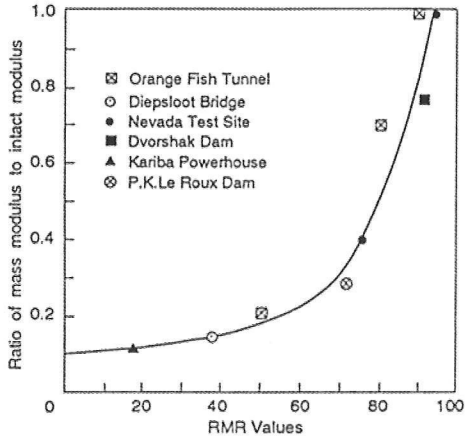

Fig. 3.3: Correlation between the RMR and the ratio of the deformation moduli of compact rock to jointed rock for various concrete dam foundations (Beniawsky 1975).

The ECM (Equivalent Continuum Model) is based on the mean values for large rock mass areas and consists of the transformation of a discontinuum into a fictive continuum with the same behaviour. Thereby, the mechanical effects of the joints must be included in the parameters used in rock mass description. This model may be justified in cases in which stress propagation is not hindered by the joints and the joint spacing remains narrow compared to the thickness of the dam body's base. It cannot be used, however, for the planning of injections, since the geometry of the flow paths cannot be

described as required for the flow description of liquids with varying flow characteristics [*102*].

It is the goal of modern calculation methods to represent the rock fabric, characterized by joints, as realistically as possible using geometrical models, so that representative parameters determined by laboratory testing can be assigned to the individual fabric elements, like rock types and joints.

Stability analyses require:

- Not so much a determination of the tensile strength, which in any case should not be considered due to the presence of joints.
- Nor of the compressive strength of the rock, which in most cases sufficiently exceeds the required values.
- But primarily of parameters for the description of the behaviour under shear stress, also in this case particularly of the joints and joint fillings.

3.4 ROCK MECHANICAL PARAMETERS

Since the 1960s tests have been performed for Austrian arch dams to determine the rock mechanical parameters [18, 19, 32, 54, 104]. Only some experiences shall be recorded below.

3.4.1 Compressive and tensile strength

Tests to determine the compressive and tensile strength cannot be carried out in situ due to the high loads that must be applied. For laboratory testing, the petrographic and structural characteristics of the test specimens, particularly of the fracture areas must be exactly defined. Generally, test evaluations must consider the stress state in the fracture areas. However, the tensile strength is of only minor significance, since it should not be considered, at least transversally to the joints in the rock mass.

The number of laboratory tests on geologically comparable fracture areas should be so chosen as to justify a statistic evaluation of the test results. The load direction must be determined according to the desired location of the fracture area (Czech 1990).

3.4.2 Shear strength

In general, the shear strength of the joints is of decisive importance for the properties of the rock mass. It can be determined using:

- Axially symmetric triaxial laboratory tests for very short shear paths, e.g. for underground structures or the foundation of buildings.
- Direct laboratory as well as in-situ shear tests, e.g. for the foundation of dams, with load cycles that result in short shear paths in both directions.
- Radial shear tests for long shear paths, e.g. for determining the stability of slopes.

The shear strength is determined by the cohesion and roughness of the fracture area. The roughness of a joint can be characterized in accordance with two constituents: (Fig. 3.4):

- Macro roughness (waviness), designated by the angle $\Theta_{1\kappa}$ and the wave length l_1.
- Micro roughness k as a deviation of the joint wall from the waviness, designated by the relative roughness.

$æ = k/2a_j$ (aj = half the joint width).

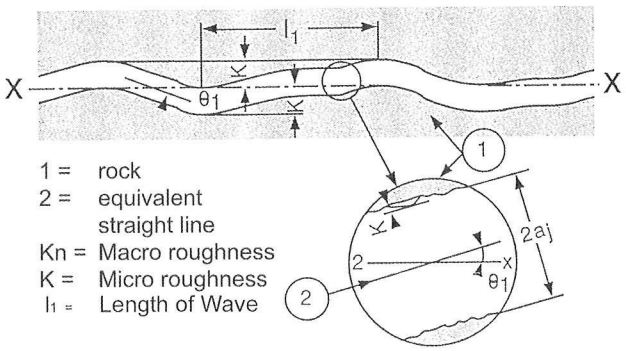

Fig. 3.4: Characterization of the roughness of joints (Louis 1967).

In the last decades, attempts were made to determine the effects of the roughness on the mechanic and hydraulic properties using the parameter

JRC (Joint Roughness Coefficient).

Its representative determination is however problematic.

In general, only the micro-roughness affects the results of laboratory tests, the waviness of the shear planes the results of in-situ shear tests; therefore, as the shear plane length in the load direction increases, in most cases also higher shear strengths result.

However, if during testing in the load direction the wave length exceeds the length of the shear plane, the shear strength can decrease with increasing shear plane.

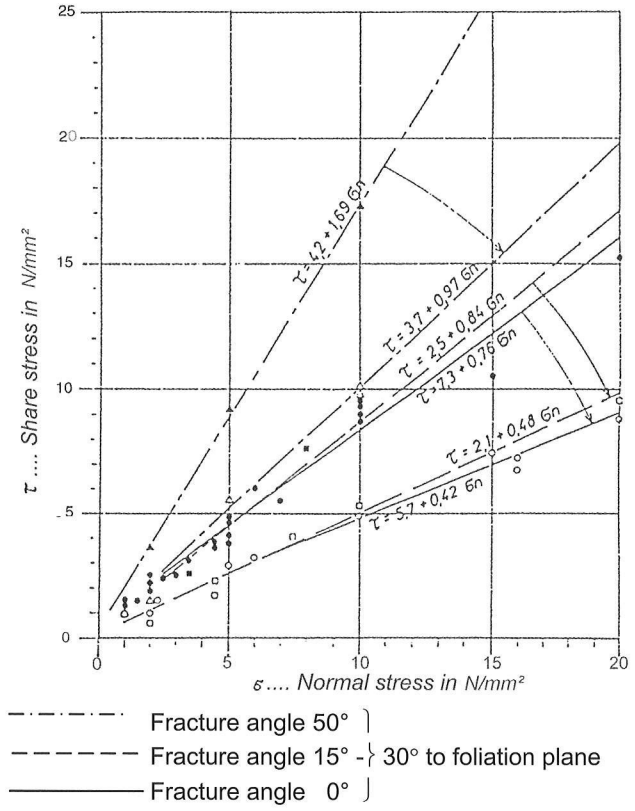

Fig. 3.5: Mohr - Coulomb fracture line for intact granite gneiss [18].

Laboratory tests

Numerous laboratory tests were performed to determine the rock mechanical parameters of the underground of the Schlegeis arch dam in the Zillertaler Alps [18]. Petrographically, the underground consists of middle to coarse-grained granite gneiss of varying composition. The mechanical properties of the rock were for the most part determined by the quantitative mineral content of the constituents, particularly the mica content. Part of the samples were immersed in water for one week. With these samples, water absorption remained below 0.005 percent in weight and did not affect the strength properties. The high number of individual tests with geologically comparable fracture areas made it possible to carry out a statistical evaluation (Fig. 3.5).

With small shear planes, however, the scale effect or waviness cannot be determined even by carrying out a great number of tests.

In-situ tests

In many cases, triaxial tests are carried out in situ on rock blocks separated laterally from the surrounding rock by cuts or bores. Due to the high loads required, the shear plane must be limited to 0.5 - 1 m^2. If testing continues beyond the maximum shear strength or if the residual shear strength is determined by repeated shearing, several such tests must be performed under equal geological conditions in the shear planes to enable a complete description of the shear behaviour (Fig.3.6).

For the 220 m high Dabaklamm arch dam project, which was not realized, extensive rock tests were carried out, including an in-situ shear test on a 56 m^3 large rock block that rested on a joint oriented parallel to the surface with an inclination of 45° (Fig. 3.7). This rock block with a bearing area of 21 m^2 was separated from the surrounding rock by a 0.5 m wide,

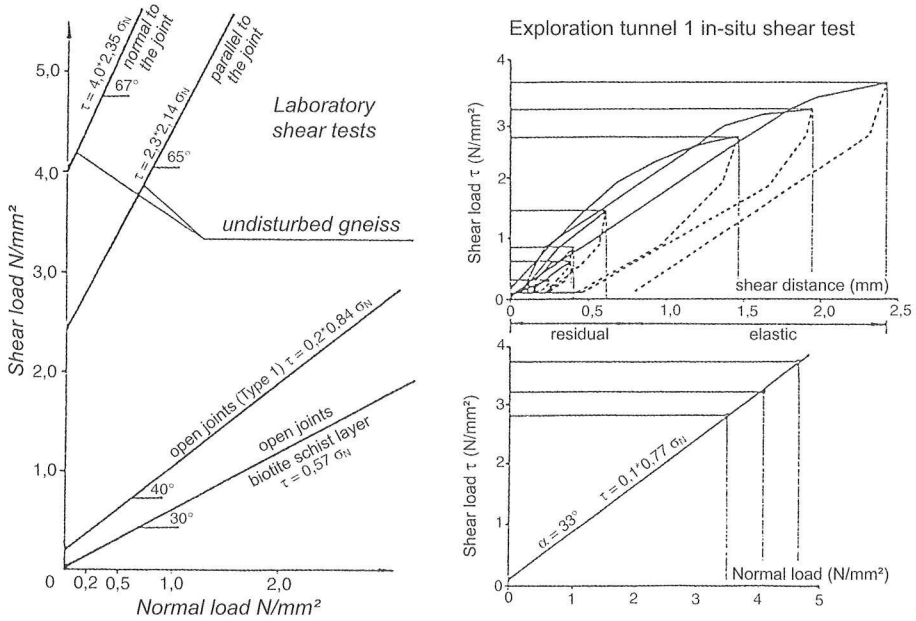

Fig. 3.6: Comparison of in-situ and laboratory shear test results.

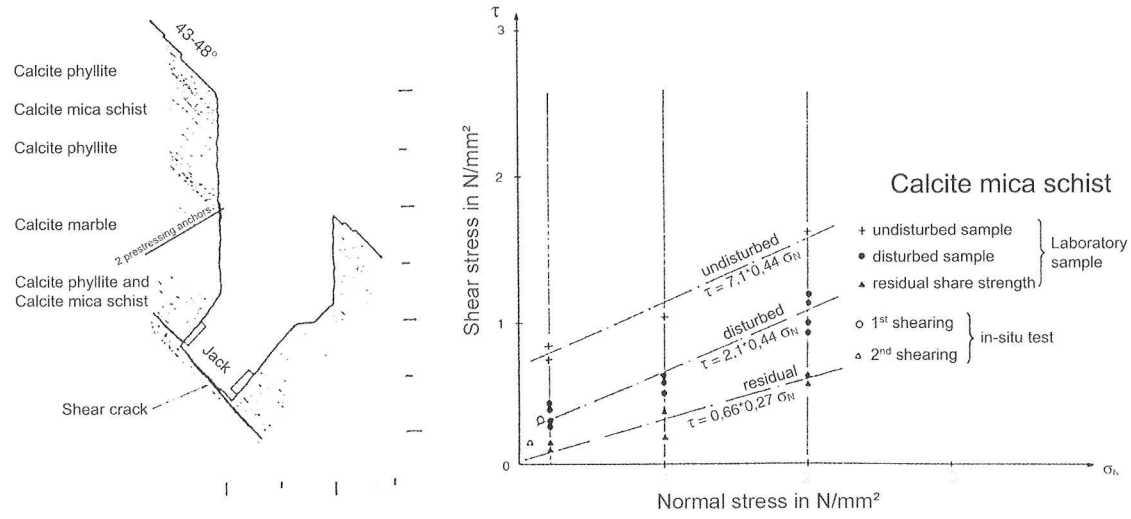

a) Test set-up b) Summary of the test results

Fig. 3.7: Shear tests for the dam site of the Dabaklamm arch dam.

2.5 m deep and 5 - 6 m long slit. Six jacks of 100 tons each were installed in this slit, with their line of action parallel to the line of fall. The rock block lying above was secured using several 20-ton anchors. The shear plane lay, as was determined after shearing, in calcite phyllite or calcite mica slate.

The test set-up is illustrated in Fig. 3.7a. The test results (Fig. 3.7b) are listed together with the results of laboratory tests on rock samples consisting of calcite mica slate with a high mica content. The results of the tests show a high degree of correspondence.

3.4.3 Deformation behaviour under compression

The deformation behaviour of the rock fabric, like its strength, is decisively influenced by the fabric. This influence is determined by

- the orientation and state of the joints,
- the filling of joints with alluvial soil or pulverized material and/or water,

and affects above all the stress propagation – the stress field – under load.

The laboratory tests to determine the deformation behaviour of rock under compressive stress follow a similar procedure as those for concrete displaying the same characteristic development.

The deformation behaviour under uniaxial compression is usually determined in laboratory tests on rock prisms. With these the transverse strain remains unconfined. In the rock mass, however, this may be only true in the case of open joints with narrow spacing. As joint spacing increases, the restraint on the transverse strain also increases, so

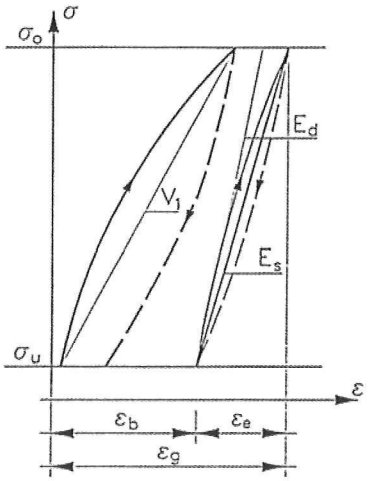

σ_u ..... Lower compressive stress
σ_o ..... Upper compressive stress
V_1 ..... Deformation modulus upon first loading
E_s ..... Static modulus of elasticity
E_d ..... Dynamic modulus of elasticity
ε_b ..... Permanent specific strain
ε_e ..... Elastic specific strain
ε_g ..... Overall specific strain

Fig. 3.8: Definition of the parameters for the deformation behaviour of rock and concrete.

that the parameters for the deformation behaviour in triaxial tests should be determined, at least mathematically taking the transverse strain measured during testing into consideration.

$$\nu = \frac{\sigma_a \varepsilon_r - \sigma_r \varepsilon_a}{2\sigma_r \varepsilon_r - \varepsilon_a (\sigma_r + \sigma_a)} \qquad E = \frac{\sigma_a - 2\sigma_r}{\varepsilon_a}$$

ν = Poisson's ratio

σ_a = Longitudinal stress
ε_r = Elastic transverse strain
σ_r = Transverse stress
ε_a = Elastic longitudinal strain
E = Modulus of elasticity

These theoretical elasticity correlations show that the deformation modulus increases with increasing transverse stress, ultimately approaching the infinite, when the transverse strain is completely restrained. This tendency can be of importance for intact rock masses.

According to standards, the modulus of elasticity is determined after several load cycles, when, following the load cycle, there is no longer an increase in residual deformations. Upon first loading, a lower deformation modulus is achieved both in rock and concrete. This must form the basis for the deformations generated during the pouring of concrete and first filling of the reservoir.

Laboratory tests

On compact rock, the deformation parameters can be determined relatively easily; also an anisotropy can be determined by examining test specimens taken from three directions perpendicular to each other (Tremmel 1970). These tests are particularly practicable and appropriate, if the rock body is relatively uniform with wide joint spacing, like the underground of the Schlegeis arch dam [19].

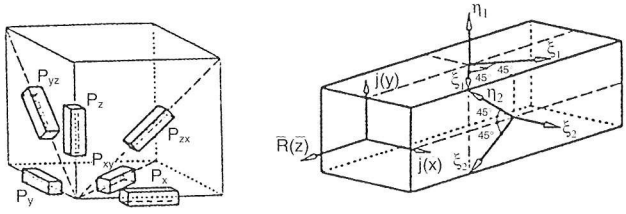

Fig. 3.9: Direction of the rock prisms and strain gauges [19].

To determine the anisotropy of the deformation moduli, 18 rock prisms, 10 x 10 x 30 cm, were cut from a large granite gneiss block in 6 different directions (Fig. 3.9), so that three test specimens were available for each direction. Four strain gauges were fixed in the middle third of each lateral surface. For each prism, measurements in 7 different directions were taken. The readings taken in the same direction on opposite surfaces were then averaged.

As is generally known, the deformation behaviour of a homogenous anisotropic body is determined by 21 elastic constants derived from an equation system. From the relation of stress to deformation tensor inherent in the elasticity tensor the 9 components of the deformation tensor can be established, utilizing all symmetries.

$$\begin{pmatrix} E_1 & \nu_{12} & \nu_{13} & & & \\ & E_2 & \nu_{22} & & & \\ & & E_3 & & & \\ & & & G_{32} & & \\ & & & & G_{31} & \\ & & & & & G_{12} \end{pmatrix}$$

E Modulus of elasticity, G Shear modulus, ν Transverse strain

The elastic parameters were established according to the diagram above (moduli in KN/mm^2, transverse strains dimensionless), e.g. for the load step 0 – 20 N/mm^2.

$$\begin{pmatrix} 17.61 & 0.056 & 0.005 & & & \\ & 7.46 & 0.042 & & & \\ & & 15.42 & & & \\ & & & 6.33 & & \\ & & & & 7.75 & \\ & & & & & 6.51 \end{pmatrix}$$

Table 3.2 Matrix of the deformation parameters [19].

The measurement results obtained from one rock prism (Fig. 3.10) clearly show larger deformations at lower than at higher load steps. Since the measurements could not be continued up to failure, decomposition of the rock as an indication of the onset of failure was as yet not discernable.

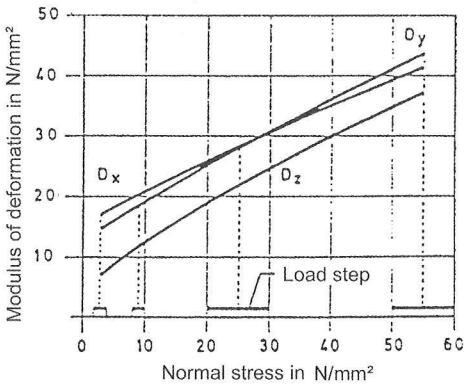

Fig. 3.10: Load-dependent, anisotropic deformation moduli.

Remarkable, however, is that all deformation parameters increased with increasing load due to the initially "loose" stratification of the rock grains as well as to the largely orthotropic behaviour.

In-situ tests

In-situ tests as well can determine the expected

deformation behaviour of the rock mass only to a limited extent. This is due to two reasons:

a) The load-dependent rock volume will reach or even exceed the REV only with very narrow joint spacing. However, as long as the rock volume affected by the load remains below the REV, the results will be influenced by random inhomogeneities within the test area and show, therefore, a large deviation. In plate loading tests this influence extends to a depth that corresponds approximately to double the diameter of the load plate. Therefore, a circular load area of 0.5 m^2 corresponds approximately to a test rock volume of 0.6 m^3.

b) Stress propagation, and hence the stress field, are influenced by the condition of the joints the true nature of which can hardly be determined. However, in order to convert the measured deformation into a deformation modulus the in-situ stress field must be known.

The influence of a jointed and therefore anisotropic rock on stress propagation and thus on the evaluation of tests carried out to determine the rock mechanical parameters has been known for a long time (Krsmanovic 1964), but until now has only rarely been taken into consideration (Fig. 3.11).

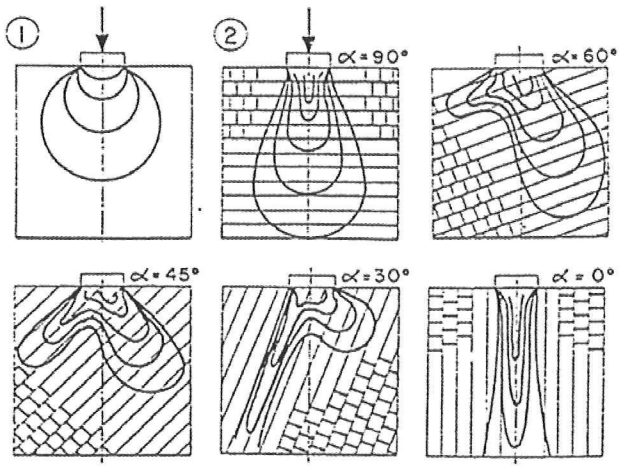

1) Continuum 2-6 Discontinuum

α Angle between load and foliation plane

Fig. 3.11: Stress propagation in the continuum and in stratified ground.

For the evaluation of plate loading tests, an elastic-isotropic semispace is generally assumed. However, if the shear stresses enabling the stress propagation can no longer be absorbed in the joints, the compressive stress will decrease considerably slower in the load direction with increasing distance and remain within a narrower range than set down in the idealised homogenous design assumptions (Fig. 3.11). Therefore, the actual deformation modulus is higher than if derived from the simplified formulas.

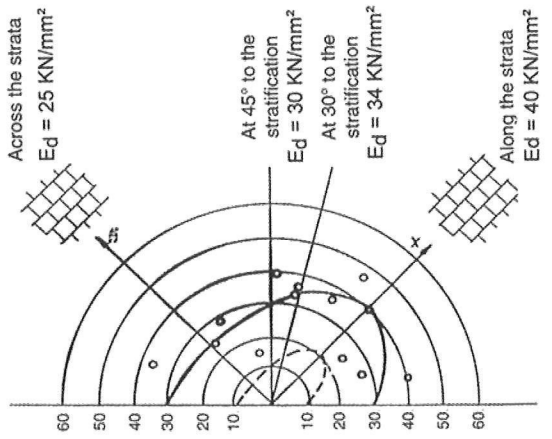

– – – Converted static deformation modulus

Fig. 3.12: Dynamic deformation moduli in various directions (Gaziev 1971).

The anisotropic dilatation of a borehole under internal pressure can be measured using dilatometers in bores that determine the deformation parameters in various directions. However, since the rock mass affected by the load usually corresponds to the bore diameter, the results are not really representative, at least for jointed rock. They are strongly influenced by random inhomogeneities in the test area and show, therefore, a large variation.

Plate loading tests in tunnels cover a larger rock volume. Preferably, these should be carried out with radial pressure direction on two opposite tunnel walls.

In the underground of the Zillergründl arch dam three plate loading tests were carried out to determine the deformation behaviour of the compact gneiss (M1), normal (M3) and parallel (M2) to a fault zone. The rock compressions were measured using multiple extensometers at a depth of 0.5 m, 1.0 m and 3.0 m respectively. Decomposition of the tunnel intrados by bursting occurred to a very limited extent only (Fig. 3.13).

The load - displacement diagrams illustrate the typical (Fig. 3.8), load-dependent deformation behaviour. The readings of multiple extensometers show the decrease in deformations approximately up to the tunnel diameter.

Evaluation of the test results can be improved upon, by taking measurements at increasing distances

from the loaded bore edge, from the onset of stress decrease and taking the decomposition zone into consideration. In the decomposition zone (= thickness measured by the shortest extensometer) the stresses were assumed as for fractured rock (i.e. no transfer of tensile stresses) and in the remaining area as for homogenous rock. Improved results are achieved, if the joint orientation and anisotropy are taken into account as well.

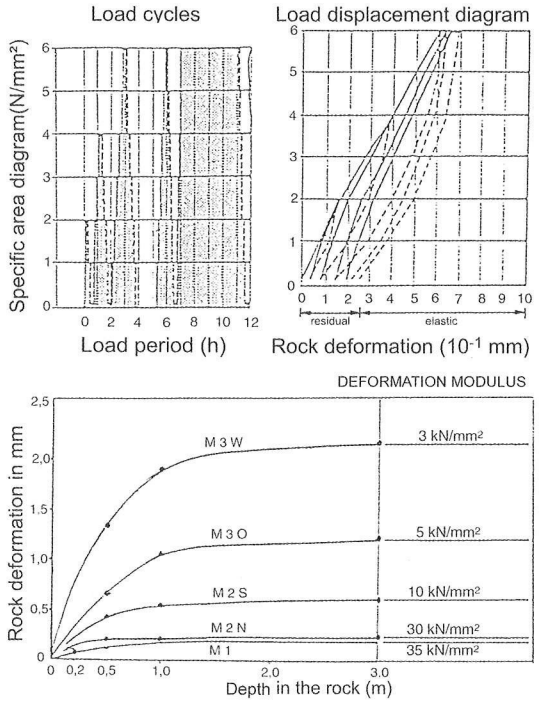

Fig. 3.13: Test results of a plate loading test in the tunnel [55].

The determined deformation moduli lay between 35 kN/m^2 in intact gneiss and 3 kN/m^2 normal to the fault zone. The residual deformations during repeated load cycles reached approximately 25% of the overall deformations.

In-situ test results should be directly applicable to design calculations. However, this can only be achieved by means of the rather costly radial jack test (Lauffer 1960, Seeber 1999) that was developed for pressure shafts to determine the sup-porting effect of the rock on the lining under internal pressure. Yet, consideration of the short load length, compared to the length of later pressure shaft, requires that the measured deformations along the loaded surface are overlaid in an appropriate manner (Tremmel 1960).

For the foundation of a concrete dam, the uncertainties inherent in the conversion of measured deformations into parameters still apply. In addition, the rock volume covered by the in-situ test still differs from the rock volume underneath the structure by two to three powers of ten.

δ_1 .. displacement at the tunnel edge
δ_2 .. compression of the decomposition zone
r ... radius
a_1 .. excavation edge
a_2 .. decomposition zone
σ_r .. radial stress
σ_t .. circumferential stress

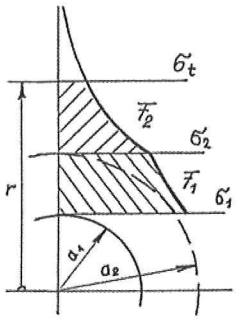

$a_1 < r < a_2$ ..fractured rock: $\sigma_r = p_F \cdot \frac{a}{r}$, $\sigma_t = 0$

$r > a_2$ .. intact rock: $\sigma_t = p_F \cdot \frac{a_1 \cdot a_2}{r^2}$

$$F_1 = p_F \cdot \int_{a_1}^{a_2} \sigma_{r1} \cdot dr = p_F \cdot a_1 \cdot \ln \frac{a_2}{a_1}$$

$$F_2 = p_F \cdot \int_{a_2}^{\infty} \sigma_{r2} \cdot dr = p_F \cdot a_1$$

$$V_1 = p_F \cdot \frac{F_1}{\delta_2}, \quad V_2 = p_F \cdot \frac{F_2}{\delta_1 - \delta_2},$$

Fig. 3.14: Sectional determination of the deformation moduli.

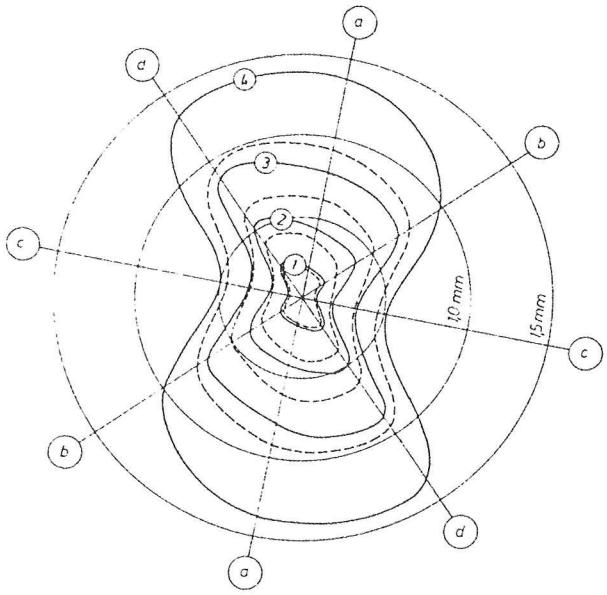

Fig. 3.15: Mayrhofen hydropower plant, pressure shaft: anisotropic deformation of the tested cross section [26].

Large-scale seismic tests yield mean values for larger areas. In addition to the plate loading and radial jack tests, therefore, seismic tests were carried

out along the abutment area of the Zillergründl arch dam between the bores for the extensometers, so that a correlation could be set up between the dynamic and static modulus of elasticity (Fig. 3.16).

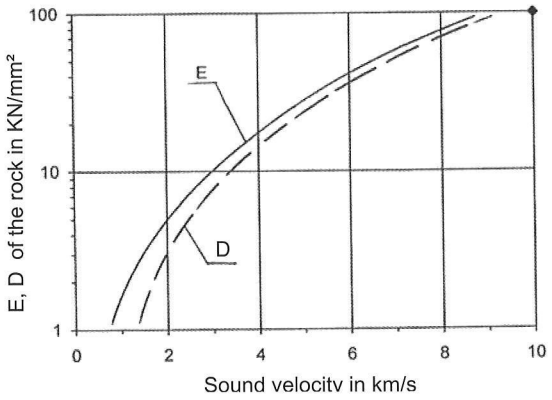

Fig. 3.16: Correlation between sound velocity and the deformation moduli.

The gneiss on the right-hand slope had wide joint spacing (mostly several meters). The joint spacing on the left-hand slope was considerably narrower. The seismic test results, however, showed only minor differences between the two slopes, whereas the fault zones were clearly discernable. Subsequent deformation measurements during dam operation confirmed these results (Fig. 3.17).

In conclusion it can be said that presently the commonly used parameters for the deformation behaviour under compressive stress:

– Are, in theory, correctly determined in laboratory tests under in most cases unconfined transverse strain; the influence of joints, however, is largely ignored.

– Are determined in in-situ tests that at least partly take into account the joint influences but do not consider the true stress field and cannot, therefore, lead to analytically correct parameters.

– Do not take into account the varying deformation behaviour upon first loading and after several load cycles as well as the residual displacements.

The stage of development of the present FE-procedures would make it possible to consider the joint structure and anisotropy. It is to be desired that these procedures be used not only in rock mechanical calculation, but also in the evaluation of tests, particularly of in-situ tests. Realistic parameters could then be inferred and used as a basis for rock mechanical calculations.

3.4.4 Deformation behaviour under shear stress

Basically, a distinction must be drawn between the shear deformations of the massive rock body and the displacements in the joints. The deformations of the more or less homogenous and isotropic rock body confined by the joints can be at least approximately deduced according to the theory of elasticity using the shear modulus and the transverse strain.

Generally, however, these will form only a small part of the overall deformation. Of greater importance for a realistic calculation of the discontinuum are the shear deformations in the joints. The length of the displacement path along the joint due to the stress has a decisive influence on the shear strength and must, therefore, be taken into consideration when selecting the shear test method (see 3.4.2):

The usual charting of the displacements along the joint surfaces (Fig. 3.18) as a function of the shear stress under constant normal stress shows the known more or less steep load decrease after attainment of the maximum shear strength τ_{peak} until the residual

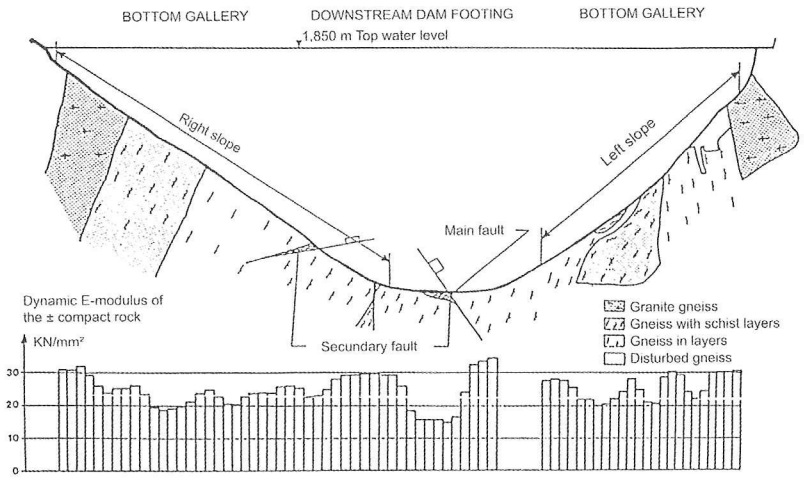

Fig. 3.17: Cross section of the Zillergründl dam site; results of the seismic tests[55].

shear strength τ_{res} is reached, at which point the displacements continue to increase without changes in the load.

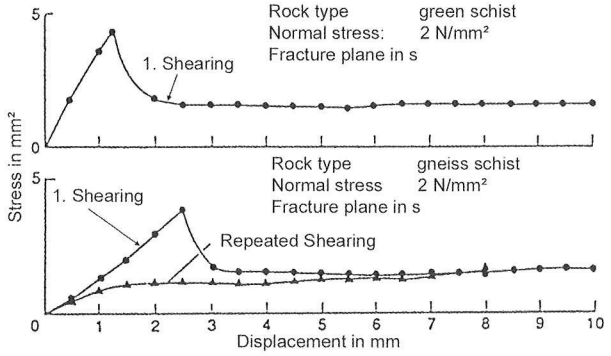

Fig. 3.18: Shear stress – displacement in one fault surface (Czech 1990).

If the displacement path before reaching τ_{peak} is defined as a function of the ratio τ/σ, a comparably low deviation of the displacements under various normal stresses results. If the area prior to fracture is considered, i.e. before reaching τ_{peak}, the displacement can be defined as a linear function based on the ratio τ/σ (Fig. 3.19), hence:

$$\Delta s = Q \cdot V_S \text{ mit } V_S = V_S' \cdot Q/N, \text{ bzw.} = V_S \cdot \tau/\sigma$$

where V_S [mm/m] may be referred to as the displacement modulus . Accordingly, the dimension of the displacement modulus is defined as the length of the displacement path per force unit. The basic difference to the usual stress-strain relation is that the displacement is approximately equal at each point of the joint, whereas the deformation resulting from the usual stress-strain relation is the sum of the displacements along the length of the load direction.

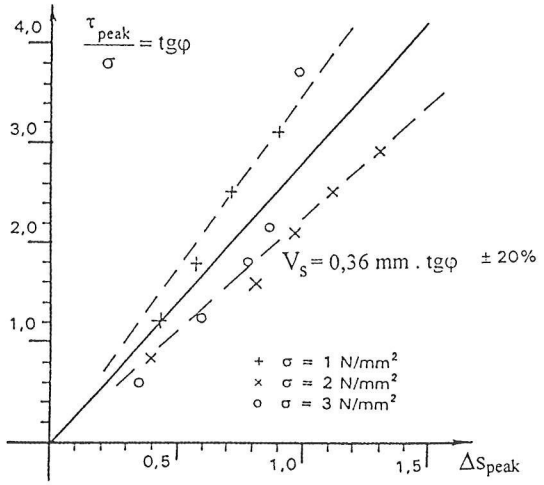

Fig. 3.19: Displacement modulus [32].

These tests require that the shear planes be geologically comparable in regard to petrography and roughness. Different joint surfaces or e.g. mica layers of varying thickness will, of course, considerably influence the displacement.

3.5 IN SITU STRESSES

The methods commonly used to determine the stress state in the rock mass, as for example the Doorstopper method, measure strains that are then converted into stresses on the basis of the assumed stress-strain relations using the formerly determined deformation modulus. Thereby, an isotropic rock mass is presumed. Recent investigations (Kummerer 1993) have revealed that the apparent deviations of these test results can be reduced, if the anisotropy in the behaviour of the rock mass is taken into account as well.

In this context reference shall also be made to tests using hydraulic pressure cells in a semicircular cut slot. In this case as well, the problematic nature of stress propagation should make it more difficult to evaluate the test results. Thereby, first the narrowing of the slot as a result of the slot cutting is measured and subsequently the pressure along the pressure slot required to re-establish the original slot width. This method ignores the effective shear stresses parallel to the slot in the undisturbed state as well as the stress gradient above the slot depth that doubtlessly exists near the rock surface, especially around tunnel intrados, since the compensatory pressure is applied evenly and frictionless. The effects of an anisotropy should approximately compensate each other during unloading and loading.

3.6 SCALE EFFECT

The scale effect usually denotes the difference between the parameters derived from tests performed on comparatively small rock volumes, either in situ or in the laboratory, and the parameters used to describe the actual behaviour of the structure or the underground. It is a general term, since this difference is due to several causes:

– The laboratory test results on specimens of rock, just like the test results on specimens of concrete, are dependent upon the form and size of the specimen, load set-up, and the rate and period of loading

due to simplifications of the stress field and the disregard of the time-dependent behaviour.

– Differences resulting from the varying size of the rock volume covered by the test and the dam, with otherwise equal boundary conditions, must be predominantly assigned to the irregular distribution of the inhomogeneities.

– Rock, just like concrete, has a granular structure with more or less strong cementing attributes. As with concrete, according to standards, the largest grain size should be smaller than 1/3 – 1/4 of the smallest specimen dimension. This can be of importance e.g. with conglomerates.

Examinations based on the theory of fractals (Carpintieri 1993) have shown that the strength values decreased using a logarithmic quantity of the specimen size. According to the definition, the lower limit of this apparent decrease in strength should be reached, when the size of the specimen corresponds to the REV.

Experience has shown that the variation of the test results decreases with increasing size of the loaded rock body, since the mean value of the statistically distributed inhomogeneities varies less (Fig. 3.20).

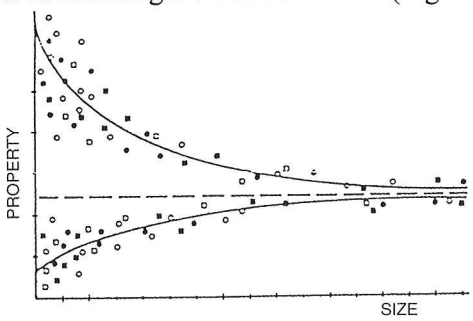

Fig. 3.20: Variation of the test results as a function of specimen size.

In the rock mass, the influence of foliation planes and joints must be considered as well, since they influence the stress propagation and the deduction of representative parameters.

The problems are different in regard to direct shear tests at given joints, in which the shear length should reach at least double the wave length of the macro roughness in the direction of the shear length. If this is not possible, then the lower limit value of the shear strength present in nature can be considered the measured shear strength.

The results of the ISRM Commission on Scale Effects and of the two workshops on this subject (Loen 1990 and Lissabon 1993) can be summarized as follows:

– Basically, as specimen size increases, both the variation of the test results (Fig. 3.20) and the strength (Fig. 4.10) diminish, since the effect of random inhomogeneities decreases proportionately.

– In situ stress measurements should on the average lead to equivalent results, if the available test methods are correctly applied and evaluated; although of course small-scale tests (e.g. overboring) will tend to determine local stress peaks or stress decreases.

– The hydraulic properties are mainly dependent on the joint system, hence on the determined rock volume, since the permeability of the intact rock can generally be ignored in this context. They can change according to the stress field.

The report concludes that the determination of the REV is actually still unresolved and will require further research.

3.7 DESIGN EARTHQUAKE

In characterizing earthquakes, a distinction must first be drawn between intensity and magnitude. Basically, the relation of these two dimensions is dependent on the distance of the site from the epicentre and/or depth of the focus and the geological formations in between. This may partly explain the great variance of the formulas specified in literature for these relations. It should be possible to achieve a reduction of this variance for small distances, if the distance of the considered point is measured not from the epicentre but from the active fault or its end points (Fig. 3.21).

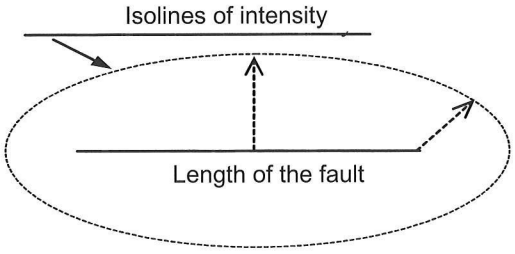

Fig. 3.21: Isolines for measuring the distance from the active fault.

The problems raised by classifying accelerations according to the 12 steps of the Mercalli-Sieberg scale can be seen in the figure below comparing the results of various authors (Fig. 3.22).

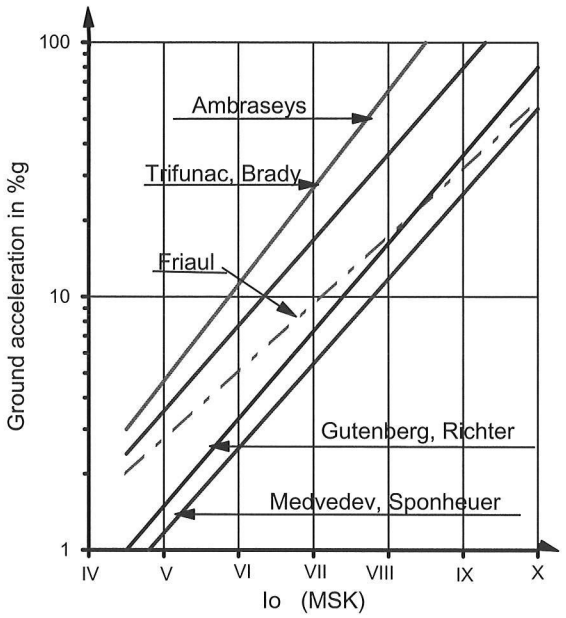

Fig. 3.22: Correlations between intensity and peak ground acceleration (Sägesser 1977).

In the old chronicles, earthquakes are evaluated according to the damages caused. The well-known 12-step Mercalli-Sieberg scale is therefore an intensity scale according to which the earthquake intensity is determined on the basis of the earthquake effects.

The Richter scale, on the other hand, deals with the magnitude that is a logarithmic measurement based on the measured vibrational energy generated by the earthquake. Trials on the correlation of these two scales (e.g. Gumensky 1957) ignore, among other things, the duration of the earthquake on which the vibrational energy is dependent. In addition, the varying damage susceptibility of different construction methods that have been developed over the centuries make a classification more difficult. Therefore such classification should serve as a reference but on no account replace measurements.

The determination of an effective peak ground acceleration suffices for the design of a structure, only if the actual dynamic loading of the structure is converted into a static replacement load. Thereby, among other things, such factors as the local ground conditions, the importance of the structure and the distribution of the earthquake load along the height of the structure must be considered as well (ENV 1998 - 5). 'Real' dynamic calculations must include the time-dependent vibration behaviour.

3.8 HYDRAULIC DESCRIPTION

3.8.1 Definitions

First it is necessary to clarify the various definitions that are usually used to describe the water conductivity of the ground.

The TRANSMISSIVITY T [m²/s] is measured e.g. using water pressure tests and corresponds to the product of the hydraulic conductivity K [m/s] and the thickness d [m] of the aquifer, which is of course fundamentally different from the cross section of the water flow: $T = K \cdot d$.

The measure of transmissivity is 1 Lugeon = 1 litre/min per m length of borehole at a pressure of 10 bar in the grouted section of the borehole, hence:

$$1\ \text{Lu} \ldots [\text{dm}^3/\text{min}] \text{ or } 1.67 \cdot 10^{-5}\ [\text{m}^2/\text{s}].$$

The HYDRAULIC CONDUCTIVITY K [m/s], according to the empirical Darcy law for laminar parallel flow: $q = K \cdot I \cdot A$

corresponds to the proportionality factor K between the water flow rate q [m³/s] and the product of the hydraulic gradient I [-] and the overall cross-sectional flow area A [m²]. For granular soils, 1 Lugeon is equivalent to a hydraulic conductivity of $K = 1.3 \times 10^{-7}$ m/s for a 3" borehole diameter and 1.5×10^{-7}/s for a 2" borehole diameter.

The hydraulic conductivity K_J of the single joint is of decisive importance in evaluating the groutability of jointed rock (Louis 1974):

$$K = \frac{W_m}{e} \cdot K_J + K_M$$

where W_m = mean joint width
e = mean joint spacing
K_J = conductivity of joint
K_M = conductivity of rock matrix

The PERMEABILITY k [m²] is a geometric characteristic value of the permeated medium as a function of the effective cross-sectional flow area. It is a result of the transmissivity or conductivity, taking into consideration the properties of the liquid passing through (Table 3.4):

$$k = \left(K \cdot \frac{\eta}{\gamma} \right).$$

The unit of permeability is 1 Darcy = 10^{-8}cm².

As has already been pointed out by Lugeon, when

Krsmanovic D, Milic S.: Modell Experiments on Pressure Distribution in some Cases of a Discontinuum. Felsmechanik und Ingenieurgeologie, Supplementum 1, 1964.

Kummerer J., Stäuble H.: Auswertung felsmechanischer Versuche am Beispiel der Vorarbeiten für eine Krafthauskaverne. Felsbau 1990, Heft 4.

Lauffer, H.: Ein Gerät zur Ermittlung der Felsnachgiebigkeit für die Bemessung von Druckstollen- und Druckschachtauskleidungen. Geologie und Bauwesen 1960, H. 2/3.

Lauffer H., Seeber G.: Design and Control of Linings of Pressure Shafts, based on Measurements of the Deformability of the Rock. ICOLD 1961, Q 25, R 91.

Lenhardt W.: Zur Risikobewertung bergbau-induzierter Seismizität. Felsbau 1998/1.

Lenhardt W.: Erdbebenkennwerte zur Berechnung der Talsperren Österreichs. Bericht an das BMfLF, Öst. Staubeckenkommission, 1996, unveröffentlicht.

Lenhardt W. A.: Zur Abschätzung von Erdbebenbelastungen. Felsbau 1996, Heft 5.

Londe P.: Three Dimensional Method of Analysis for Rock Slopes (in french). In: Ann. pônts et chaussées, 1065, No. 1, pp 37 - 60.

Louis C.: Strömungsvorgänge in klüftigen Medien. Universität Karlsruhe, Inst. f. Grundbau und Bodenmechanik, Heft 30, 1967.

Louis C.: Rock Hydraulics. In Rock Mechanics (Ed. Müller L.), pp 299-388; Int. Centre for Mech. Sciences, Udine 1974.

Probabilistics: Int. Conf. on Probabilistics in Geotechnics, Technical and Economic Risk Evaluation; Graz; Ed.: R. Pöttler, Verlag Glückauf GmbH Essen.

Reitmeier W.: Die Lagekugel - ein Hilfsmittel zur Lösung von Aufgaben der Felsmechanik. In "Beiträge zur Felsmechanik", Schriftenreihe des Lehrstuhls für Grundbau, Boden- und Felsmechanik an der TU München, Heft 10, 1982.

Seeber G.: Druckstollen und Druckschächte. Enke Verlag, 1999.

Tremmel E.: Ausweitung des kreiszylindrischen Hohlraumes unter örtlichem Innendruck. Öst. Ingenieurarchiv 1960.

Tremmel E.: Das Verformungsverhalten von Gneis. Mit R. Widmann. ISRM 1970, 2-40.

Wells D.L., Coppersmith K.J.: New Empirical Relationships among Magnitude, Rupture Length, Rupture Width, Rupture Area and Surface Displacement. Bulletin Seismological Society of America, Vol. 84, No. 4, ppa 974 - 1002, August 1994.

4. CONCRETE [102]

4.1 INTRODUCTION

Concrete, known since Greco-Roman times, has had a great influence on the architectural style of the last century, more so than any other construction material. Even though today's expertise in concrete technology makes it possible to design and to produce concrete with specific properties as required, the properties of concrete are still dependent on various external influences. These are specified in the guidelines for concrete testing in order to procure comparable results. In many cases, however, these are not really comparable to the actual influences the structure will be exposed to during its working life. Test evaluation as well is often based on much too simplistic assumptions. A more detailed examination of the guidelines for the determination of concrete properties shows clearly that a distinction must be drawn between actual and apparent influences and, therefore, between test strength and actual strength (Fig. 4.1).

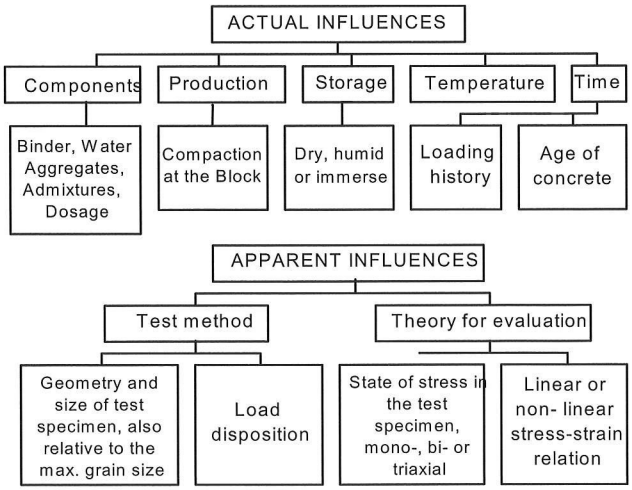

Fig. 4.1: Influences on concrete properties.

These actual and apparent influences on the results of tests carried out to determine the most important concrete properties have been known to experts for a long time (see e.g. from Rüsch 1959 to Geymayer 1985) and shall be summarized below from a statics point of view.

Generally, concrete for large dams is subject to the same technological problems as in all other constructions. However, for dam concrete some assessment criteria are of particular importance, which are almost of no significance for example in evaluating slender or reinforced structures:

– The construction of very massive concrete bodies causes internal stresses that with increasing concrete block size can no longer be ignored.

– Dams are a type of structure that though rarely overloaded actually have to bear the full extent of the design load over long periods.

– The deformation behaviour is important not only in regard to the deformation of the dam body itself - its continuous comparison with the calculation results forms one basis of safety monitoring - but also in regard to the often decisive concrete and rock stresses along the interface with the rock underground. With arch dams, differences in stiffness can cause considerable restraint stresses particularly, if the deformation modulus of the underground equals or exceeds that of the concrete.

All findings in the field of concrete technology, as a basis, must be included in an optimal development of dam concrete. Below, concrete technological aspects such as the mineralogy of aggregates, crushed or naturally rounded aggregates, sieve curve, binders and admixtures etc. shall be dealt with only so far as they are important for test evaluation. In other cases, reference must be made to the extensive expert literature. Therefore, the following observations will focus on those properties of concrete that are essential in assessing concrete dam constructions:

– The crack resistance of green concrete during concrete dam construction.

– The strength and deformation characteristics under service conditions during the lifetime of the concrete dam.

4.2 CRACK RESISTANCE OF GREEN CONCRETE

4.2.1 Introduction

The main problem in the development of mass concrete is the development of a binder that offers an optimal relation of heat and strength development to the available aggregates and the clinker raw material. The required final strength of the concrete is more or less given from the start due to the maximum stresses. The time-dependent development of the concrete strength, however, must still be exam-

dent variation in the deformation and relaxation characteristics implicitly into consideration. The test results show that under slow load increase the fracture strain is almost twice as high as under standard load increase.

In the 1980s a new test method was at last developed that, though requiring a complex test set-up, comes closest to the actual conditions, its sole precondition being the determination of the expected temperature variation in the concrete (Springenschmid 1985). In this test, a concrete beam fastened at both ends is forced to undergo the temperature variation expected in the structure. The beam is poured in the test direction so that measurements can be taken immediately after concrete placing.

Through the force required to stabilize the beam length, the actual thermal stresses in the concrete can be easily determined.

Subsequently, the beam is cooled until failure. In this test, the time and temperature-dependent parameters for the determination of the volumetric changes due to the temperature changes are implicitly taken into consideration as well. Only the temperature variation in the structural concrete must be determined in advance. For this, sufficiently exact methods are available (see section 4.2.4). This test best reflects the actual processes in the concrete block of the dam (Fig. 4.6).

Comparative tests using this method were carried out for binders of varying composition and with the required binder dosages. The test results showed that the temperature and hardening development could be considerably influenced by the choice of binder. Despite the comparatively high temperature increase, binder B had the highest crack resistance, since at the time cracking occurred the concrete

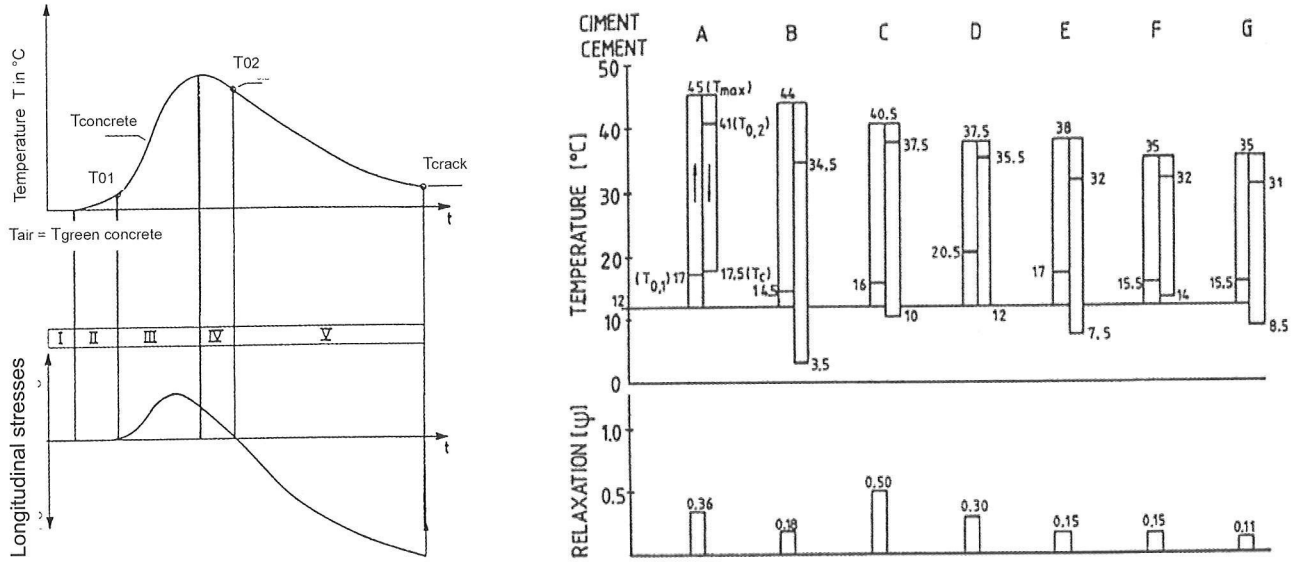

Binder		A	B	C	D	E	F	G
Compressive strength (28 days)	N/mm²	37.3	33.3	39.2	34.3	37.6	30.7	28.7
Tensile strength (28 days)	N/mm²	2.6	2.2	2.5	1.9	2.2	2.0	2.0
Adiabatic heat development	kJ/kg C	3,72	3,42	3,21	2,93	2,88	2,66	2,65
Temperature increase in concrete T_{max}	in °C	33	32	28.5	25	26	23	23
Zero stress temperature T_{02}		29	22	25.5	23	20	20	19
Crack temperature T_c		+5.5	-8.5	-2	0	-4.5	+2	-3.5
Relaxation (ψ)		0.36	0.18	0.50	0.30	0.15	0.15	0.11

State II ... Stress-free heating
III .. Pressure build-up due to heating
IV . Pressure drop due to cooling
V ... Tensile stresses due to cooling

Fig. 4.6: Test results for various binders (Springenschmid 1985).

temperature was at its lowest, while the binder with the lowest hydration heat did not have the highest crack resistance due to the slow hardening process Using the above-mentioned method, it is also possible to evaluate the stress relaxation and thus the residual stresses still present at impoundage begin. Cooling of the test specimen is stopped shortly before the crack temperature is reached. This temperature is then maintained and the stress decrease observed until an approximately stable condition is achieved. Subsequently, the residual stress σ_r can be deduced and should be taken into consideration in the evaluation of the tensile stresses during the lifetime of the concrete dam.

4.2.3. Thermal stress development in green concrete

The various influences on temperature and stress development in green concrete (Fig. 4.7) are largely dependent on the factor of time, while the strength and the deformation modulus are also dependent on the concrete temperature during hardening. Only the thermal diffusivity and thermal expansion may be assumed to be constant.

Each calculation of thermal stresses comprises two steps:

- Calculation of the development in the thermal stress field as against a 'zero' stress-temperature field.
- Calculation of the restraint stresses generated due to the restraint of the temperature-dependent volumetric changes.

The theoretical assessment of the crack resistance or of the distance from the fracture strain must be based on the factors listed below:

- Mean and extreme daily load graphs of the air temperature during construction.
- Time-dependent changes in the binder's heat development to determine the time-dependent concrete temperature.
- Temperature of the concrete during pouring.
- Time-dependent changes in the deformation and strength characteristics taking slow deformations into account as well.
- The parameters of cooling, if required, such as arrangement of the cooling pipes, temperature and flow rate of the cooling water.

For analytical calculations, a computer programme was developed using the method of finite differences [*40*]. It comprises two steps:

- Determination of the temperature field in the concrete as a function of time.
- Calculation of the stresses corresponding to these temperature fields.

The development of the temperature field in the concrete is defined on the basis of the equation for thermal conduction by:

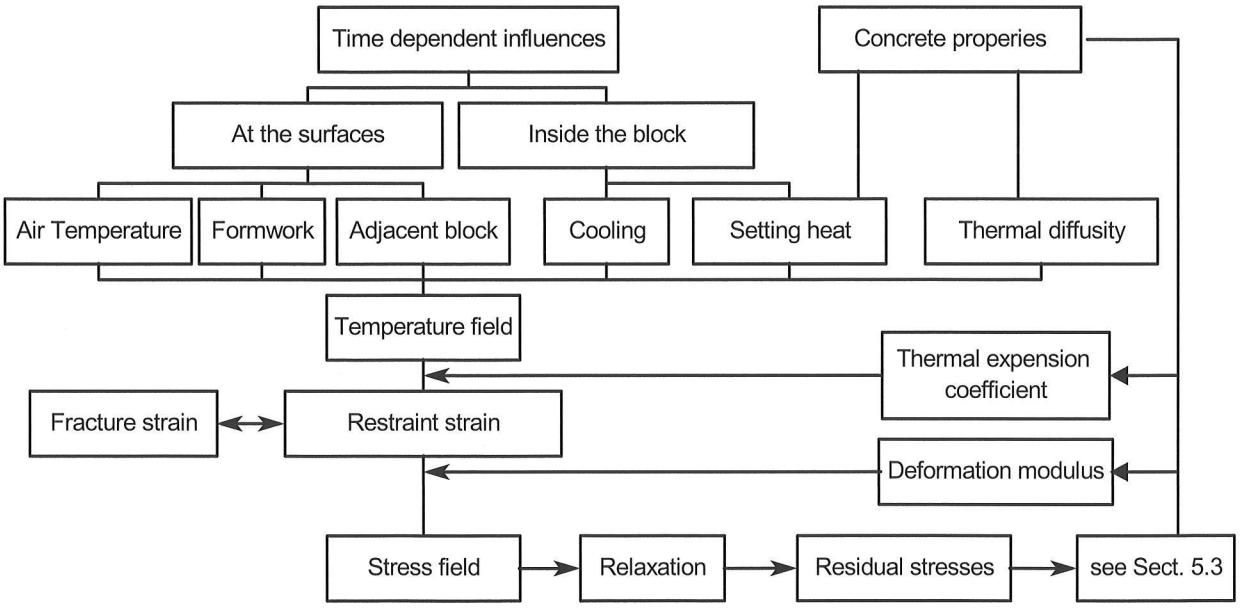

Fig. 4.7: Calculation of the thermal expansions and stresses in green concrete [*40*].

$$a \cdot \Delta\Theta_t - \frac{\partial\Theta}{\partial t} + W_{n,t} = 0 \quad \text{with } a = \frac{\lambda_B}{c \cdot \gamma}$$

where:

a ... thermal diffusivity of the concrete in m²/h
λ_B ..... thermal conductivity of the concrete
c ..... specific heat of the concrete
γ ..... density of the concrete
Θ ..... temperature field at time t
t ..... time variable in hours
$W_{n,t}$. heat development or cooling in point n at time t

The locus-dependent temperature field at time t (Fig. 4.6):

$$\Delta\Theta_t = \left(\frac{\partial^2\Theta_t}{\partial x^2} + \frac{\partial^2\Theta_t}{\partial y^2} + \frac{\partial^2\Theta_t}{\partial z^2} \right)_{n,t}$$

can be easily converted for the method of finite differences, e.g.:

$$\frac{\partial^2\Theta_t}{\partial x^2} = \frac{1}{\Delta x^2}\left(T_{x-\Delta x,y,z,t} - 2T_{x,y,z,t} + T_{x+\Delta x,y,z,t}\right).$$

To improve the convergence of the method, the time-dependent temperature variation T in point n at time t + Δt is extrapolated from the temperatures T, T - ΔT and T - 2Δt using a regression parabola (Fig. 4.8).

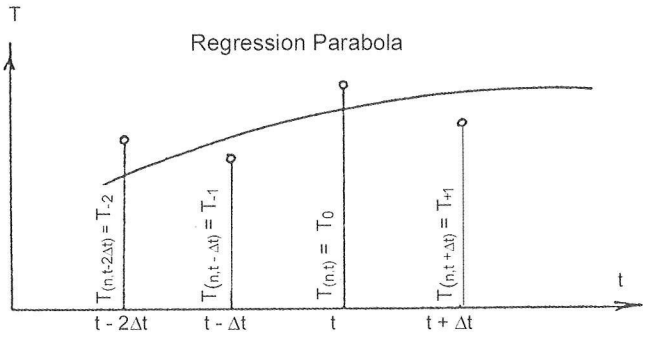

Parabola $T_{n,t+\Delta t} = b_0 + b_1 \cdot (\alpha\Delta t) + b_2 \cdot (\alpha^2\Delta t^2)$

Tangent $T' = b_1 + 2b_2 \cdot (\alpha\Delta t) = \frac{\partial\Theta_t}{\partial t}$

Fig. 4.8: Assumption of the temperature development.

An adjustment analysis supplies the coefficients b_i; following several conversions, the difference equation of the thermal conductivity for temperature T in point n at time t + Δt is defined by:

$$T_{n,t+\Delta t} =$$

$$-\frac{20\Delta t}{11}\left(a.\Delta\Theta_t + W_{t,n}\right) + \frac{1}{11}\left(T_{n,t-2\Delta t} + 7T_{n,t-\Delta t} + 3T_{n,t}\right)$$

The boundary conditions at the surface (air temperature, formwork) can be fulfilled e.g. by assuming a fictive external point with the corresponding air temperature and a heat-transfer coefficient. Thereby, for example, the presence of formwork with or without insulation can be taken into consideration by putting the corresponding heat-transfer coefficient into the formula (Mandry 1961).

This extremely adaptable method for the calculation of two and three-dimensional temperature fields makes it possible to determine the time-dependent variation of the concrete temperatures at any point in the calculation model, taking into consideration:

- The sequence of pouring in the given block and adjacent blocks.
- The date of form stripping.
- The turning on and off of the cooling system, etc.

In the next step, in which the stress fields corresponding to these temperature fields are calculated, these points define a net of finite elements, either in relevant two-dimensional sections or three-dimensional systems. Therefore, the results of the temperature field calculations at a specific time can be directly applied to the stress calculations.

These calculations must be repeated for several points in time, taking the time-dependency of the deformation modulus into consideration. Starting with the initial stress-free state at time t = 0, the stresses (n,t at time t in point n) are given by:

$$\sigma_{n,t} = k_t \cdot \sigma_{n,t-1} + \Delta\sigma_{n,t}$$

where:

$\sigma_{n,t}$ stress in point n at time t
k_t correction factor considering the reduced stress due to creep
$\sigma_{n,t-1}$ during period Δt
$\Delta\sigma_{n,t}$ ... stress increase in point n during period Δt = t-(t-1)

The resulting stress field indicates the points with the highest tensile stresses that can then be charted over time. Comparison with the tensile strength at the same point in time gives the time-dependent variation in the crack resistance:

$$S_t = \frac{\beta_{n,t}}{\sigma_{n,t}}$$

and thus, ultimately, also the lowest crack resistance. Using this method, it is possible to analytically compare the effects of the properties of various binders and the efficacy of constructional measures.

4.2.4 Cracks inside the concrete block

Cracks inside dam bodies can develop in hardened concrete primarily in the region near the dam base, where, due to cooling after attaining the highest concrete temperatures at the dam base, the volumetric changes of the concrete (α_t . ΔT) are restrained most. Since the measured volumetric change due to temperature variation (ε') proceeds stress-free, the fracture state is defined by:

$$\alpha_t \cdot \Delta T - \varepsilon' = \varepsilon'' < \varepsilon_{kr}$$

where ε' . measured strain
ε'' confined strain
ε_{kr} fracture strain
α_t thermal expansion coefficient
ΔT temperature difference

The relation of the deformation moduli of concrete and rock has only little influence on the restraint of deformations due to temperature variations [*67*].
Furthermore, the restraints on the deformations induced by temperature changes, at a distance from the dam base corresponding approximately to half the block width, have largely subsided (Townsend 1965).
Recently attempts have also been made to calculate the potential crack behaviour of cracks perpendicular to the construction joint using fracture-mechanical methods (Linsbauer 1988).

4.3 INFLUENCES ON CONCRETE PROPERTIES

To ensure that test results are comparable, the guidelines of most countries contain specific requirements, listed in Fig. 4.1, for testing the mechanical properties of concrete.

4.3.1 Actual influences

The composition of concrete will not be discussed in this paper, reference should be made to the extensive literature existing in this field.
In regard to the production of concrete it shall only be pointed out that:
– The pouring direction of the test specimens influences the test results and should be so chosen as to ensure that the most unfavourable parameters result. The compressive strength under a load in the pouring direction, e.g. for the load case dead load, is on the average 10% higher than transverse to the pouring direction, as for example in arch stresses.
– The compaction at the block must achieve the same quality as that of the test specimen. To increase the strength, therefore, the water-cement ratio can only be reduced to a limited extent.
Until testing, the storage conditions for the test specimen must be so determined as to ensure the lowest test strength (Bonzel 1963, Kaltenböck 1976); current standards often specify conditions that result in the highest strength. A test specimen stored in humid conditions can have a 20% lower compressive strength, but a 20% higher tensile strength than a test specimen stored in dry conditions.
In construction and bridge engineering, the test specimen age is generally 28 days due to the form stripping dates. In dam construction, the hardening process is considerably slower due to the lower temperature of the binder. In addition, higher loads are applied at a considerably later date. It is therefore justified to set a test specimen age of 180 days and sometimes even of 365 days. However, in doing so the hidden reserves due to post-hardening may involuntarily be abandoned.
The loading rate and period are generally specified in the test standards. They have a decisive influence on the test strength (Fig. 4.9). However, this influence of time is mostly ignored. As concrete dams are subjected to cyclic long-term loading, normal load cases should be based at least on the fatigue strength. For the special load case of earthquakes the short-term strength can be used.

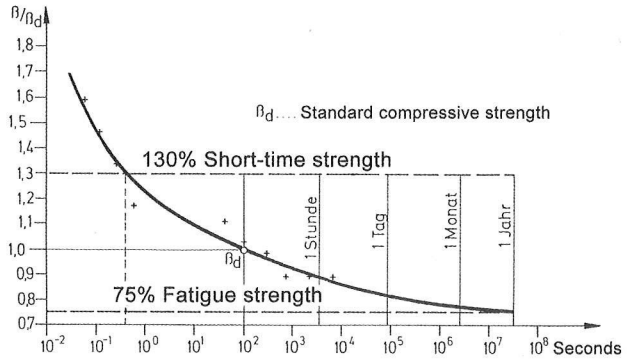

Fig. 4.9: Compressive strength as a function of the load period [33].

The temperatures during setting should of course not be below 5°C, since lower temperatures result in correspondingly longer hardening periods.

4.3.2 Apparent influences

Apparent influences are, in particular, the effects of a simplified evaluation of the test results. Today, these can no longer be justified.

The compressive strength β_C is the only strength in which the fracture stress is not calculated for the fracture areas. The geometry and size of the test specimen (Fig. 4.10) as well as the type of loading (with or without friction, Fig. 4.11) considerably influence the stress distribution and thus the location of the fracture areas.

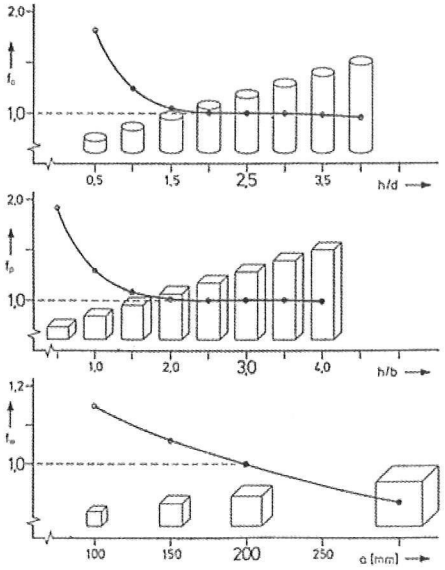

Fig. 4. 10: Shape factors for the compressive strength of concrete (Schickert 1981).

The fracture stress is always calculated using the same formula:

$$\sigma_c = \frac{P}{A}.$$

However, this value is only relative to the stress in the fracture area.

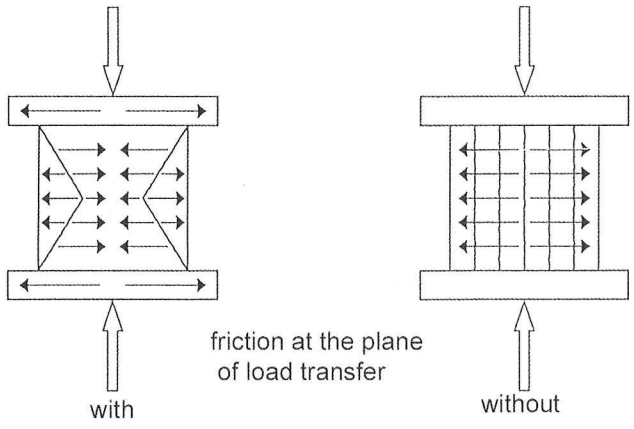

Fig. 4.11: Fracture patterns in compression tests.

Recent examinations have shown that the dependency of results on test specimen size, the so-called scale effect, can be explained by the fractal dimension of the fracture areas which in turn is dependent on the related grain size of the aggregates (Carpentieri 1993). Whether or not these relations apply only to the range of the possible test specimen sizes or also to the extrapolated REV and/or structural dimensions still needs to be examined.

According to Griffith (1920), initially local tensile stress peaks occur at the aggregate grains transverse to the load direction causing microcracks parallel to the compressive stress direction. As the load increases, the tensile stresses increase as well while the microcracks lengthen until to the point of continuous failure. In compression tests as well, failure occurs when the tensile strength β_t is exceeded due to – initially local – transverse tensile stresses. The measured transverse strain, therefore, comprises the sum of these crack widths plus the lateral strain. More recent considerations infer from the fracture patterns in compressive strength tests that with inhomogeneous, brittle materials such as concrete the compressive strength represents only an 'apparent' property dependent on the simultaneous tensile stress (Stavrogyn 1995).

If the local tensile stress peaks are substituted by an equivalent tensile stress $\overline{\sigma_t}$ along the entire fracture plane in proportion to the simultaneous compressive stress σ_c:

$$\overline{\sigma_t} = \sigma_c \cdot \frac{\beta_t}{\beta_c},$$

it must be added to the lower principal stress σ_{II}^{o} in the case of biaxial stresses, thus taking the 'internal' tensile stresses $\overline{\sigma_t}$ into consideration as well:

$$\sigma_{II} = \sigma_{II}^{o} - \sigma_I \cdot \frac{\beta_t}{\beta_c}.$$

Due to the low absolute distance from the tensile strength, it must be compared to principal tensile stress comprising all secondary stresses that are usually ignored.

The tensile strength β_t as well is determined using various types of tests leading, of course, to varying test results (Fig. 4.12).

Evaluation of the tests to determine the tensile bending strength β_{bt} is based on the Navier theory for slender beams while the beam is actually compact

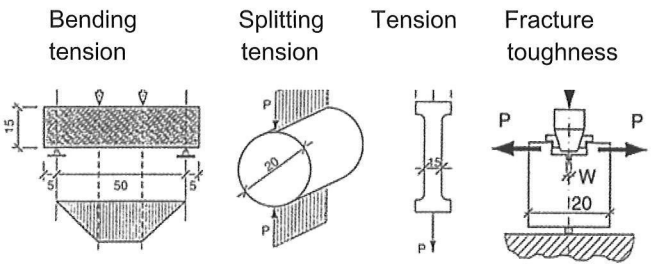

Fig. 4.12: Load set-up in various tests for the determination of the tensile strength.

and should at least be determined according to the slab theory [*17*], presuming a non-linear stress-strain relation (Gebauer 1956). According to the slab theory, the splitting tensile strength β_{st} is based on a biaxial stress state. The fracture starts from inside the test specimen; dependency on the geometry and size of the test specimen is low.

The difference between splitting tensile strength and tensile strength is probably due to the relatively rapid drying process from the surface to the inside during open-air storage. This drying results in a thin zone with surface microcracks, that cannot take part in the transfer of tensile stresses. For a tensile bar with a diameter of 100 mm, a dry boundary zone with a depth of only 5 mm suffices to explain the difference. Comparative tests on test specimens stored in humid conditions until testing have, therefore, produced similar results in tensile and splitting tensile tests (Raphael 1984).

In literature, the relation of the results of the various test methods to determine the tensile strength is defined with a certain variation range, that is also dependent on the aggregate and its grain shape, by:

$$\beta_t : \beta_{st} : \beta_{bt} = 1 : 1.2 : 2$$

The fracture toughness β_{ft} as well is a measure of the tensile strength. It is the only parameter that is correctly determined using an evaluation method based on the same theory as the fracture-mechanical calculation methods. A theoretically correct comparison of strength to stress is, therefore, possible.

4.4 THE USABLE STRENGTH OF CONCRETE

4.4.1 General

Deduction of the usable concrete strength from the concrete test results should comprise three steps:

- Using statistic methods, the value that with sufficient probability will not fall below the maximum stress in the structure must be determined based on the individual test results taking the variance during production and testing into consideration.
- Using a correction factor that takes the expected conditions in the structure into consideration, if these deviate from the conditions and assumptions during the performance and evaluation of the tests; following these two steps the decisive strength is determined.
- Using a safety factor which defines the difference between the maximum stress in the structure and the decisive strength.

In addition, the reduced tensile strength in the horizontal construction joints, particularly in the annual joints, must be considered since this reduction cannot be entirely avoided even with very careful handling.

4.4.2 Statistic methods

The use of statistic methods not only requires a sufficient number of individual values determined under comparable conditions, but also that the deviations from the mean values must always be random and therefore subject to "normal distribution". In general, the Gaussian distribution is used. This presumes a symmetric deviation from the mean value, but also the theoretical possibility of negative strength values. Theoretically correct, therefore, would be the use of the logarithmic normal distribution. The differences between these two methods are slight and certainly not decisive.

Using these methods, the most important statistic parameters for checking the constant quality of concrete during production can be determined:

- The mean value and the variance s of the test results.
- The variation coefficient as the ratio of test variance to mean value.
- The fractal, the parameter that will not be attained with a probability of w %.

When determining a correction factor to indicate the relation of test strength to actual strength, the varying conditions during testing and in the structure must be taken into consideration. However, it must also be considered that the calculation methods based on the FEM are no longer based on the bar

of 1 year each. The load was applied in three load steps of 2.5 N/mm² each. At each step the load was held constant for approximately 2 months. The maximum stress of 7.5 N/mm² corresponded approximately to the highest stress in the arch dam.

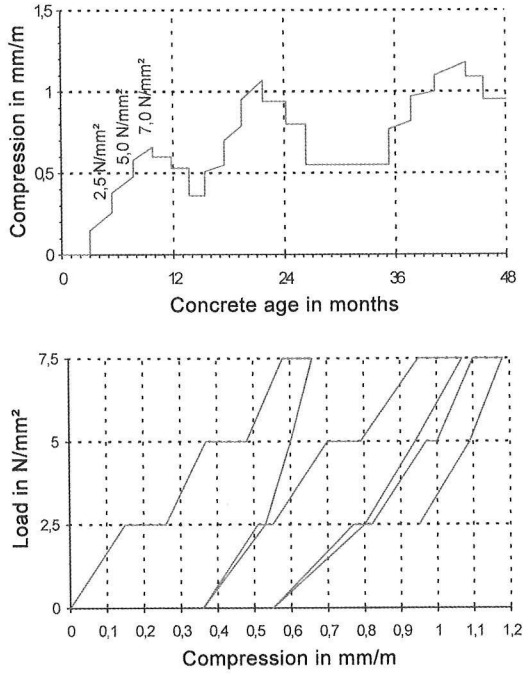

Fig. 4.15: Deformations in three load cycles.

Another group of concrete prisms was subjected to one load cycle each, at the test ages of 0.5, 1 and 3.5 years (Fig. 4.16).

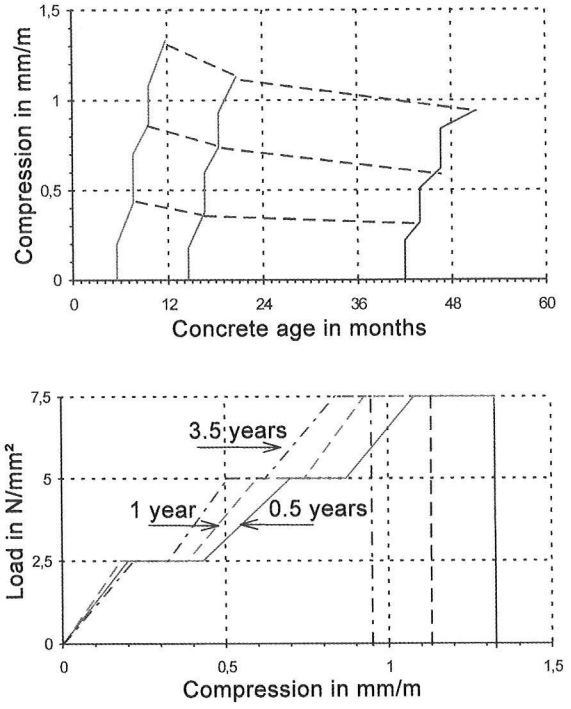

Fig. 4.16: Deformations in 1-year load cycles and with varying test ages upon load begin.

All test results show uniform tendencies:

– The creep deformations increase the deformations under short-term load by up to 100 %.

– The residual deformations reach approx. 60 % of the deformations under short-term load.

d) Long-term bending tensile test

In the third points of a concrete beam, measuring 30/30/165 cm, the load was increased in 12 load steps of one week each, and at each step by a load corresponding to a flexural stress of 0.175 N/mm² up to a maximum flexural stress of 2.1 N/mm². The measured strain on the underside of the beam reached $1.6 \cdot 10^{-6}$ at the final load step, corresponding to a long-term flexural deformation modulus from the bending tensile test of approximately 13 kN/mm² (Fig. 4.17).

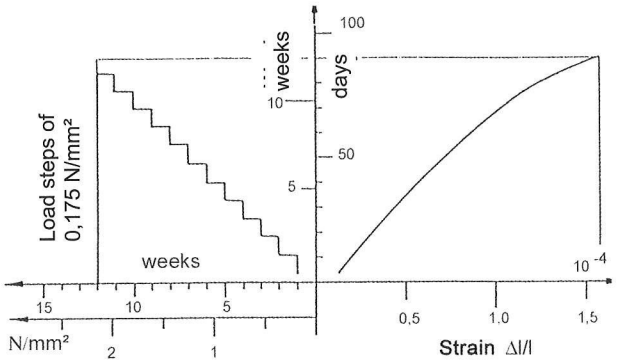

Fig. 4.17: Long-term bending tensile test.

e) Stress relaxation of green concrete

To determine the stress relaxation for the thermal stresses during concrete setting, a relaxation test was carried out. Within 21 days a compressive stress of 3 N/mm² was applied. The stresses were measured for 2 months under constant strain (Fig. 4.18). The results showed that approx. 20 % of the initial stress remains in the concrete.

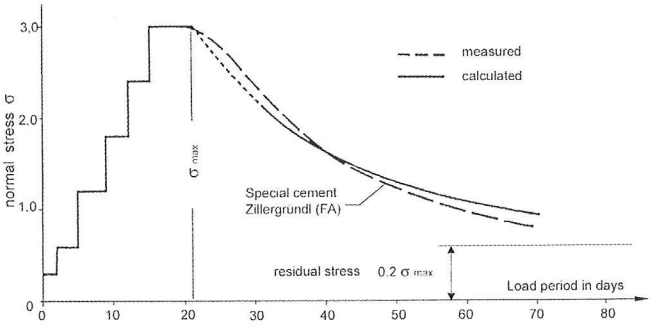

Fig. 4.18: Stress relaxation of the core concrete of the Zillergründl arch dam.

The dependency of the deformation behaviour on concrete age and load period has been known for a

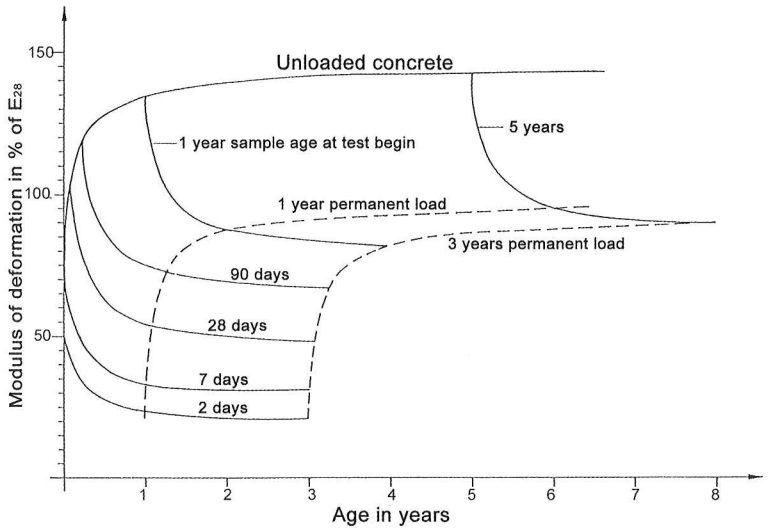

Fig. 4.19: Deformation modulus of concrete as a function of concrete age, load begin and load period (ACI 1976).

long time but is not sufficiently taken into consideration (Fig. 4.19).

4.6 DURABILITY OF CONCRETE

Chemical influences that could affect the properties of concrete, such as alkaline expansion, are purely concrete-technological concerns and shall not be dealt with in this paper. It shall only be recommended that the compatibility of all concrete components be examined.

With dam concrete, the water tightness and frost resistance are of especial importance, particularly at the concrete surface. Therefore, face concrete with a higher binder dosage is often used at the surfaces and core concrete with a lower binder dosage inside the dam.

4.6.1 Water tightness

Like all other concrete properties, the water tightness must be determined according to specific guidelines. Unlike the test results of other concrete properties, the test results of various water tightness tests can be compared, namely by determining the coefficient of hydraulic conductivity according to Darcy for the flow in porous media, since these no doubt ensure the required laminar flow.

The test pressure should be 1.5 times the maximum storage level. The depth of penetration after a test period of 14 days should not exceed 10% of the thickness of the face concrete. Based on this, it is possible to theoretically determine the period after which the water will have leaked through the entire thickness of the dam wall. This value, however, is more a theoretical comparative value, since the increasing leakage is counteracted by other influences, e.g. the pressure drop due to the increasing flow path and drying from the downstream face.

4.6.2 Frost resistance

The frost resistance of concrete is of special interest particularly for concrete dams in cold regions as for example in the Alps. Tests to determine the frost resistance are based on the assumption that water enters the concrete pores and that the volume increase of the pore water after having passed from the liquid to the solid state causes strains and thus tensile stresses in the concrete. If the fracture strain or the tensile strength is exceeded, microcracks will form and the modulus of elasticity will decrease. Finally, this can destroy the concrete. It thus follows that concrete has higher frost resistance, if:

- Less water can penetrate the concrete.
- The (constant) volume increase after the pore water has passed from the liquid to the solid state causes lower tensile stresses under the same specific strains due to a higher deformability of the concrete, i.e. a lower deformation modulus.

In the test, the variation of the modulus of elasticity is determined after repeated alternation between immersed storage at room temperature and dry storage in the cooler.

This test method shows that the frost resistance is dependent basically on two other concrete properties, namely water tightness and deformation behaviour.

Immersed storage alone is certainly sufficient for testing the concrete of the downstream dam face, since there the conditions correspond to those of

as compared to former conditions. This seems to be rather unconsciously accepted.

From the viewpoint of the structural engineer, the concrete testing requirements must include:

- Determination of the storage conditions ensuring the lowest strengths.
- Evaluation of the strength values according to similarly highly developed calculation methods based on the same theoretical assumptions as those commonly used in static methods. Different test methods to determine the same properties must lead to the same results.
- In uniaxial compressive strength tests, the standard compressive stress does not refer to the fracture area. Although it is proportional to the actual fracture stress, if the test specimens have the same geometry, this relation can vary with other test specimen geometries, particularly under multiaxial stresses.
- In regard to the deformation behaviour a distinction must be drawn between the deformation modulus under first loading and the modulus of elasticity. This difference may be of fundamental importance at the dam base and for the evaluation of the measurements upon first filling the reservoir.
- The effects of a permanent load corresponding to the design load on the strength and deformation behaviour must be clarified and taken into consideration when determining the effective strength.

REFERENCES

ACI Committee 207, Mass Concrete for Dams and other massive Structures. ACI Journal, April 1970

ACI : Manual of Concrete Practice 1976.

Bombich A.A. et al.: Concrete Temperature Control Studies. Tennessee-Tompgee Waterway Projects. J.E. McDonald, Vicksburg.

Bonzel J.: Über die Biegezugfestigkeit des Betons. Düsseldorf. Betontechnische Berichte 1963.

Carpintieri A.: Fractal nature of material microstructure and size effects on apparent mechanical properties. Journal Mechanics and Materials, 1993.

Catharin P.: Die Hydratationswärme des Zementes und ihre Bedeutung. Zement und Beton 1971, H. 58/59

Dahms J.: Normalzuschlag. Zement-Taschenbuch 1984, Bauverlag Wiesbaden.

Dungar R.: A viscoplastic bounding surface model for concrete under compressive and tensile conditions and its application to arch dam analysis. 2nd Int. Conf. on Constitute Laws for Engineering Materials. Tuscon, Arizona, Jan. 1987.

Eidel'man S. et al: Cracks in Blocks of the Bratsk hydroelectric station dam. Investiia Vsesoiuznogo Nauchno-Issledovatel'skogo Instituta Gidrotekhniki, imeni B.E. Bedeneva, Vol. 79, 1965.

Gebauer F.: Über die Biegezugfestigkeit des Betons und ihre Mitwirkung im Stahlbetonbalken. Bauplanung und Bautechnik, Wien, 11.Jg, 1957, Heft 7.

Geymayer H.: Zur Problematik des Druckversuches. Sicherheit und Verläßlichkeit von Betonbaustoffen. TVFA TU Graz, Tätigkeitsbericht 1986/87.

Hatano T. et al.: Aseismic design criteria for arch dams in Japan. COLD 1967, Q 35, R 1.

Huber H.: Der Einfluss von gebrochenen Gneiszuschlagstoffen auf den Beton der Zemmkraftwerke. Dissertation, Universität Innsbruck.

Huber H.: Kölnbreinsperre - Neue Wege in der Technik des Massenbetons. Beton und Stahlbeton 1979, Heft 5.

Huber H.: Unveröffentlichte interne Berichte der Materialprüfanstalt Straß.

Kaltenböck H.: Einfluss der Nachbehandlung von Würfelproben auf die Druckfestigkeit des Betons. Zement und Beton, 21. Jg., Heft 1 (1976).

Linsbauer H.: Abkühlungsprozess in Massenbeton - Einfluss von externen Zwangsbedingungen auf Rissbildung und Rissverhalten. 5. Int. Seminar Wasserkraftanlagen; TU Wien 1988.

Mandry W.: Über das Kühlen von Beton. Springer Verlag 1961

Newmark N.M., Rosenblueth E.: Fundamentals of earthquake engineering. Practice-Hall, N.J. 1971

Raphael J.M.: Tensile strength of Concrete. ACI-Journal March/April 1984, Title Nr. 81-17.

Rüsch H.: Physikalische Fragen der Betonprüfung. Zement-Kalk-Gips, 1/1959.

Schickert G.: Formfaktoren der Betondruckfestigkeit. Berlin, Die Bautechnik 2/1981.

Springenschmid R.et al.: Thermal stresses in mass concrete. ICOLD 1985, Q 57: Vol.II, pp 57-52.

Stavrogyn A.N.: Statistical theory of strength, deformation and failure of rocks. 2. Int. Conf. on Mechanics of jointed and faulted Rock, A.A. Balkema 1995, sowie persönliche Mitteilung.

Stucky A., Derron M.: Problemes thermiques posés par la construction des barrages-réservoires, Sciences & Technique, Lausanne 1957.

Townsend C.L.: USBR Practices for control of cracking in arch dams. Journ. of the Power Division, Proc. Amer. Soc. Civ. Eng. 85 (1959), S. 129 - 135.

Townsend C.L.: Control of cracking in mass concrete. Engineering Monograph Nr. 34, 1965.

Wesche K.: Baustoffe - Beton 1985

Wicke M.: Versuchsbericht des Inst. für Stahlbeton- und Massivbau, Universität Innsbruck, 1974 (nicht veröffentlicht).

5. ARCH DAM DESIGN

5.1 INTRODUCTION

To opt for the construction of an arch dam, the following requirements must be met:

– Due to the concentrated and therefore higher loads acting on the abutment area than in the case of embankment dams, the dam must rest on very stable rock.

– To ensure the economically efficient production of concrete of adequate and uniform quality, suitable aggregates must be available in sufficient quantity in the immediate vicinity of the dam site.

– For cement meeting the requirements, the transport distance to the construction site must be within economically acceptable limits.

– The crest length should not exceed seven times, better yet five times the dam height. This geometrical limit is required for static reasons, since the bearing capacity of the arches decreases with increasing length relative to the dam height and the required vertical cross sections approximate those of gravity dams. In such a case, however, the higher construction expenses are no longer offset by the concrete cubature saved.

5.2 FIRST ESTIMATION OF THE MAIN DIMENSIONS

Design engineers of arch dams have always been interested in at least approximately estimating the prospective dam volume and abutment thickness maximally required in the centre section prior to the actual design. Therefore, formulas for the estimation of the dam volume V, the thickness of the crest arch d_c in the arch crown, the base thickness d_B and the thickness $d_{0.45H}$ in the centre section as a function of valley form were already developed early on (Fig. 5.1):

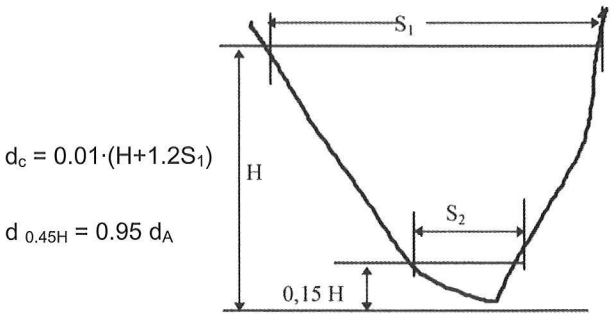

$$d_A = \sqrt[3]{0{,}0012 H . L_1 . S_2 \cdot \left(\frac{H}{133}\right)^{\frac{H}{133}}}$$

$$V = 0{,}000\,002\ H\ .\ S_2 \left[\frac{(H+0{,}8S_1)^2}{S_1+S_2}\right] + 0{,}0004 H S_1 (H+1{,}1\,S_1)$$

Fig. 5.1: Estimation of the main data of an arch dam (USBR 1938).

The geometrical parameters of several arch dams are listed in annex A-1. A comparison of the theoretical values V_{USBR} to the actual values V_{act} (Fig. 5.2) shows, however, a comparatively large variation.

Another assumption is based on the water load acting on the valley cross section at the dam site above the foundation surface. In this case, the variation is quite a bit lower, apart from a few exceptions (Fig. 5.3). Grengg (1961) described the relation water pressure : dam volume as an 'economical design success'.

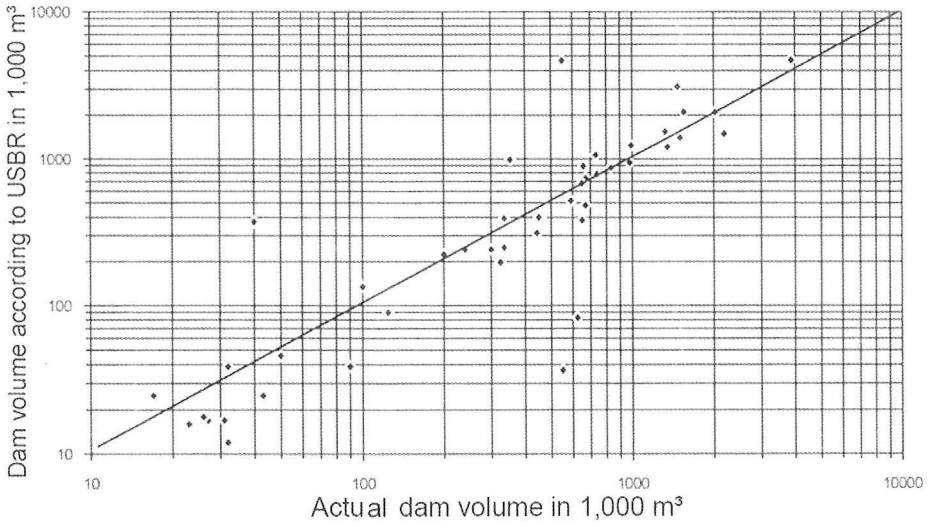

Fig. 5.2: Comparison of the theoretical volume V_{USBR} to the actual volume V_{act}.

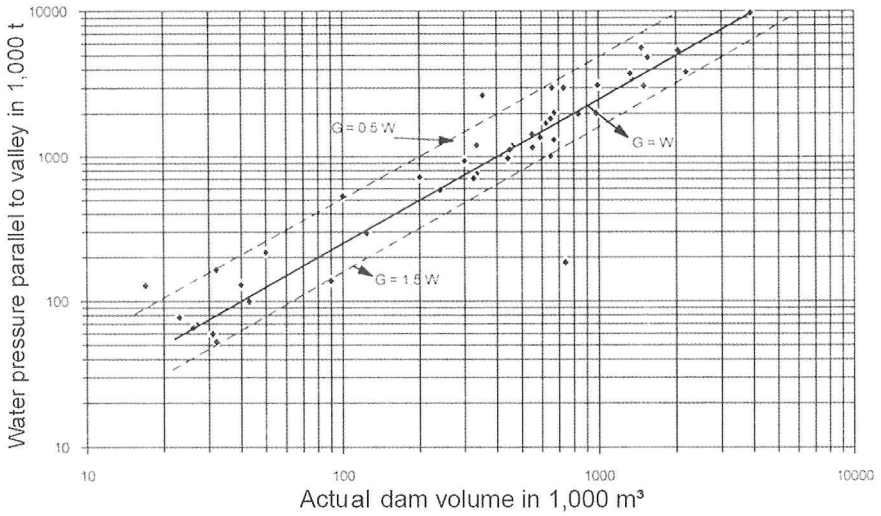

Fig. 5.3: Comparison of the water pressure W parallel to the valley to the actual volume V_{act} of various arch dams.

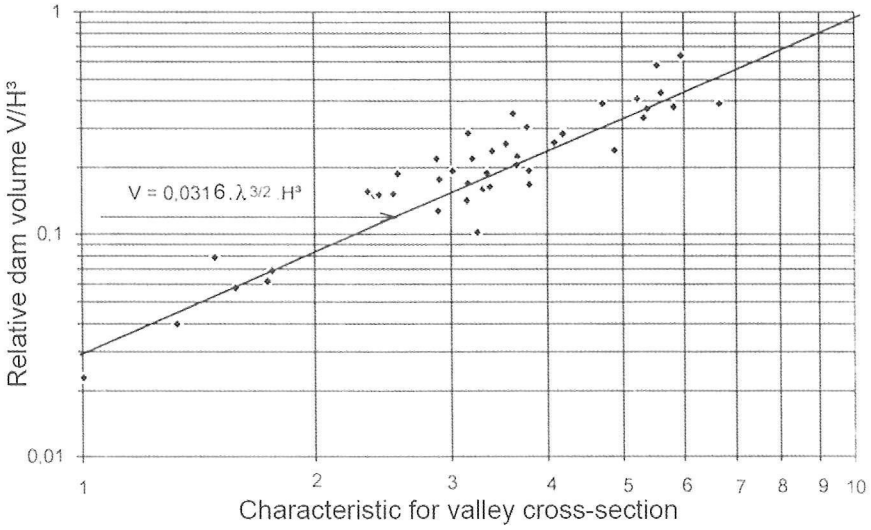

Fig. 5.4: Relative dam volume as a function of the valley characteristic.

The results can be somewhat improved upon, if for the estimation of the dam volume a characteristic λ_D is introduced for the valley cross section based on a proposal of the USBR (definitions see Fig. 5.1). Particularly the volume of arch dams can be better

$$\lambda_D = \sqrt{\frac{S_1 + S_2}{0{,}15H^2}}$$

estimated on the basis of this relation (Fig. 5.4). The base thickness in the centre section, however, varies widely (Fig. 5.5).

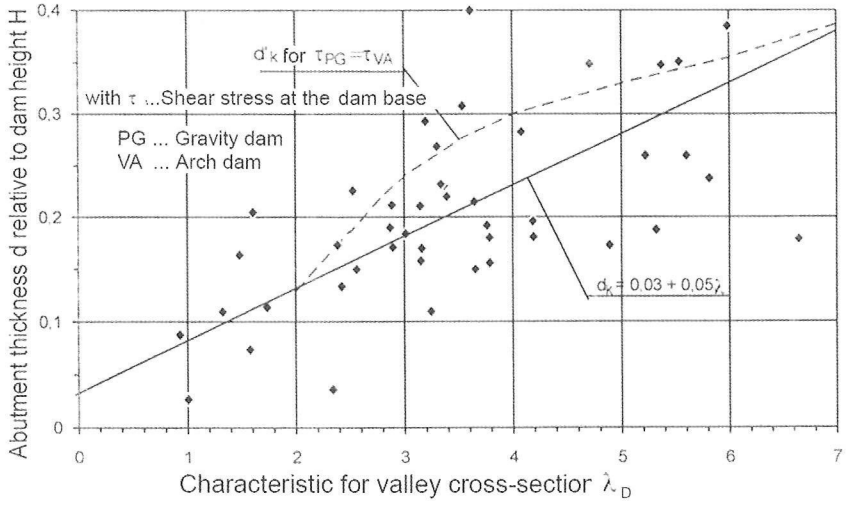

a) empirical mean based on empirical values (see A1),
b) static with given shear stress (see Fig. 5.34).

Fig. 5.5: Estimation of the abutment thickness in the centre section.

The 'slenderness coefficient' C (Fig. 5.6) does not sufficiently take the cross section of the valley shape into consideration:

$$C = \frac{(\text{upstream dam surface})^2}{\text{concrete volume x dam height}} = \frac{A^2}{V \cdot H}$$

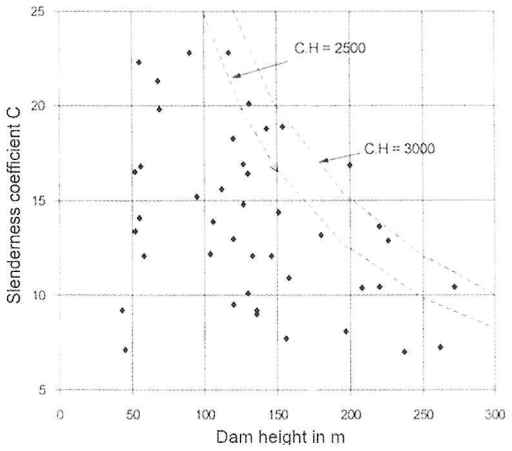

Fig. 5.6: 'Slenderness coefficient' (Kaech 1953).

A closer examination of this formula reveals that with:

$\frac{A}{V} = \frac{1}{d_m}$ where d_m = mean dam thickness

$\frac{A}{H} = b_m$ where b_m = mean valley width

$C = \frac{b_m}{d_m}$ results.

In this formula above all the dam height is no longer taken into consideration. Therefore, a 1 km long gravity dam with a height of 30 m would have a higher 'slenderness coefficient' than a slender 200 m high arch dam with a crest length of 300 m. This can be of importance, for example, for the evaluation of arch gravity dams.

Fig. 5.6 shows that the slenderness of arch dams can be better evaluated on the basis of C' = C·H should remain below 2,500, since arch dams with a higher slenderness seem to have an above-average susceptibility to damage. On the basis of this condition, the minimum volume

$V \geq \frac{F^2}{2{,}500}$ can be estimated as well.

5.3 STATIC ANALYSIS OF THE DAM BODY

5.3.1 A short summary of the history of calculation methods (according to Schnitter 1976)

While the fundamental assumptions of the scientific design for the considerably older embankment dam construction was not made possible until the developments of Terzaghi, Casagrande and others in the 1920s, the theoretical foundation for the calculation of gravity dams were developed at a considerably earlier date. Based on the linear elasticity theory of Navier, Sazilly demanded in 1853 that not only the sliding stability be observed, as done previously, but also that specific allowable stresses in the dam body must not be exceeded as well. Requirements that were complemented in 1881 by Rankine's insistence on the avoidance of tensile stresses and finally by Lévy in 1895 who also demanded that the uplift pressure be taken into consideration.

An arch dam can be considered a doubly curved thick shell of variable thickness and curvature, and variable compliance along the circumference of its foundation. Comprehensive realistic solutions for the entire structure are only possible in certain cases. All methods developed up to now that have been put to actual use are based on the division of the shell structure into individual elements that are more easily calculated (Fig. 5.7).

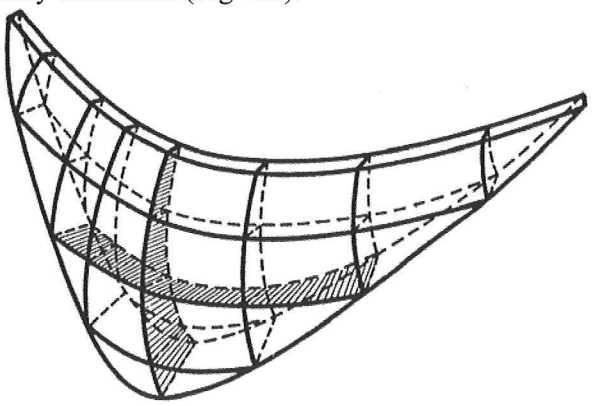

Fig. 5.7: Imaginary division of the shell structure.

A short summary of the development of calculation methods for arch dams is outlined below. (Schnitter1876):

- Based on beam analyses:
  - Single circular arches using the heel formula (Navier 1826) for the 43 m high Zola cylindrical arch dam (1854) and the Salmon Creek constant angle arch dam (1914) according to L. Jorgenson.
  - Arch – cantilever method according to Woodgard (1904) as a basis for the load distribution method by H. Ritter (1913), with adjustment of the radial displacements of the arches and one cantilever beam in the centre section.

- Variable curvature arches according to E. Gruner for the 55 m high Montsalvens arch dam in 1920.
- Arch calculation initially with elastic restraint by fictively lowering into the bearing area (Vogt 1925), then using spring constants (USBR 1938, Mladyenovitch 1966). The deformation moduli of the rock underground along the dam base between rock and concrete vary and can also be assumed to be different for varying directions.
- Trial Load Method (TLM, USBR 1938) with unit triangular loads for 3 (of 6) independent deformation directions.
- Algebraic Load Method (Jurecka 1949, Tonini 1964), subsequently referred to as LDM (Load Distribution Method).
- Consideration of all 6 deformation components (e.g. Serafim 1974).
- On the basis of the theory of shells, the Finite Element Method (FEM) was developed in the middle of the 20th century, based on the theory of thin or thick shells, lastly including also variable thickness and curvature.

COMPARISON OF THE TWO METHODS

LOAD DISTRIBUTION METHOD

In the crossing points of both lamella systems:

- The normal and shear stresses are continuous.
- The bending lines and therefore also the tangents at the bending lines in the crossing points are continuous.
- The interactions of the loads acting on the underground along the dam body are given; in the underground however only in a first approximation.
- Consideration of the uplift pressure of any form and dimension does not present any problems.
- The requirement of uniform deformations is fulfilled in the axial points, but not in the corresponding points at the surface.
- The stresses at the surface are calculated from the cross sections in the axial points.
- Whether realistic results are achieved is dependent on the number of deformations considered (max. three displacements and three torsions around the axes corresponding to the displacements) and on the assumptions for the distributions of the normal and shear stresses, but not on the number of beams of the calculation model (opt. 5 arches).
- It has as yet not been possible to theoretically verify the convergence of the method. Comparative calculations have, however, shown that assuming a continuous abutment surface in the longitudinal section with 5 arches and the corresponding 9 cantilever beams (equivalent to 25 crossing points) or 6 x 25 = 150 equations, gives sufficiently exact results. An increase in the number of lamellas did not significantly affect the results.

FINITE ELEMENT METHOD

In the nodal points of adjacent elements:

- The normal and shear stresses are not continuous across the element boundaries.
- The tangents at the bending lines are only continuous, if the moments in the nodal points are considered.
- The interaction of the loads acting on the underground both along the dam body and the underground are given.
- Consideration of the uplift pressure requires specific developments.
- The requirement of uniform deformations is fulfilled in the nodal points, but not in the areas between them.
- The stresses are extrapolated from the Gaussian to the nodal points.
- According to the theory of elasticity, singular points and thus stress peaks occur at the upstream and downstream dam base, which make it more difficult to evaluate the relevant stresses in precisely these decisive areas.
- Whether realistic results are achieved is dependent on the theoretical assumptions and on the shape and number of the elements.
- With the transition from finite to infinite elements, the convergence of this method can be theoretically verified for all element types. Comparative calculations have however shown that type, dimension and number of the elements have a significant influence, so that thousands of equations must be solved.

The designations LDM or FEM, therefore, only characterize the basic concepts of the two method groups. Both methods can be based on simplifications of more or less consequence, so that it is impossible to predict how realistic the results will be. In both methods the theoretical assumptions for the shear stress distribution in the shell surface area are of essential importance for the calculation results. More sophisticated assumptions for calculating the elements according to the LD method could improve the results without loosing its advantages, namely its descriptive character and low number of equations required. Step-by-step calculation during reservoir filling should make it possible to consider the time-dependent deformation behaviour by correspondingly adapting the deformation modulus .
This rough outline can of course only point out the problematic nature of both calculation methods. A more detailed comparative analysis of the extent of the influence of the respective disregarded factors exceeds the scope of the present paper but would certainly merit a separate critical study.

5.3.2 Static calculation methods

Investigation of dams by calculation can have various goals (Fig. 5.8):
– During the design phase, static calculation as realistically as possible, which requires several parameters and can be based on widely varying theories.
– During dam operation, analysis of the measurement results using statistic and hybrid models. This can serve two purposes:

- To calibrate the deterministic models during the initial storage periods. All calculation methods are, of course, only approximation methods; their theoretical bases and parameters must, therefore, be examined.
- To check the safety of the dam during its entire lifetime so as to be able to discover any anomalies in the dam behaviour as early as possible and to take appropriate corrective measures, if required. (see chapter 7).

For the design, only such calculation methods should be used that have already proven their worth in an examination of the prototype.
Also more advanced calculation methods, with improved theoretical foundations to achieve more realistic results must be subjected to this verification.
Static calculations, however, will allow a direct comparison with the actual behaviour of the structure only, if the rheological properties of concrete and rock are also included in the calculation methods. The calculation results can only be verified by measuring the deformations of the prototype, since at present it is not possible to carry out sufficiently exact stress measurements in the dam concrete during the long period, particularly in the case of high arch dams, between concreting begin and at least the first full storage level. The deformations measured on the prototype must, however, be divided into elastic and time-dependent deformations (chapter 7), to allow a comparison with the calculations.

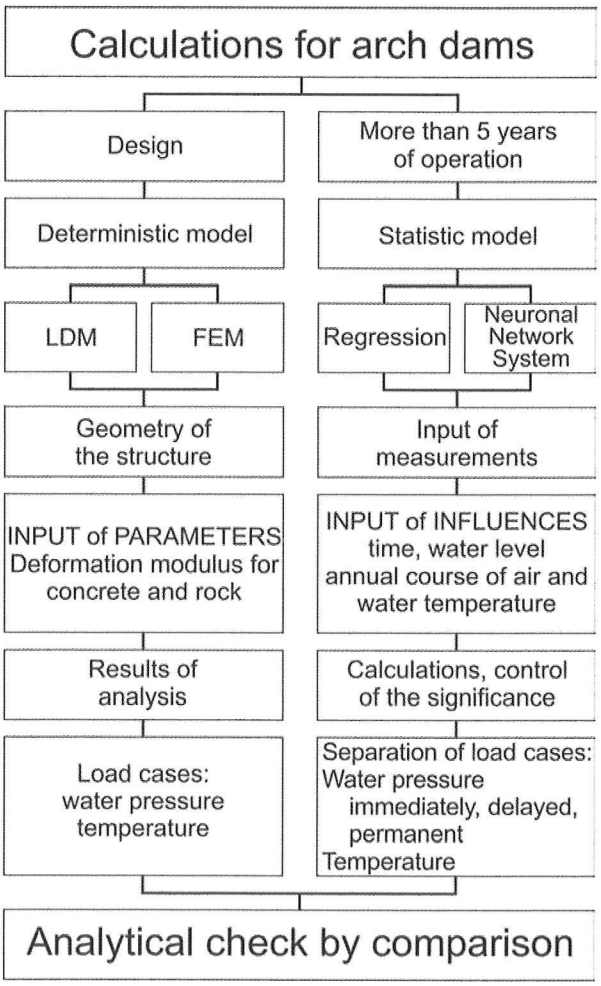

Fig. 5.8: Execution of the calculation methods.

5.3.3 Load cases and calculation assumptions

As with all other statically indeterminate systems, the loads acting on the structure can be attributed to:
– 'Permanent' loads, such as dead load and water

pressure normal to the dam surface and in the joints, possibly also silting-up, ice pressure, vibrations etc.
– Restraint stresses due to the restraint of deformations, e.g. along the dam base, or volumetric changes due to temperature variation, shrinkage and swelling, which are partly or even completely relieved by relaxation.
Below, only the three main load cases shall be discussed.

Dead load case

Up to now, concrete dams have in most cases been poured in blocks due to concrete-technological reasons. Formerly, these were separated by cooling joints, in the last decades increasingly only by vertical contraction joints. Today, continuously poured concrete dams are also constructed, using specially developed low-shrinkage concrete RCC (Roller Compacted Concrete).
The static system for the dead load case is largely dependent on the construction method:
– If the blocks are poured individually and the block joints are grouted after completion of the entire dam but before filling of the reservoir, the blocks must be calculated as independent vertical blocks.
– If during concrete placing the reservoir is already filled by stages, but is again emptied in time before the block joints are grouted, it will be necessary to verify the justification of assuming independent blocks (see section 8.2.4).
– If the reservoir is filled after concrete placing but not completely emptied and the concrete not sufficiently cooled before grouting of the block joints, the dead load of the newly poured blocks will act on the monolithic arch below them, resulting in an entirely different distribution of the stresses.

Water load case

There are two kinds of loading due to water pressure:
– The water pressure acting upon the dam body - normal to the upstream surface - is clearly given by the assumption of the reservoir level. Unlike buildings and bridges, however, dams must bear the maximum load permanently or over long periods at the very least.
However, this water load cannot be exceeded and is given:
- In standard load cases, by the top water level during normal operation.
- In exceptional load cases, by the dam crest plus the overflow height.

– Joint water pressures act normal upon the walls of the joint system. In large areas, the joint water pressure can be divided into three orthogonal components, two of which are of importance:
- Along the dam base the upward vertical component, i.e. the uplift pressure, which in many cases is superposed along the dam base as stress on the results of static calculations. However, it would be more correct to directly include the uplift pressure as an external load in the static calculation of dam body, and thus also in the calculation of deformations. This would result:
  At the dam base, in a reduction of the abutment resultant's vertical component and thus followed by a reduction of the sliding stability (see Fig. 8.14).
  Within the dam, in an increase of the existing vertical compressive stress and thus in an improvement of the safety against the lengthening of surface cracks. According to fracture-mechanical calculations, the difference between the pressure acting on the upstream face and the uplift pressure should not exceed 100 m on the water column.
- In the underground a horizontal component in the downstream direction, on the grout curtain which should not exceed a certain dimension on account of the static stability of the downstream foreland. It also causes an increase in the radial displacement and must, therefore, be considered in the calculation of deformations.

Usually, the maximum water pressure is assumed upstream of the grout curtain, downstream a linear decrease in the uplift pressures from 25% - 50% of the maximum water pressure to the level of the downstream foreland (Fig. 5.9). This assumption results not only in an upward vertical force in the dam body, but also in a momentum in the downstream direction.
In general, additional loads e.g. due to silting-up or ice pressure, waves or wind, play only a minor role.

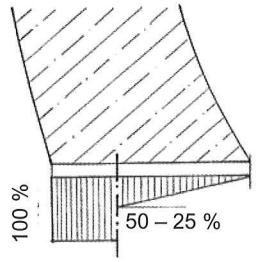

Fig. 5.9: Assumption for the uplift pressure.

Temperature load case

During the lifetime of the concrete dam, the concrete temperatures will vary around the mean annual temperature. The amplitude of these variations is given by the climatic conditions, water temperature, storage levels, dam thickness as well as by the thermal diffusivity of the concrete (Ritter 1943, Stucky 1957). Only in extreme cases was an attempt made to create an air cushion by means of a downstream curtain in order to shield the dam surface from extreme temperature drops.

To calculate the influence of temperature, depending on dam thickness, the daily, monthly or annual variations of the air and water temperatures at the dam site must be given. The actual temperature in the dam cross section can be substituted by a linearized temperature distribution between the upstream and downstream face under the condition that the cross-sectional deformations are equivalent (Fig. 5.10).

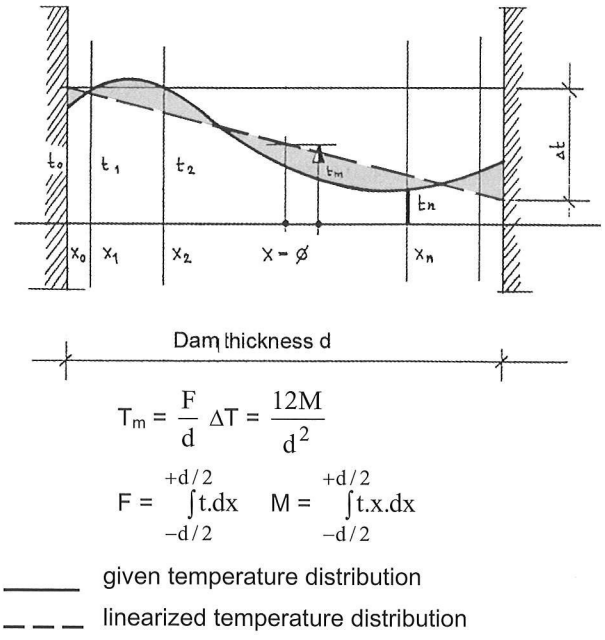

Fig. 5.10: Given and linearized temperature distribution.

The deformations of the individual lamellas or elements are calculated based on the linearized temperature distribution and introduced into the equation system in the same way as those due to an external load. The influence of the (in Fig. 5.10 hatched) difference to the actual temperature distribution is usually ignored.

5.4 ROCK MECHANICAL ANALYSIS OF THE UNDERGROUND

As part of the overall dam design, rock-mechanical analysis, like all other static calculations, is based on three groups of input data (Fig. 5.11):

- Geometrical description of the rock structure to be calculated (see section. 3.2), i.e. of the geological composition, rock fabric and rock elements.
- The properties of all rock elements, such as strength, time-dependent deformability, including joints (see section 3.3).
- External loads, i.e. the dam's abutment forces, groundwater pressures due to seepage flows, primary stresses particularly at the foot of steep, high valley flanks, tectonic and seismic influences.

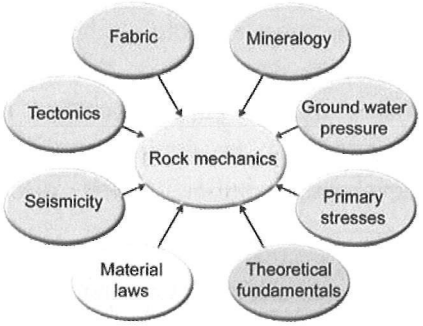

Fig. 5.11: Aspects to be considered in rock mechanical calculations [114].

In the field of rock mechanics as well, the methods for the determination of those components that form the basis of all mathematical models (Fig. 3.1) have not made progress, particularly in regard to:

- The geometrical description of the rock fabric; a task for geologists, as a basis of all mathematical models.
- The formulation of realistic material laws for the various elements of the rock fabric with their deformability, strength and hydraulic properties to be a task for rock-mechanical engineers. In many cases, the results of the usual tests reflect the actual conditions in nature only insufficiently, since, due to the simplified assumptions and evaluations that may

be of use in comparing test results, they often differ considerably from the actual conditions in nature.
At this point, attention shall once more be drawn to the basic requirements of mathematical models. They should:
– Only be based on parameters that can actually be determined in the field.
– Enable the prediction of the future behaviour of the structure and underground on the basis of in-situ and laboratory tests.
– Provide a valuable support for, but not replace mental effort, precisely because of the problematic nature of two, in principle, obvious basic requirements mentioned above.
As is generally known, research endeavours in the fields of the first two basic requirements have not kept pace with the mathematical development of the calculation methods (Hoek 1994), so that the third requirement assumes particular importance. Therefore, rock-mechanical calculations must at least also be carried out as parameter studies in order to be able to assess the influence of the various assumptions.
Selection of the most suitable mathematical model will ultimately be dependent on the availability of reliable bases for the points specified above. A distinction must also be drawn between two and three-dimensional, continuum and discontinuum models.

5.4.1 The time-old question: Continuum or discontinuum?

Due to its jointed structure, rock naturally is considered an anisotropic discontinuum and must, therefore, be calculated as such to achieve realistic results. Basically, thanks to the developments in regard to similar problems in soil or continuum mechanics, taking anisotropy into consideration no longer presents any problems. It has also become possible to introduce non-linear stress-strain relations. However, due to the difficulties encountered in the geometrical description of rock as discontinuum, from the in-situ description to the mathematical model, rock is in many cases considered a continuum (Equivalent Continuum Model ECM), the global parameters of which implicitly take the joints into consideration.
Continuum methods will give sufficiently representative results:
– With narrowly jointed rock or with joint spacings that remain below one tenth of the lowest dam width at the dam base.
– If stress propagation is not hindered by the joints due to reduced shear stress transfer.
– In overall stress and deformation calculations particularly, if deformations due to normal stresses prevail.
Consideration of rock as a discontinuum will be necessary, if:
– The spacing of continuous joint surfaces corresponds to the smallest structural dimension at the dam base.
– Displacements due to shear stresses parallel to the joints prevail and therefore particularly, if the residual shear strength τ_{res} in the joints is exceeded.
As is generally known, shear displacements occur predominantly in the joints and less in the rock in between. Larger deformations cause a decrease in the shear strength; in such cases, continuum methods could lead to incorrect safety estimations.
The influence of joints on the progress of displacements parallel to the rock surface with increasing depth is compared in the parameter study below (Fig. 5.12) based on assumptions according to the ECM-model and an explicitly simulated joint.
In an elastic analysis according to the continuum model, horizontal joints were determined based on an orthotropic material law. The shear modulus was so assumed as to ensure that the horizontal displacement at the dam base corresponds to that of the discontinuum model. The displacements along a perpendicular line below the upstream face of the dam was continuous, the gradient corresponded to the shear distortion of the fictive material.
To describe the non-linear material behaviour in the joint in the discontinuum model, the cohesion, angle of friction and residual friction must be defined; in addition, the exclusion of the transfer of tensile stresses is assumed as well. In this case, the discrete joint around the continuum is described as an elastic isotropic homogenous material.
The results of the analysis show the expected concentration of the significant horizontal displacements in the discretely simulated joint, where the critical

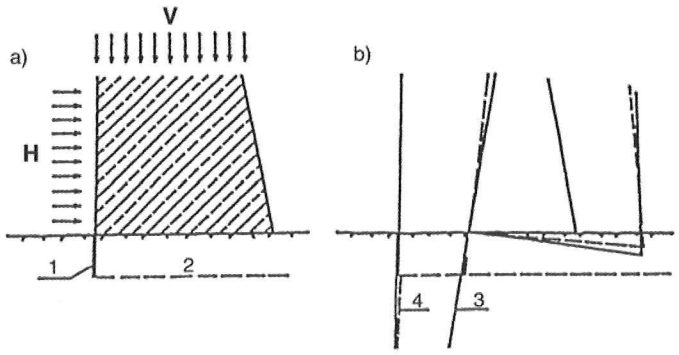

a) ... Load set up b) ... Displacements
1 ... Vertical crack 2 ... Horizontal joint
3 ... Deformations in the continuum
4 ... Deformations in the discontinuum

Fig. 5.12: Influence of a joint ± parallel to the rock surface on the horizontal displacements in the underground [83].

shear distance can be exceeded and sliding can occur. Calculation of the sliding stability based on a continuum model can, therefore, result in an overrating of the sliding stability.

Also to evaluate the groutability of the rock mass it is absolutely essential to consider the rock mass as a discontinuum. The usual evaluations of water pressure tests are based on the assumption of an even flow through the test area. This may suffice for the calculation of seepage flows or evaluation of seepage losses and thus also in deciding whether sealing measures will be required. In the rock mass, however, seepage occurs almost exclusively along the joints, seepage through the intact rock can generally be ignored. Therefore, the planning of injection work cannot be based on the assumption of even seepage, since selection of the appropriate grouting material and the grouting procedure is dependent on the geometrical dimensions of the flow paths. Their conductivity must be determined when evaluating water pressure tests. The different flow properties of water and grout can then be taken into consideration as well (section 3.8).

In summary, it can be said that for overall stress, deformation and seepage calculations, mathematical models based on a continuum may suffice in many cases. In cases, however, in which the displacements or seepage along the individual joints may play an essential role, the considerably more realistic model based on a discontinuum must be used.

5.4.2 Deformations at the concrete – rock interface.

Investigations of the foundation must fulfil the tasks listed below:

– Determination of the deformations, since these influence the distribution of the forces within the dam body, as well as of the stresses along the dam base.

– Determination of the stability of the underground on which the structural stability of the dam is dependent.

– Determination of the seepage flow around the dam and/or through the grout curtain so as to allow for the consideration of the joint water and uplift pressures in the calculations.

The static loads acting upon the rock underground can be attributed to the influences dependent on the storage-level (Fig. 5.13):

– Abutment forces of the dam.

– Water load in the reservoir.

– Changes in the joint water level due to the storage level; for these, the influence of the grout curtain and drainages must be taken into consideration as well.

In addition, silting-up must also be considered. It is dependent on the geological conditions in the catchment area, operational management (efficiency of flushing) and time.

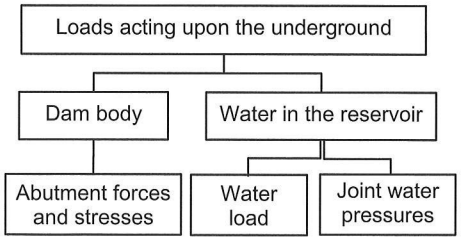

Fig. 5.13: Loads acting upon the underground.

All deformations in the underground comprise:

– Direct elastic deformations (resulting from the assumption of the modulus of elasticity).

– Delayed elastic deformations (with the assumption of a corresponding deformation modulus, these are included then in the calculated deformations).

– Permanent deformations due to the load history; these are generally ignored in static calculations.

The dam body can be considered a shell. At the edges of its foundation on the rock underground restraint stresses are generated as edge disturbances which, as the restraint of deformations increases,

can generate considerable additional local stresses and extend to a distance from the dam base corresponding to approximately half the shell thickness.

Abutment forces

Initially, the direction of the three-dimensional abutment forces along the circumference of the arch dam resulting from the LD method but having yet to be calculated based on the FE method, can be clearly illustrated using the spherical projection.

Nr.	R T	α_v °
1	2,613	31
2	2,481	16
12	6,868	27
13	6,464	27
21	10,275	25
22	10,003	29
28	12,192	28
29	12,513	33
33	11,646	41
34	11,940	39

α_v .. Angle of the abutment resultant against the horizontal.

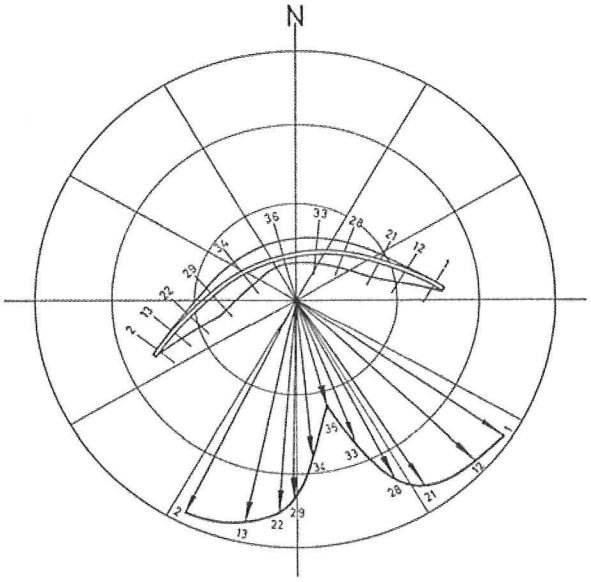

Fig. 5.14: Representation of the direction of the three-dimensional abutment forces [32].

The term propagation angle [32] enables a first descriptive evaluation of the foundation of arch dams. A propagation angle defines the smallest angle of a cone whose axis through the downstream dam base corresponds to the direction of the three-dimensional abutment resultant and whose surface touches the rock surface. Under average rock conditions, this angle should not fall below 25° - 30°. Thereby, a distance from the dam base corresponding to triple the dam base width should be taken into consideration. Comparative investigations have revealed that the direction of the three-dimensional abutment resultant is basically dependent on the valley shape and can only be slightly influenced by the shape of the arch dam (Fig. 5.15). If the angle is smaller, more detailed rock-mechanical investigations and additional safety measures, if required, must be carried out.

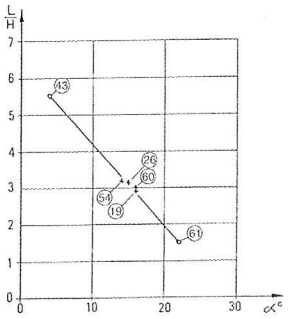

19 ... Limberg, H = 120 m
26 ... Drossen, H = 112 m
43 ... Schlegeis, H = 130 m,
54 ... Kölnbrein, H = 200 m
60 ... Zillergründl, H = 180 m
61 ... Dabaklamm (Projekt), H = 220 m

L/H . Crest length : Dam height

α .... Angle between the arch dam axis in the longitudinal direction of the valley and the horizontal projection of the largest three-dimensional abutment resultant.

Fig. 5.15: Direction of the maximum abutment resultant as a function of the valley cross section [39].

Influence of the size of the downstream foreland

The influence of the abutment forces' propagation angle on the stresses should be low, since:

– The deformations normal to the dam base and thus the restraint conditions remain largely constant.

– The displacements parallel to the dam base influence the stresses in the dam body only, if the dimension of these displacements along the circumference varies widely from section to section.

Displacements, however, considerably influence the dam's sliding stability resulting from the foundation conditions. Structures subjected to repeated loading can, of course, bear several hundreds of thousands of load cycles without an adverse effect on their load bearing capacity. Shear tests have, however, revealed that the number of allowable load cycles without decrease in the shear strength is low. With weak zones parallel to the dam base and a small propagation angle, special attention must be paid to the extent the shear strength and friction angle decrease under repeated loading or whether the

increase in the maximally occurring horizontal displacements at least does not decrease from year to year during normal operation.

To take the influence of the deformability of the underground into consideration, spring constants are introduced into the calculation of the dam body according to the LD-method. These are usually determined assuming an elastic isotropic semispace for the components of the abutment forces normal, radial and tangential to the dam base as the surface of this semispace . FEM-calculations are often based on similar simplifications, if the underground can only be simulated in a general way, for example using boundary elements. In this method, however, merely the topographic simulation of the rock surface downstream of the dam enables a more realistic determination of the stress propagation from the abutment into the underground. The influence of this stress propagation is discussed below in more detail.

For the underground itself, the assumptions listed below apply (Fig. 5.16):

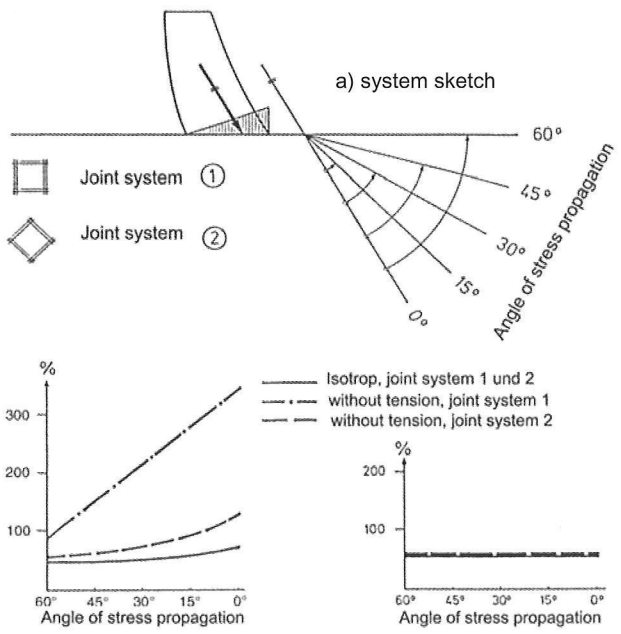

b) Radial displacement c) Vertical displacement
relative to the displacement in the elastic isotropic semispace

Assumptions:

- Isotropic and homogeneous with two joint systems perpendicular to each other:
- Parallel and normal to the dam base.
- 45° inclination to the dam base.
- Joint systems cannot transfer tensile stresses.
- To the elements of these joint systems different properties were assigned than to the weak zones in between.

Sound rock: V = 20 kN/mm² G = 9.1 kN/mm²
Weak zones: V = 0.4 kN/mm² G = 0.2 kN/mm²

Fig. 5.16: Deformations of the dam base as a function of the size of the downstream rock surface and joint systems [32].

From this follows that the displacements normal to the dam base are neither significantly influenced by the joint systems nor by the position of the downstream rock surface, as long as the propagation angle does not noticeably restrict stress propagation. As can be expected, both these factors exert a considerable influence on the displacement in the downstream direction parallel to the dam base.

When the upstream tensile stresses in the rock exceed the tensile strength and the propagation angle decreases, the shear stresses will increase rapidly as the remaining load-bearing section decreases and will only slowly be relieved with increasing depth. Their influence increases depending on the orientation of the joint systems. Therefore, the position of the downstream rock surface influences the deformations at the dam base most, if one direction of the weak zones is approximately parallel to the dam base (joint system 1). Under the given assumptions, the overall displacement is already approximately twice as large as the displacement that would occur, if an elastic isotropic semi space were assumed.

The influence of the downstream rock surface and weak zones is, however, negligible, as long as the angle between land surface and abutment force does not fall below 30°.

In regard to the calculation results, it shall also be pointed out that the transverse tensile stress decreases with the decrease of the downstream rock foreland, in accordance with the lower splay of the stress trajectories.

The influence of radial weak zones

The influence of a varying deformability along the circumference of arch dams is examined using the FE-model, with which both boundary cases are easily simulated:

– Initially, based on the mesh, the spatial behaviour of the underground is determined. In nature, this would correspond approximately to an isotropic underground.

– If the nodal points between the individual slabs of the underground are loosened, the elastic springs assumed to be independent of each other are simulated in the underground by independent slabs. In nature, this would correspond approximately to a radially foliated underground. In its foliation planes, shear stresses cannot be transferred.

The results of a comparative study [69] show that initially the influence of the coupling of the rock slabs is low, remaining in any case below that of the simplifications in the geometrical representation of the rock fabric and material laws. As expected, these lie between those of a homogenous and 'uncoupled' underground. This, however, also confirms that it is allowable to use a simplified simulation of the underground based on springs or boundary elements or to ignore the coupling in the underground.

Finally, it must be pointed out that these simplified analyses can, of course, only indicate tendencies in the behaviour of the underground subject to varying influence factors, which must be examined in more detail, if so required. Detailed investigations of the effects of the abutment forces of arch dams on and in the underground as well as the underground's retroactive effect on the dam are nowadays taken for granted.

The increasing efficiency of computers facilitated the development of more sophisticated mathematical models and thus also of considerably more realistic examinations than was previously the case; however, this is only true, if the structure and material laws of the foundation are representatively determined.

5.4.3 Tensile stresses along the dam base and in the underground

Tensile stresses that can cause cracks or the opening of joints in the underground can be expected to occur in three directions perpendicular to each other: normal and parallel to the dam base as well as parallel and transverse to the valley.

Tensile stresses normal to the dam base

Tensile stresses normal to the dam base can lead to the opening of joints parallel to the dam base, particularly below the upstream dam surface. Usually they are examined in detail.

They represent one criteria for evaluating dam design and can be considerably influenced by the shaping of the dam body. Two influences affect the dimension of the tensile stresses:

– The ratio of the deformation moduli of concrete and rock. The less deformable in the vertical direction the rock underground is, compared to the dam concrete, the higher the restraint degree will be and thus also the vertical tensile stress along the upstream dam base (Fig. 5.17).

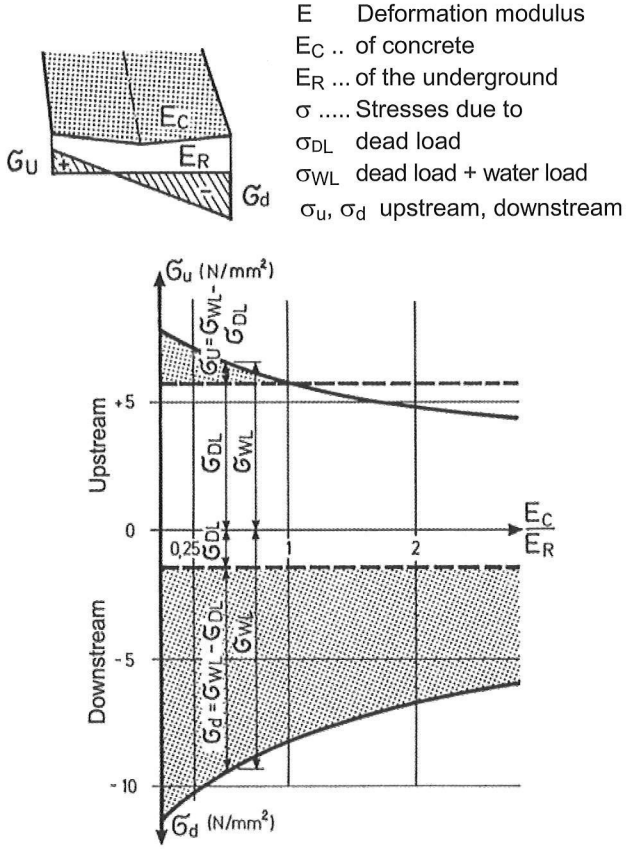

Fig. 5.17: Influence of the ratio of the deformation moduli of concrete and rock on the stresses along the upstream dam base [*70*].

– Loads acting upon the reservoir. It has been known for decades that the reaction of the reservoir bottom and slopes to the filling of the reservoir varies widely. Both a narrowing as well as expansion of the valley could be observed; for the reservoir bottom, however, hardly any observations exist.

In regard to gravity dams with open block joints, this behaviour is hardly of significance. However, with monolithic dams such as gravity dams with grouted block joints or arch dams, it can result in additional vertical stresses along the upstream dam base.

To assess the deformations of the reservoir boundary due to a superimposed water load, a distinction must be drawn between two theoretical models:

– Model based on permeable reservoir slopes, in which the joint water pressures in the jointed rock adapt to the water level in the reservoir. In this case, the deformations of the reservoir bottom and slopes will be small. The joint water pressure acts as uplift pressure and upon the grout curtain as well.

– Sheet model, in which the reservoir is assumed to be lined with a fictive impermeable sheet. Therefore, neither the groundwater level nor the joint water pressures will be affected. The maximum water load acts upon the boundary of the reservoir, but not as uplift pressure or upon the sealing apron.

To examine the influence of a deformation of the reservoir bottom according to the sheet model, the spatial, monolithic shell must, of course, be used as a basis. Examination of a plane section would give far too favourable results (Fig. 5.18). A foreland with a sealing apron shifted towards the upstream face shows a similar effect. If a sealing apron that is assumed to be absolutely impermeable is inclined towards upstream, this, too, causes additional vertical stresses (Gell 1986).

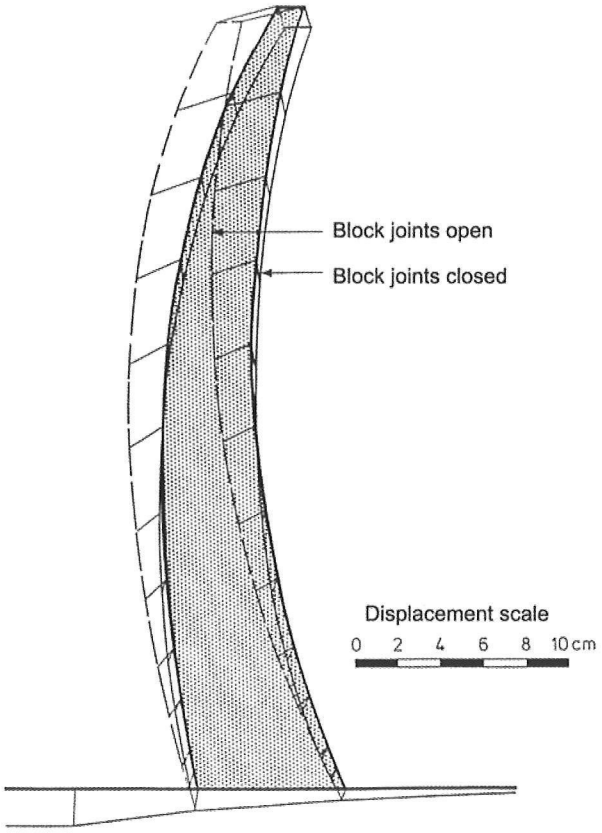

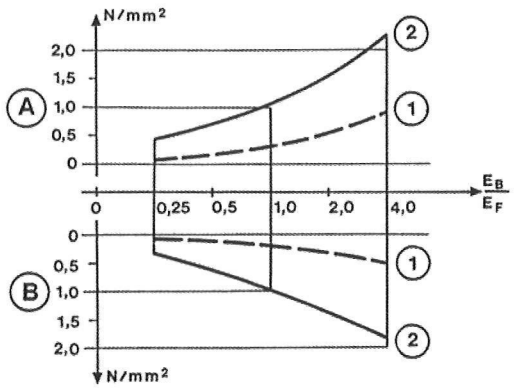

A .... Upstream face (tensile stresses)
B ..... Downstream face (compressive stresses)
1 ..... Open block joints
2 ..... Grouted block joints

Fig. 5.18: Influence of the reservoir load on the vertical stresses along the dam base [*71*].

Horizontal tensile stresses in the longitudinal direction of the valley

The horizontal tensile stresses parallel to the rock surface in the mountain - valley direction are generated by the horizontal component of the abutment resultant (= transverse force at the dam base), causing displacements in the downstream direction in which the upstream rock foreland can only participate, if horizontal tensile stresses are transferred. With dam height and valley form given, the transverse force can hardly be influenced by the shape of the arch dam.

In reality, the theoretical distinction between vertical and horizontal tensile stresses does not exist. Inclined principal tensile stresses, however, do occur; their direction is basically determined by the ratio between the two calculable components.

The problematic nature of these tensile stresses has been known for a long time (Henny 1929):

'...The danger of such tensile stresses is that:

– They increase with increasing dam height.

– Possible cracks or expansions of existing rock joints can spread from the upstream base under the dam; the resulting water flow can cross the natural

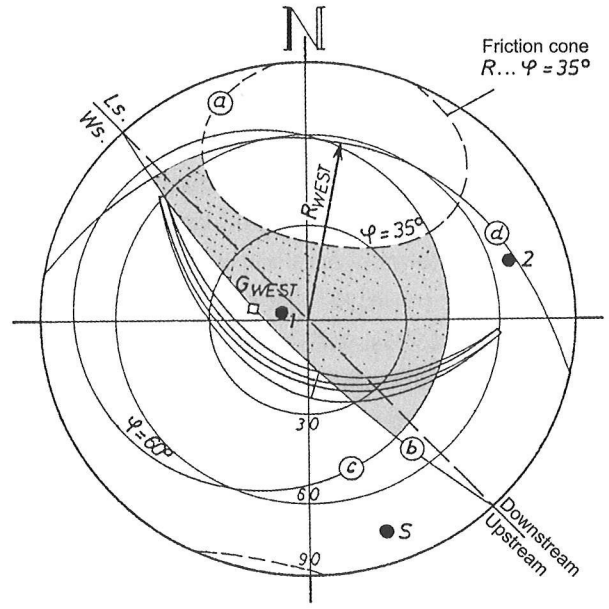

Area of critical joints
S ... Foliation planes

a) the angle of possible shear planes to the resultant must be larger than the joint friction angle;
b) they must exit downstream of the dam;
c) they can be effective on their own only, if their angle to the rock surface is smaller than 60°;
d) in potential shear planes components of the resultant must lie in the direction of the rock surface.

Fig. 5.22: Determination of critical rock bodies using the spherical projection (Pacher 1967, unpublished).

Finally, also an analytical method was developed, which takes the statistic distribution of the parameters for the joint structure and of the rock-mechanical properties into consideration as well (Trunk 1993).

5.4.5 Summary

Today, the joint analysis of the interaction between the arch dam and its underground has become a matter of course. A reliable predetermination of the reaction of the underground faces difficulties in three subsections, which form the basis of all calculations:

– Realistic determination of the, for the most part, heterogeneous structure of the underground using statistic methods.

– Determination of the rheological, mechanical and hydraulic properties of the individual rock elements by means of improved evaluations of the laboratory and in-situ tests based on theories equally advanced as those used in rock-mechanical calculations.

– Incorporation of the improved bases in the mathematical model for the analysis of the underground. To date, this can only be done using simplifications.

The usual simplifications of the structure complex geometrical of the underground reduce the advantages according to the FE-method, so that in many cases the EC-method and thus spring constants or boundary elements are considered sufficient.

5.5 DYNAMIC ANALYSIS OF THE DAM BODY

5.5.1 Introduction

For a dynamic analysis of arch dams:

– the theory on which the calculation method will be based, and

– the definition of the external loads corresponding to this theory

must be determined in advance.

5.5.2 Calculation methods

The assessment of the lowest Eigenfrequency constitutes one basis of dynamic calculation methods, for which approximation methods are sufficient :

– Calculated approximation methods, e.g. according to the formula (Geiger 1923) (Fig. 5.23).

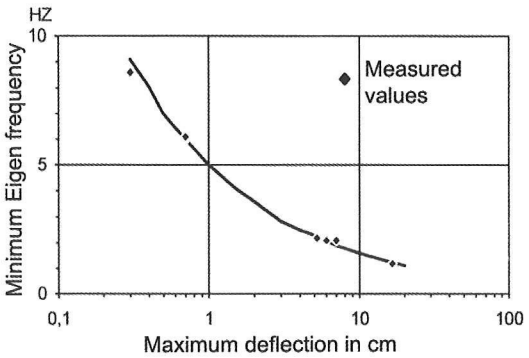

$$\omega_G = 5\sqrt{\alpha.\beta / \delta_{max}} \quad \text{in [Hz]}$$

where α = Coefficient for distributed masses, ~ 0.8
β = Ratio $E_D : E_S$;
E_D .. Dynamic E-modulus,
E_S .. Static E-modulus
δ ... Maximum deflection in the load case of full storage level due to water load

If β is substituted by ~ 1.25:

$$\omega_G = 5 / \sqrt{\delta_{max}} \quad \text{results.}$$

Fig. 5.23: Lowest characteristic frequency according to Geiger (see annex A - 3).

Since both the deflection and the Eigenfrequency are functions of the stiffness of the structure, this relation appears to be justified for the assessment. Several comparative values are listed in the table in annex A - 3 and show satisfactory conformity with the values measured at the structure.

– Empirical methods. A summary of the values determined on the prototype in vibration tests shows a clear dependency on the height of the structure with a comparatively low variation (Fig. 5.24). The tests also revealed decreasing characteristic frequencies, probably due to the increasing damping with increasing reservoir level, in conformity with the calculations. Thereby, the ratio of the Eigenfrequencies, both with a full and empty reservoir, is dependent above all on the ratio of the reservoir level variations to the dam height and is expected to lie between 1.1 and 1.2.

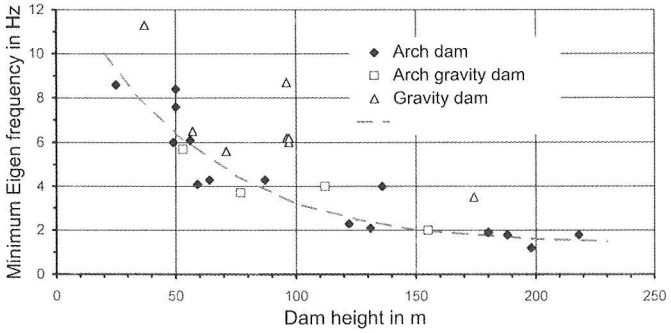

Fig. 5.24: Empirical assessment of the lowest Eigenfrequency (see table in annex A - 4).

For the calculation of the loads several methods have been developed:

– Loading by means of a static replacement load.

– Assumption of modes of vibration for the dam body, usually a symmetrical and an asymmetrical wave (Copen 1967). For each considered point, the static replacement load is calculated from the product of the covibrating mass assigned to this point and the calculated deflection in this point.

– 'Real' dynamic calculation of the dam body step by step. The effort required for a 'real' dynamic calculation in steps appears not to be justified, since it provides only an apparent increase in accuracy in regard to the variation range of the calculation assumptions.

– Pseudo dynamic calculation using the response spectrum.

5.5.3 Load assumptions

The static replacement load or the ordinate of the covibrating water mass was initially determined assuming a stiff vertical wall (Westergaard 1933) for symmetrical and asymmetrical modes of vibration. Later these values were improved using an electrical analogy model and extended to include inclined walls (Zangar1952).

Using the FE-method, dynamic calculation methods were finally developed, in which the vibrations of the dam were coupled to the water in the reservoir as well as to the underground. This made it possible to directly calculate the covibrating water mass for each vibration mode of the dam (e.g. Obernhuber 1995).

Even earlier on it was proven (Federhofer 1933) that the covibrating water mass decreases with higher modes of vibration n proportional to the spacing of the nodes (Fig. 5.25):

$n/(n^2 - 1) \rightarrow a/\pi$

where

n .. n th mode vibration

a .. spacing of vibration nodes

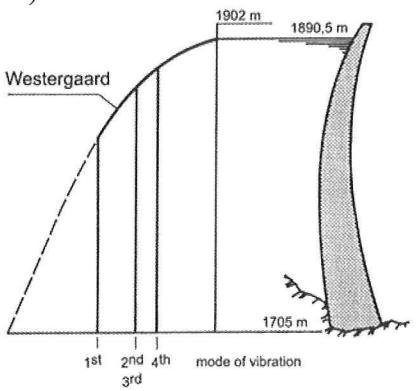

Fig. 5.25: Limitation of the covibrating water mass with higher modes of vibration for the Kölnbrein arch dam (Federhofer 1933).

For the 'real' dynamic calculation of the structure, however, the variation over time of the extremely irregular stimulating vibrations of the underground at the dam site must be known. However, it is almost impossible to determine these vibrations.

Therefore, a calculation method using the so-called response spectrum is usually applied, which is initially independent of the structure. The response spectrum can be deduced comparatively easily using the Duhamel integral based on a one mass exciter (Clough 1970) as an envelope for several stimulating vibrations determined using a random generator (Großmayer 1978). The European earthquake standard EC8 specifies response spectra for three different ground classes, on which these

double curved dam shell requires some experience and is discussed below in more detail.

5.6.2 Dam body

As with the load distribution method, the basic elements of shaping can be best illustrated by an imaginary division of the structure into two load-bearing systems, the horizontal arch lamellas and the vertical cantilever lamellas. The basically unavoidable bending stresses in the arch lamellas can, of course, be kept low, if the shape of the arch follows as far as possible the catenary arch for the external load acting upon the arch. Assuming at one level a constant water pressure corresponding to the depth of the arch level below the top water level, the circular arch inevitably results as the optimal arch form, which, therefore, was almost exclusively used until a few decades ago. According to the well-known heel formula, the compressive stress of the circular arch remains constant under hydrostatic loads (Fig. 5.28):

$$\sigma = \frac{p \cdot r}{d}$$

From this, the lowest possible arch thickness d_{min} results, assuming a maximally allowable arch stress σ_{all} and taking the greater length of the outside of the arch upon which the water load acts into consideration.

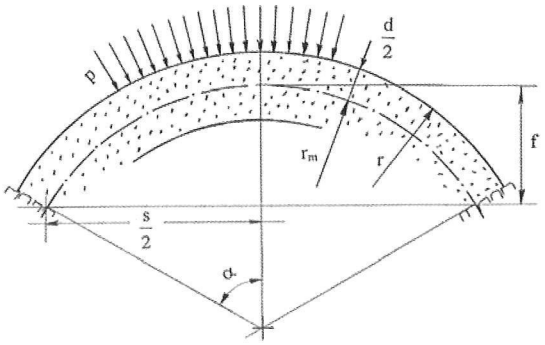

$$d_{\min} = p \cdot \frac{r}{\sigma_{perm}} \cdot \left(1 + \frac{d}{2r_m}\right)$$

Fig. 5.28: Geometric illustration.

Generally, the arch stress will reach a decisive value in regard to the allowable compressive stress of concrete only, if the dam height exceeds 150 m (Fig. 5.29); it can, however, be used as a measure of the general stress level of arch dams. Thereby, the water pressure p corresponds to the water level of the considered horizon below the normal design top water level, a surcharge due to flood is classified as a special case.

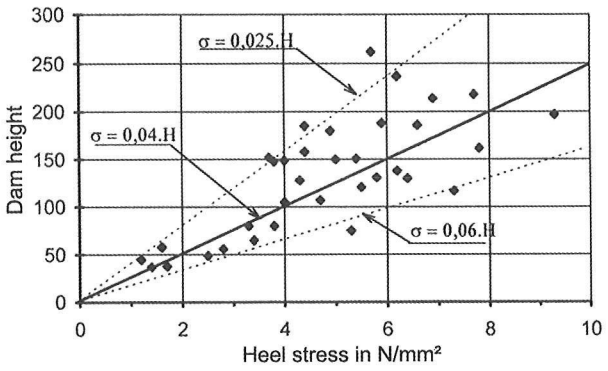

Fig. 5.29: Maximum arch stress of several arch dams (see annex A).

To assess the maximum allowable arch stress, the bending line of the vertical centre section shall serve as a basis (Fig. 5.30). According to the LDM, the radial displacements result basically from the compression of the horizontal arches as a result of:

– Shortening due to the normal stresses (from the part of the water load acting upon the arch).

– Concrete temperature variations; in alpine regions, their effect over the year is opposed to the storage level variations of seasonal storage reservoirs.

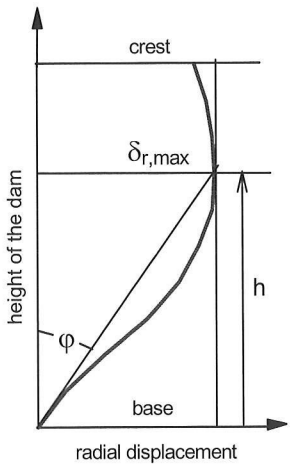

Fig. 5.30: Bending line and torsions in the centre section.

The bending area resulting from these radial displacements determines, however, also the torsions at the dam base and thus the unwanted restraint stresses dam base: the smaller the largest radial displacement, the lower the torsion, restraint moments and the bending stresses at the dam base will be. From this it follows that the bending stresses at the dam base can be reduced in two ways:

– The usual increase of the dam thickness at its base; this requires the lowest cubature, but also results in an unwanted stiffer restraint of the vertical load-bearing lamellas and an unwanted load transfer from the horizontal to the vertical lamellas with higher restraint moments.
– Strengthening of the arches at mid-height of the arch dam; this requires a higher concrete cubature, but also increases the stiffness of the entire dam and reduces its mean stress level.

Therefore, the allowable arch stresses can be the higher, the higher the deformation modulus of the concrete and the narrower the valley in relation to the dam height is.

The vertical tensile stresses due to the dead load at the downstream dam base as well as in the upper third section of the dam height at the upstream face of the independently assumed blocks are decisive for the shape of the vertical sections. Before grouting of the contraction joints, the vertical tensile stresses should not exceed approximately 1 N/mm² or remain below 1/3 of the simultaneous compressive stress at the other cross-sectional boundary.

Calculations according to the Load Distribution Method have shown that the load acting upon the arch decreases from the crown to the abutment, since the lateral vertical sections absorb an increasing portion of the horizontal water load due to their increasing stiffness. However, this also means that no longer the circular arch, but rather an arch with a radius of curvature increasing from the crown to the abutment comes closer to meeting the requirements of a catenary arch (Fig. 5.31), since the geometrical condition for a catenary arch under a load normal to the axis is defined by:

$$p_\varphi \cdot \rho_\varphi = p_k \cdot \rho_k = p_s \cdot \rho_s = N$$

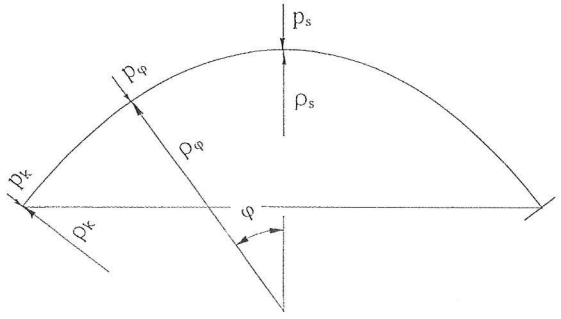

Fig. 5.31: Geometry of a thrust line arch [1,3,4].

According to the heel formula, a smaller radius of curvature in the arch crown also results in a lower arch stress or lower arch thickness. The use of arch shapes with variable radii of curvature brings about not only an improved approximation to the catenary arch and thus a reduction of the bending stresses in the arch, but has also the advantage of an additional parameter for an improved adjustment of the arch geometry: a circle and parabola, for example, are defined by three points, whereas the definition of a ellipse requires 5 points.

Only the restraint of torsions at the abutments, which is determined basically by the width of the dam base and the deformability of the underground, causes an unavoidable restraint momentum, which in most cases requires thickening of the abutment.

If, from the start, the circle or parabola is the shape of choice for all horizontal sections over the entire dam height, the margin for further adjustments to the valley shape or force line remains narrow. If, however, a general arch form is assumed, for example a conic shape, two further points, e.g. quarter points, can be chosen. The crown equation of the conic shape has proved useful:

$$x^2 + (1 - \varepsilon^2)\,(y - y_s)^2 - 2\rho_s \cdot (y - y_s) = 0$$

By the selection of ε (eccentricity of the conic shape), the arch shape can be altered considerably:

ε < 0..	Ellipse with the large axis transverse to the valley
ε = 0..	Circle
0 > ε < 1	Ellipse with the large axis parallel to the valley
ε = 1	Parabola
ε > 1	Hyperbola

The modification of ε, however, must be continuous over the entire dam height in order to guarantee a smooth dam shape. Determination of the tracing data of the dam surface as well requires the continuous specification of the arch parameters as a function of the dam level. In addition, experience has shown that a decreasing radius of curvature from the crown to the abutment at the lowest dam levels contributes to a decrease in the bending moments. By choosing conic shapes for the arches, this goal can be continuously met by choosing hyperbolas in the crown area followed by a parabola, ellipses (with the large axis in the longitudinal direction of the valley) to the circle and possibly to ellipses

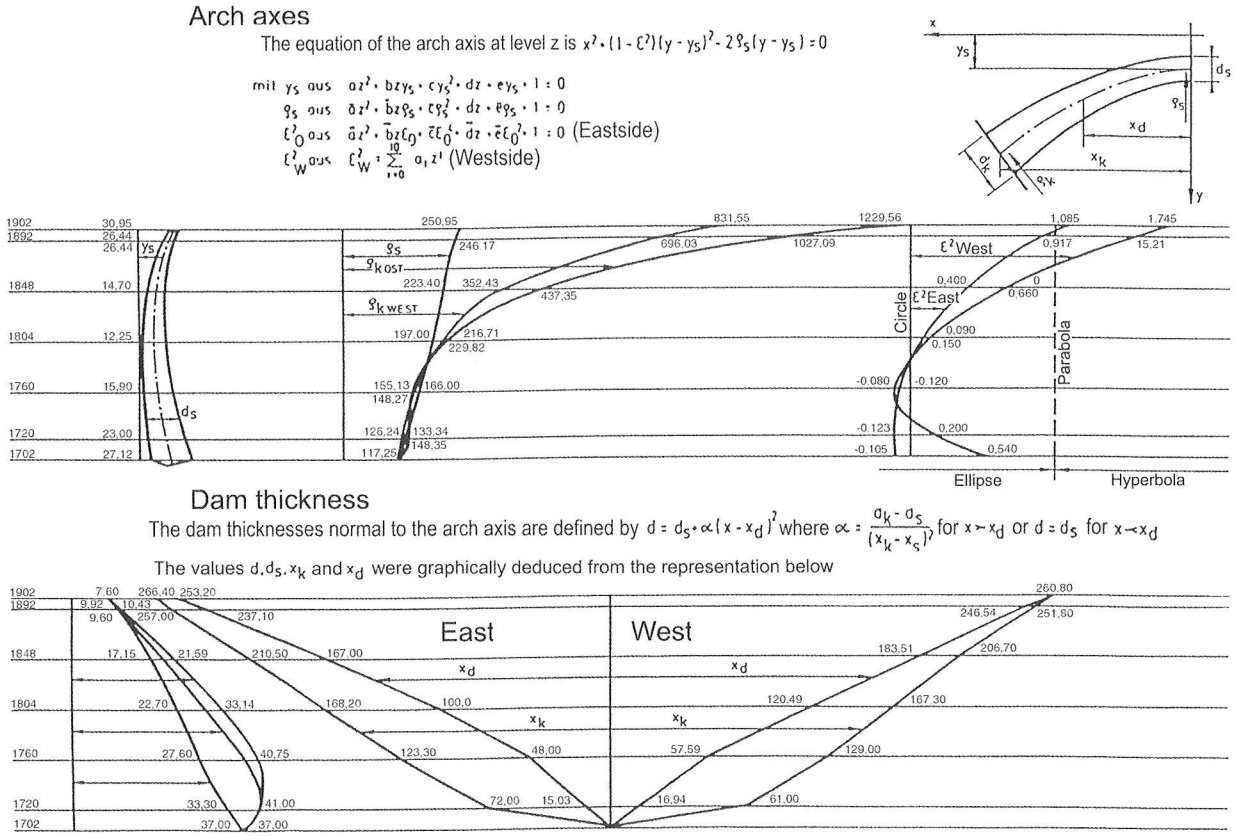

Fig. 5.32: Geometrical data of the Kölnbrein arch dam [25].

(with the large axis transverse to the valley) in the lowest dam section.

An example of this type of shaping is the Kölnbrein arch dam shown above (Fig. 5.32).

Since static calculations according to the LDM are based on the arch axis, determination of the axes of the horizontal and vertical lamellas has proved useful for this method. For static calculations according to the FE method, the external surfaces (taking into account $\varepsilon_W \neq \varepsilon_L$) could be defined as the corresponding conic shell as well.

To assess the abutment thickness, not only the bending stresses, but also the shear stresses could be relevant. These can sometimes cause higher principal tensile stresses within the dam than at the surface [75] and are thought to have caused damages at several newly constructed arch dams (Lombardi 1987). A first analytical attempt to assess these shear stresses along the perimeter of arch dams did not take into account the valley shape (Fanelli 1992). An empirical assessment of the horizontal force at the dam base that takes the valley shape into consideration, based on the results of static calculations of several arch dams and confirming the dependency on the valley shape, can facilitate the determination of a minimum base strength.

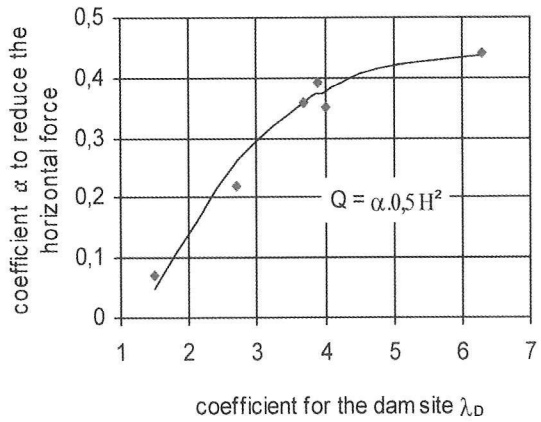

Fig. 5.33: Empirical estimation of the transverse force at the basis of the centre section [106].

This horizontal force causes not only horizontal tensile stresses in the underground (see Fig. 5.19), but also inclined principal tensile stresses within the dam, which to date have only rarely been examined. An estimation of the shear stresses at the dam base can be deduced from the abutment thickness (Fig. 5.6) and the base shear force (Fig. 5.33) as a function of the valley characteristic λ_D (Fig. 5.34).

$$\tau' = \frac{Q}{H.d_k} = \gamma_W \cdot \frac{1}{2} \cdot \frac{\alpha}{f_2(\lambda_D)}$$

where $Q = \alpha.\gamma_W . \frac{1}{2} H^2$ (Fig. 5.44)

and $d_A = H.f_2(\lambda_D)$ see Fig. 5.6

For gravity dams:

$$\tau'_G = (0.67 \div 0.59)\gamma_W$$

applies.

where $d_A = (0.75 \div 0.85) \cdot H$

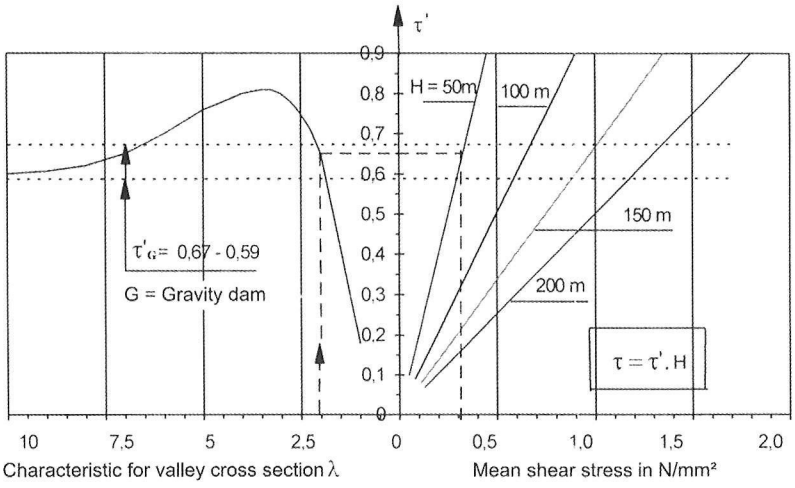

Fig. 5.34: Estimation of the mean shear stress τ at the dam base.

If the shear stresses along the base of arch dams should not exceed that of equally high gravity dams, the required thickness of the dam base can be deduced from the above diagram (see also Fig. 5.6). Together with the radial normal stresses which are ignored in the slab theory, the transverse tensile stresses resulting from the vertical compressive stress (these are, however, much reduced due to the restraint of the transverse deformations at the dam base) and the possible residual tensile stresses from the construction period, the inclined principal tensile stresses can be determined.

5.6.3 Constructional possibilities for the design of the dam base

Comparatively often, cracks parallel to the abutment surface are generated in the concrete or rock along the upstream dam base, no doubt the area most subjected to tensile stress. Here, two different media impact on one another: the more or less slender, homogenous concrete body and the jointed semi space of rock, so that restraints and thus additional stresses are unavoidable. Especially in this area, inaccuracies in the assumptions as well as intentionally or unintentionally disregarded influences can add up to inadmissible quantities, particularly in the case of high dams with comparatively high stress levels.

To avoid shallow cracks in the area of the upstream dam base, a perimetral joint over the entire dam thickness, the so-called 'pulvino', was introduced into arch dam construction already in the 1930s, and was later succeeded by various structural formations, particularly in the upstream dam third section. Even though the effectiveness of such a three-dimensional perimetral joint is questioned and could only be confirmed in some cases by measurements along the upstream dam base (Marazio 1991), the basic idea of these joints shows that the upstream third section of the dam base plays only a subordinate role in the structural stability of arch dams with full reservoir. Analogously, the same applies to the downstream third section of the dam base with empty reservoir, with only one reservation: these joint openings must at least be limited in their depth not only to guarantee the safety against overturning towards the upstream face in the dead load case but also to ensure a long-term shear transfer at a high reservoir level and with the closed joint.

At this point, attention shall be drawn to the fact that arch dams, whose reservoir levels compared to dam height vary widely during normal operation, are subject to cyclic stresses, particularly in the region of the dam base. This must be taken into consideration when designing joints subjected to periodic opening and closing.

The optimal height of the perimetral joint above the dam base was discussed as well (Rescher 1993). The results of this research showed that with all arch dams:

– The restraint moments (and thus also the flexural stress) decrease rapidly with increasing distance from the dam base, so that the tensile zone at the upstream face and thus the effect of the perimetral joint remains lower than at the dam base.

– The low local decrease in the stiffness of the cantilever beam cross section due to an open joint - in this case the descriptive character of the LD method again proves useful - does not cause a

significant load transfer, so that the position, direction and quantity of the resultant remain largely unchanged in the section normal to the dam base.

– The same state as without perimetral joint is soon regained due to the stress propagation below the open perimetral joint.

– Thus also the stress distribution along the dam base is affected less with increasing distance of the joint from the dam base.

This, however, means that the effectiveness of a perimetral joint is limited to the immediate vicinity of the abutment surface and that its effect on the stress distribution at the dam base steadily decreases with increasing distance. (Fig. 5.35).

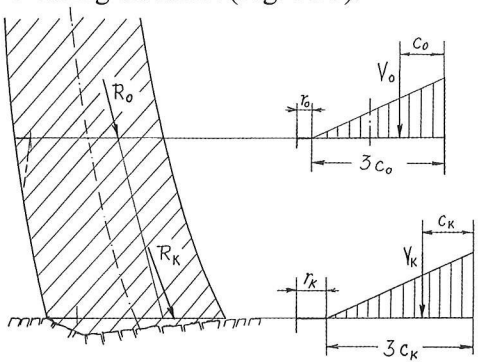

Fig. 5.35: Force and stress curve with a high perimetral joint.

Although cracks in the concrete and rock around the upstream dam base hardly affect the structural stability if the reservoir is full, they can considerably reduce the effect of the grout curtain, which is usually located in this area, since its permeability is also dependent on the stress respective deformation state. The grout curtain should be located in an area in which the stress variation due to reservoir level variations between top water level and minimum operating level remains as low as possible. This requirement is even more important, if the reservoir level variation is high compared to the dam height. So as to be able to utilize the compressive prestressing due to the dead load, the injections for the grout curtain should be finished before a significant compressive stress due to the dead load becomes effective during placing of concrete.

The monitoring and recording of seepage is very important in order to ensure an early discovery of these joint openings or cracks. Since the danger of erosion in concrete and rock is only a long-term concern, there is sufficient time for corrective measures to become effective. The dimension of the seepage can be used as a measure of the extension of the cracks or joint openings. From this, however, it is not possible to directly infer a significant decrease in the load-bearing performance. From the increase in seepage as a function of the reservoir level the safety against uncontrollable seepage can be deduced (Fig. 7.5 – 7.7).

For the Zillergründl arch dam, therefore, a design was chosen in the middle third section of the dam abutment (Fig. 5.36), in which:

– The perimetral joint between the upstream face and inspection gallery is located as close as possible to the rock surface and the bottom concrete in between is strongly reinforced.

– A concrete apron founded at the same level as the dam and sealed against the dam using an elastic sealing wedge.

– The grout curtain near the upstream end of the concrete apron is located below an injection gallery, which is accessible at its centre and at both ends from the dam during operation so as to facilitate post grouting, if required.

Detail A: Radial section, concrete apron, block joint

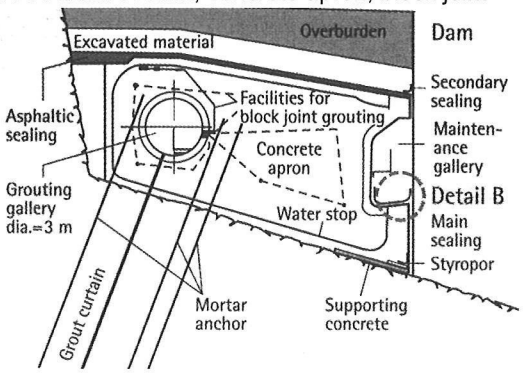

Detail B: Main sealing in the maintenance Gallery

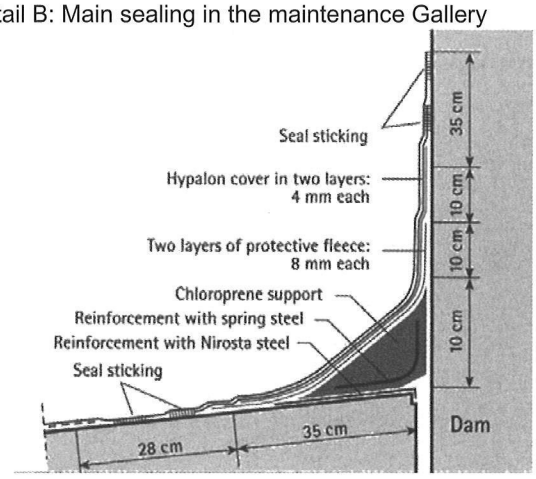

Fig. 5.36: Design of the Zillergründl arch dam in the abutment area.

The problem of water pressure in these joints requires, however, more detailed consideration (Carrère 1994). In general, a seal is placed near the upstream surface, so that no water pressure can occur in the joints. If, however, water enters at full storage pressure into a small initial crack above the joint, the crack can propagate into a region, in which the compressive stresses normal to the crack plane stop the crack propagation. The pore water pressure in concrete can cause similar effects, since it is determined by the pressure at the upstream face, if it has its effect close to a free concrete surface at the joint. With arch dams higher than 100 m, the difference between the water pressure acting upon the upstream face and in the perimetral joint must not exceed 100 m.

If, however, the joint is left open towards the upstream face, a seal must be installed in the joint if the joint ends at a control gallery. During installation, care must be taken to ensure that the full water pressure acting upon the entire joint tape width can be absorbed. An installation of these seals must, therefore, be well considered, statically as well as structurally (Fig. 5.37).

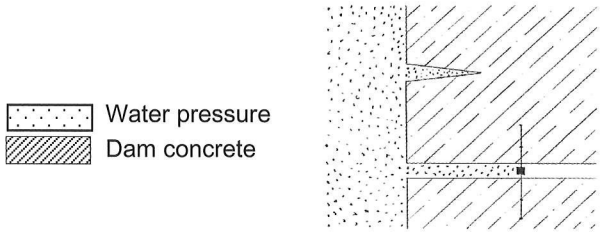

Fig. 5.37: Water pressure in cracks at the upstream face and in the perimetral joint.

Cavity shapes in highly stressed areas, such as the bottom gallery or the lowest inspection gallery, should be so designed that they follow the principal stress trajectories (Fig. 5.39). Thereby, unwanted additional tensile stresses can be avoided, which otherwise would be generated due to the required deflection of the compressive stress trajectories (Stäuble 1993).

Non-linear calculations assuming an open joint at the upstream dam base and maximum water pressure in the joint have shown that the deformation behaviour and the stresses of the dam body (Fig. 5.38) are only slightly affected.

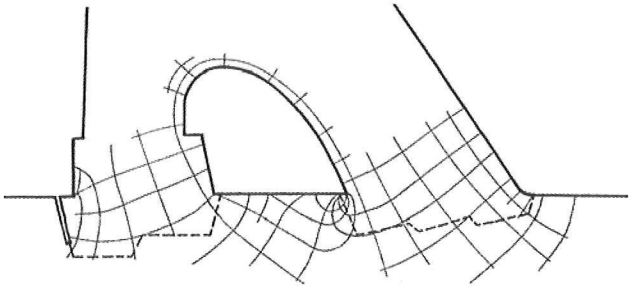

Fig. 5.38: Principal stress trajectories with the load case dead load + water pressure (Steinböck 1959).

5.6.4 Summary

To evaluate the load-bearing capacity of arch dams, it is common practice worldwide to use the ratio of compressive strength to principal compressive stress. A more rigorous definition is based on the crack resistance, evaluation of which must take the principal tensile stresses into consideration. In the prototype, the load-bearing capacity of the statically highly indeterminate system will still be significantly higher due to the load and stress transfers into less stressed areas.

However, in order to avoid seepage, special care must be taken to prevent cracking or opening of joints in the area of the upstream dam base by carrying out appropriate constructional measures.

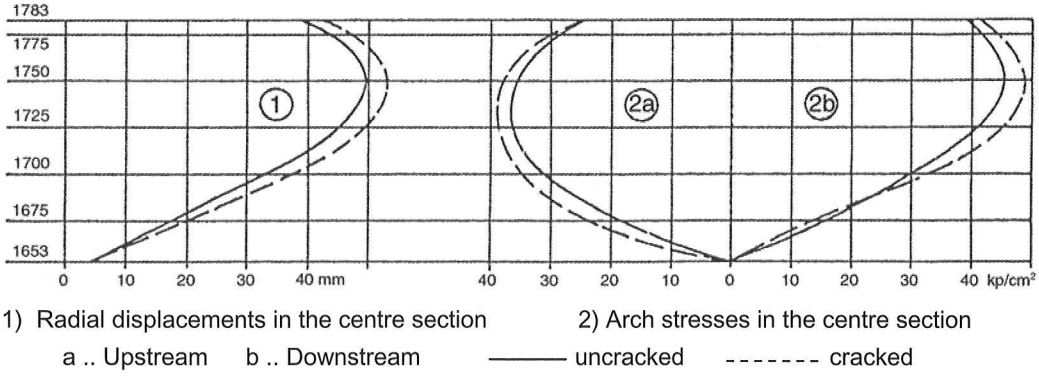

Fig. 5.39: Schlegeis arch gravity dam, influence of a joint open towards the upstream face on the deflections and arch stresses in the centre section [*35*].

Fracture-mechanical methods, however, cannot be used either to predict the formation of initial cracks or to assess their influence on the stability of the structure. Fracture-mechanical methods can only be used to determine, whether an existing crack will have the tendency to lengthen under given conditions and, if so, in which direction lengthening will occur. Therefore, it would be more exact to refer to these methods as 'Analytical Crack Control' (ACC).

Particularly with high arch dams, the tensile stress considered allowable is decisive for the required concrete volume and thus for the construction costs. It is, however, also of particular importance due to the low absolute distance to the tensile strength. Therefore, the allowable principal stress in the upstream region near the abutment should be defined, taking into consideration a possible penetration of water into initial cracks [106]:

$$\sigma_{t,all} = \beta_t - 1 - w - \sigma_r - 0.1\sigma_c \quad \text{in N/mm}^2$$

where

- $\sigma_{t,all}$ Allowable principal tensile stress,
- β_t ... Tensile strength of the concrete,
- 1 ... Safety margin to the fracture strength, (corresponds to 100 m on the water column),
- w ... Water pressure at the considered level (only at the upstream face and dam base),
- σ_r ... residual tensile stress due to hardening of the concrete
- σ_c ... Simultaneous principal compressive stress.

For the determination of the principal tensile stress at the abutment within the concrete body, the uplift pressure and, as a radial normal stress, a possible residual tensile stress resulting from the construction period must be taken into consideration as well.

With arch dam heights above 100 m,

$$w + 1 + \sigma_r + 0{,}1\sigma_c > \beta_t \text{ can result,}$$

so that a compressive stress at the considered point can become necessary in order to definitely prevent cracking.

5.7.2 Structural design at the upstream dam base

Particularly for high arch dams, the basic requirement for this maximally stressed area is watertightness even, if unexpected tensile stresses or cracks should occur. The permeability of the rock underground is dependent on the stress or deformation state (Bellier 1967). Therefore, to prevent seepage, the stress or deformation state in the plane of the grout curtain should not fall below the level present at the time of completion of the injection process assuming a normal load case. If the grout curtain should be installed in an area which is affected as little as possible by stress changes, there are three possibilities:

- Under the dam in the zone of the zero line, i.e. in the upstream third section of the dam.
- Under a pedestal separated from the dam (e.g. Verwoerd, SA), which requires at least in part the installation of a perimetral joint with a respective seal.
- Upstream of the dam, which requires the installation of a concrete apron (Fig. 5.35) connected to the dam body by a reliable durable seal. Using this design, the uplift pressure can be considerably reduced.

Which design is used, must be decided in each individual case; both safety-relevant and economic aspects will have to be considered. In any case, the assumptions for the uplift pressure will have to take into consideration the structural design of the region around the upstream dam base. In addition, the exceptional load case of a sealing element failure and its effects must be examined.

5.7.3 Model tests

Since the 1950s, model tests for arch dams have been carried out using various scales (1:100 to 1:500) and model materials (various casting resins and gypsum-kieselghur mixtures). Selection of the model materials must take into consideration not only the deformation modulus, but also the transverse strain and tensile strength.

The usefulness of model tests for checking the static analysis of arch dams with their spatial load-bearing performance has decreased in importance in the age of computers, which no doubt require less simplifications thereby enabling much more realistic calculations of the arch dam shell. In addition, using models, even today it is hardly possible to:

- Simulate the structure of the underground of the dam realistically.
- To determine the influence of the joint water pressures or uplift pressure.
- The effects of temperature changes.
- To enable the consideration of the effect of the dead load on independent blocks, special measures are necessary.

In addition, model tests allow an increase in the water load; however, only the influence of cracks on the stiffness, but not the water pressure in the cracks, is taken into consideration in the determination of the ultimate load. This, however, presupposes the use of a model material which reproduces the concrete properties as realistically as possible in the model scale.

5.8 SUMMARY

The design of arch dams requires the close cooperation of experts from various fields, such as geology and rock mechanics, concrete technology, static and dynamic analysis, test and measurement techniques. The reciprocal coordination of these special fields and incorporation of the individual results in the overall design is of particular importance.

The geological and rock-mechanical investigations can only be checked when additional findings gained during construction are available (see section 6.1). On principle, rock-mechanical calculations should only be evaluated based on the results of parameter studies, since they can only be determined with a certain degree of variation.

For the analysis of arch dams, only methods or software should be used which have been proven to reflect the actual conditions by comparing them with the measurement results on the prototype.

The structural design of arch dams at the abutment area, particularly the location of the grout curtain, must be examined in detail as well. The influence of the periodic deformation changes of the underground on the grout curtain due to reservoir level variations can be reduced by means of a - partial - perimetral joint or by shifting the grout curtain towards the upstream end of a concrete apron.

The monitoring systems, which constitute an essential part of the project, must guarantee the permanent supervision of the design criteria and thus the constant safety of the dam.

REFERENCES

Bellier J.: Le Barrage de Malpasset. Traveaux 1967.

Carrère A.: Arch dams, uplift and design criteria: are heel base joints useful ? Hydropower and dams, November 1994.

Casagrande A.: Control of seapage through foundations and abutments of dams. First Rankine Lecture, Geotechnique 11, 161-183, 1963.

Dolcetta M., Marazio A., Bavestrello F.: The Peripheral Joint at Arch Dams. Felsbau 1991, Heft 2.

Fanelli M.: Analysis of arch dams by the principle of minimum potential energy. Theory of Arch Dams, Southampton 1964, Pergamon Press.

Federhofer K.: Über die Eigenschwingungen eines dünnwandigen, allseits von Flüssigkeiten umgebenen Hohlzylinders. Sitzungsberichte der mathem. -naturwiss. Kl., Abt. 2a, Bd. 172, Heft 5 u. 6

Fishman Yu.A.: Investigation into the mechanism of the failure of concrete dams rock foundation and their stability analysis. ISRM, 1979, Vol. 2, 147-152.
Analysis of displacements of concrete shear blocks and concrete dams on rock foundation by field measurement results. Field Measurements in Geomechanics, Zürich, Vol. 2, 865 - 874, 1983.

Großmayer R.: Grundlagen einer stochastischen Theorie zur Ermittlung des Erdbebenrisikos von Bauwerken. ÖIAZ 1978.

Gumensky D.B.: Earthquakes and earthquake resistant design. American Civil Engineering Practice, Vol. 3, John Wiley & Sons, 1957.

Henny D.C.: Classification, selection and adaption of high dams. ASCE, Papers and Discussions, 11, 2327-2336, 1929.

Hoek A.: The Challenge for Input Data for Rock Engineering. ISRM News Journal, Vol. 2, Nr. 2, 1994

Huber B., Linsbauer H.N.: Erdbebenschäden an Talsperren, selektive Beurteilung. Felsbau 1996, H. 5.

Jörgenssen : Über Gleichwinkelmauern. Deutsche Wasserwirtschaft 1938, Heft 2

Jurecka W.: Beiträge zur Berechnung von Bogenstaumauern nach dem Lastaufteilungsverfahren. Dissertation TH Graz, 1949.

Kaech A., Lombardi G.: Alcune considerazioni sulle dighe ad arco. Schweizer Bauzeitung 1953, Nr. 38.

Kansai Electric Power Company: Static and Dynamic Behaviour of Kurobe Dam, 1988

Kettner R.: Zur Formgebung und Berechnung von Gewölbemauern. Schriftenreihe 'Die Talsperren Österreichs, Heft 8, 1959.

Lenhardt W.: Erdbebenkennwerte zur Berechnung der Talsperren Österreichs. Bericht an das BMfLF, Öst. Staubeckenkommission, 1996. Unveröffentlicht.

Leroy M.: Le calcul des barrages voutes par les derniers perfectionnements de la methode du Trial Load. Publications de la Faculté des Sciences Appliquées de l'Université de Liége, n° 25, 1971.

Linsbauer H.: Fracture mechanical models for characterizing crack behaviour in gravity dams. 15th ICOLD Congress, 1985.

Lombardi G.: Querkraftbedingte Schäden in Bogensperren. Vortrag vor dem Schw. Nat. Kom. für große Talsperren in Bern, 1987; Wasser, Energie, Luft 1988.

Londe P. et al.: Stability of rock slopes, a three dimensional study. Journal of the soil mechanics and power division, ASCE, SM 1, Jan. 1969.

Londe P. et al.: Stability of rock slopes, graphical methods. Journal of the soil mechanics and power division, ASCE 96, pp 1411 - 1434.

Ludescher H.: Felsmechanische Untersuchungen anlässlich der Verstärkung der Kölnbreinsperre. Felsbau 1991, Heft 2.

Marazio A., Dolcetta M., Bavestrello F.: The Peripheral Joint at Arch Dams. Felsbau 1991, Heft 2.

Mladyenovitch V.: Déformation des fondations de barrages. Travaux, Nov., Dec. 1966; Paris

Obernhuber P. et al: Reservoir - Dam - Soil Interaction, a comparative Study. Proc. of Int. Conf. on Soil Dynamics and Earthquake Engineering. Greece, May 1995.

Rescher O.J.: Zur Statik der Gewichtsstaumauern. 1965

Rescher O.J.: Arch dams with an upstream base joint. Water Power, March 1993.

Ritter H.: Die Berechnung von bogenförmigen Staumauern. Dissertation Karlsruhe 1913.

Ritter M.: Temperaturverlauf und Wärmespannungen in Mauern bei oszillierenden Außentemperaturen. 7. Bd., Abhandlungen IVBH, Zürich 1943/44. Int. Ass. for Bridge and Structural Engineering Publications.

Sägesser R.: Neue Erdbebenrisikokarten der Schweiz. Mitteilungen der Schweizer Gesellschaft für Boden und Felsmechanik Nr. 97, November 1977, Bern.

Schüller H.: Die Limbergsperre. Festschrift anlässlich der Fertigstellung der Hauptstufe des Tauernkraftwerkes Glockner - Kaprun, TKW 1951

Serafim L.: Complete adjustment Method in analysing arch dams. ASCE Proceedings ST 8, August 1970.

Steinböck W.: Die Staumauer am großen Mühldorfersee. Schriftenreihe 'Die Talsperren Österreichs, Heft 10, 1959.

Stäuble H., Wagner E.: Comments on the arrangement of grout curtains with special regard to uplift pressures in case of large Dams. Int: Workshop on Dam Safety Evaluation, Grindelwald 1993

Tremmel E.: Zur elementaren Berechnung von Gewölbemauerlamellen veränderlicher Dicke. Festschrift Oberstufe des Tauernkraftwerkes Glockner Kaprun. TKW 1955.

Tremmel E.: Estimation of the Influence of forced Vibrations on the stresses imposed on Arch Dams. ICOLD 1961, C 14.

Tonini : Automation of arch dam analysis. Theory of Arch Dams, Southampton 1964, Pergamon Press.

U. S. Bureau of Reclamation: The Trial Load Method, Denver 1938.

Westergaard H.M.: Water pressures on Dams during earthquakes. Transactions ASCE, Vol. 98, 1933, pp. 418-433.

Yamazumi A.: Influence of the Hyogoken-Nanbu Earthquake on Japanese Dams. Felsbau 1996/5.

Zangar C.N.: Hydrodynamic pressures on Dams due to horizontal earthquake effects. Engineering Monographs Nr. 11, USBR, Denver, May 1952.

Zenz G. et al: Nonlinear Earthquake Analysis of Wiederschwing Arch Dam. IACMAG'97, Vol. IV, Wuhan, China, 1998.

Zhang X.: Vibration Response on Arch Dams with Time - Lag between abutments. Int. Symp. on Earthquake and Dams. Beijing 1987.

6. PLANNING TASKS FOR THE CONSTRUCTION PERIOD

6.1 GENERAL

From the technical point of view, quality management is of particular importance and requires continuous surveillance of site operations, whether:

- The design assumptions for the rock fabric model and elements of the underground are being sufficiently verified by additional geological findings during excavation, boring and grouting of the grout curtain. Otherwise, the project engineer may have to review whether the project must be adapted to the altered conditions.
- A very careful excavation process could prevent loosening of the dam underground.
- Grouting of the grout curtain has resulted in the required water tightness of the underground.
- The preparation plant for the aggregates can guarantee the required sieve curve and the optimal grain shape and whether the coarse grains show signs of abrasion after preparation, in which case provisions for recleaning may have to be made.
- During the production of fresh concrete, the on-site batch plant can ensure that the dosage variation of the individual components is as low as possible so as to guarantee uniform concrete quality.
- The horizontal construction joints are treated according to the guidelines so as to guarantee an optimal bonding between old and new concrete.
- On the block, the fresh concrete achieves optimal compaction.
- The allowable maximum concrete temperature is not exceeded.
- Cracks have formed, particularly at the concrete - rock interface.
- The planned concrete temperature at the time of block joint injection is not exceeded.
- During block joint injection, the prescribed maximum grout pressures are not exceeded and/or no undue block joint expansions have occurred.

Below, only such problems will be discussed which relate to the design assumptions for site operations and surveillance.

6.2 CONCRETE

6.2.1 General

Even if in laboratory tests the aggregates used in concrete development are taken from the same source as for dam construction, the, by several powers of ten, higher volume requirement as well as the industrial preparation on site will create entirely different conditions than in the laboratory. At large alpine construction sites, where concreting work can only be carried out during the summer half-year, it has proved successful to perform a very closely monitored test run of the entire construction site equipment in the autumn prior to the first actual concreting season, to produce several 10,000 m³ of trial concrete while also monitoring whether the required parameters of the concrete have been attained. During the winter break, based on the experience thereby gained, the adjustment of the construction site equipment or the composition of the concrete can be improved, if required.

6.2.2 Monitoring of the crack resistance of green concrete

During pouring, monitoring must ensure that the allowable maximum temperature of the concrete is not exceeded. A direct verification of the absence of cracks by means of core drilling radial at the dam base a may be required in individual cases.

Observing the required maximum temperature

The maximum temperature of concrete during curing may be decreased in several ways: [67]:

- Concrete-technological measures, such as cool binders or low dosage (see section 4.2).
- Constructional measures, such as:
  - A longitudinal joint for larger dam thicknesses; this, however, involves several difficulties, such as additional expenditures for formwork, the delayed pouring process and subsequent grouting of the additional construction joints, as well as the risk of joint lengthening due to cracking at their ends.
  - Reduction of the pouring lifts, which is particularly useful in the first layers at the rock surface (Fig. 6.1).
- Reduction of the pouring temperature on site (precooling):
  - Sprinkling of the prepared aggregates, to keep heating due to sunlight exposure at a minimum. At the Zillergründl site (a.s.l. 1,750 m), the pouring

temperature could be reduced by approximately 1° to 2° in fair summer weather.

- Partial replacement of the mixing water by the addition of flake ice, taking the overall water quantity in the fresh concrete and the characteristic moisture of the aggregates into consideration. Thereby, the pouring temperature could be reduced by up to 2° per 10 kg of ice added per m³ of fresh concrete.

At the construction site of the Zillergründl arch dam for example, using these measures, pouring temperatures of 6°C to 10°C could be maintained in the summer months.

– Reduction of the temperature increase during hardening (postcooling):

– Reducing the height of the pouring lifts by half (from 3 m to 1.5 m) at air temperatures around 5°C resulted in a decrease of the maximum concrete temperature by 6°C; at air temperatures around 15°C, however, only by 2°C (Fig. 6.1).

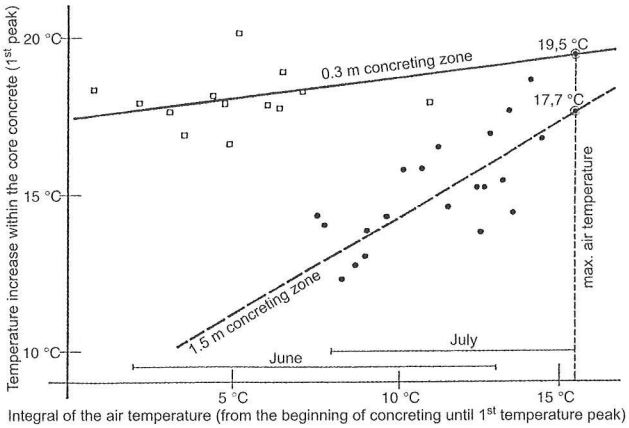

Fig. 6.1: Influence of the air temperature on the temperature development of core concrete.

- Installation of an internal cooling system. As experience has shown, the temperature peak in green concrete can thereby be reduced by approximately 2°C and the additional heat build-up after pouring of the subsequent lifts can also be absorbed thus achieving an overall temperature decrease of 3 - 4° C (Fig. 6.2).

The loops of the cooling pipes of the internal cooling system should be fed whenever possible directly at the lift centre. In this area as well, their spacing should be narrower than near the dam surfaces. The difference between the water temperatures at the inlet and outlet as a gauge of the heating carried off should be measured at least in some of the lifts in

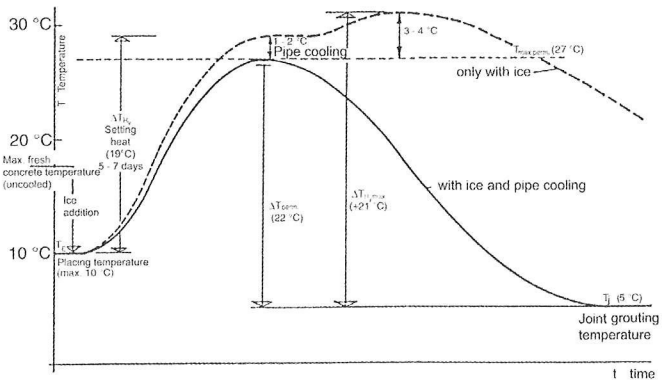

Fig.6.2: Temperature variation in the core concrete of the Zillergründl arch dam (Huber 1987).

which the concrete temperatures are observed as well. The in most cases large temperature gradient to the cooling pipes can cause short cracks; these, however, will reclose and subsequently heal after the cooling has been turned off and the temperature equalization attained.

From the extensive measuring programme for testing the theoretical assumptions (see section. 4.2.4), testing of the crack resistance is described below in more detail. During concreting of the Zillergründl arch dam, one measuring line each was installed in two lifts with lift heights of 1.5 m and 3.0 m in the vicinity of the dam base in order to measure the temperatures and linear expansions of the concrete. The measurement of the maximum linear expansion during the first 15 months (Fig. 6.3) showed its variation along the measuring length and the variation over time at one measuring point (Fig. 6.4). The difference between the measured and the calculated linear deformation corresponded to the restraints and remained considerably lower than the fracture strain determined in tests, so that cracking could be excluded. These results were confirmed using core drilling and in water pressure tests with uraninite water.

6.2.3 Checking of the parameters of the structural concrete during and after pouring

To be able to produce concrete of uniform quality during the entire construction period, the constant quality of all components and the observance of the prescribed dosage must be continuously checked (Huber 1987).

The following aspects should be checked:

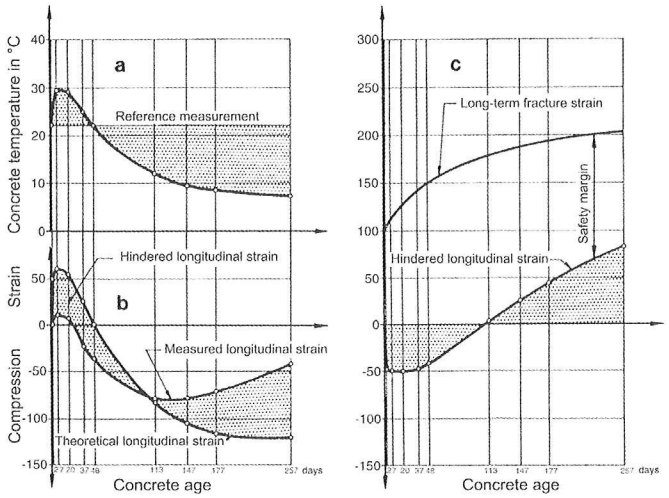

a ... Concrete temperatures b ... Strains
c ... Comparison of fracture strain to restrained linear deformation

Fig. 6.3: Zillergründl arch dam, variation over time of the strains at one measuring point.

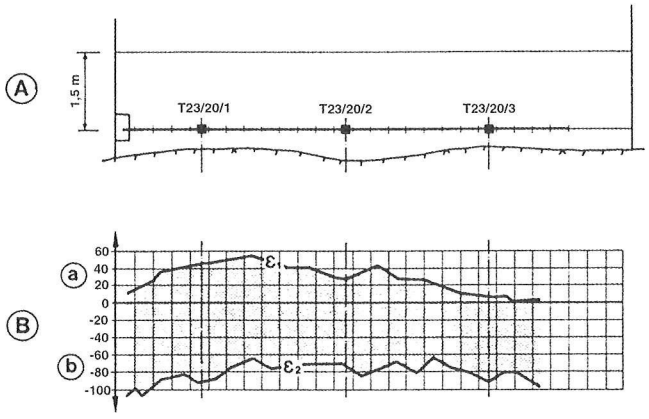

A ... Measuring line B ... Maximum strains
a ... Compression b ... Strain

Fig. 6.4: Zillergründl arch dam, maximum strains along a measuring length.

– Age and storage of all delivered binders as well as strength and heat development must comply with the specifications.
– Optimal adjustment of the aggregate preparation plant to ensure the prescribed grain shape and sieve curve, particularly in the fine sand range.
– Continuous checking of the dosage of all concrete components. This is facilitated by using modern concrete mixing plants fitted with electronic weighing and dosage devices, and devices that automatically measure the moisture of the aggregate components to ensure the required W/C-ratio, enabling a continuous comparison of required to actual values.

6.2.4 Checking of the parameters of ready-mixed concrete

During the entire concreting period, all relevant parameters for the determination of the composition of concrete during concrete development must be checked:
– Strength and deformation properties must be tested using the same test specimen sizes and under the same conditions as during concrete development. In addition, the development of these parameters should be monitored over a longer period than was possible during concrete development. Finally, the strength development should be tested as well using drill cores from the structural concrete (horizontal and vertical); the test results should be compared to the laboratory test results taking the dependency of the results on the size, shape and direction of the test specimens into consideration.
– Water tightness and frost resistance must be tested as during concrete development.

6.3 POURING ZONES SEQUENCE

6.3.1 Introduction

One means of rationalizing construction is through the construction site equipment, which determines the pouring speed and thus the construction period. The equipment includes:
– Aggregate preparation and onsite batch plant.
– Cable cranes.
– Devices for the formwork and compaction of concrete.
Possibilities for the reuse of cable cranes are very limited. To optimise various design variations of cable cranes, their efficiency under the given conditions and locations, as well as other influencing factors, a computer programme was developed.
Based on this, not only the shortest possible concreting period, but also the most favourable sequence of the pouring blocks can be determined. In addition, it facilitates an improved adjustment of the required efficiency of the most important devices in the production chain.

6.3.2 Factors influencing the construction period

Assuming that the shape, size and topographical location of the concrete dam have been determined, a

few structural details still remain to be clarified that can influence the construction period. Their design, however, can only be varied within certain limits.
These structural requirements can be subdivided into:
– Concrete-technological requirements concerning the prevention of thermal cracking and allowing for only a very narrow margin of play. They include:
  • Spacing of the contraction joints.
  • Height of the individual pouring lifts within the blocks.
  • The respective permissible maximum and minimum differences in height between two adjacent blocks.
  • The minimum and maximum interval between two successive pouring lifts.
– Requirements dependent on the construction site equipment for concrete placing. These allow for a larger scope of design variations and include the choice of:
  • Number of cable cranes, parallel or radial travelling.
  • Location of the cable crane trackage relative to the dam.
  • Topographical location and height of the pouring quay.
  • Load-carrying capacity of the cable cranes and/or contents of the pouring buckets.
  • Possible minimum distance between to adjacent cranes.
  • Working speed of the cranes (travelling speed of the crane bridges, lifting of empty buckets and lowering of full buckets).
– Requirements more or less predetermined by the working conditions on site. These include:
  • Date at which the rock foundation is ready for the first pouring lift.
  • Number of cable crane working hours during a 24-hour day.
  • Sequence of working days and days off, revision periods, concreting and stop periods, predetermined limitation of the dam height at the end of each working period.

6.3.3 Programme organisation

The programme was developed as a deterministic simulation programme based on the assumption that both preparation and batch plant have sufficient capacity and the cable cranes are capable of simultaneous travelling and lifting or lowering of the bucket. Taking all given restrictions into consideration, the pouring sequence and thus the construction period can then be calculated; for specific dates, the respective concreting stage attained can be printed out. If various possible pouring lifts still remain, either the lowest lift or the lift requiring the most concreting work can then be chosen.
At the end of each working period, the time needed to set up the formwork and to pour the concrete as well as the concrete volume placed are printed out.

6.3.4 Example

The programme was first used in the concreting of the Schlegeis arch gravity dam, 1969 - 1971. The results of a variation study are summarized in Fig. 6.5. Construction of the dam, which has a height of 131 m and a crest length of 725 m, required a concrete volume of 980,000 m³. The chosen lift height was 2.45 m, the waiting time between when pouring of the lower lift ended and pouring of the lift above began was 3.5 days. Double this waiting period was required for the lifts poured directly onto the rock.
The variation study revealed that (Fig. 6.5):
– Neither the waiting period nor a block width variation within realistic limits had a significant effect on the overall concreting period.
– An increase in the lift height from 2.45 to 3.0 m would not have considerably changed the concreting period even if the waiting period had been extended from 3.5 to 4 days.
– Installation of 3 instead of 2 cable cranes of the same unit capacity would not have resulted in a significant reduction of the concreting period due to the increasing influence of 'unfeasible' areas.
– A significant reduction of the construction period could have only been achieved by increasing the bucket content from 6 m³ to 9 m³. This, however, would have required a larger preparation and mixing plant.
Similar studies were later carried out for the Kölnbrein (height 200 m, concrete volume 1.56 million m³) and Zillergründl (height 185 m, concrete volume 1.35 million m³) arch dams. Also in the case of these dams, the results of the variation studies

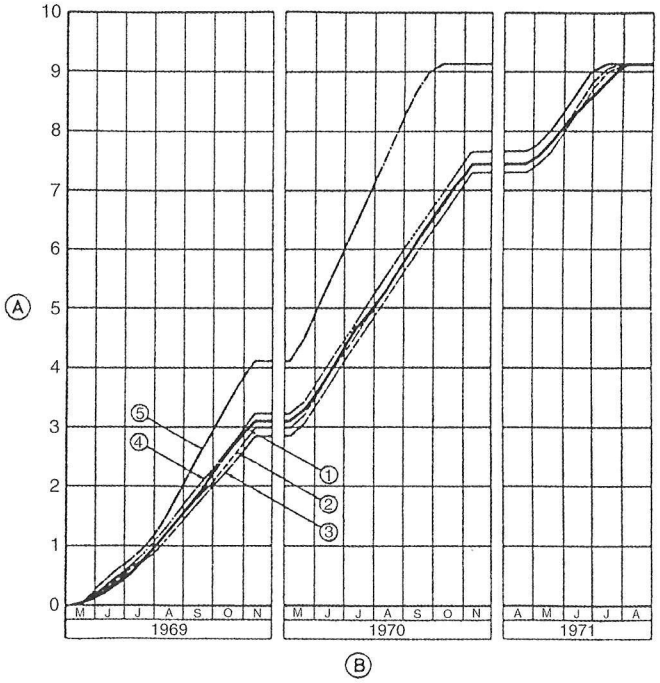

A ..... Concreting output 100,000 m³
B ..... Concreting years
1 ..... Actual concreting output
2 ..... Calculated concreting output (under the same assumptions)
3 ..... Waiting period 4 days
4 ..... Lift height 3 m
5 ..... Bucket content 9 m³ instead of 6 m³

Fig. 6.5: Variation comparison for the concreting of the Schlegeis dam [*30*].

performed in the course of reviewing offers were confirmed during construction.

With the higher dams, the optimum height of the pouring quay was slightly below the crest height. The attained rising speeds of the four highest Austrian arch dams are listed in Fig. 6.6.

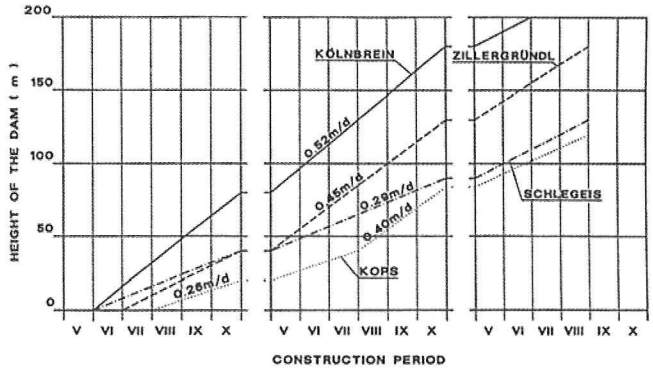

Kops (1965 – 1968),
Schlegeis (1969 – 1971),
Kölnbrein (1974 – 1977),
Zillergründl (1984 – 1987)

Fig. 6.6: Mean rising speed of the pouring level at Austrian arch dams [*86*].

6.4 GROUTING OF CONTRACTION JOINTS

6.4.1. Introduction

Concrete, particularly at a young age, is subject to volume decreases due to cooling during and after hardening as well as shrinkage, the restraint of which corresponds to strain or tensile stresses in the concrete. All concrete structures are subdivided into pouring lifts in order to ensure that these stresses remain below the fracture strain and/or tensile strength.

Therefore, also mass concrete dams are subdivided into vertical blocks. Formerly, cooling joints of 0.5 – 1.0 m width were often installed, which were filled with concrete after cooling. In recent decades, however, it has become common practice to concrete the intermediate blocks onto the previously concreted blocks. The radial contraction joints are installed at a spacing of maximally 20 m and are in many cases fitted with vertical ribs that can prevent mutual radial displacements but not vertical displacements during construction.

6.4.2. Influences on the block joint width

Volume decrease of concrete

The temperature-dependent volume decreases of concrete result from the temperature difference between the maximum temperature during curing and the mean annual temperature. The thermal expansion coefficient usually lies between α_T = 0.5 and 1.2 x 10^{-5} per °C and is dependent above all on the mineralogy of the aggregates.

The difference between the maximum temperature during curing and the mean annual temperature lies, as previous experience has shown, between 20 and 30° C, so that the reduction of the block widths is 0.10 – 0.36 mm per m width. The expansion of the subsequently concreted blocks during heating is, however, restrained by the previously concreted adjacent blocks, so that in most cases only a part of the above-mentioned temperature differences causes tensile stresses.

The volume decrease due to shrinkage results above all from the drying of the concrete, which is naturally low with mass concrete structures. Tests have shown that in these cases shrinkage is maximally defined by α_S = 5 x 10^{-5}.

Deformations during construction

In arch dams with vertical curvature, compressive and bending stresses are generated due to the dead load; these are generally determined in static analysis. The displacements of the independent concrete blocks during pouring - in the lower part of the dam upstream, in the upper part, depending on the curvature, downstream - that result in a change of the block joint widths are usually not determined, since they are not of importance for the later behaviour of the dam during operation.

If the reservoir is already filled during concreting of the dam, but again emptied before grouting of the block joints, additional displacements will occur upstream relative to the concreting date, which will result in larger block joint widths. To date, these displacements have only rarely been measured, since measuring devices for this purpose were only available in special cases during concreting.

During concreting of dams, the vertical compressive stresses due to the dead load generate horizontal transverse strains, thereby opposing the expansion of block joints.

Impoundage causes compressive stresses in the arch that completely disappear after emptying of the reservoir. After drawdown, a residual compression of the concrete results, that comprises approximately 25 % of the overall deformation and contributes to the expansion of the block joints.

The width of block joints can also be increased by a, - ignored in the following -, residual horizontal component of the abutment displacement that increases with the storage periods, if it is not compensated by a corresponding displacement of the dam blocks in the downstream direction.

Example (Widmann 1990)

The Kölnbrein arch dam shall serve as an example for approximately assessed influences on block joint widths:

– Cooling down to the joint closing temperature results in a volume decrease and thus in an expansion of the block joint widths. If the effective cooling for expansion is defined by $\Delta T = 20°C$, and the thermal expansion coefficient for gneiss aggregates by $\alpha_T = 0{,}8 \times 10^{-5}$, a shortening of

$$\Delta T \times \alpha_T \times L = 20 \times 0.8 \times 10^{-5} \times 20 \times 10^3 = 3.2 \text{ mm}$$

results for block lengths of 20 m.

At the foundation area, the block joint widths cannot expand due to the restraint of the strains. At the measuring level of the inspection gallery V (distance from the foundation maximally ½ d_a), the expansion will reach approximately half this value.

For mass concrete, the volumetric changes due to shrinkage may be considered negligible, particularly within the blocks and thus also at the measuring point of the block joint widths.

The vertical dead load (Fig. 6.8) causes a transverse strain which results in a reduction of the block joint widths. Based on a deformation modulus of $V = 13$ kN/mm², calculated from the horizontal displacements for initial loading (Fig. 8.15), and a transverse strain of $\nu = 0.15$, the transverse strain in the inspection galleries with a block length of 20 m is given by:

$$\varepsilon_q = \frac{\sigma}{V} \cdot \nu \cdot L$$

at measuring levels	KG1	KG2	KG3	KG4	KG5
the mean vertical compressive stress is in N/mm²	0	1.4	2.1	2.3	4.0
the transverse strain	0	-0.3	-0.5	-0.6	-0.9 mm

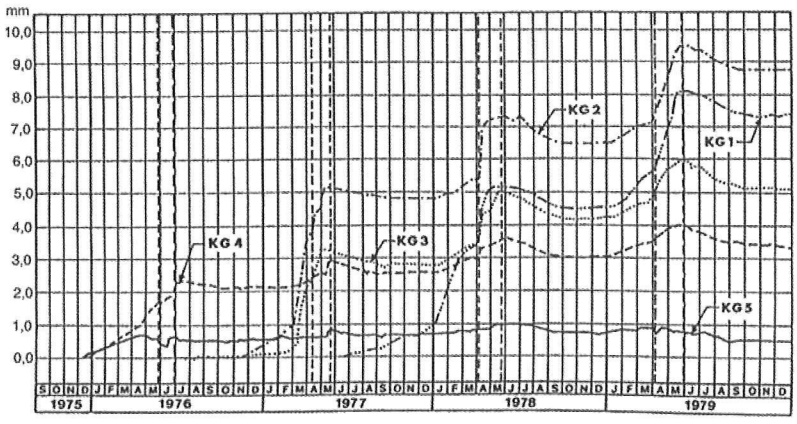

Fig. 6.7: Kölnbrein arch dam, measured mean block joint widths at the measuring levels.

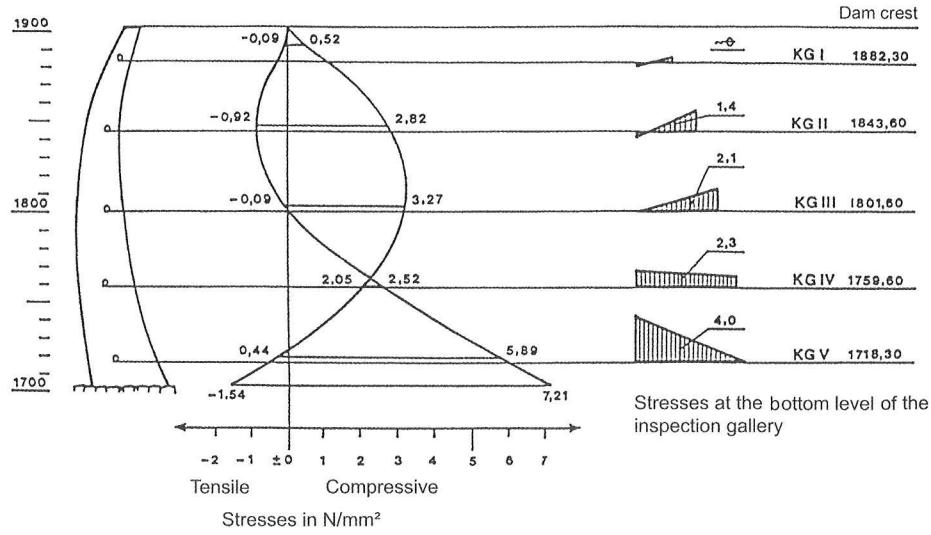

Fig. 6.8: Kölnbrein, dead load stresses in the centre block.

– Full storage in 1979 up to the top water level of 1,902 m caused horizontal compressive stresses and/or compressions of the concrete (Fig. 6.9). If the residual deformation under initial loading is assumed to make up 25 % of the overall deformation, in accordance with the results of concrete tests, the mean shortening of the blocks in the horizontal tangential direction is calculated from:

$$\varepsilon_\sigma = \frac{\sigma}{V} \cdot 0.25.L$$

at measuring levels	KG1	KG2	KG3	KG4	KG5
with a compressive stress σ_m in N/mm² of					
	5.0	7.1	6.4	4.8	2.2
a block joint expansion in mm of					
	1.9	2.7	2.5	1.9	0.8.

At the time each level is concreted, the block joints are closed due to the concreting of the subsequently concreted blocks. Since the simultaneous intermediate storage causes a horizontal deformation of the dam body towards the downstream face, drawdown results in a displacement of the dam body in the opposite direction up to the position corresponding to the bending line of the block, assumed to be independent due to the dead load. Only the part of the dead load that lies above the respective pouring level has an effect on these deformations (Fig. 6.10). If the radial displacement of the centre block until grouting of the block joints can be assumed by approximation to equal the lengthening of the arch

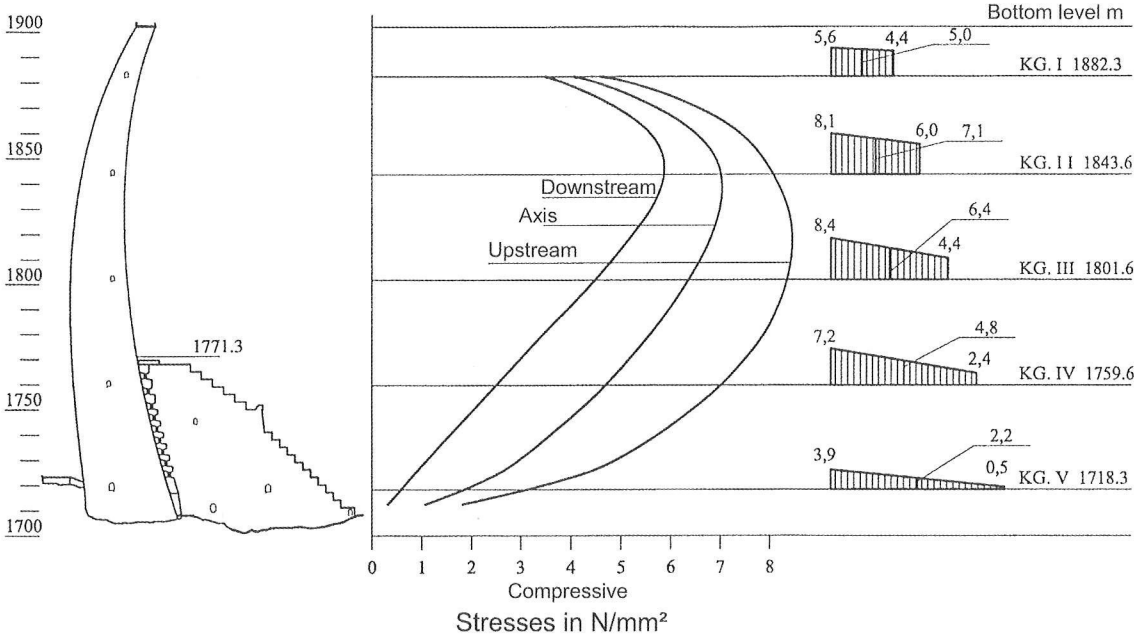

Fig. 6.9: Kölnbrein, arch stresses at full storage 1979.

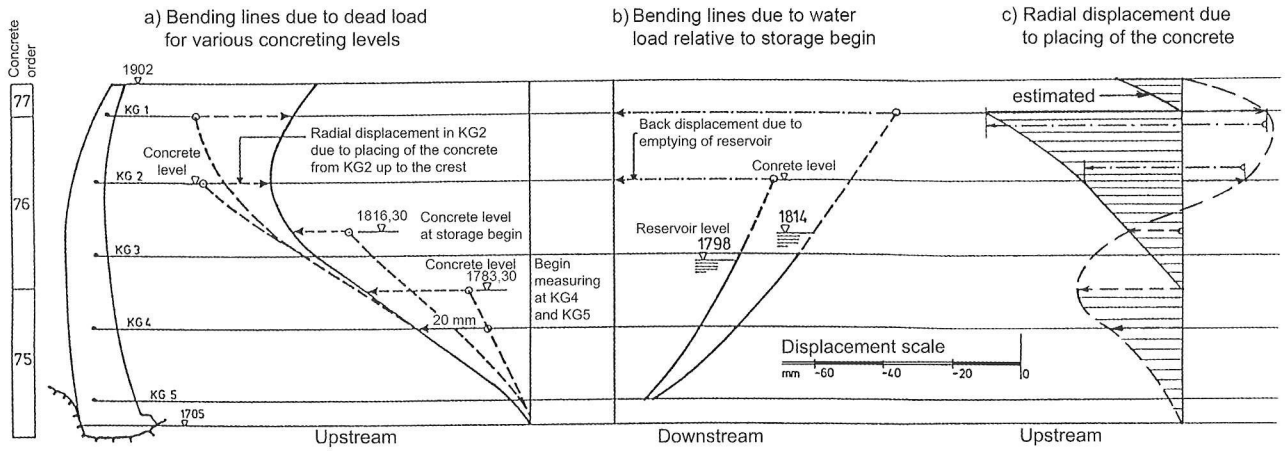

a) Bending lines due to the dead load of the concrete block below the considered level

Radial displacement due to the dead load of the concrete block above the considered level

Bending line due to the dead load of the entire block

b) Measured back displacement due to emptying of reservoir

c) Radial displacement of the blocks during concreting and the moment of joint grouting.

Below 1,816.3 m, the concrete height at storage begin, only the radial displacement due to the dead load below this level, must be taken into consideration; above this level also the displacement during emptying of reservoir.

Fig. 6.10: Radial displacements in the centre block of the Kölnbrein arch dam during concreting due to the dead load until grouting of the block joints in 1978.

and thus the sum of the block joint widths changes, the values listed below result:

at measuring levels	KG1	KG2	KG3	KG4	KG5
according to a radial displacement of					
	60	28	26	20	4 mm
with a block joint number of					
	28	24	20	15	10
a mean change of block joint widths					
	2.1	1.2	1.3	1.3	0.4 mm

It must be pointed out that the block joint widths were only measured at one point of the cross section, which cannot be representative of the overall cross section. With this reservation, the following conclusions can be drawn:

The lower measured values in the inspection galleries 4 and 5 may be attributable to the fact that the joint expansion due to the residual compression of the arches during the storage periods was compensated for by the radial displacement of the conical blocks at the dam base.

The higher measured values in the inspection galleries 1 and 2 confirm that the required arch prestressing to improve the arch effect was attained, but decreased later due to the residual compression of the concrete.

Table 6/1: Theoretical and measured block joint widths.

	Control gallery				
Horizon	1	2	3	4	5
Calculated estimation of the block width due to					
Cooling	3,2	3,2	3,2	2,4	1,6
Transverse strain due to dead weight	0	-0.3	-0.5	-0.6	-0.9
Concreting and impounding	2.1	1.2	1.3	1.3	0.4
Permanent widening due to arch compression	1.9	2.7	2.5	1.9	0.8
Sum	7.2	6.8	6.5	5.4	1.9
Measured widening of the block joints					
Estimated widening until start of measurements	-	-	-	0.5	1.0
Measured widening (Fig. 6.7) max	8.1	9.4	6.0	4.0	1.0
permanent	7.3	8.7	5.1	3.4	0.6
Sum max	8.1	9.4	6.0	4.5	2.0
Sum permanent	7.3	8.7	5.1	3.9	1.6

The measured negligible vertical displacements at the foundation area - upstream settlements, downstream liftings - confirm as well that prestressing of the upper dam third section did not result in a change in the vertical abutment stresses and deformations.

6.4.3. Statics of block joint grouting

Since complete grouting of the entire joint area is required to ensure the monolithic effect of the arch dam shell, the grout pressures must not fall below specific limits. On the other hand, the additional loads acting upon the blocks, due to the grout pressure effective in the joint, limits the dimensions of the sections that can be grouted in one step. The static stresses acting upon the dam blocks due to grouting of the block joints are caused:

– In the tangential direction, if the adjacent joints are open or subjected to a lower pressure than the joint to be grouted.

– In the radial direction, if two adjacent joints are grouted simultaneously or the adjacent joints are filled with water or with grout that has not yet hardened.

The stresses considered to be allowable for these loads define the upper limit of the allowable grout pressures, while their lower limit is determined by the requirement that complete grouting of the block joints must be ensured. This lower limit is defined, on operational grounds, by the pressure triangle resulting from the height of the section and the specific weight of the grout. This load is overlaid by a uniform overpressure that ensures that the grout spreads over the entire joint surface and that it can be measured at the injection section's upper vents, which must be closed immediately after the grout has first begun to flow out.

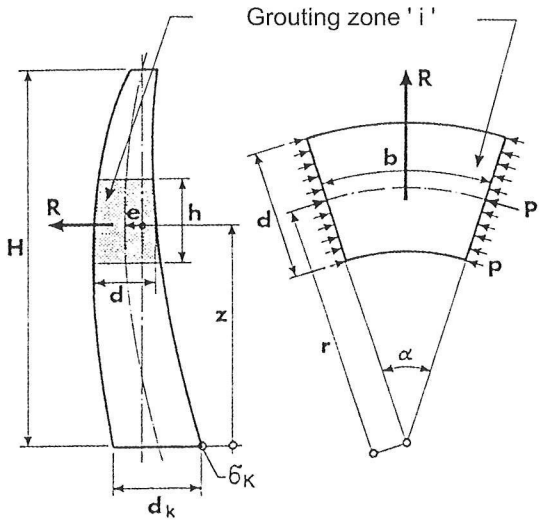

Block width at the cylinder of reference b_0

at level z ... $b_z = b_0\,\beta_z$ mit $\beta_z = \left(\frac{r_z}{r_z - e_z}\right)$

Fig. 6.11: Primary injection, radial stresses.

Tangential stresses

For primary injections, the block joints may be assumed to be largely open, so that the tangential stress at the lower construction joint of the respective injection section will be decisive. This stress increases with the height of the injection section and block width and is independent of dam thickness. The bending and shear stresses can be estimated based on examinations according to the slab theory.

Due to the superposition of the stresses resulting from block joint injection and the dead load of the block, tensile stresses can occur in the construction joints. This may require either a reduction of the height of the injection section or the filling of the adjacent joint with water.

To check the injection process, the tangential deformation at the upper end of the injection section should be monitored as it may indicate a change in the block joint width. If the adjacent joints are open, double the expansion of the block joint is measured until the blocks rest against each other.

Radial stresses

Radial stresses are generated in two ways:

– If two adjacent joints are grouted simultaneously or if the adjacent joint is filled with water or grout that has not yet sufficiently hardened, the hydraulic pressure acting normal upon the block joint walls between the two block joints causes a force component

Radial force $R_z = 2{\cdot}P \cdot \sin \alpha/2 = R = p{\cdot}h \cdot\cdot \left(\frac{d}{r}\right) \cdot \beta_0 \cdot \beta$

for triangle fluid pressure $p = p_F = ½{\cdot}\gamma{\cdot}h$

for constant over pressure $p = p_U$

Abutment moment $M_K = R_z \cdot z$

relative to H $M_{K,max} = p \cdot \frac{H}{h}\left(\frac{d_z}{r_z} \cdot \frac{z}{H}\right)_{max} \cdot b_0 \cdot \beta_z$

Section modulus at the abutment, downstream

related to H ... $W_K = \left(\frac{H}{d_k}\right)^2 \cdot (b_0) \cdot \beta_k \cdot \frac{3-\lambda^2}{6.(3-\lambda)}$

Vertical stress along the downstream dam base

$$\sigma_v = p\frac{h}{H} \cdot \underbrace{\left\{\left(\frac{d_z}{r_z} \cdot \frac{z}{H}\right)_{max}\right\}}_{m'} \cdot \underbrace{\left\{\left(\frac{H}{d_k}\right)^2\right\}}_{w'} \cdot \underbrace{\left\{\frac{\beta_z \cdot 6 \cdot (3+\lambda_k)}{\beta_k \cdot (3-\lambda_k^2)}\right\}}_{æ}$$

$$\sigma_v = p \cdot \frac{h}{H} \cdot \sigma' \quad mit\ \sigma' = m' \cdot w' \cdot æ$$

in the upstream direction due to the curvature of the dam. If the dam body underneath the injection section to be grouted can already be considered a monolith, again only the construction joint at the lower boundary of the injection section must be examined. However, if this injection forces the lower block joints to open, the effect of this force up to the monolithic area, in an extreme case even down to the foundation area, must be examined.

If the adjacent joint has already closed, the grout sufficiently hardened and the dam block below can be considered a monolith, which can be assumed during post-grouting in subsequent years, the stresses acting upon the dam in the radial direction are considerably lower. The radial force in the considered level (Fig. 6.11) is proportional to the ratio of dam thickness to arch radius and height of the injection section. This ratio also determines the arch stresses at full storage level (heel formula), which must be lower for low dams than for high dams. This may explain the at first unexpected result of a comparative study, namely that even in arch dams of various heights, the vertical stresses resulting from block joint injection vary only slightly due to the radial forces.

In the most unfavourable case of a free-standing block up to the foundation surface, the stresses acting upon the this area are primarily determined by the ratio of abutment thickness to dam height and are therefore only slightly dependent on the absolute dam height.

The influence of the dam curvature in the vertical and horizontal direction can be summed up by a dimensionless coefficient æ (Fig. 6.11), which has been determined to be 1.15 ± 10%, based on a comparison of 30 arch dams of heights between 40 and 220 m.

The decisive maximum abutment moment and thus estimation of the vertical tensile stresses at the foundation surface according to Fig. 6.11, where æ = 1.15, enables a quick determination of the number of the required injection sections. The assumptions on which the calculations are based may, however, be considered to be rather unfavourable, since measurements of the stresses, strains and settlements at the foundation area of the three highest Austrian arch dams have not shown any significant changes during block joint injection.

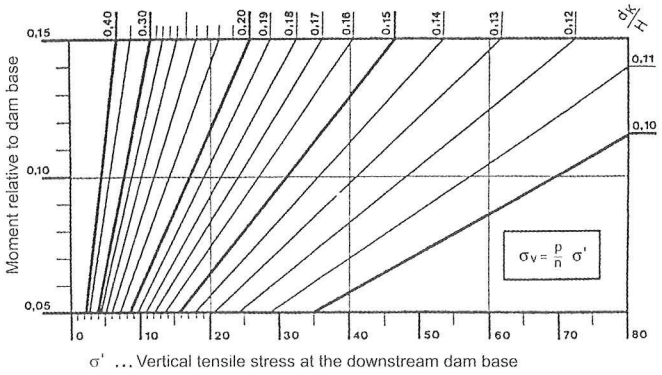

Fig. 6.12: Evaluation of the calculations according to Fig. 6.11.

The actual pressure acting, on average, upon the entire joint surface during primary injection may largely correspond to the theoretical assumptions; during post-grouting, however, it will be considerably lower, since due to the narrow joint widths only part of the joint surfaces can be grouted. Therefore, the actual stresses are not only dependent on the nominal pump pressure, but also on the quantity grouted under high grout pressure as a measure of the joint surface covered.

Superposition of the stresses of individual blocks

The tangential shear stresses resulting from the injection of adjacent sections act in opposite directions; therefore they neutralize each other and need not be taken into consideration in the overall stresses acting upon the dam.

The equidirectional radial stresses, however, could, in theory, superpose each other over the entire height of the dam, if the grout pressure in the grouted joints is maintained. This assumption, however, appears unjustified for various reasons:

During grouting of the upper sections, the pressure in the lower block joint is relieved; in some cases, this may result in a partial opening of the joint. This has been confirmed by recent measurements.

Since grout pressures cannot be considered as permanent loads, stress relief further decreases the residual compressive stresses that may possibly still be present.

Higher reservoir levels and thus higher arch stresses are only attained after block joint injection. During the subsequent lowering of the reservoir level, permanent arch compressions can even result in a reopening of the block joints. Possible horizontal

compressive stresses due to block joint injection will not, therefore, be permanently present in the dam.

6.4.4. Grouting

Grout

As with all other injections, the penetration capacity of cement suspensions is basically determined by the ratio of the narrowest joint width w_j to the decisive grain diameter d_{95} of the cement, which shall be

$$w_j : d_{95} \geq 5.$$

According to the European Standard 196, d_{95} of mean normal cement is 50 µm, so that only joint widths that are at least 0.25 mm wide can be grouted.

For post-grouting, therefore, fine cement with $d_{95} <$ 16 µm should be used, in order to be able to also grout joint openings exceeding 0.08 mm.

Grout pressure

Selection of the grout pressures requires detailed consideration. The grout pressure required at the pump results from the:

- Height of the injection sections.
- Flow resistance in the pipe lines, inlet and vent valves as well as in the block joint itself.
- The possibly required overpressure at the upper boundary of the injection section.

If the height of the injection section is 20 m and the specific weight of the grout 1.5 t per m³, the minimum pressure at the lower boundary of the injection section is 3 bar; to this must be added the flow resistance in the valves and pipe lines which is at least 2 bar. The lowest effective grout pressure for a 20 m high section is, therefore, approximately 5 bar, with the exception of the short-term opening pressure of the valves. This pressure can be sufficient for primary grouting. For post-grouting, the flow resistance in the, due to primary grouting, generally considerably narrower block joints will have to be overcome; pump pressures of up to 20 bar are, therefore, usually used. Since by that time the monolithic effect of the arch dam is largely given, the stresses acting upon the dam due to the grouting of a joint section can be ignored; this was confirmed by measurements of the radial displacements during post grouting. Therefore, static verifications for post-grouting are generally not carried out.

Injection method

The block joints are grouted from the bottom to the top, from the flanks to the centre or from the centre to the flanks.

Prior to injection, the pipelines - often the block joints as well - are flushed using water in order to check whether they are free. With some arch dams, prior to the grouting of one block joint, the adjacent joints are filled with water; the counter pressure thereby attained is maintained during injection. This provides a lateral support for the blocks and considerably reduces or even eliminates the tangential stresses. In this case, however, each individual block will be subject to the full radial stresses.

Careful consideration of each individual case is required to determine the most favourable method.

Monitoring of block joint injection

Initially, the pressure and flow of the grout prior to entering the injection pipelines is monitored using pressure and flow recorders. To open the valves, a higher pressure is required, which, however, will immediately drop after opening; subsequently, the prescribed pressure will be maintained. When the grout exits at the vents, these can be closed and the overpressure can be measured. For primary injection, pressures of up to 3 bar, for post-grouting pressures of up to 8 bar may be used. The effective pressure in the joints will then be approximately midway between the pressure at the inlet port and vent.

The tangential deformations as a measure of the actual stresses generated during injection, determined by means of joint expansion measurements at the lower and upper end of the injection section, indicate the effective pressures in the joints much better, providing a representative basis for the determination of the allowable injection pressure. Checking the width of the adjacent joints will prove useful as well.

In addition, monitoring the radial displacements of the dam at several levels during injection would also be useful so as to be able to measure possible additional vertical stresses; during primary grouting, however, the plumb lines are generally not yet in operation.

Even after deducing the grout quantity that has remained in the injection pipes and/or possibly exited at the surfaces, the conversion of the injected quantity of solids into block joint widths is subject to high uncertainties, since:

– transfers into injection sections above or below, as well as
– filling of inhomogeneities or air voids in the concrete
can hardly be determined.

6.4.5 Empirical values

Additional stresses due to block joint injection

The calculated temporary additional vertical tensile stresses during primary injection at the upstream dam base have a wide variation range and are dependent not on the absolute dam height, but primarily on the ratio of abutment thickness to dam height d_a/H.

Cement absorption

Comparison of grout consumption to joint width for the Kölnbrein arch dam (Fig. 6.13) reveals a certain proportionality, but with a relatively high variation. Another reason why such a comparison is problematic is that the width changes are measured only at the point where the inspection gallery cuts the block joint. This point, however, must not necessarily be representative of the entire injection section covering an area of several hundred m².

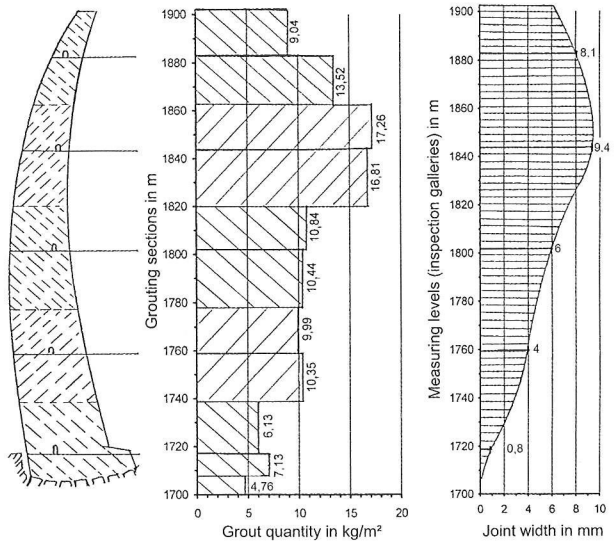

Fig. 6.13: Kölnbrein arch dam, measured grout consumption and block joint widths at the measuring levels.

A comparison of the specific cement consumption (Table 6/2) of various arch dams, relative to the unit volume of concrete (per m² joint area/block width), shows that they vary widely and are independent of the dam height. They are influenced by many other factors as well, such as concreting and storage history.

Table: 6.2: Cement consumption during block joint injection of high arch dams.

Name	Height	Cement consumption in kg	
	m	per m² joint area	per m block width
Mauvoisin	237	13.00	0.72
Kölnbrein	200	11.45	0.57
Zillergründl	185	3.80	0.19
Emosson	180	18.00	1.00
Curnera	153	12.20	0.76
Zervreila	151	13.00	0.72
Moiry	148	17.60	1.10
Gigerwald	147	8.00	0.44
Limmern	145	8.60	0.50
Valle di Lei	143	5.90	0.49
Schlegeis	131	3.80	0.22
Punt dal Gall	130	10.80	0.60
Nalps	127	8.50	0.53
Kops	122	9.60	0.60
Santa Maria	117	6.90	0.38
Cavagnoli	111	21.00	1.40

6.5 SUMMARY

Optimisation of the construction site equipment by adapting the capacity of the most important individual units, particularly of the cable cranes, to the concrete-technological requirements and topographical conditions can contribute significantly to an economical construction progress.

The supervision of all construction phases by experienced experts, such as confirmation of the geological design bases and of the conformity of the guidelines for the execution of construction, constitutes an essential part of the structure's quality management.

The guidelines for block joint injection must be determined based on detailed investigations in order to ensure that its purpose, i.e. the guaranteed monolithic load-bearing capacity of arch dams consisting of individual blocks, is achieved.

In addition, detailed documentation of all determined data is required.

REFERENCES

Huber H., Döpper H.: Massenbetonprobleme bei der Bogenmauer Zillergründl. In: Vertrauen in die Kraft des Wassers, Tauernkraftwerke AG; Verlag Koska, 1987.

Widmann R.: Die Gewölbemauer Kölnbrein, Projektierung, Bau und erste Betriebsjahre. Interner Bericht der ÖDK, 1990, Internal report.

ÖDK, TKW: Internal reports.

7. SURVEILLANCE DURING OPERATION

With the beginning of modern dam construction, the importance of surveillance to guarantee dam safety was recognized. This task will remain important as long as dams are in operation.

7.1 ORGANISATION OF SURVEILLANCE

Each dam owner is obliged to employ an expert and competent supervisor, the dam representative, who will be responsible for:

- Control of the dam condition and maintenance, carried out by a dam warden who shall be stationed as near as possible to the dam.
- Evaluation of the prescribed measurements and the preparation of an annual report on the condition of the dam and appurtenant works.
- Timely initiation of all necessary corrective measures in case of exceptional events.

To guarantee safety, supervision by a team of experts independent of the owner or project engineer is also of essential importance (Fig. 7.1). In addition, a dam record must be kept, in which all observations and exceptional events (e.g. floods and earthquakes, including all observed data) must be recorded.

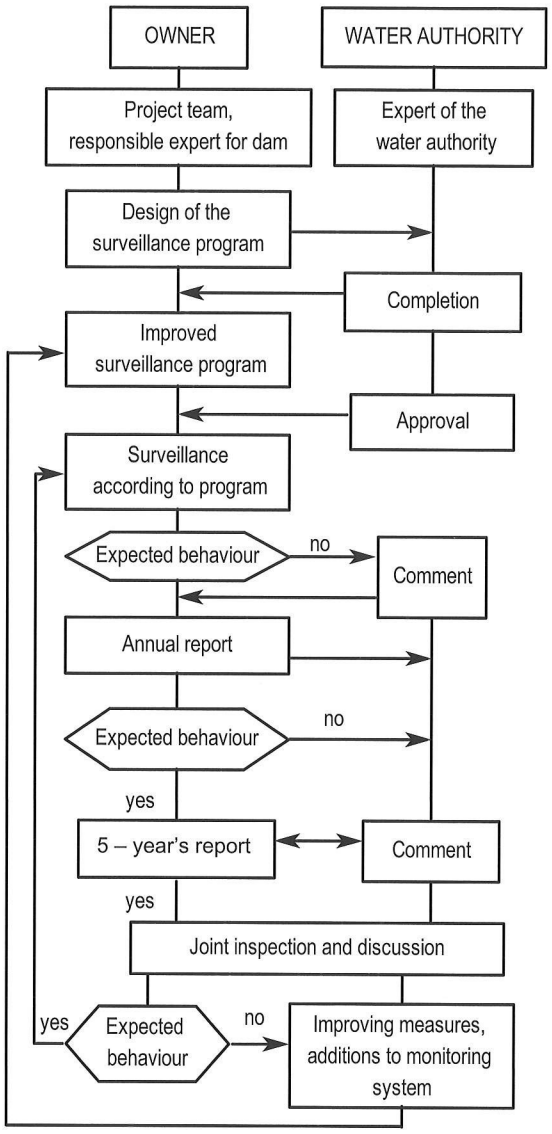

Fig. 7.1: Organisation of surveillance.

7.2 SURVEILLANCE TASKS

In general, safety surveillance during operation comprises three different fields (Fig. 7.2):

- Condition checking to ensure the continuous functional reliability of the dam, appurtenant works and monitoring system.
- Behaviour monitoring including the performance and evaluation of the prescribed measurements of the dam and underground.
- Control of the reservoir slopes.

7.2.1 Checking the condition

Checking the condition of the dam, including all appurtenant works, comprises:

Inspections: Regular local inspections of the dam, reservoir slopes and the area below the dam are of especial importance. A location drawing (supplemented by detail drawings, if required) must contain all important locations such as surveying points, springs or potential sliding surfaces of the reservoir slopes and below the dam; potential cracks and wet areas within the dam body - photographic documentation may facilitate the discovery of such changes - should form the basis of these inspections.

Appurtenant works: The functional reliability of all appurtenant works is based on:

- Keeping the intake and discharge channels free.
- Maintenance of the mechanical systems.
- (Remote) control system.

The appurtenant works' functional reliability must be permanently ensured by careful maintenance and must, therefore, be checked at least once a year. Spillways must be checked prior to the reservoir level reaching the height at which the retention volume will no longer suffice to accommodate a possible flood wave (see section 2.3.3).

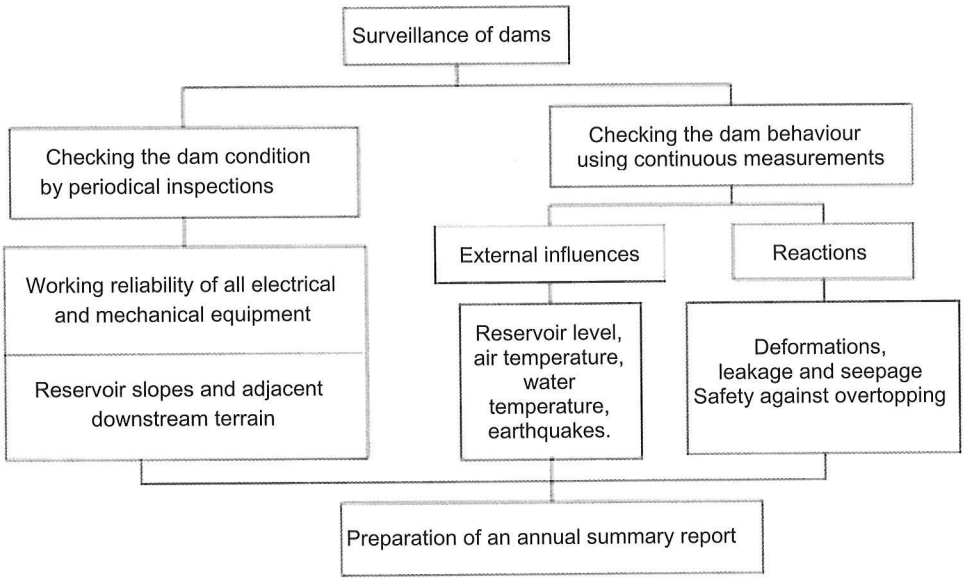

Fig. 7.2: Surveillance

Reservoir slopes: The valley flanks of the reservoir and the downstream dam foreland must be inspected at least once a year as well as after heavy rainfall or strong earthquakes. An engineering geologist familiar with the area should take part in these inspections. Areas that are particularly susceptible to slope movements should be checked regularly using modern geodetic measuring techniques of sufficient accuracy, in order to be able to keep track of any changes in the movement speed, possibly in connection with rainfall or storage periods. Areas that are especially sensitive or inaccessible for longer periods can be visually monitored using a television system.

The importance of direct surveillance for the discovery of damages as early as possible is illustrated by an empirical summary (Table 7/1). Approximately 2/3 of all damages were discovered by direct surveillance, i.e. local inspections; this, however, could also be attributed in part to the less extensive monitoring system of older dams.

Table 7/1: Methods used to discover damages [58].

	Concrete dams	Embankment dams	Total
Visual inspections	361	590	951
Measurements: Water flow	71	87	158
Water pressure	20	26	46
Pore water pressure	-	39	39
Water chemistry	8	6	14
Displacements	45	85	130
Material tests	38	6	44
Total	543	839	1,382

7.2.2 Measured parameters

Basically, a distinction must be drawn between parameters that determine (Fig. 7.2):

- The influences on the structure, such as reservoir level, air and water temperature, flood and earthquakes.
- The structural reactions of the structure, such as displacements, torsions, block joint widths, stresses and strains.

The necessary interval between all measurements is determined based on the daily temperature load graph. If the daily temperature load graph varies by more than half the measurement tolerance, the interval between measurements will have to be shortened.

Earthquakes: If earthquakes are to be expected at the dam site, seismographs should be set up which allow the vibrations to be recorded in three directions perpendicular to each other.

7.2.3: Measuring systems

Measuring systems require correct maintenance - by a specialist for each type of measuring instrument - as well as expert collection and evaluation of the measured data. The basis for each evaluation is an ordered collection of all measured data of verifiable correctness and plausibility, which are available at any time and can be related to each other in any way needed.

Errors that can falsify measurement results and must be eliminated prior to evaluation include:

- Optimal calibration of the measuring instruments, taking the instrument constants into consideration.
- Determination of the temperature sensitivity.

– Avoidance of zero errors, e.g. due to insulation defects or residual elongations of invarwire extensometers.
– Measuring accuracy; thereby, a distinction must be drawn between reading accuracy and system accuracy.
– Avoidance of errors in transmission, which may either result from repeated transcriptions of the measured value or, in the case of remote measurements, be due to insulation and frequency problems in the lines.

Almost all measurements are relative measurements referring to a certain state at a certain time. Geodetic measurements as well, in the last analysis only determine displacements relative to a point that is assumed to be non-displaceable. The zero measurement should be repeated several times at short intervals to eliminate random measuring errors.

The interruption of a measurement series, e.g. due to the failure of the measuring instrument, may cause problems in long-term evaluation. These measurement breaks can be bridged using regression analysis, with which the preceding period can be analysed and the probable measured value, at the time the measurements will be resumed, can be estimated.

Only temperature, water quantity and water pressure measurements give absolute values and can, therefore, be discontinued and resumed at any time, without adversely affecting the measurement series.

The direct measurement of the stresses (e.g. due to overboring) as well, reflects the state at a given time and is independent of a measurement series.

If measurement and calculation point are not identical, the measured values must be converted correspondingly. For conversion to the theoretical axial point at the dam base (Fig. 7.3), the torsions must be measured as well.

7.2.4 Evaluation of measurements

Measurements of the behaviour of all dams can be divided into two periods:

– During the first approximately 10 normal operating years an extensive measurement programme must be carried out. Based on the results, a representative mathematical model should be prepared. The mathematical models can be subdivided into deterministic models (their parameters must be calibrated based on the measurement results), statistic models (e.g. regression analyses) and hybrid models (combination of static and statistic models).
– During the subsequent operating years, relevant measurements at representative points, selected on the basis of the experience gained during the initial years, suffice for the monitoring of dam safety.

Therefore, to evaluate the status of a dam, the project must include a monitoring system adapted to the specific characteristics of the dam and, if possible, to the calculation points as well. Until verification of the operational reliability of a possibly automatic remote monitoring system, all measurements must be carried out on site.

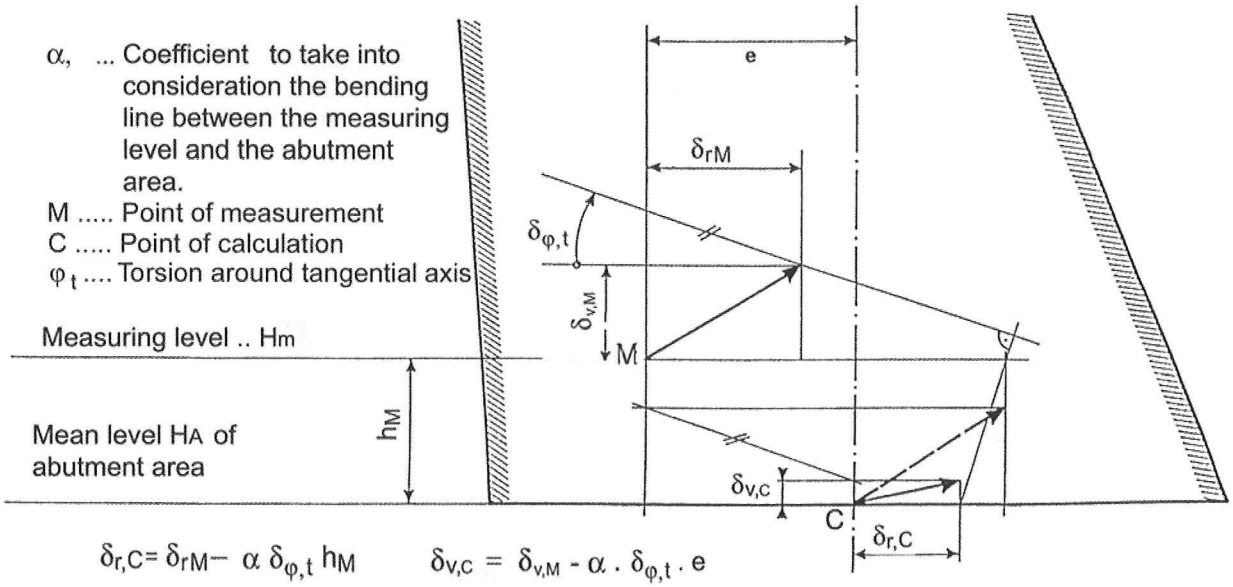

Fig. 7.3: Conversion of measurements from measurement point to calculation point.

Equal measurement results under equal external influences indicate that dam safety remains constant. For this, a few measurement points suffice, e.g. summation measurement of all drainage water quantities or measurement of the radial and vertical displacements of the arch crown. This direct comparison is, however, rendered more difficult by the time-dependent behaviour of concrete and rock, since their behaviour is not only dependent on the quantity of the loads, but also on the load history.

Evaluation of the measured behaviour should be based on a comparison of the, according to the static calculation methods, expected behaviour to the observed values. Since all measurement results reflect the reactions of the structure to the sum of all external influences, the share of the various external influences in the measured value must first be determined (Fig. 7.4).

7.3 SAFETY MONITORING

7.3.1 During construction

With higher arch dams, the reactions of the underground to excavation and concreting of the dam should be investigated prior to construction. The original state should be determined based on a definite zero measurement (i.e. the mean of various measurements carried out at short intervals); the measurements can be re-continued later, when the construction schedule allows. Thereby, primarily the displacements in the vertical direction in the vicinity of the upstream and downstream face should be monitored. This can be done in various ways:

- Levelling in the drainage gallery, which is usually driven at or just below the excavation base prior to the actual excavation in the valley bottom.
- Invarwire units for the inverted pendulums in the bores that should be drilled after the injections for the grout curtain, but before the beginning of concreting. At least one of these units should include the drainage gallery underneath the dam and be included in the geodetic levelling.

Within the dam body, the following aspects are of interest during concreting:

- Stresses and/or strains along the dam base.
- Concrete temperatures from the beginning of concreting of the respective lift, to verify the effectiveness of the measures taken to ensure that the maximum allowable temperature is not exceeded.
- Block joint widths; these should be measured long before the grouting of the block joints and should be carried out at short intervals particularly in the injection zone during injection work, in order to determine the effect of the injections.

7.3.2 During operation

In general, dams can be considered safe, if depending on the storage level and outside temperatures, which must therefore always be measured:

- The significant deformations of the dam body and foundation during operation correspond to

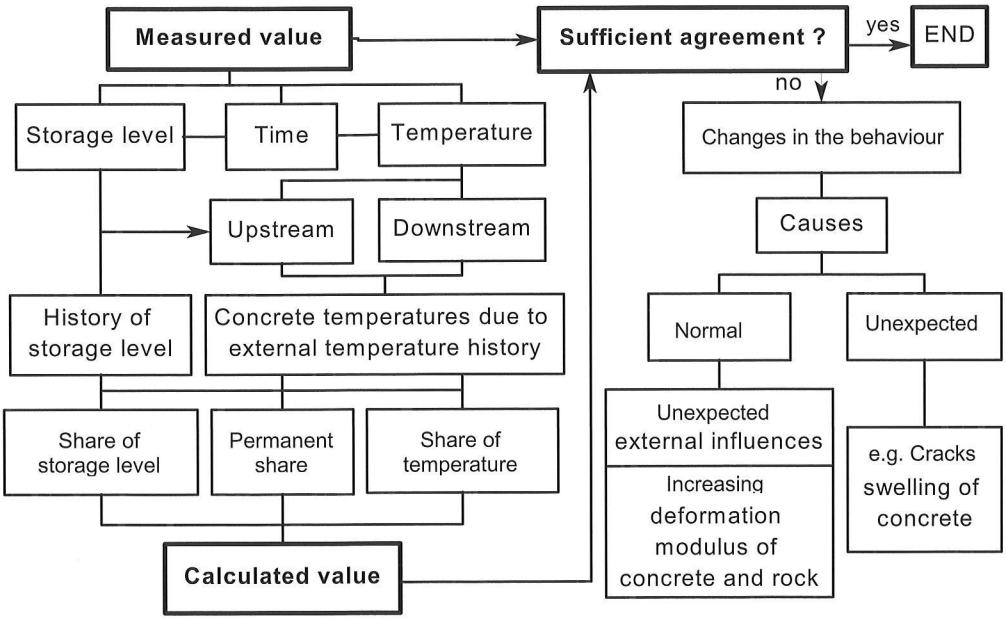

Fig. 7.4: Verification of the measured values by calculation.

the predetermined values and the increase in residual deformation decreases with time.

– A suitable drainage system within the dam body and underground produces a constant allowable seepage quantity as a constant function of the storage level, without changes in the uplift and groundwater pressures.

Displacements: At all concrete dams, the radial horizontal displacements at the crest of the highest block are generally measured using pendulums or inverted pendulums and non-contact reading. For gravity dams with open block joints, the other blocks should be monitored using block joint measuring chains (Tauernmoos gravity dam, ÖBB) to measure their relative displacements. With this dam type, measurement of the crest displacement suffices, since deformations along the dam base are reflected in the displacements of the dam crest, which have at least the same dimension.

With arch dams, changes in the deformation behaviour of the dam body, e.g. long-term changes of the deformation modulus or swelling of concrete, can be determined based on integral measurements of the deformations in the crown of the crest arch; not, however, local changes such as cracks or larger deformations in the vicinity of the dam base.

From the measured deformation behaviour of a dam, a safety factor can be directly deduced, only if hybrid models are used. Even if the measured deformations remain below the calculated values, this does not indicate higher safety, since other factors may be more decisive:

– A higher deformation modulus of the concrete, without changes in the stresses.

– A higher deformation modulus of the underground causes higher restraint stresses along the dam base.

– A three-dimensional structure has six degrees of freedom; if in the calculation less degrees are taken into consideration, e.g. only the three displacements in the nodal points using the FE-method, smaller deformations may result on the stiffer prototype, but also higher restraint stresses.

Cracks: Monitoring of cracks will prove useful during the entire lifetime of the dam.

The acoustic emission method would enable an early discovery and localization of cracking, but is too costly to be included in general monitoring, since the range of each individual highly-sensitive instrument is too narrow and evaluation very difficult, requiring special experts.

In several concrete dams, vertical drainages were installed parallel to the upstream face to limit and enable an early localization of cracks. Their distance from the upstream face should correspond to the critical crack length (Fig. 5.41).

Design flood: To check the design flood, the reservoir level variations during each flood event, at least however the reservoir level upon arrival of the flood wave and the highest reservoir level attained, as well as the discharge quantities should be recorded. Based on this data and using the reservoir depth - volume curve, the hydrological data of the inflowing flood wave can then be deduced. For dams with a small retention volume in comparison to the flood inflow, the peak inflow, for dams with relative large retention volumes the water load of the flood wave will be decisive. After a sufficient number of operating years, the probability of overtopping the spillway crest can be determined.

Seepage: Water quantity measurements are summation measurements covering a specified area or even the entire structure; for higher or longer dams, a subdivision into sections will prove useful in order to improve accuracy and discover discontinuities early. This is particularly important in regard to the early discovery of impending changes, before any significant changes in the deformation behaviour can be observed. With larger seepage quantities, monitoring of the suspended solids quantity will prove useful as well.

Monitoring of seepage requires at least:

- Continuous monitoring of the seepage quantities through leakage points and drainages; the latter should be installed at an appropriate distance from the grout curtain, to avoid excessive gradients.
- As well as monitoring of the uplift and joint water pressures using piezometers, whose measuring length - to measure the uplift pressures at the dam base as well - should exceed the joint spacing in the rock, to avoid faulty measurement results.

A safety factor against inadmissible seepage according to the newly proposed definition (Fig. 2.3) can already be directly deduced from the variation in the

seepage quantity at the first filling of the reservoir. The permeability of the underground and thus also seepage is dependent on the deformation or stress state, which in turn is determined almost exclusively by the storage level. If on the basis of the observed conditions (Fig. 8.55) a hyperbolic curve of the seepage quantities as a function of the storage level is assumed (Fig. 7.5), then [113]:

$$q = q_0 \frac{1+\alpha}{1+\alpha-\beta} \text{ results.}$$

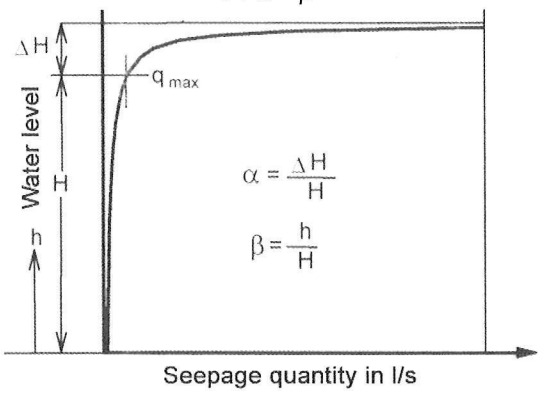

where q_0 = Seepage quantity at minimum operating level
q_{max} = Seepage quantity at top water level
H = Reservoir level variation between top water level and minimum operating level
ΔH = Fictive increase of the top water level
h = Reservoir level above minimum operating level

Fig.7.5: Hyperbolic curve of the seepage quantity.

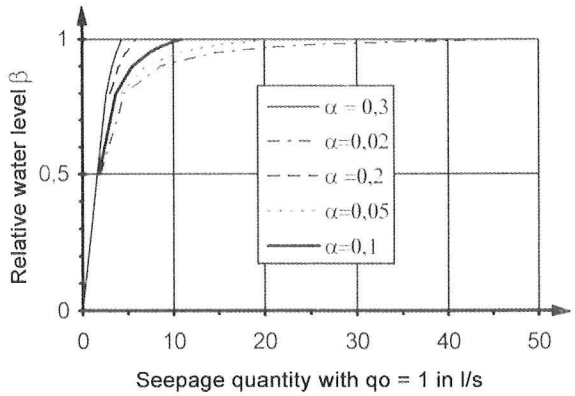

Fig. 7.6: Variation of the seepage quantity as a function of storage level for various values of α.

α is defined by the ratio of measured seepage quantities at top water and minimum operating level based on the relation specified above (where b = 1) (Fig. 7.6). Thus 1+ α becomes a measure of the safety against inadmissible seepage at a fictive increase of the reservoir level and thus also of the safety against inadmissible vertical tensile stresses along the dam base (Fig. 7.7).

The concrete temperatures must be measured in those vertical blocks, in which the pendulum devices have been installed. At the measuring levels, which should correspond to the calculation levels, several measurement points are required, depending on the dam thickness; their spacing should increase from the dam surface to the dam centre. For analysis, the annual water temperatures over the entire water depth are required as well.

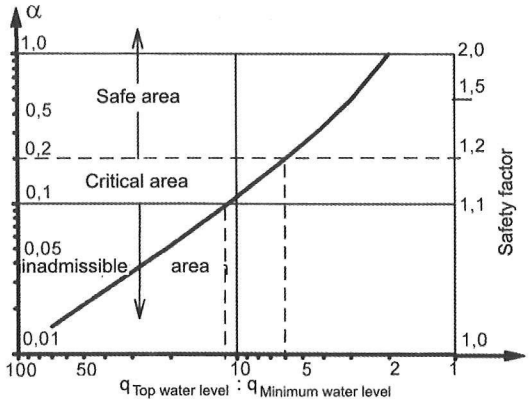

Fig. 7.7: Deduction of the safety factor.

Additional measurements should be carried out in areas, where, as experience during the first filling of the reservoir has shown, they will prove useful, i.e. where an unexpected behaviour of the dam, underground or reservoir slopes was observed.

7.4 MEASUREMENTS TO ANALYSE THE BEHAVIOUR

For a more comprehensive determination of the actual behaviour of the dam and underground, the mesh of measurement points must be denser and more behaviour characteristics must be measured.

7.4.1 Displacements of the dam body

In arch dams with a valley characteristic of ≥ 3, pendulum devices should be installed not only in the highest vertical section, but also at the quarter points of the crest arch. With the pendulum devices, not only the radial but, with only minor additional effort, also the tangential displacements can be measured in all inspection galleries in the horizontal planes. If, in addition, Invarwire extensometers are installed in the pendulum shafts in the dam and/or bores in the underground, also the vertical displacements and thus the direction of the overall

displacement can be measured at the same positions. In slender arch dams with large vertical curvature, it may become necessary to subdivide the pendulum units. In addition, clinometer measuring chains (at least double row) can be installed along a vertical section; from the measured tangents at the bending line, its shape and thus the displacement along the crest can be deduced.

To also determine the displacements of the anchor points of the pendulums and invarwire and thus the absolute displacements of the dam body, geodetic precision measurements must be carried out at least twice a year, if the selected reference points are really sufficiently non-displaceable. To check the reliability of the zero measurement, it should be repeated at short intervals. In the polygonal tensile measurements and levellings also the pendulum and Invarwire measurement points should be included, particularly in the bottom and crest area. Visur lines from these measurement points to the reference points in the downstream foreland can also indicate displacements of the pendulum anchor points.

Finally, distance measurements between the valley flanks should complete the geodetic measurement programme and provide additional information.

7.4.2 In the underground,

The decrease in deformations with increasing vertical distance from the dam base are of interest particularly in the evaluation of the seepage flow paths. To measure the deformations section by section, multiple extensometers (for flat, longer measuring lengths roller-guided bar extensometer) can be used. For short measuring lengths, separate extensometers may be useful due to the simpler construction, since the costs for short bores are relatively low. Using sliding micrometers, many measurement points along the borehole are possible, facilitating the localization of local deformations, e.g. with cracks transverse to the bore.

7.4.3 Torsions

Torsions at the dam base around:

– The horizontal tangential axis are usually measured using clinometers. With large dam bases and a high deformation modulus of the rock underground relative to the concrete, radial clinometer measuring chains may be required due to a possible curvature of the cross section.

– The horizontal radial axis are negligible and therefore generally ignored.

– The vertical axis in the arch abutment can be measured:

- Indirectly, by installing tangential extensometers in pairs in the vicinity of the downstream and upstream dam face, more or less completely depending on the length of the extensometers.
- Geodetically using visur lines directed at reference points in the downstream foreland, at least twice a year both at high and low reservoir levels.

7.4.4 Stresses and strains

In theory, stresses measured at specific points of the dam body would facilitate a direct comparison to the calculated values. In practice, however, stresses can only be measured via the deformations; for this, various methods can be used:

– Measurement of pressure changes in the pores due to the deformation of the surrounding concrete, using telepressmeters installed in the direction of the principal compressive stress. If a compressive stress is applied prior to measurement begin, pressure drops, that is tensile stresses can be measured as well.

– Measurement of diameter changes in the bores, e.g. using dilatometers in a plane transverse to the drilling direction.

– Using overboring, strain changes due to the unloading of the drill core can be measured in the plane transverse to the drill core. This method produces absolute values, but is only suitable for individual measurements.

– Measurement of strain changes in various directions by installing teleformeters; the measuring lengths should exceed approximately triple the maximum grain diameter of the concrete. Using this method, the principal stresses can be determined.

When evaluating the stresses, attention must be paid to the fact that on the one hand temperature-dependent strains do not cause stresses, and that on the other hand temperature-dependent stresses due to restraint stresses do not cause strains.

Measured strains should include the three-dimensional state and can be measured in various directions using teleformeters.

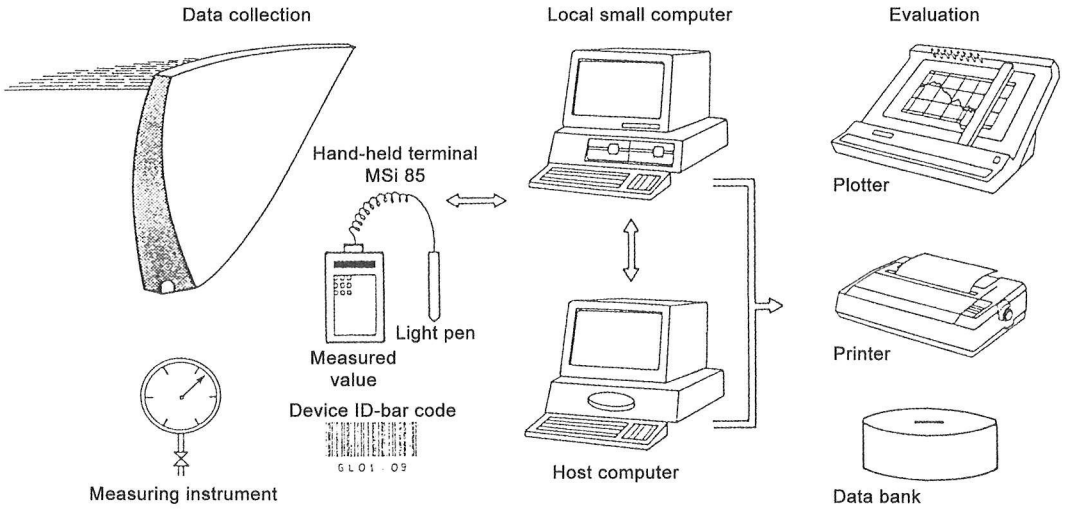

Fig. 7.8: Scheme of automated remote monitoring (Eiselmayer 1987).

The actual stress state is then calculated, based on the stress-strain relation. The respective deformation modulus should be recalculated based on the simultaneous overall deformation of the dam. Confined strains, i.e. restraint stresses, however, cannot be determined.

7.4.5 Summary

Careful performance and evaluation of all measurements, together with regular inspections, will ensure that all unwanted changes are discovered and therefore all requisite measures for proper maintenance are carried out in time.

7.5 REMOTE MONITORING AND AUTOMATION

7.5.1 General

The goal must be continuous monitoring, since changes in the dam behaviour, which can directly lead to failure, generally come about slowly. Expert and reliable personnel for daily routine work is not only costly; there is also the risk that, due to the monotony of keeping measuring records for years, changes may one day be overlooked.

Therefore, automated recording, collection and evaluation of measured data, which are transmitted to permanently occupied centres, has been increasingly used for the continuous monitoring of limit values(Fig. 7.8). This facilitated not only improved documentation for the evaluation of the dam condition, but also continuous monitoring of dams either located far-away or practically inaccessible during some seasons. Studies have shown that a considerable amount of overall costs is required for the basic equipment - such as transmission of measured data and terminals including plotters - so that the quantity of measured values plays only a subordinate role.

Generally once a week visual inspections including direct manual measurements of all instruments are carried out, during which all measured values including those that are not automatically recorded, must be collected. For these measurements, a mobile hand-held terminal was developed enabling rationalized and improved data collection (Fig. 7.9). The measuring points are identified by bar codes and compared to the specified sequence of measurements by the hand-held terminal. The measured value is fed in, its plausibility checked by comparing it to the respective previous measured value, then it is converted into the final value and stored. Subsequently, the stored measured values can be directly transmitted into the data bank of the central computer for further evaluation.

This method absolutely requires unvarying inspection procedures, immediately discovers measuring errors making repeat measurements unnecessary and eliminates the possible sources of error that may occur during the repeated transmission and conversion of measured values into corresponding lists as was commonly done previously.

7.5.2 Definition of limit values

Automation of safety monitoring must comprise two steps:

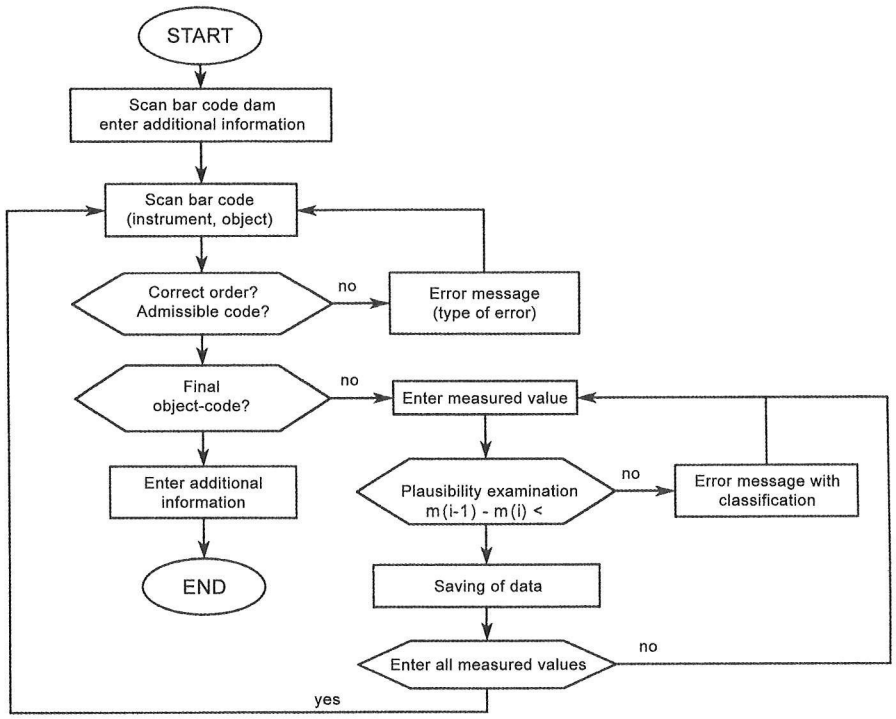

Fig. 7.9: Flow chart of software for the hand-held terminal (Eiselmayer 1987).

– plausibility checking of the measured values; and only then
– comparison to required or limit values.

Plausibility checking should discover errors in the measuring instrument, measuring method or transmission of the measured values. If an unusual measured value is confirmed by an immediate repeat measurement as well as by manual measurement on site, the entire structure must be inspected by responsible experts and a detailed analysis of all measured values must be prepared.

In any case, the further measures must be determined by qualified experts and should not be anticipated by an automatic alarm.

During the first filling of the reservoir the dam should be supervised by a team of experts; in this phase, therefore, automation of limit value checking is rather used to check the functional reliability of the transmission equipment. For subsequent storage periods, empirical values are then available, which must be included in the definition of the limit values. Full automation of limit value checking will really prove useful only after several storage periods.

Limit values can be determined in various ways:

– By determining extreme values to be used irrespective of the reservoir level and season. Thereby, however, the external influences on the dam are not taken into consideration. Thus a seepage increase at low reservoir level, resulting in values which are usually measured at higher reservoir levels, can already indicate that unfavourable changes are developing. On the other hand, if the deformation exceeds the previous maximum value, this may be attributable to below-average air temperatures or a high storage level for an exceptionally long period, without this being and indication of unexpected behaviour. Fixed limit values will be useful above all for daily storage reservoirs and smaller dams which play only a minor role.
– Flexible limit values are more expressive, since they can be defined depending on the storage level and season, based on previous experience or appropriate mathematical models and by taking the storage and temperature history into consideration. To predetermine flexible limit values, deterministic or statistic mathematical models can be used:

Deterministic models generally do not take the actual rheological behaviour of the rock and concrete into consideration. However, during first reservoir filling, comparison to the measured values and calibration of the deformation parameters is only possible using deterministic models.

Statistic models can only be prepared based on a measurement series spanning several years. Using regression analyses, the extent of the various external influences on the measured value, i.e. the reaction of the dam, is back-calculated. In this way, for the respective measured value it is possible to de-

duce a required value from external influences that are easily determined, such as time, reservoir level and air temperature, which can then be compared to the actual value. Using these models, a conversion to realistic, physical parameters must be ensured to avoid misinterpretations.
Hybrid models are a combination of the two models mentioned above. After calibration of the parameters using statistic models, the calculation results must with sufficient exactness reflect all measured deformations, particularly the bending surface of the dam and the displacements and torsions at the dam base. Then, the various safety factors can be checked and if required the theoretical bases for future dams improved,; this should be utilized as far as possible.

7.5.3 Tolerance limits

Due to unavoidable measuring inaccuracies and simplifications in the mathematical models, tolerance ranges must be allowed for in the definition of limit values. Dam safety is affected only, if the tolerance range is exceeded due to a more or less rapid increase of deviations from the expected value (Pürer 1986). Only then, more extensive monitoring will be required, provisions for which must be included in the operating regulations. To ensure the vigilance of the monitoring personnel and to avoid its being undermined by frequent, unnecessary fault indications, the tolerance range chosen should not be too small for in-plant checking.
The regression analysis, on which determination of the limit values is based, should not be carried out for the period immediately preceding the measured value to be evaluated, since slow changes can then not be discovered.

7.6 EVALUATION OF MEASURED VALUES

To determine the extent of the various influences on the individual measured values, various statistic methods can be used:
- Linear Multiple Regression Analysis (LMRA);
- Non-Linear Multiple Regression Analysis (NMRA);
- Neuronal Network System (NNS).

Using the latter, the best adaptation to the given measured value variation may be achieved, but the optimal determination of the extent of the external influences on the measured values, which is required both for prognoses and comparison to the measured values, must still be verified.
To determine the increase in the deformation modulus, the NMRA should prove useful above all for the first 10 - 20 operating years. The LMRA is the basis of all evaluation examples specified below.

7.6.1 Regression analysis

Using the LMRA, the external influences are represented only by two measured parameters that are easily measured and always available [11]: the time-dependent storage level and temperature variation as well as the time-dependent, residual share of the creep of rock and concrete. Therefore, the regression formula for displacement δ at time t is given by:

$$\delta = a_0 + \delta_B + \delta_T + \delta_W.$$

The residual deformations δ_B at time t will increase primarily during the initial storage periods and are defined by:

$$\delta_B = a_1 (1 - e^{\frac{t}{t_B}}).$$

With t_B, the period must be chosen, after which the increase in residual displacements will presumably have ceased.
The relationship between the temperature field in the concrete and thus the temperature-induced deformations of the dam body and the external temperatures is very complex and can only be approximated even using regression analysis. The slow advance of external temperatures to the inside of the dam body, which is largely dependent on the temperature history, requires that a respectively longer period be taken into consideration with increasing dam thickness. It can be determined in three fundamentally different ways:
- Direct determination of the dam body's deformations based on the concrete temperatures.
- Based on the measured external temperatures, taking the temperature history into consideration, and setting up a relation between the external temperatures and the respective deformations.
- Based on a "characteristic concrete temperature", usually measured in the centre top section of the dam, assuming that this characteristic concrete temperature always reflects the same temperature

field in the entire dam. The prior external temperature history is ignored, which may be justifiable for small dam thickness.

Using the LMRA, the displacements due to temperature δ_T are related to the mean annual load graph of the air temperature $\delta'_{T,t}$ and the daily deviations from this annual load graph $\delta''_{T,t}$. Thereby, the influence of the water temperature is implicitly related to the storage level:

$$\delta_T = \delta'_{T,t} + \delta''_{T,t}.$$

In a first calculation step, the mean annual load graph of the temperatures is determined and then related to the respective annual load graph of the deformations $\delta'_{T,t}$. The daily deviations of the temperatures from the mean annual load graph were defined by $\delta''_{T,t}$. Thereby, with increasing dam thickness, a longer preceding period must be taken into consideration, whose length in days should at least correspond to the dam thickness in meters.

The water pressure is clearly given by the storage level h and is introduced into the regression analysis using the definition:

$$\delta_W = \delta'_{W,t} + \delta''_{W,t.}$$

Where $\delta'_{W,t}$ defines the immediate elastic share and $\delta''_{W,t}$ the delayed elastic share, thus the influence of the load history as well as creep. The immediate elastic share is usually defined using a power equation:

$$\delta'_{W,t} = \sum_{1}^{n} h^n$$

The decisive exponents n can be determined based on the significance of their share in the overall value (see section 7.6.2). The exponents 1 and 3 have proved optimal for the displacements along the crest and a linear equation at the dam base.

Based on the preceding storage level history, the delayed elastic share is given by:

$$\delta''_{W,t} = a_1.h_{t-i} + a_2.h_{t-2i} + a_3.h_{t-3i}$$

where i defines the length of the preceding period, resulting from the period of creep that must be taken into consideration.

Finally, it shall be pointed out that this method can of course be used not only for deformations, but also for all other measured parameters.

7.6.2 Evaluation of the results of a regression analysis

To evaluate the usefulness of a statistic method, various parameters can be used. These include (Table 7/2):

- "t" values for the significance of the influence of the various variables. Using these values, the general regression formula can be reduced to the significant terms in each individual case.
- Variation coefficients "v", i.e. the mean variation in relation to the variation range of the calculated values, assuming a normal error distribution.
- Multiple correlation coefficient "R" or the reliability factor R^2, which defines the share of the measured value determined by the chosen equation.
- Absolute mean error deviation Θ.

Table 7/2: Examples for the parameters of several regression analyses [*69*].

	Block	Displacements					Water flow	
			max		v		q_{max}	Θ_w
		R^2	δ'_B	δ_{el}	v_{EL}	e_V		
		mm			%	mm	l/s	
Limberg	7	0.96	0.73	19.7	4.3	2.0	0.03	0.01
	0	0.98	-1.00	29.5	2.9	2.0	0.012	0.05
	8	0.96	-0.15	19.1	4.1	2.0		
Drossen	0	0.98	4.80	55.1	2.7	2.5	1.25	0.30
							0.20	0.10
Mooser	7	0.97	-0.74	27.8	3.6	2.0	0.60	0.05
	1	0.98	-0.72	32.7	3.2	2.0	0.35	0.05
	8	0.96	-0.77	22.7	4.4	2.0		

Legend: Blocks 0,1 ... centre blocks
Blocks 7,8 ... lateral blocks
δ_B .... residual deformation
δ_{el} ... elastic deformation
v_{el} ... variation coefficient, relative to δ_{el}
e ..... range of allowable measured values
q_{max} max. water ingress into bottom gallery left and right flank

Comparing the parameters of dams of various sizes shows that the absolute variation range of the deformations is generally between 1 und 2 mm and is less dependent on the extent of the overall deformation. This could mean that the variation primarily results from inaccuracies that inevitably occur on the way from the measuring instrument to the computer.

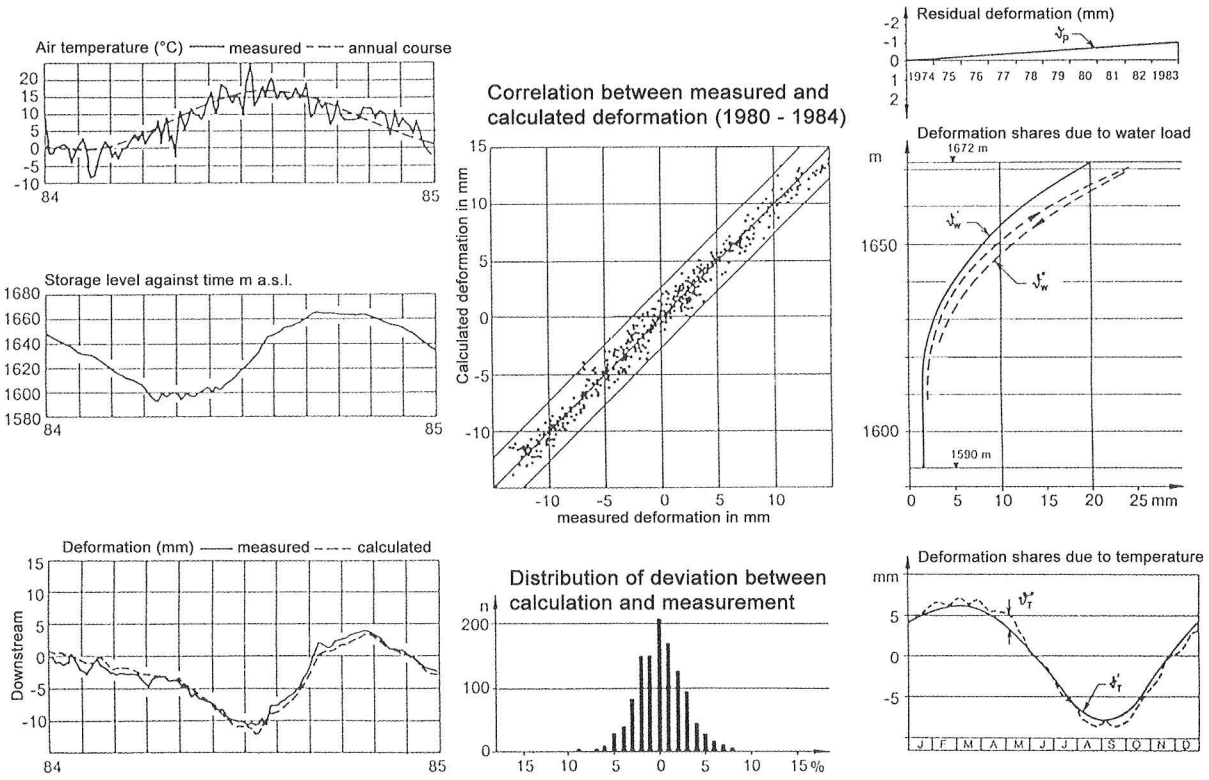

Fig. 7.9: Comparison of the regression analysis results for the crest of the Limberg arch gravity dam 1974 - 1983 to the actual displacement in 1984.

7.6.3 Application example

An example of a regression analysis result is illustrated in Fig. 7.9. It shows the various shares of the main influencing factors in the overall crest displacement of the Limberg arch gravity dam

Of particular interest is the distribution of the differences between the measured and calculated values.

The results show a symmetrical error distribution probably caused by random deviations. According to this analysis, a residual displacement of the crest by 1 mm had occurred during the observation period, a rather negligible dimension. Taking the load history into consideration, the hysteresis cycle is clearly defined.

7.7 SUMMARY

As with all other technical structures, monitoring plays an important role in ensuring dam safety, since damages generally take a long time to develop before they actually endanger the stability of the dam. Therefore, the monitoring programme including regular inspections and measuring instruments constitutes an essential component in each project.

If these recommendations are observed, developing damages can be discovered and remedied in time, ensuring dam safety.

REFERENCES

Breitenstein F., Eiselmayer M.: Überwachung von Talsperren bei Wasserkraftanlagen. Vertrauen in die Kraft des Wassers, Koska Verlag 1987

Köhler W.: Einsatz neuronaler Netze bei der Talsperrenüberwachung. Verbund - Forschungsbericht 1996, Wien.

Leobacher A., Liegler K.: Langzeitkontrolle von Massenbewegungen der Stauraumhänge des Speichers Durlassboden. Felsbau 1998, Heft 3.

Melbinger R.: Die Genehmigung und Überwachung der Talsperren in Österreich. Öst. Wasserwirtschaft 1991, Heft 5/6.

Pürer E. et al.: Application of statistical methods in monitoring arch dam behaviour. Water Power, 12/1986.

SNCOLD: Zustandsüberwachung von Stauanlagen und Checklisten für visuelle Kontrollen. Schweizer Nationalkomitee für große Talsperren, 1997.

8. MEASUREMENT RESULTS AND THEIR STATIC EVALUATION

8.1 INTRODUCTION

Before evaluation:
– The plausibility of the measured values must be checked.
– Data banks must be available allowing direct access to all measurement series as well as any combination thereof.
– The measurement series should be smoothened for static evaluation.
The goals of measurement result evaluations are:
– Evaluation of long-term tendencies as a criterion for possible changes in dam safety; thereby the time-dependent behaviour of concrete and rock must be taken into consideration.
– Back analysis of input parameters, such as the deformation parameters of concrete and rock by representing the relations between abutment forces and displacements.
– Comparison of calculated to measured values; thereby, special care must be taken that the location and direction of the measured and calculated values correspond to each other.
– Determination of the relations between various measured values, such as extensometer measurements and seepage.
– Clarification of the causes, if the calculated and measured values do not correspond to each other.
– Changes in the long-term behaviour of the dam body or underground under constant external influences can – but must not necessarily – indicate the onset of changes in dam safety. In regard to the changes, a distinction must be drawn between changes that:

- Can be attributed to the rheological properties of concrete and rock, including, for example, a reduction in the elastic range under storage conditions as well as a diminishing increase in residual deformations as the number of storage cycles increases.
- Indicate unexpected changes in the concrete, e.g. volume increase due to swelling resulting in upstream displacements and lifting of the dam crest which in turn can cause cracking.
- Are due to cracks in the concrete or joint expansions in the rock, which may be indicated by a slow, but also sudden increase in water inflows.

In the section below, various measurement and evaluation techniques shall be illustrated by discussing the at times unusual measurement results of several arch dams.

8.2 THE EFFECT OF CHANGES IN CONCRETE TEMPERATURE DURING OPERATION

Determination of the temperature influence on dams comprises three tasks, the determination of:
– The external influences.
– The concrete temperatures resulting from these external influences.
– The displacements and stresses due to the changes in concrete temperature.
External influences include air and water temperatures as well as insolation. For arch dams of small thickness, the annual load graphs of the air temperature should be superposed by the corresponding daily load graphs, since their influence on the deformations can amount to several mm. The water temperatures in the Schlegeis reservoir, for example, were measured at the crest of the centre block by recording 35 temperature profiles over the entire year (Fig. 8.1).

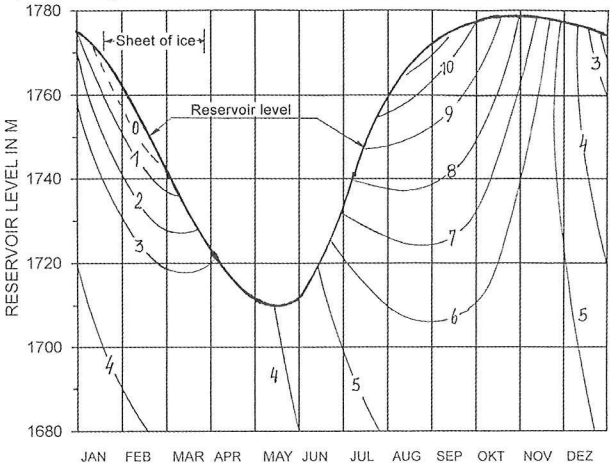

Fig. 8.1: Schlegeis reservoir, annual water temperature variation in the vicinity of the upstream dam surface.

Calculation of the temperature field within the dam body based on the time-dependent variation of the external temperatures is very complex (an approximation method was discussed in section 5.3.4). In general, the concrete temperatures are measured at several levels chosen in accordance with the calcula-

tion system. Depending on the dam thickness, 3 - 7 transducers should be installed in each measurement cross section; their spacing should increase from the dam surface to the centre and the measured values should be read daily or up to every 2 weeks.

The concrete temperature fields during the summer and winter for the Schlegeis arch dam are illustrated in Fig. 8.2. What is remarkable is that in the winter the concrete temperatures in the upstream top section of the dam were significantly higher than downstream despite the low reservoir level. This can be explained by the fact that the upstream dam surface faces south: Insolation during the day warms up the area near the surface, preventing the radiation of internal warmth to the upstream face. Therefore, slightly higher temperatures should already be assumed for the south side in the design. At the lowest measuring level near the dam base, however, only very small temperature changes could be observed.

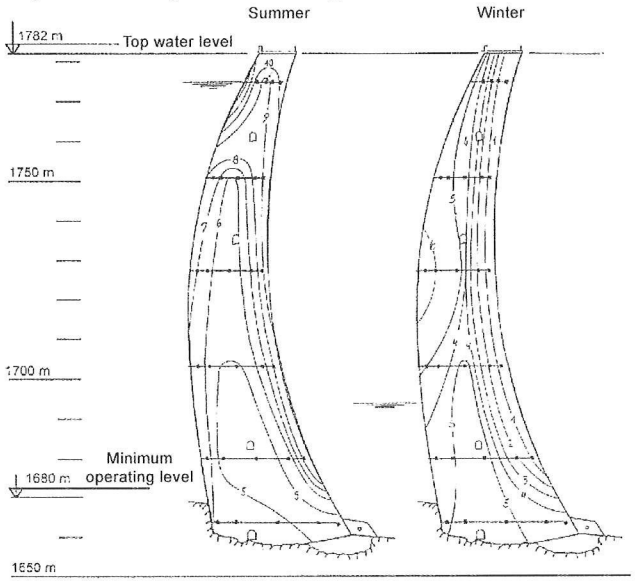

Fig. 8.2: Schlegeis arch dam, temperature fields in the concrete.

The influence of the changes in the temperature field, as compared to the initial state at the time of the respective first block joint injection, on the stresses and deformations of the dam body could be determined, ultimately, by directly assigning the measured temperature field to the elements of the static calculation. It is, however, simpler, and therefore common practice, to deduce the linearized concrete temperature variation in each measurement cross section from these measurement results (see Fig. 5.15) and to carry out the static calculation based on these values. The stresses due to the deviation of the actual from the idealised temperature distribution in the dam cross section are usually ignored as is the stress state at the time of the block joint injection.

Evaluation of the concrete temperature measurements confirmed the expected strong dependency of the annual amplitude of the concrete temperature changes on the dam thickness (Fig. 8.3):

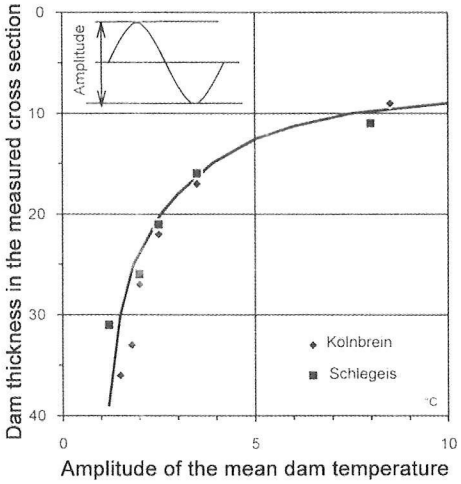

Fig. 8.3: Decrease in the amplitude of the concrete temperature variations in the dam centre with increasing dam thickness.

The temperature gradient corresponds to the reduced temperature difference at both dam surfaces, as compared to the outside temperature variations, relative to the dam thickness. While the uniform temperature variations lead to volume changes, i.e. radial and vertical displacements but only low restraint stresses, the torsions due to the temperature gradient are strongly restrained and cause, therefore, predominantly restraint stresses.

The influence of the concrete temperature changes on the annual variation in radial displacements in the centre section was determined using regression analysis (Fig. 8.4). As could be expected, with increasing dam thickness, i.e. from the top to the bottom:

– The amplitude of the radial displacements decreases.

– The phase delay increases by approximately 5 weeks.

The abutment displacements due to concrete temperature changes can be ignored.

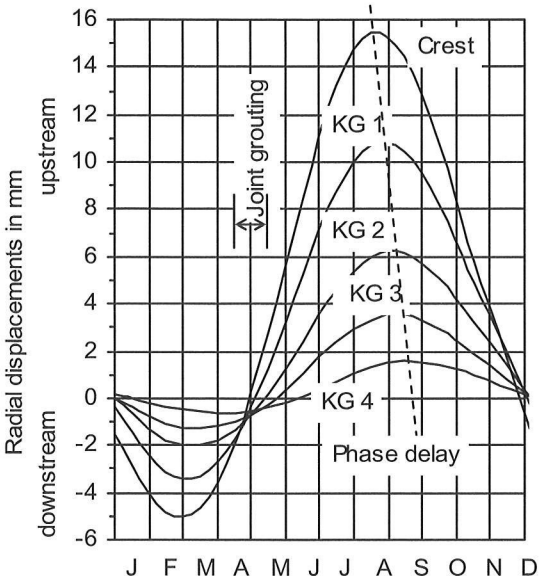

Fig. 8.4: Schlegeis arch dam: Mean annual variation in the radial displacements at the measuring levels of the centre section due to temperature variations.

8.3 HORIZONTAL RADIAL DISPLACEMENTS

8.3.1 Displacements of the dam body

The displacements of the dam body are determined by the deformations of the dam body itself and the deformations of the underground at the dam base. In general, examinations do not distinguish between their individual shares in the overall deformation.

Gerlos arch dam as an example for abnormal long-term behaviour

The 39 m high Gerlos arch dam constructed in the final years of the second World War as a weekly storage reservoir (length of the crest arch 69 m), with an artificial abutment at the left valley flank, was only monitored using geodetic measurements of the horizontal and vertical displacements along the crest, in keeping with the technological development of the time. Due to rockslides on both valley flanks downstream of the dam, the dam was first rehabilitated in 1964 (Fig. 8.5) by the construction of a downstream gravity dam supporting the valley flanks and the arch.

The annual amplitude of the displacements of the crest arch at the crown of approximately ±1.5 mm in the radial direction and ±0.4 mm in the vertical direction results primarily from the temperature changes. However, deviating from the usual reversible behaviour, residual displacements with an approximately linear increase over time were observed (Fig.8.6):

upstream in the horizontal direction of the crest arch
- at the crown ..... 1.6 mm/year
- in the vicinity of the abutment ..... 0.6 mm/ year

of the gravity dam
- at the inspection gallery level ..... 0.2 mm/ year

upward in the vertical direction in the centre section of the arch dam at the level of
- the crest (36 m above the dam base) ..... 2.2 mm/ year
- the inspection gallery (27 m above the dam base) ..... 1.5 mm/ year
- the gate chamber (12 m above the dam base) ..... 0.4 mm/ year

the left abutment in the direction
- of the arch tangent ..... 0.2 mm/ year
- upward ..... 0.8 mm/ year

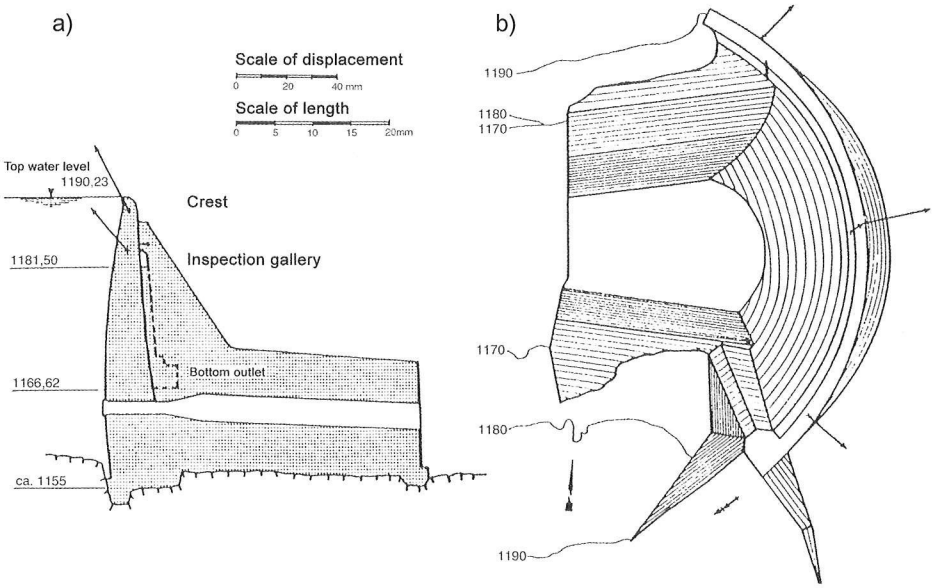

a ... Displacements in the centre section, observation period May/72 - May/84

b Horizontal displacements along the crest, observation period December/64 - May/84

Fig. 8.5: Gerlos arch dam, location drawing and centre section with the displacement vectors [64].

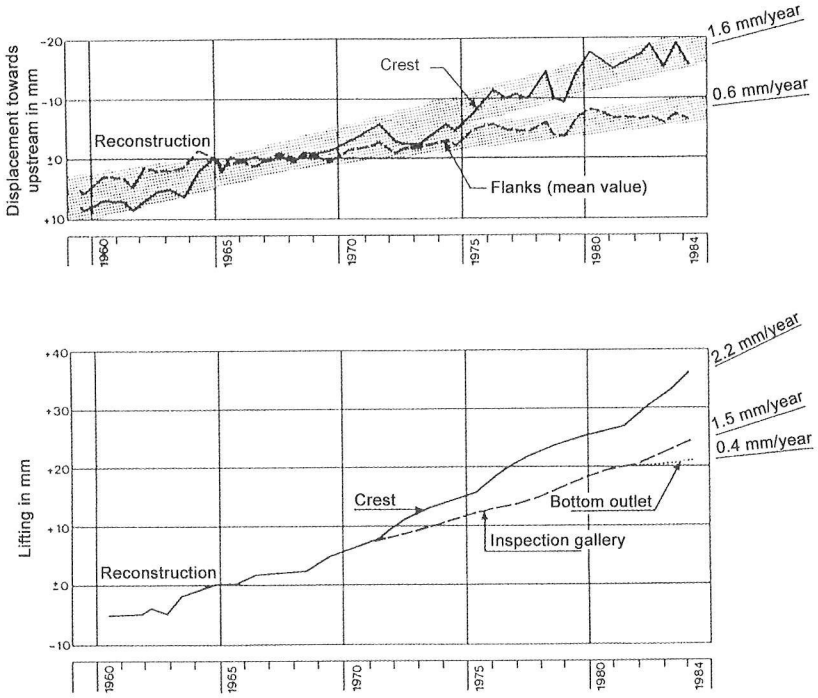

Fig. 8.6: Gerlos arch dam, displacements of the crest arch at the crown between 1960 - 1985 in the radial and vertical direction [64].

On the other hand, no significant tendency towards liftings at the crest of the gravity dam built downstream of the original dam or towards changes in the chord length could be observed. Following lengthy concrete technological examinations, the cause was confirmed as suspected to be the low alkaline expansion of the dam concrete. Upstream, this atypical behaviour resulted in a web of surface cracks, necessitating an extensive rehabilitation of the dam (Stäuble 1997).

Limberg arch gravity dam

In the years 1948 - 1951 the Limberg arch gravity dam (height 120 m, crest length 357 m, concrete volume 446,000 m³) was constructed on calcite mica slate.

Following three intermediate storage periods in 1949 (33% of the ultimate storage level, 1950 (50%) and 1951 (96%)), the first full storage level was attained in 1952. The measuring systems for continuous monitoring basically included three pendulums in the centre section (block 0) and in two lateral blocks (block 7 (right) and 8 (left)), weir flowmeters to determine water leakages into the bottom gallery resting immediately upon the rock as well as 46 measurement positions to monitor the uplift pressures. 45 temperature sensors, several telepressmeters and more than 100 teleformeters completed the very extensive measuring equipment, considering the technological development of the time. Geodetic measurements (crest levelling and downstream bending surface) were carried out as well.

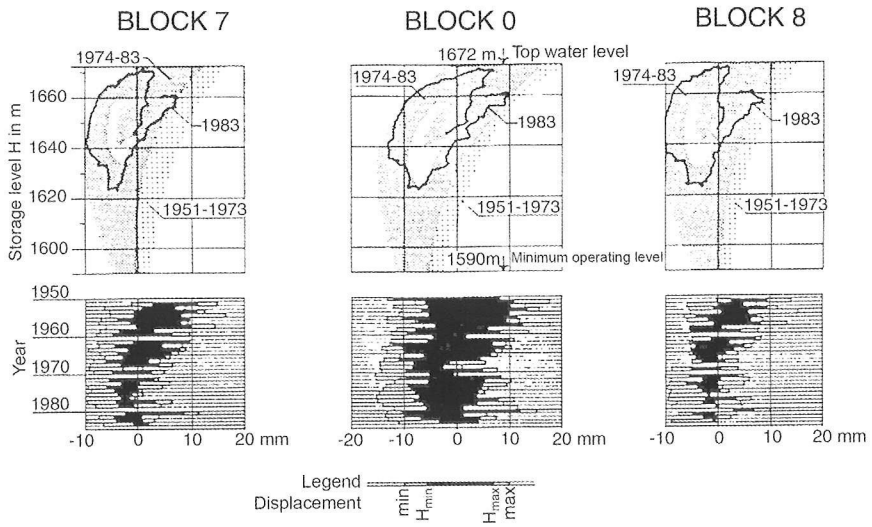

Fig. 8.7: Limberg arch gravity dam, radial displacements along the crest in the blocks 7, 0 and 8 [64].

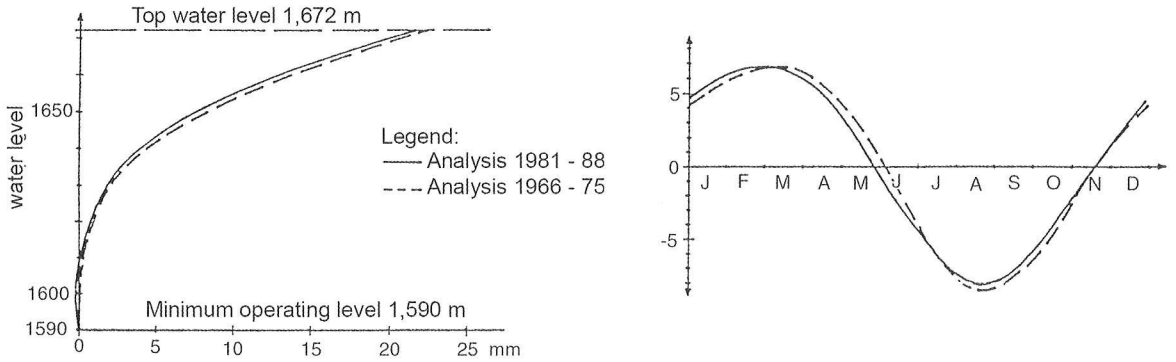

a ... radial elastic displacement due to water load

b ... annual radial displacements due to temperature

Fig. 8.8: Limberg arch gravity dam, comparison of the regression analyses for the radial displacements of the crest arch crown in 1966/75 and 1981/88.

The previously usual representation of the annual extreme displacements (Fig. 8.7) by representing the measured values of the annual storage level range cannot indicate long-term tendencies, since the annual reservoir level and air temperature load graphs are not synchronous and the load and temperature history cannot be taken into consideration.

A multiple linear regression analysis produced more telling results, indicating an upstream residual displacement of the crest by approximately 6 mm in the centre block and 4 mm in both lateral blocks in the initial 15 years, which slowly decreased following the sealing of a cable channel at the crest.

The evaluations [6] of the initial storage periods showed for the crest arch crown an annual elastic radial displacement of 31 mm due to reservoir level variations and of ± 9 mm due to temperature changes. Subsequent examinations of two periods 15 years apart (Fig. 8.8) showed for the by that time constant behaviour an approximately:

– 23 mm storage-dependent elastic displacement
– and a ± 7 mm temperature-dependent displacement,

without a significant increase in residual displacements. This behaviour indicates an increase of the concrete deformation modulus by approximately 25 % since storage begin.

Schlegeis arch dam

The Schlegeis arch dam was constructed from 1967 to 1971 in the central gneiss of the Zillertaler Alps; with a height of 131 m and a crest length of 725 m, the dam required a concrete volume of just under 1 million m³ and was equipped with an extensive measuring programme. In addition to the up to that time usual measurements, the radial displacements along the dam base were measured as well using 3 inverted pendulums in up to 70m deep bores. Additional invarwire extensometers were installed in the plumb line shafts in the dam body and underground, so that the vertical displacements of the dam body as well could be measured at all inspection gallery levels.

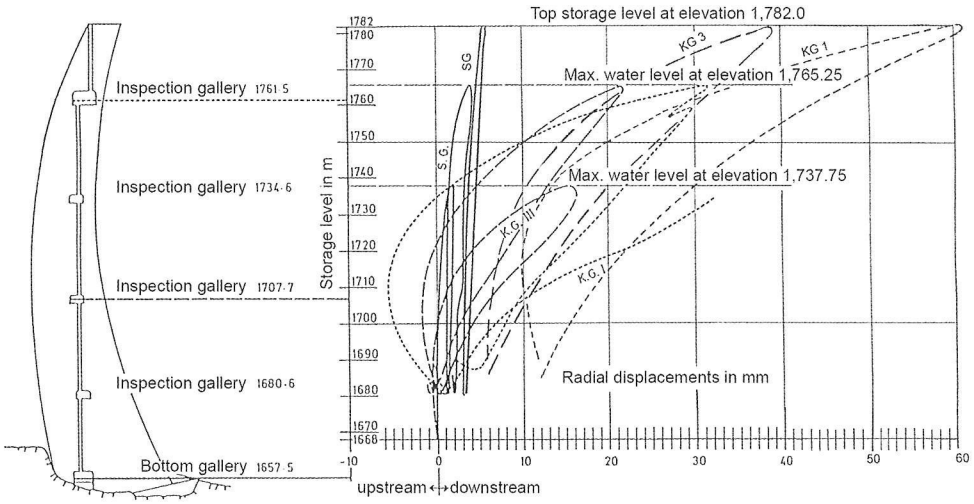

Fig. 8.9: Schlegeis arch dam, storage-dependent radial displacements in the centre section during the initial storage periods [26].

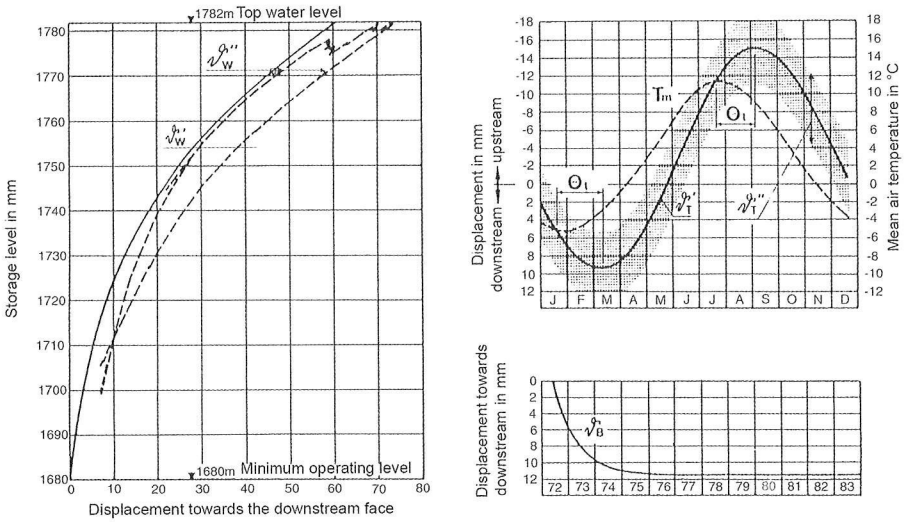

Fig. 8.10: Schlegeis arch dam, results of the regression analysis for the radial displacements of the crest arch crown 1972/83 [64].

The behaviour of the radial displacements of the crest arch crown during the step by step increase of the reservoir level until attainment of the first full storage level after 4 years corresponded to the stress-strain relations as assumed for the determination of the modulus of elasticity (Fig. 8.9).

The results of the regression analysis for the crest arch crown during 10 years following the first top storage level show (Fig. 8.10) a rapid decrease in the increase of residual deformations, the influence of the load history and a phase delay of Θ_t between the load graph of the mean air temperature and that of the temperature-dependent displacements $\left(\delta'_T \text{ and } \delta''_T\right)$.

Analysis showed that:

– 95 % of the residual deformations had settled approximately three years after the first full storage level in 1973 or 6 years after first partial storage in 1970 and reached approximately 15% of the overall deformation.

– The immediate elastic storage-dependent share of the displacements corresponds to a concrete elasticity modulus of 25 kN/mm² and the delayed share reaches up to 15% during a long-term high storage level;

– To the mean annual air temperature of +3° ± 12°C corresponded a crest displacement of ± 12 mm in the crown with an approximately one month delay and that the influence of temperatures deviating from the long-term mean can amount to up to ± 4 mm.

In regard to the results, it should be mentioned that the correlation coefficients as a measure of how well the measured values were attributed to the external influences lie above 0.95 and the standard deviation as a measure of the quality of the regression is below 4‰.

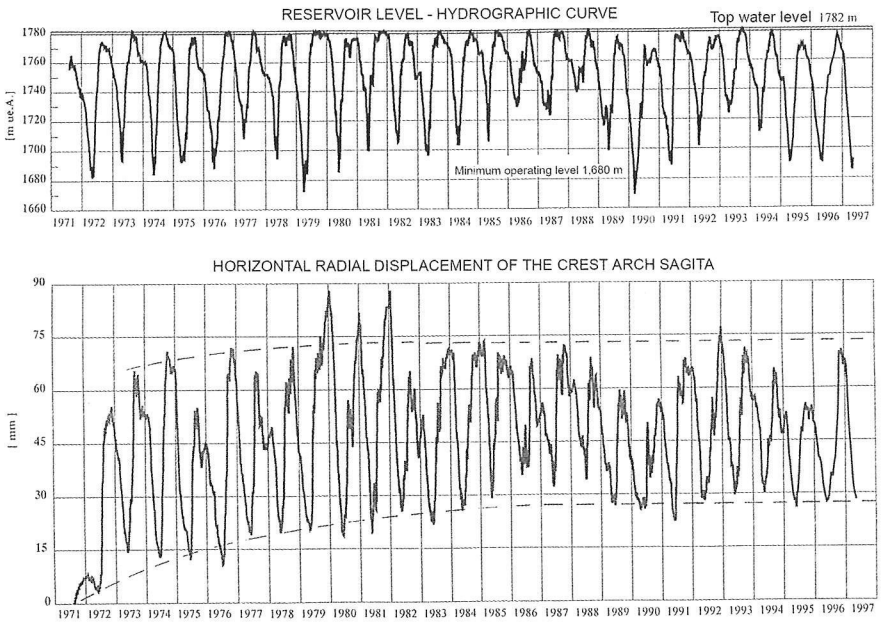

Fig. 8.11: Schlegeis arch dam, radial displacements of the crest arch crown 1971 - 1997.

The time-dependent variation in

the radial displacements of the crest arch crown from the beginning of first partial storage until 1997 (Fig. 8.11) as a function of the storage level shows the characteristic normal graphs.

The residual deformations reached approximately 27 mm and had settled after 15 storage periods (= load cycles). The amplitude of the annual variations in the radial displacements decreased from approximately 58 mm in the year of the first full storage level to approximately 44 mm after only 8 years. The thermal properties of the concrete are independent of its age and load history, so that the decrease in deformations can only be attributed to an increase of the deformation modulus by approximately 25%. In particular, it must be pointed out that, despite a low increase in residual displacements up to 1997, the maximum displacements did not increase from 1978 onward, as they were compensated by an increase in the deformation modulus.

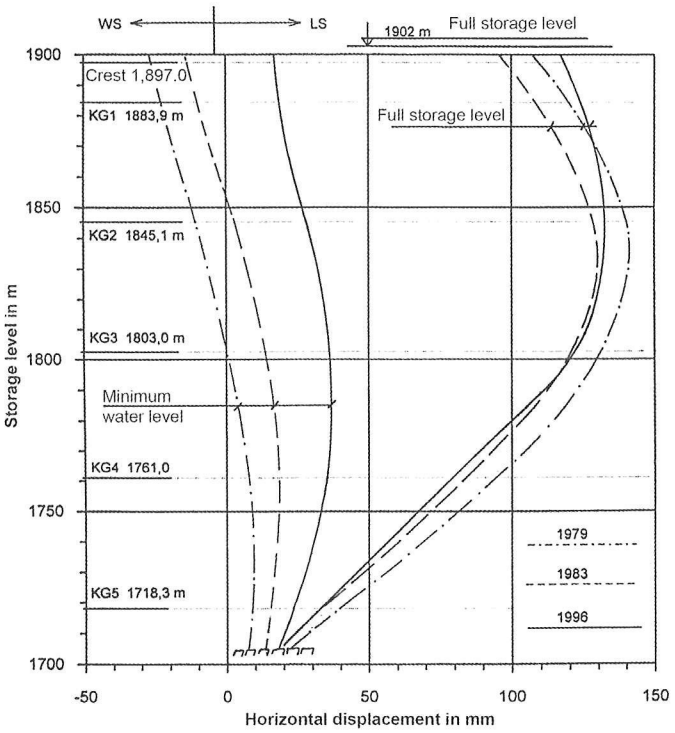

Fig. 8.12: Kölnbrein arch dam; bending lines of the centre section at full storage level in 1979, 1983 and 1996.

Kölnbrein arch dam

The almost 200 m high Kölnbrein arch dam with a crest length of 625 m and a dam volume of 1.55 million m³ was concreted from 1974 to 1977. The first full storage level was attained after three intermediate storage periods in 1979 [44]. Thereby, cracking occurred in the highest dam blocks, originating in the upstream third of the dam base at approximately ¾ of the full storage level and spreading, with increasing storage level, diagonally upwards in the upstream and diagonally downwards in the downstream direction [*70*]. These cracks were only discovered when investigations were carried to find the causes of the inadmissible seepage. Following lengthy examinations of the causes and various rehabilitation variants, the arch dam was finally rehabilitated from 1993 to 1995 by the construction of a downstream supporting concrete block (Ludescher 1996). The measurement results of this dam are therefore of particular interest.

The changes in the bending lines in the centre section as the number of the storage periods increased (Fig. 8.12) show that the overall deformation has not increased despite the residual displacements. The amplitude between the radial displacements at the lowest and highest storage level which decreased from 150 mm (1979) to 120 mm (1983) and 105 mm (1996), can only be due to the 50% increase in the deformation modulus of the concrete since attainment of the first full storage level from approximately 13 kN/mm² in 1979 to 17 kN/mm² in 1983 and 20 kN/mm² in 1996. An influence of the supporting structure on the radial displacements at the crest is not discernible.

8.3.2 Displacements at the dam base

Schlegeis arch dam

The arch gravity dam rests on a practically uniform two-mica gneiss whose foliation planes run approximately parallel to the right dam flank and dip steeply against the downstream face (Fig. 8.13). The gneiss is traversed by large-spaced and several dm thick soft interbeds of biotite schist lying in the foliation planes. In the near-surface area, various surface-parallel expansion joints were observed.

A summary of the maximum radial displacements at the dam base, measured using horizontal 50 m long extensometers and inverted pendulums reaching to a depth of 70 m into the underground (Fig. 8.14) shows that the displacements on the right valley flank are considerable higher than on the left valley flank.

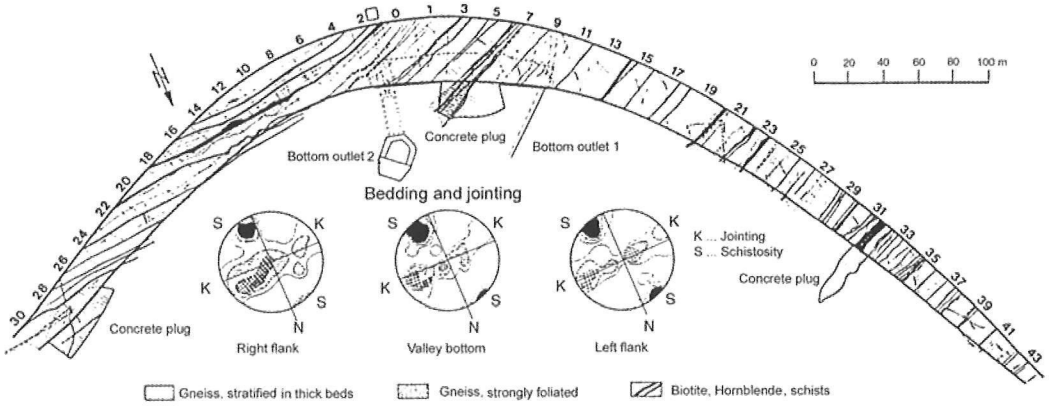

Fig. 8.13: Schlegeis arch dam, geological mapping of the dam base [61].

This behaviour can be explained by the structure of the underground. On the left flank, the foliation dipping steeply towards the downstream face runs approximately radial through the dam base and on the right flank approximately tangential; on the left, therefore, the abutment forces act upon the foliation heads and on the right upon the foliation planes. The rather continuous variation in the displacements, which were measured using various measuring systems, confirms that the anchor points both of the plumb systems and extensometers can be assumed sufficiently non-displaceable in the considered displacement direction.

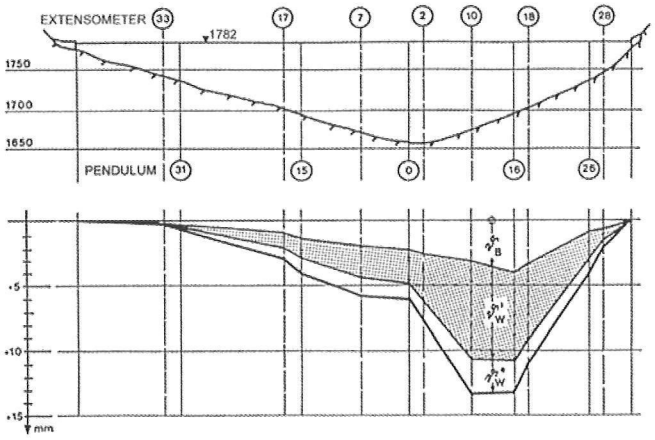

Fig.8.14: Schlegeis arch dam, radial displacements along the dam base [61].

The standard plotting of the radial displacements along the dam base (Fig. 8.15) shows in the centre section a non-linear increase in the displacements with increasing storage level.

If however, the radial displacements are plotted as a function of the overall water pressure load acting upon the dam (Fig. 8.15), an almost linear increase in the displacements with increasing storage level results, since also the transverse force at the dam base increases approximately linear with the overall water pressure load.

a) as a function of the storage level

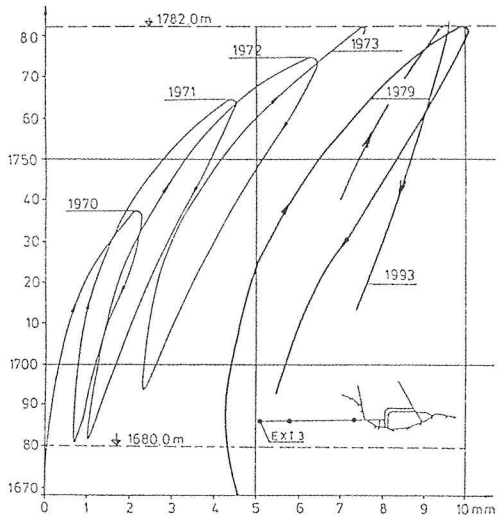

b) as a function of the overall water load

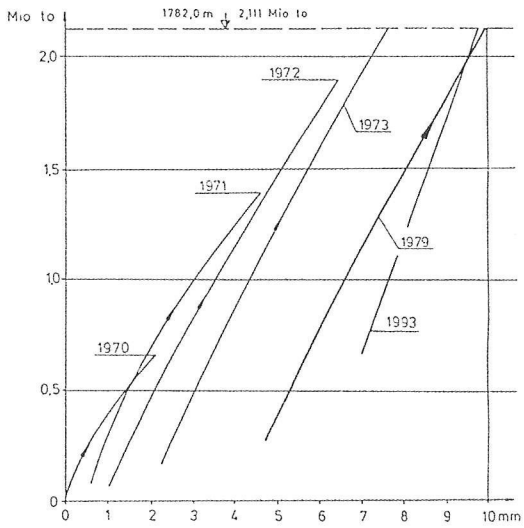

Fig. 8.15: Schlegeis arch dam, radial displacements along the dam base in the centre section until first full storage level [*52*]

The absolute highest values for the displacements along the dam base were measured in the lower part of the right slope (block 10) using up to 50 m long extensometers directed horizontally towards upstream (Fig. 8.16). The development of these displacements over time shows that the residual displacements had largely settled 10 years after attainment of the first full storage level.

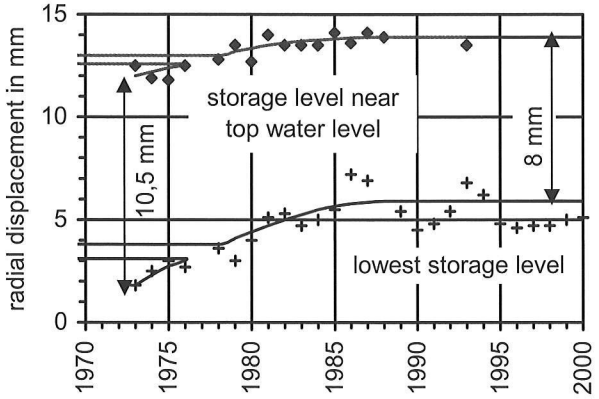

Fig. 8.16: Schlegeis arch dam, radial displacements along the foundation of the measuring block 10 between 1973 and 2000 [61].

The diagram shows the largest and smallest displacements during the initial 27 years. In this period, the residual deformation reached approximately 4 mm or just under 30% of the overall displacement. The maximum displacement had, however, only increased by approximately 2 mm; therefore, the elastic displacement had decreased from approximately 10.5 mm to 8 mm indicating that the deformation modulus in the rock had increased by approximately 25% after 15 load cycles.

For the investigations discussed below to determine the deformation parameters of the rock underground, various definitions must first be clarified: (see also Fig. 3.8):

– E_0 defines the value of the modulus of elasticity resulting from the immediate elastic storage-dependent share of the deformations.

– E_1 defines the value of the modulus of elasticity resulting from the elastic storage-dependent displacements including the delayed elastic share.

– V defines the value of the deformation modulus resulting from the inclusion of the residual deformations.

In a first approximation, the ideal moduli of elasticity and deformation of the underground can be determined comparatively easily assuming an elastic isotropic semispace. If the immediate elastic storage-dependent share is assumed to be a function of the share of the overall abutment force acting in the displacement direction (Fig. 8.17), moduli of elasticity E_0 between 11 kN/mm² (block 18) and 60 kN/mm² (blocks 7 and 17) result. Taking the delayed deformations into consideration, a somewhat lower deformation modulus E_1 between 10 kN/mm² (block 18) and 50 kN/mm² (block 17) results.

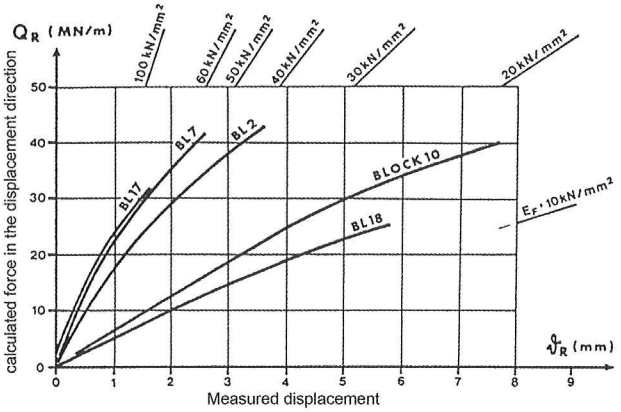

Fig. 8.17: Schlegeis arch dam, deformation moduli for the elastic storage-dependent share of the abutment displacements at first full storage level [61].

A comparison of these values reveals quite plausible relations, but also the problematic nature of deducing representative deformation parameters for the structure from test results. The deformation parameters deduced from various tests were consistently lower, lying approximately between 7 kN/mm² and 21 kN/mm² for the modulus of elasticity E_1 and approximately from 10 kN/mm² up to 30 kN/mm² for the modulus of elasticity E_0. This can be explained by the fact that in an underground with only few joints the transverse strain is restrained; as is generally known, this results in a reduction of the deformations or in an increase of the parameters for the deformation behaviour.

The following regression analysis [61] for the radial displacements of block 10 at the foundation refers to a period of 12 years following the injection of the contraction joints of the entire dam in the spring of 1972, since only from that date on the monolithic effect of the entire arch dam for bearing the water load seems to be ensured. In 1970 and 1971 two partial storage periods (50% or 70% of the full storage level) had already taken place, so that these

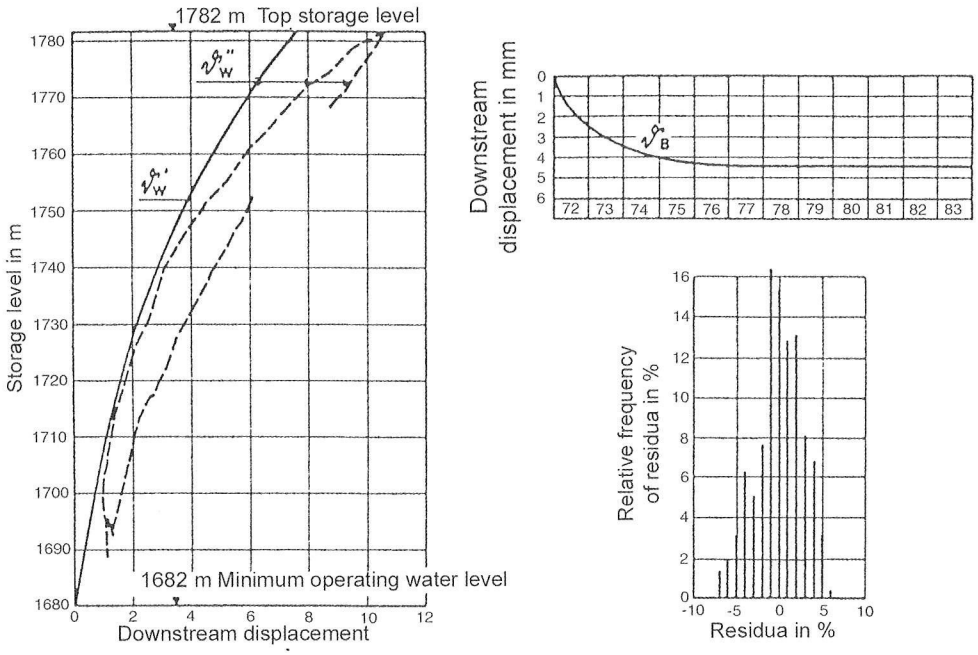

Fig. 8.18: Schlegeis arch dam, results of the regression analysis 1972/83 for the radial displacements at the foundation of block 10.

evaluations do not include the overall residual deformations (Fig. 8.18).

The results of a regression analysis for the block with the largest displacements initially show that:

– The temperature influence on the displacements at the dam base can be ignored.

– The residual displacements had basically settled 7 years after first partial storage began and accounted for almost 30% of the overall displacements.

– The delayed share of the displacements reached approximately 30% of the elastic displacements as well. The hysteresis cycle, also generally known from all concrete and rock tests, could be clearly determined in the regression analysis.

Kölnbrein arch dam

The arch dam rests on granite gneiss, which is very massive at the right flank, particularly at the right slope foot, more plate-like at the left flank and traversed by schistose zones in the valley base, particularly at the left slope foot (*86*).

While preparing for rehabilitation, geological investigations confirmed the presence of steep cracks in the rock under the upstream face of the arch dam (Fig. 8.19). The variation of the measured horizontal displacements (Fig. 8.20) during the previous storage periods shows the influence of the inclination of the abutment forces towards the dam base.

After decreasing the water pressure under the dam by constructing a fore-structure and an additional

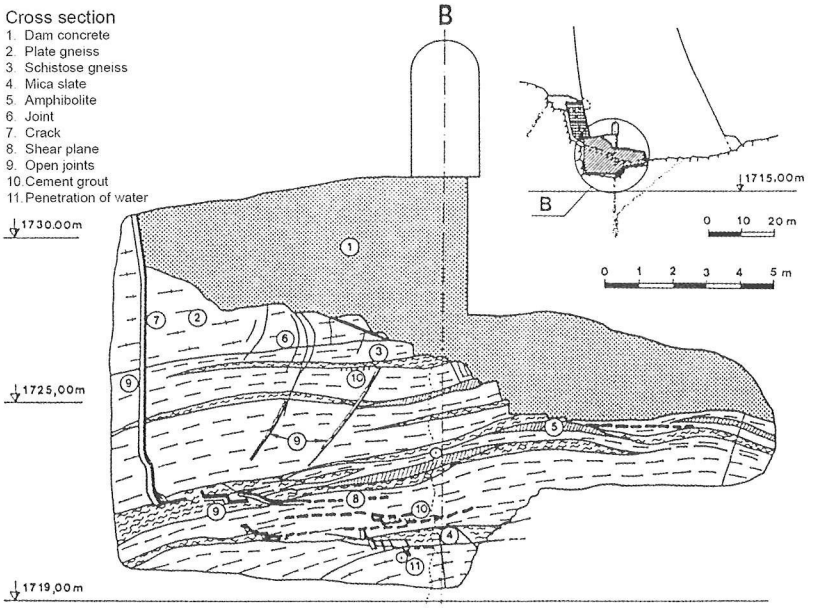

Fig. 8.19: Vertical section of a geological survey under the dam base at the right slope foot, block 20, (Demmer, 1982).

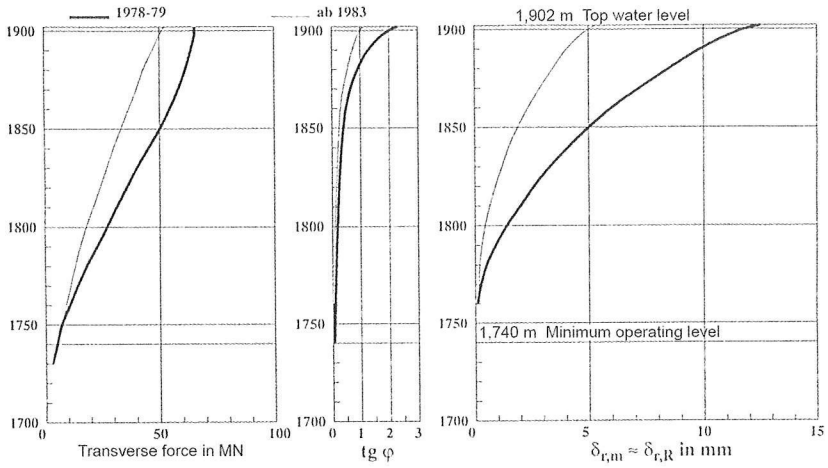

Fig. 8.20: Elastic radial displacements of the centre block at the dam base.

upstream grout curtain as a first partial rehabilitation measure, the displacements decreased in proportion to the lower radial horizontal force; they did, however, not decrease after halving the shear stresses by constructing a downstream supporting arch (Fig. 8.20). A comparison of measured to calculated displacements revealed that, as the number of load cycles increased, the displacements decreased per load unit by a displacement modulus of 0.47 mm/MN for the storage periods of 1978/79 and from 1983 on by a displacement modulus of 0.39 mm/MN, i.e. by approximately 20 %.

8.4 VERTICAL DISPLACEMENTS

8.4.1 Vertical displacements at the dam base

The vertical component of the stresses as well is primarily determined by the two main load cases, dead load and water load. The dead load case is usually calculated for the blocks assumed to be independent (the justification of this assumption is discussed in more detail in section 8.6.1); for the subsequent water pressure load case, however, the monolithic arch is then effective. Superimposing both load cases - acting in the opposite direction as regards the vertical stresses along the dam base- presumes an elastic behaviour of the structure and underground. If analysis is based on the deformation behaviour, for the sake of a more descriptive representation, the dam body and rock base must be considered separately.

Initially, the dead load of the dam body acts upon the rock base; the settlement depression reaches its maximum value in the vicinity of the upstream dam base. The concrete blocks - prior to block joint injection - follow these deformations without additional stresses. Depending on its stiffness, the monolithic dam body will turn in the downstream direction during impounding, due to the horizontal water pressure. The rock foundation can follow this turning or lifting under the upstream half of the dam base only up to a certain rock surface level, which will remain below the level prior to the beginning of concreting due to the residual share of previous settlements. If the dam body continues to turn, vertical tensile stresses will first be generated along the upstream face, as long as the dam body "pulls along" the rock underground. After exceeding a limit value, the joint rock-concrete will open or, which is rather more probable, the shallow joints in the rock under the dam.

Already the usual tests to determine the deformation behaviour of concrete and rock show that their deformation behaviour is also dependent on their load history. Therefore, a distinction must be drawn between a - lower - deformation modulus for initial loading and a - higher - modulus of elasticity, which will only be reached after several load cycles; the difference between these two moduli defines the residual deformations. These influences will naturally be most effective at the base of the highest dam section, where also most damages of arch dams occur. The deformation behaviour of this section will, therefore, be discussed in more detail below.

8.4.2 Settlements due to dead load during construction.

Schlegeis arch dam

In the underground of the Schlegeis arch dam,

measurement of the settlements using extensometers was already begun during placing of concrete. Based on the settlements as a function of the superimposed dam load, deformation moduli between 11 kN/mm² and 40 kN/mm² can be estimated under the ideal assumed condition of an elastic isotropic semispace similar to the horizontal displacements (Fig. 8.21).

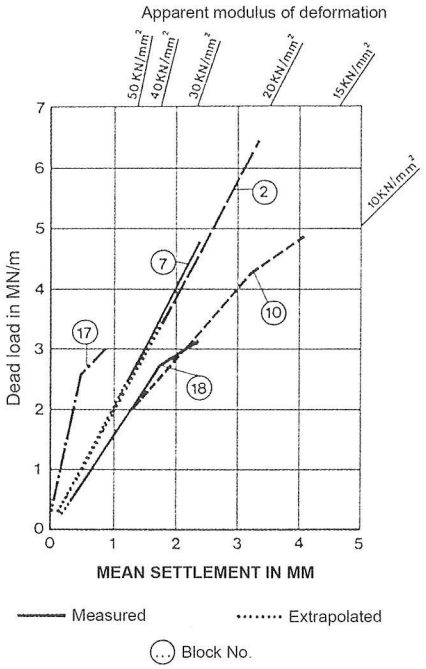

Fig. 8.21:Schlegeis dam: Deformation moduli for the settlements due to dead load [61].

Kölnbrein arch dam

Measurement of the settlements during concreting was hindered by site operations and could only be commenced after reaching a certain pouring horizon. In order to be able to estimate the settlements during the entire construction period, the existing measurements must be examined in detail to allow precise conclusions. A representative evaluation of the settlement measurements is rendered more difficult on account of various causes:

– The reading points for the mechanical measuring instruments are partly located in inspection gallery 5 that is approximately 15 m above the dam base.

– The extensometer and invarwire measuring lengths are not equally long.

– In regard to the influence of the dead load, the measurements are only directly comparable, if the reservoir is empty. Since the reservoir was already partly filled during concreting, only a lower number of measurements can be evaluated.

– Particularly at the downstream face, the measurements concerning the influence of the dead load can only be evaluated until storage begin, since subsequent measurements taken at times when the reservoir is empty will include the residual settlements resulting from partial storage after relieving of the load.

First, a conversion of the existing measured values for the dam centre at the dam base was necessary. In addition, under the simplifying assumption of an elastic isotropic semispace, the compression of the underground within the various measuring lengths under a unit triangular load was determined. The respective settlements were then calculated by superimposing these unit values using the respective surface stresses at the time of zero measurement and additional representative dates at higher concreted levels. From the difference to the zero measurement the actual deformation modulus can be recalculated.

Block 16 (centre block) illustrates (Fig. 8.22) that for the settlements at the upstream face and in the block centre the same deformation modulus of 16 kN/mm² for the first loading shows a very good calculation/measurement correspondence.

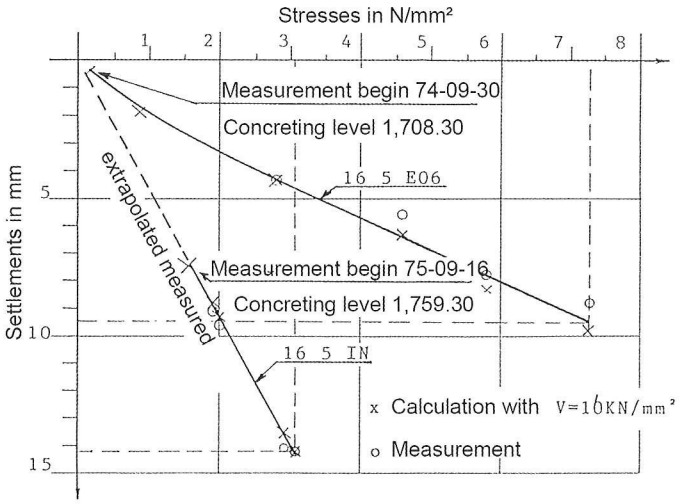

Legend:

16 5 E06 ... vertical extensometer in block 16, inspection gallery 5

15 5 IN .....invarwire measurement point in block 16, inspection gallery 5

Fig. 8.22: Kölnbrein dam: Comparison of measured to calculated settlements of the centre block during the construction period [94].

Zillergründl arch dam

The Zillergründl arch dam, with a height of 186 m and a crest length of 525 m, was constructed in the

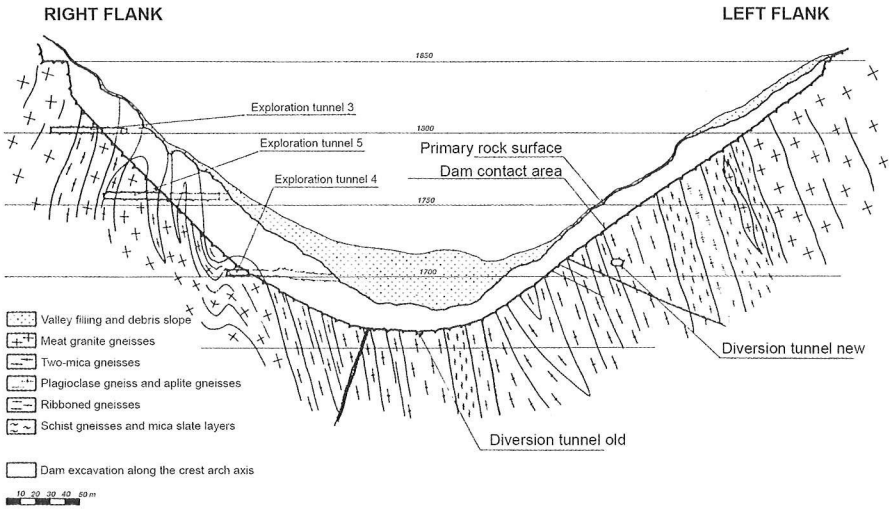

Fig. 8.23: Zillergründl arch dam, geological valley section towards upstream (*86*, Mignon 1983).

Zillertaler Alps from 1979 to 1985 and required approximately 1.4 million m³ of concrete [54]. This dam rests basically on granite gneiss with fewer joints in the right valley flank than in the left (Fig. 8.23). A steeply inclined fault zone approximately parallel to the left dam flank crosses the foundation area at the right slope foot. While the rock in both valley flanks had only a thin layer of overburden, the rock surface in the valley centre had an overburden layer up to 40 m thick.

To drain the excavation, a drainage gallery underneath the predetermined excavation bottom had already been driven before beginning excavation. Two up to 50 m long extensometers as well as levelling in this gallery made it possible to measure the vertical displacements along the dam base during excavation, placing of concrete and storage periods. Some results of these investigations are summarized below (Fig. 8.24).

During the excavation of a total of 1.7 million m³ from 1980 until the beginning of concreting in

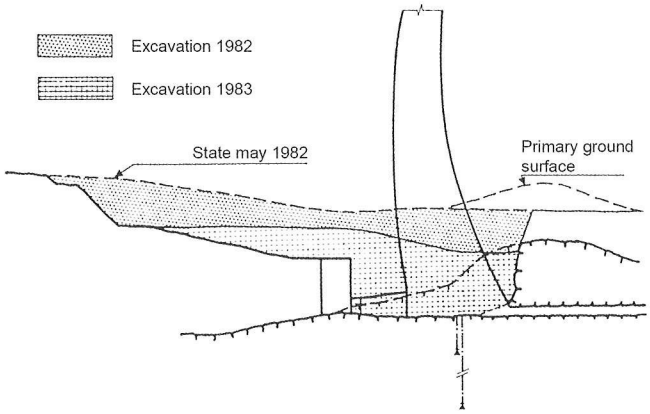

Fig. 8.24: Zillergründl arch dam, overburden and rock excavation in the valley bottom (Schöberl 1987).

September 1983, liftings of up to 8.3 mm occurred approximately concurrent with the progression of excavation (Fig. 8.25). During concreting of the dam, these liftings decreased again and as was expected, the settlement reached its maximum value of 14 mm underneath the upstream dam base, approximately 6 mm under the original rock surface.

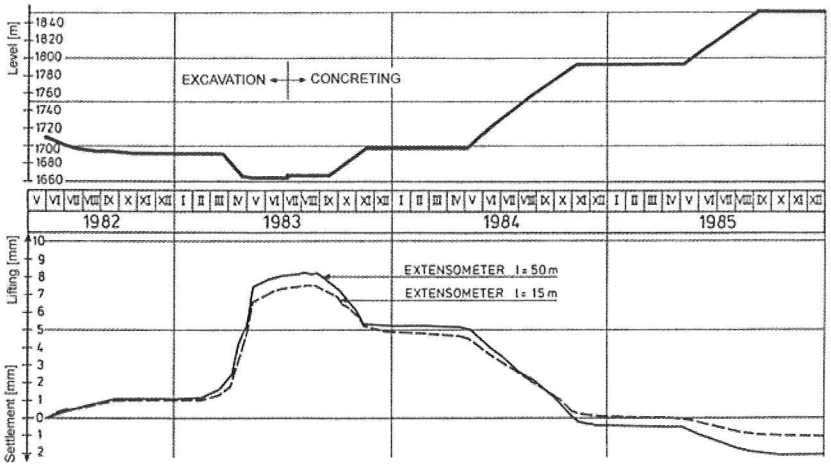

Fig. 8.25: Zillergründl arch dam, vertical displacements of the rock surface during the construction period (Schöberl 1987)

The measuring results of the invarwire extensometer anchored at a depth of 90 m, which were converted for the dam axis using clinometers, initially show during impounding the expected settlement of the dam base by 0.3 mm; subsequently, however, a lifting by approximately 1.2 mm, relative to the minimum operating level (Fig. 8.30b) and including the effect of the uplift pressure could be observed. This caused a lengthening of the dam body by approximately 9.0 mm or 6.9 x 10^{-2} mm/m dam height.

Kölnbrein arch dam

At the Kölnbrein arch dam, the weight of the impounded water (200 million m³ x 10 kN/m³) reaches 2,000 GN, the dead weight of the dam (1.6 Mio. m³ x 24 kN/m³) 40 GN, or only 2 % of the water load, and the weight of the supporting structure (0.48 Mio. m³) another 11.5 GN/m³. Since the changes in the vertical component of the overall abutment force during operation in the centre section can doubtlessly only attain part of the dead load, its effect on the anchor point of the invarwire at a depth of 80 m can be safely ignored, despite a considerably more concentrated load application.

To determine the absolute vertical displacements in the centre section of the Kölnbrein arch dam, the measurements specified below can be used (Fig. 8.31):

– Levelling in inspection gallery 1 at a level of approximately 1,882 m, relative to the portal of the passageway to the dam warden's house, at a distance of approximately 150 m from the dam abutment.

– Levelling from the portal of the access tunnel (approximately 600 m downstream of the dam base) to the pendulum devices in the lowest inspection gallery 5 at a level of approximately 1,718 m, where both the concrete bottom and the reading point of the invarwire were included in the measurement.

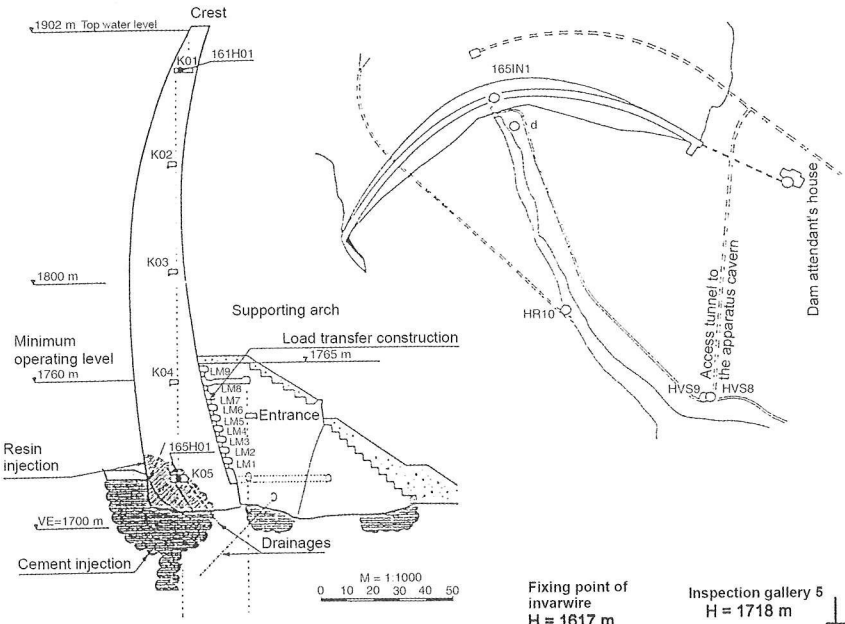

Fig. 8.31: Kölnbrein dam: Centre section, measuring system for vertical displacements.

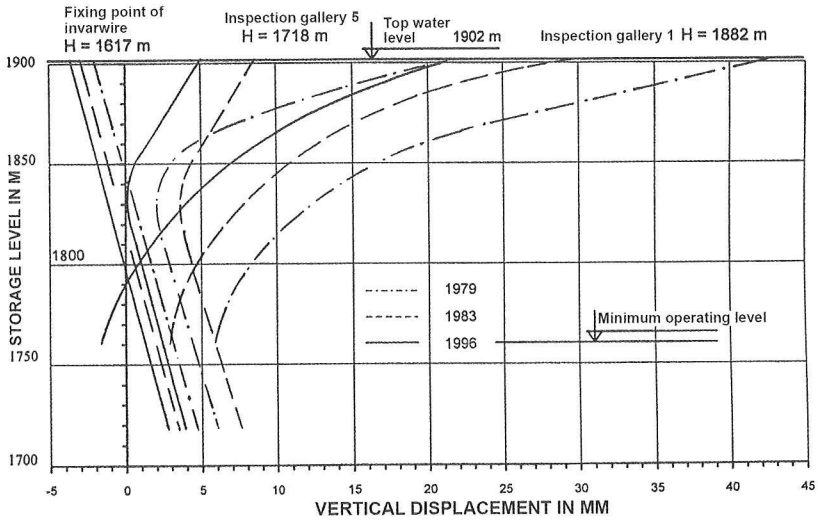

Fig. 8.32: Kölnbrein dam: Vertical displacements of the centre block [94].

– Invarwire extensometer between its anchor point at a level of 1,617 m and inspection gallery 5 (1,718 m) as well as between inspection gallery 5 and the top inspection gallery 1 (1,882 m).

The vertical displacements in the centre section (Fig. 8.32) show a similar, but significantly more pronounced variation during operation than in the case of the Schlegeis arch dam. Repeated levellings at the valley bottom, particularly during the initial storage periods, show a very low variation (~ 0.3 mm) as compared to the changes in the measured values; therefore, the rather surprising results can be assumed to be correct. The measurements refer to the beginning of the first partial storage period in the spring of 1976. Assuming that the reference points of the independent levellings can be considered unshiftable fixed points, the following storage-dependent vertical displacements result:

– Of the invarwire anchor point by approximately 6 mm, based on the geodetic absolute measurement and the length change of the invarwire during all storage periods as a linear function of the storage level; the residual settlement since measurement begin during the partial storage period in 1978 was 2 mm, thus accounting for approximately one third of the elastic deformations. The weight of the downstream supporting structure did not have a significant influence on these displacements. Underneath the two lateral measuring blocks of the arch dam at a depth of 60 m, the anchor points of the invarwire extensometers were observed to have settled by approximately 4 mm.

– In inspection gallery 5, however, widely varying displacements were measured during the individual storage periods. The extensive injection operations in the underground (111 tons of cement) since the winter of 1979/80 initially caused a residual lifting of approximately 2 mm, the construction of a downstream supporting structure from 1989 to 1992 resulted in a settlement of almost 5 mm.

- The storage-dependent vertical displacements resulted in an almost linear settlement of about 3 mm up to a reservoir level of approximately 1,830 m.
- After this reservoir level was exceeded, the lower anchor point continued to settle; the concrete body was however lifted up, resulting in a displacement which was naturally more pronounced in 1979 with a high uplift pressure, attaining 19 mm than in the years following 1983 without any considerable uplift pressure, when only 5 mm were attained.

Based on the settlement of the anchor point by approximately 6 mm under a superimposed water load of 2 N/mm² and using simplifying assumptions (elastic isotropic semispace with semicircular surface load), a modulus of elasticity of approximately 25 kN/mm² can be back-calculated that, like the residual share of deformations, corresponds satisfactorily to the preliminary investigations.

From the difference between the - extrapolated - settlements at the dam base and the anchor point, it is also possible to infer that the rock area lying in between is subjected to a compression of approximately 6 mm. Assuming that the water pressure rising up to 2 N/mm² causes a compression of the solid joint bodies while the joint widths - due to the joint water pressure - remain constant, the deformation modulus of these joint bodies as well is defined by:

$$V = 2/6 \cdot 80000 = 27 \text{ kN/mm}$$

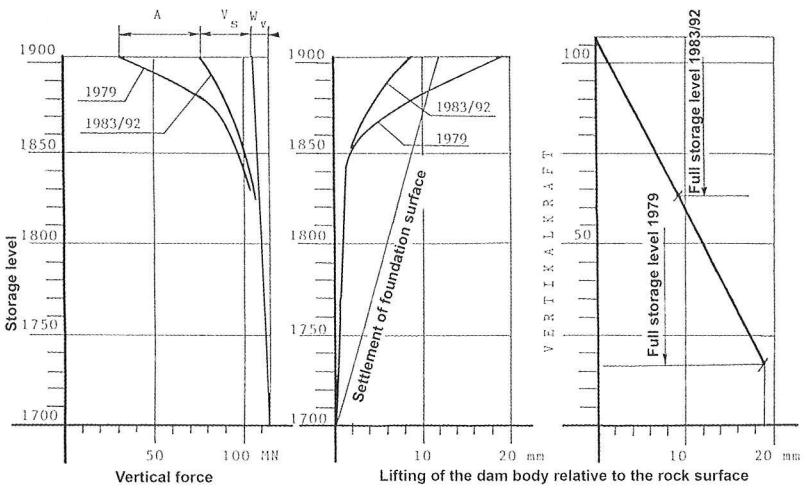

Fig. 8.33: Vertical force and vertical displacements in inspection gallery 5 as a function of reservoir level [94].

The liftings in inspection gallery 5 must be due to the corresponding reductions of the abutment resultant's vertical component. More detailed examinations revealed that this reduction of the vertical forces is caused by the influences specified below (Fig. 8.33):

- Vertical share of the water pressure at the upstream dam face W_V due to the vertical curvature of the dam body.
- Vertical shear stresses within the dam body, adding up to upwardly directed vertical forces V_S.
- The uplift force A due to the uplift pressure at the dam base or joint water pressures underneath the dam base.

During the entire observation period, a linear relation between the elastic liftings and the decreasing vertical forces could be observed.

– In the top inspection gallery, the following vertical displacements occurred:

The storage-dependent liftings in the vicinity of the crest at full storage level in 1979 attained approximately 43 mm due to the very high uplift pressure; following the reduction of the uplift pressure by the completion of a fore-structure in 1983, this lifting decreased in the same year to approximately 30 mm (amounting approximately to the same difference as in inspection gallery 5), decreasing still further to 21 mm by 1993.

The storage-dependent length changes of the dam body between inspection galleries 5 and 1, calculated from the difference between the two levellings, decreased continuously from approximately 24 mm in 1979 and 1983 to approximately 17 mm from 1993 onward.

The invarwire measurements revealed lengthening of the dam body by approximately 19 mm in 1979 and 1983, which had decreased by 1996 to approximately 12 mm.

The difference between the two levellings and the invarwire measurements indicates a storage-dependent increase in the height difference of the two levellings' reference points.

A quantitative evaluation of the causes resulting in the lengthening of the dam body revealed that:

– the seasonal temperature variation causes a length change of 4.6 mm, independent of the concrete deformation modulus as well as of the concrete age;

– the transverse strain due to the horizontal arch stresses caused an additional lengthening, that decreased from 13.8 mm in 1979 to 10 mm in the years following 1989;

– the above-mentioned decrease in the vertical force results in a reduction of the compression due to dead load;

The latter influences are dependent on the concrete deformation modulus, which increased, on average, from approximately 13 kN/mm² during impoundage in 1979 to 20 kN/mm² in 1993, as had already been determined in the evaluation of the horizontal displacements.

Settlements of the reservoir bottom

Except for the fact that even an almost impermeable reservoir bottom is very unlikely to be achieved, a number of other observations as well support the validity of the jointed rock model:

Piezometer measurements under the dam base have revealed an increasing dependency of the joint water pressures on the reservoir level with increasing depth downstream of the grout curtains; this is an indication of the impermeability of the grout curtain and points to a certain circumfluence.

Vertical extensometers, starting from the impermeable concrete plate of the fore-structure with the new grout curtain at its upstream end, constructed in 1981/82, have shown, over a measuring length of 25 m, storage-dependent elastic settlements of up to approximately 7 mm in the area of the schistose zone at the left slope foot and of 3 to 4 mm in the remaining area as a function of the deformability of the underlying rock formation. These settlements decreased as the joint water pressures under the fore-structure increased, when the drainage system of this area was closed off by way of trial.

Zillergründl arch dam

During impounding, no significant liftings of the rock foundation were measured, in contrast to the Kölnbrein arch dam; as with the Schlegeis arch dam, the vertical displacements of the dam base basically reflect only the changes in the restraint momentum due to the uplift pressure (Fig. 8.34).

Comparison to the levellings shows that the 27 m long extensometers measured approximately 2/3, the 50 m long extensometers approximately 90% of the overall settlement. The anchor points of the invarwire

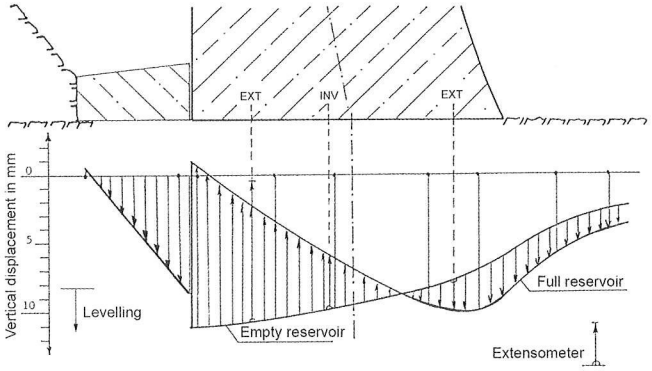

Fig. 8.34: Vertical settlements of the dam body during impounding [94].

at a depth of 80 m have settled by approximately 1 mm due to the dead load.

Another measurement, however, is of particular interest (Fig. 8.35). At the Zillergründl arch dam, a perimetral joint was installed upstream of the bottom gallery in the vicinity of the rock foundation. To monitor possible openings of this joint, another extensometer was installed underneath the joint to measure the vertical deformations of an approximately 25 m thick rock layer. The measurements revealed, in correspondence to the respective laboratory tests, a residual compression of this rock layer by approximately 30% [89]. This result is especially important because it verified that the precondition for superimposing the subsequent load cases dead load and water load, namely an elastic behaviour of the rock underground, is not given.

This by no means unexpected but often ignored fact could help to explain the occurrence of unexpected tensile stresses in this area or wider openings of the perimetral joint.

8.4.4 Summary

The arch dam zone with the highest stresses is the area around the dam base in the valley centre. Naturally, these stresses increase with increasing dam height; there-by, particularly the restraint stresses can only partly be reduced by the shape and thickness of the dam. Therefore, an evaluation of the deformation measurements is of especial importance in this area, as is confirmed by the present report.

For all three arch dams, the measuring results in regard to the vertical displacements during operation, that up to now have only rarely been considered, show a quite uniform tendency. At all three dams, a settlement was measured initially at the lowest

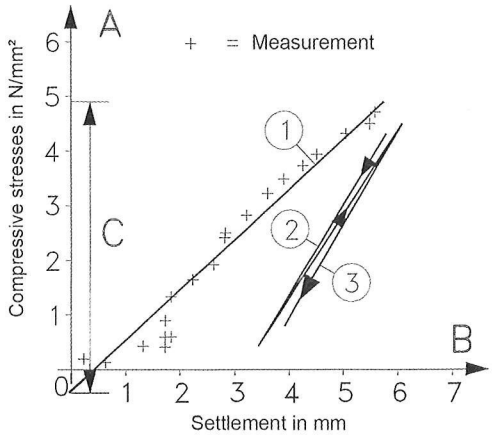

A ... Compressive stress in N/mm²
B ... Settlement in mm
C ... Calculated vertical stress
1 ... during placing of concrete
2 ... during 1st damming
3 ... during 2nd damming

Fig. 8.35: Measured vertical displacements of the rock surface under the upstream dam footing during construction and initial storage periods [94].

measuring level in the valley centre (Table 8/1). After exceeding a storage level of approximately ¾ of the maximum reservoir level, these settlements rather suddenly turned into liftings. The difference to the liftings of the dam crest finally resulted in length changes in the dam body, attributable to several causes. What is remarkable is the strong influence of the uplift pressure at the Kölnbrein arch dam, for which measurements both at a very high and very low uplift pressure were available.

The influence of the reservoir settlements on the stresses has already frequently been examined. Since possible load transfers and stress changes are dependent on the deformation variation along the dam circumference, detailed studies will still have to be carried out on the subject. Only by comparing the calculated to the measured results will a realistic determination of the conditions, particularly at the dam base, be possible.

8.5 TORSIONS AT THE DAM BASE

8.5.1 General

The bending area of the arch dam shell forces torsions at the dam base that must be compatible with the deformations of the underground normal to the dam base if the opening of cracks or joints is to be avoided. As these torsions are increasingly hindered, the restraint moments and/or bending stresses

– The load is only applied upon the completed monolithic dam, also in the case of dams constructed block by block (System C).
– The dead load of the recently poured sections acts upon the underlying monolithic, because already injected, section of the dam (System B).

Schlegeis arch dam

To check the stresses in the dead load case, telepressmeters were available in five sections along the dam base both near the upstream and downstream face; in the centre section three additional telepressmeters were installed so as to be able to better determine the stress variation between the upstream and downstream face. Other teleformeters were installed at the upstream and downstream face in 7 cross sections; each measurement point covered 5 directions at the surface for the biaxial stress state and nine directions in the interior of the dam, so that the biaxial and triaxial stress states were overdetermined. (Fig. 8.41).

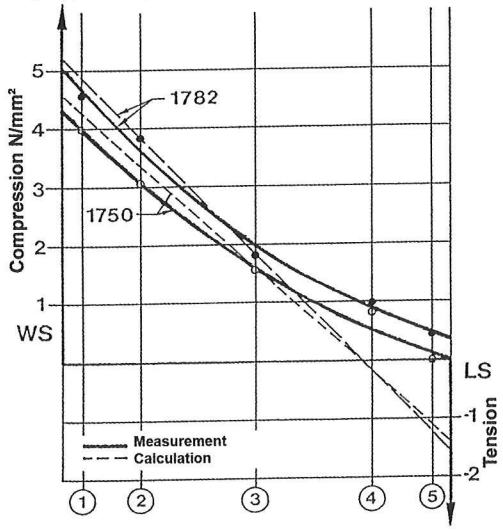

Fig. 8.41: Vertical stresses due to dead load along the foundation of the centre section of the Schlegeis arch dam [57].

The measurements showed a very good correspondence to the calculations, assuming independent dam blocks. The calculated tensile stresses along the downstream dam base could not be measured.

Kölnbrein arch dam

The influence of the assumptions specified above was determined by calculation for the 200 m high Kölnbrein arch dam and then compared to the measurement results [88].

The dam was constructed in three summer seasons, pouring had to be interrupted during the winter season (Fig. 8.42a). The block joint injections were first carried out for each pouring lift in the spring following pouring and were repeated in the following years. Impounding began only after the first winter break.

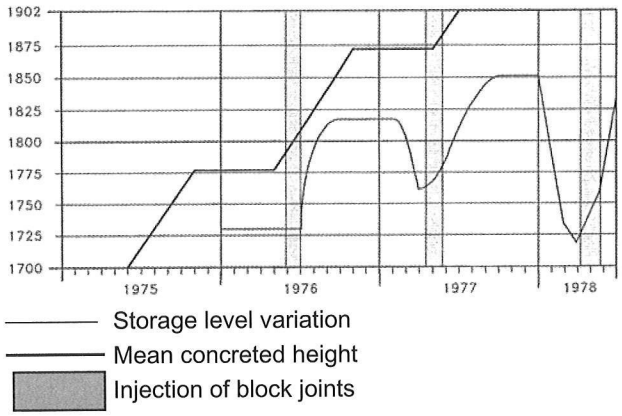

Fig. 8.42a: Pouring process and storage level variation during the construction period [88].

Therefore, the static calculations were carried out based on the following bearing systems (Fig. 8.42b):
– System 1976: Independent blocks for the blocks poured in the preceding year.
– System 1977: The weight of the independently assumed blocks poured in 1976 acts upon the monolithic zone poured in the preceding year.
– System 1978: The weight of the blocks assumed to be independent and poured in 1977 acts upon the monolithic zone poured in the preceding years.

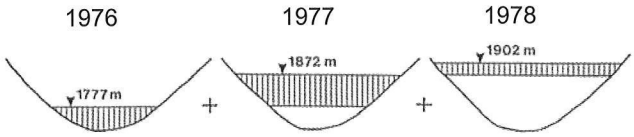

Fig. 8.42b: Static systems [88].

After the superimposition of the three steps (system B), the resulting stresses are summarized in Fig. 8.42c, as compared to the stresses according to the assumptions "independent concrete blocks" (system A) and "monolithic dam" (system C). At this point it should be noted that in the case of the Kölnbrein arch dam the assumption of a monolithic dam would lead to horizontal tensile stresses in the arches, which would exceed 1 N/mm² in the upper dam section and could therefore be hardly transferred in the block joints.

The compressive stresses at the upstream dam base

measured using teleformeters were evaluated based on a modulus of deformation of 13 kN/mm² as the mean value of the three pouring years, which had been recalculated from the measured deformations of the dam body during the first full storage period.

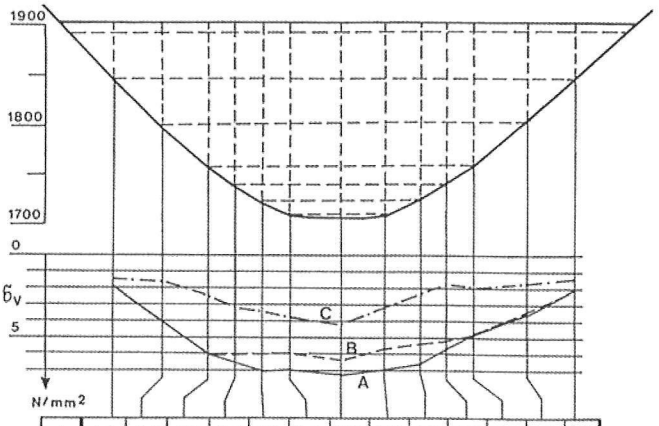

A	1,7	3,8	5,8	6,4	7,0	6,9	7,2	6,7	6,5	5,7	4,9	3,7	2,3
B	–	–	–	6,0	5,8	5,9	6,3	5,5	5,2	5,3	4,8	3,5	2,3
C	1,5	1,6	2,2	3,2	3,4	3,8	4,2	3,2	2,4	1,9	2,0	1,8	1,4
D	–	–	–	–	–	5,2	6,7	4,8	–	–	–	–	–
E	–	–	–	–	–	5,0	6,7	4,6	–	–	–	–	–

A ... independent cantilever beams
B ... successive change of the static system
C ... monolithic dam body
D ... calculated stresses for A, related to the measurement point
E ... measured stresses

Fig. 8.42c: Comparison of the vertical stresses due to dead load along the upstream dam base of the Kölnbrein arch dam based on three assumptions [88].

The stresses determined in this way show an excellent correspondence to the calculated values related to the measurement point, assuming independent cantilever beams. The differences in the flanks are probably also due to the fact that the directions of the measured and calculated stresses do not correspond.

The results of both examinations confirm the validity of hypothesis A with independently assumed concrete blocks under the dead load case, for arch dams under conditions that large annual reservoirs in the Alps are subjected to. This is true, whether the block joints are already injected and the reservoir partly filled during the construction period (as at Schlegeis and Kölnbrein) or only after pouring of the dam has been completed (as at Zillergründl).

Top storage level load case

At the Schlegeis arch dam, the stresses during impounding could be determined as well using telepressmeters (Fig. 8.43).

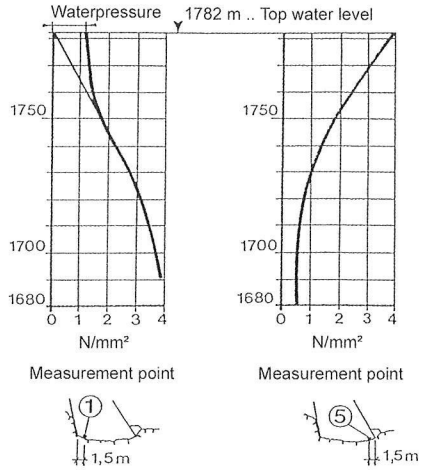

Fig. 8.43: Stresses in the centre section along the dam base during impounding [57].

The measurements at the downstream dam base of the centre block showed the expected uniform increase up to a maximum value of approximately 4 N/mm², corresponding to the calculated stresses for this area. At the upstream dam base, however, this trend underwent a change, when the reservoir level exceeded 1,750 m; in that case, only the relevant water pressure due to the reservoir level was measured. This can be explained by the fact that the uplift pressure began to rise only as of a reservoir level of 1,750 m, subsequently attaining the maximum level due to the opening of joints underneath the upstream dam base. Also these measurements confirmed, therefore, the lifting of the upstream dam base, resulting in water inflows into the bottom gallery at top storage level (see 8.8.2).

Within the dam width, the foundation is of course subjected to triaxial stresses. In this area, therefore, teleformeters covering nine measuring directions and a zero teleformeter were installed. Following an adjustment including the excess measuring directions and taking the zero teleformeter into consideration, the storage-dependent magnitude and direction of the principal stresses result (Fig. 8.44, Fig. 8.45). To illustrate the results, a spherical projection well-known from geological mappings was chosen, with the marked points representing the piercing points of the stress vectors originating at the source of the spherical projection.

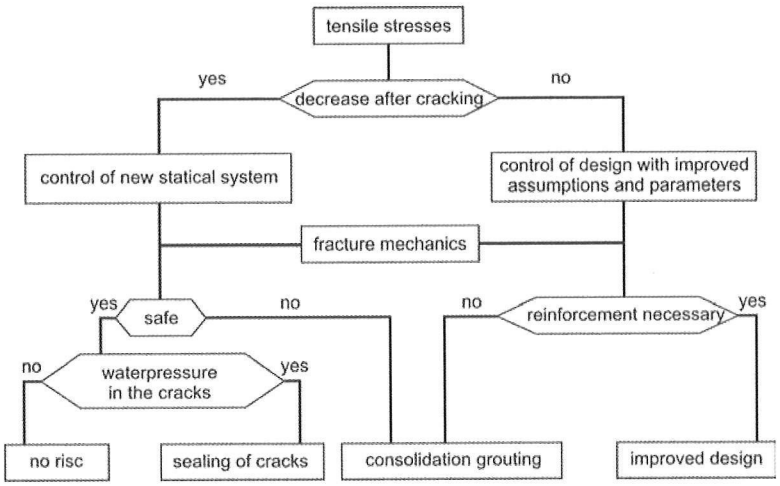

Fig. 8.49: Evaluation of cracks [*68*].

The evaluation of cracks (Fig. 8.49) will have to take the cracks' further development into consideration. If the cracks close again, because e.g. the extreme concrete temperature differences have decreased and the static system has not been affected, the occurrence of cracking will, in general, not be important and special remedial measures will therefore not be required. At the upstream surface, horizontal cracks in the upper dam third due to the downstream overhang of the dam crest will hardly be of consequence, if the reservoir level is low, since they will close again with rising reservoir level and be subject to vertical pressure at top storage level. In the lower third of the dam, where water can enter under high pressure, the possibility of crack propagation should be examined in more detail, e.g. using fracture mechanical methods (Fig. 5.41).

If, however, the cracks do not close after the cause of cracking has been eliminated or if the cracks have a significant effect on the static system, a new analysis of the arch dam based on the new static system will have to be carried out, taking the causes of cracking into consideration. This can include improved assumptions for the deformation moduli of concrete and rock, which (in rock) can vary widely along the dam base, or higher load assumptions, as e.g. the maximum water pressure in the cracks. The calculations should include rock-mechanical investigations as well, which may throw light upon the possible crack propagation.

If these examinations show that strengthening of the dam is not required, it will suffice to force-close the cracks permanently e.g. by the injection of epoxy resin. If, however, the dam must be strengthened, a new project must be prepared specifying the measures required to eliminate the causes of cracking, taking the experiences and knowledge gained in the meantime into consideration.

8.7 PERMEABILITY OF THE UNDERGROUND

8.7.1 DEFORMATIONS

The permeability of the underground and thus seepage under the dam are influenced by the deformations, since these affect the joint openings and thus the flow section. Using sliding micrometers, these joint openings can be localized enabling an effective application of possibly required corrective measures.

The horizontal forces acting at the dam base in the radial direction can be influenced only slightly by the shape of the dam; they cause unavoidable horizontal tensile stresses, particularly underneath the upstream dam base, which are basically dependent on the dam height and valley shape (Fig. 5.33) and contribute to the opening of steep joints in the rock or to the formation of corresponding upstream cracks as well as to the lengthening of the upstream dam surface. The point of origin of these cracks can shift towards the downstream face together with the zero line of the vertical stresses, assuming that the horizontal forces can only be transferred within the pressure area. The inflow of water under the pressure corresponding to the reservoir level can result in a lengthening of these cracks and joints, as an evaluation based on fracture mechanics has shown (Wagner, 1991); the depth of these cracks, however, is limited by the propagation angle of the compressive stresses due to the abutment forces.

To maintain the permeability attained during injection, the vertical stresses in the plane of the grout curtain should not fall below the level at the time of injection.

Schlegeis arch dam [37]

To check the effectiveness of the grout curtain and drainage bores, the measuring instruments listed below were installed in seven measuring cross sections (Fig. 8.50):

Three extensometers E, with measuring lengths of 5, 15 and 50 m from the foundation, were installed in a vertical plane in four directions (two in the approximate direction of the expected maximum stresses).

Piezometers P at a depth of 10, 20 und 30 m were installed underneath the dam base, with measuring lengths of approximately 2 m. One measurement series was located upstream, the second downstream close to the grout curtain and the third under the downstream dam base.

Based on the extensometer measurements, the area where an opening of joints around the upstream dam base as a function of the respective reservoir level (Fig. 8.56) is to be expected, could be clearly defined.

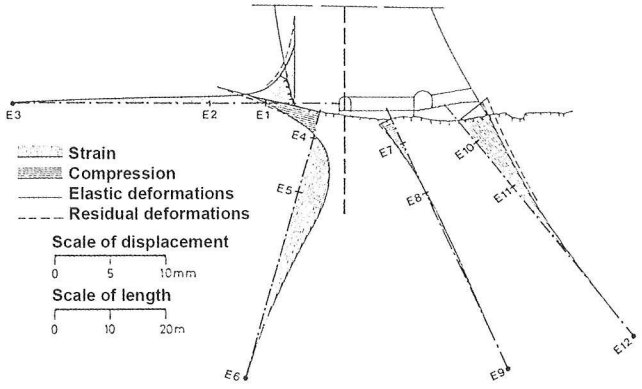

Fig. 8.51: Storage-dependent strains in the underground around the upstream dam base [61].

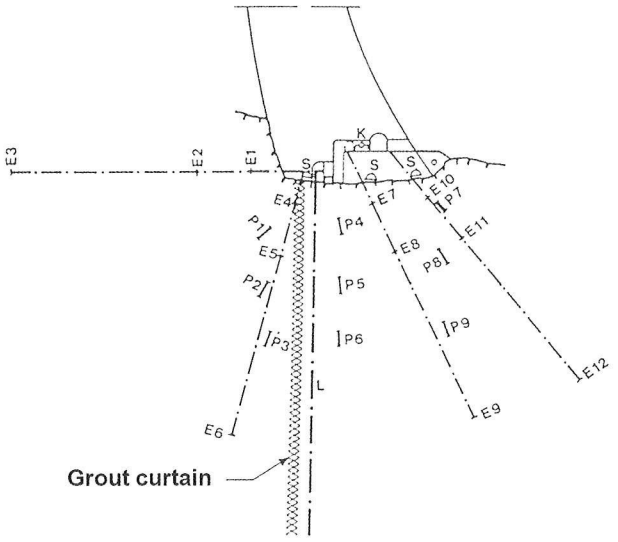

Fig. 8.50: Standard cross section including the arrangement of the measuring instruments [37].

Lengthening of the measuring lengths directly around the upstream dam base, indicating cracking in the rock or the opening of existing joints in this area, are limited to the few meters underneath the foundation; the length of the longer measuring length changed only slightly.

8.7.2 Seepage

Supervision of dam seepage is of especial importance due to the uplift pressure, particularly in the case of gravity dams, and erosion due to larger seepage quantities.

Already at the dams of the Glockner-Kaprun power plant group constructed in the 1950s, supervision included the monitoring of the uplift pressures (Fig. 8.52) and water inflows into the bottom gallery (Fig. 8.53).The uplift pressures show constant values upstream of the bottom gallery up to the respective reservoir level, downstream of the bottom gallery

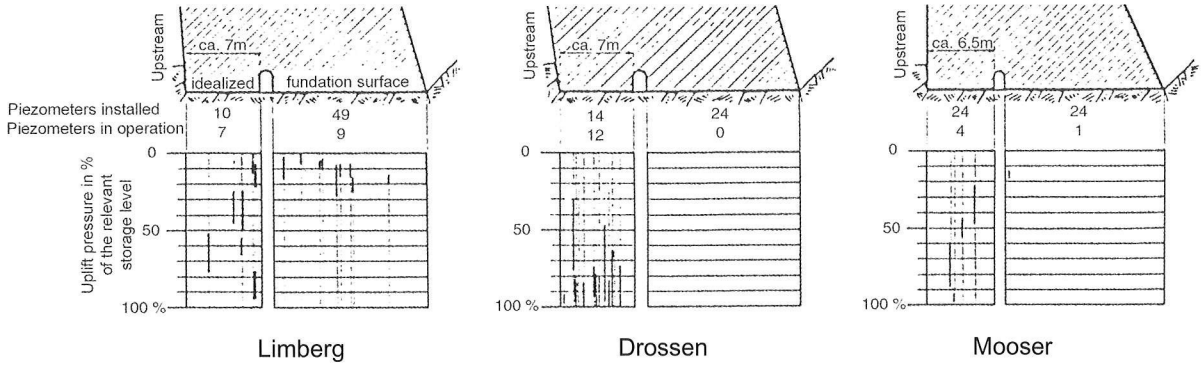

Fig. 8.52: Uplift pressures [6].

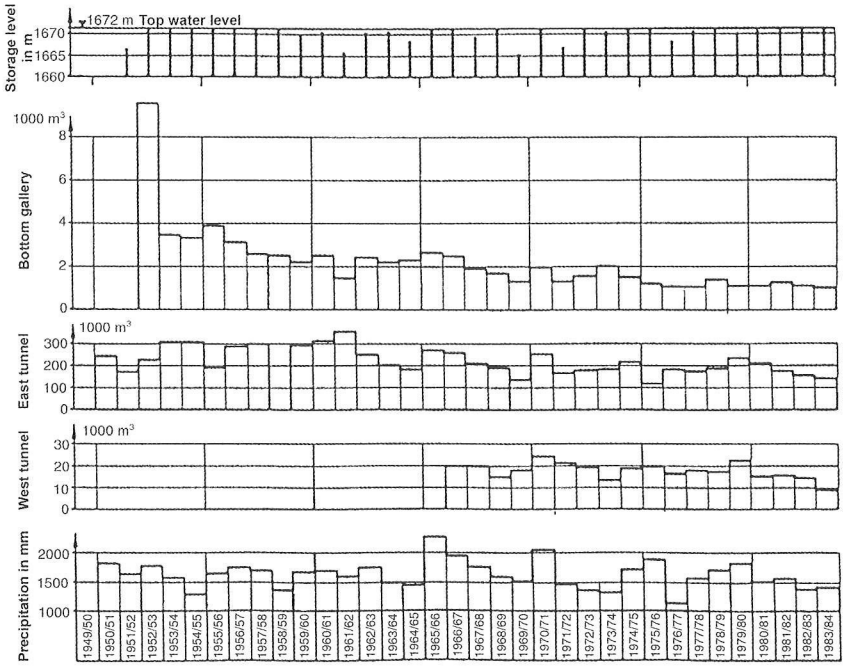

Fig. 8.53: Limberg, seepage quantities from 1950 to 1984 [64].

only few measurement points showed low values up to approximately 20% of the reservoir level.

Limberg arch gravity dam

The storage-dependent water inflows into the bottom gallery reached approximately 0.8 l/s during the first full storage year and decreased subsequently, due to self sealing, very quickly to the present value of less than 0.1 l/s. Consequently, the annual seepage load decreased as well from approximately 9,000 m³ during the first full storage year to approximately 1,500 m³ (Fig. 8.53).

Drossen arch dam

As at the other dams of the Kaprun power plant group, at the Drossen dam as well the bottom gallery rests directly upon the rock, so that the water inflow into this gallery represents an important indication of the permeability of the underground.

The sum of the water inflow (Fig. 8.54) attained approximately 7 l/s during the first full storage period in 1957 and has decreased during the subsequent storage periods to the present constant value of approximately 0.7 l/s. The annual water load decreased accordingly from 57,000 m³ to 9,000 m³.

Schlegeis arch dam

At this dam as well, the bottom gallery rests directly upon the rock, which, as experience has shown, considerably relieves the uplift pressure acting upon the dam. At the Schlegeis arch dam, however, the water inflows into the bottom gallery increased rapidly when the reservoir level exceeded approximately 95% of the maximum storage level, attaining a maximum of almost 200 l/s at top storage level, 90% of which was concentrated along a length of 150 m in the centre dam area (Fig. 8.55).

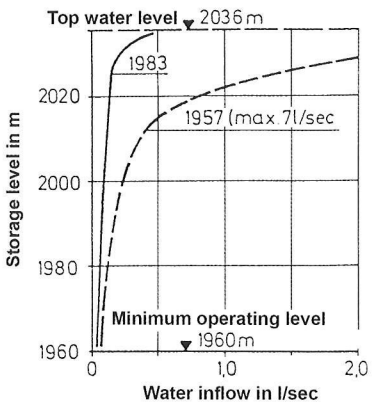

Fig. 8.54: Limberg dam, inflow into the bottom gallery [64].

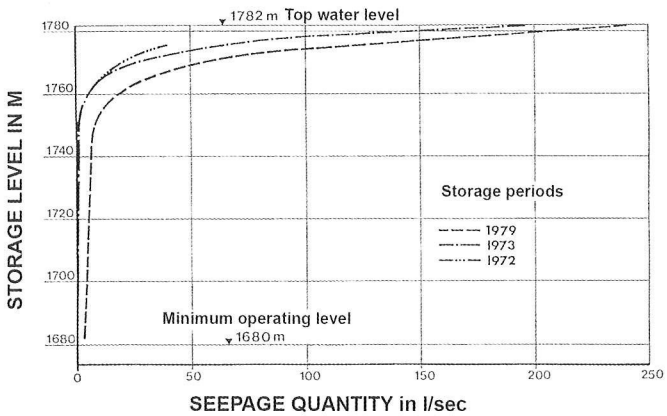

Fig. 8.55:Schlegeis dam, inflow into the bottom gallery [64].

Based on the extensometer measurements, it could be verified that seepage under the dam is limited to a very narrowly defined area, down to approximately 3 m underneath the foundation (Fig. 8.56).

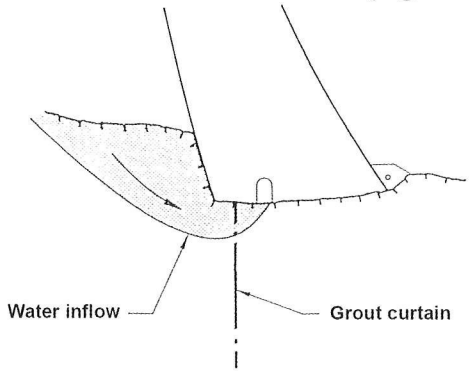

Fig. 8.56: Area of water inflows into the bottom gallery in vertical section.

Comparison of the storage-dependent variation of seepage to the length changes of the 5 m long extensometers E4 in the upstream direction (Fig. 8.50) suggested an empirical deduction of the relation between water inflow and mean joint openings (Fig. 8.57). As a measure of these joint openings, the mean value of these extensometers measurements in the three blocks of the seepage area was used. Seepage was limited to a few joints in the rock; test drills revealed that the joint rock - concrete was free of cracks. The flow rates indicated a turbulent flow at a hydraulically rough joint surface, at least for the larger water inflows.

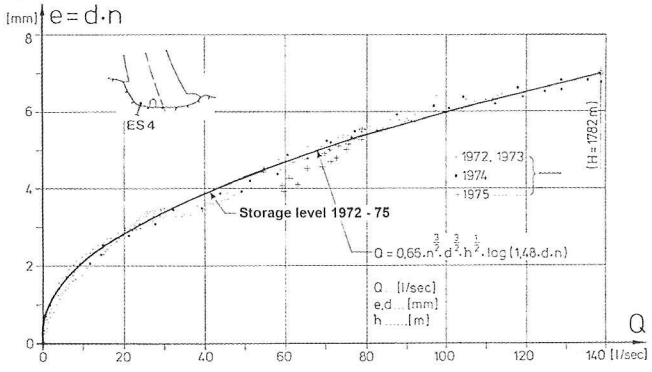

Fig. 8.57: Water inflows into the bottom gallery in the centre dam section 1972 - 1975 as a function of rock deformations [*37*].

Therefore, calculation was based on the following formula.:

$$h = \lambda \cdot \frac{L}{2d} \cdot \frac{v^2}{2g} \quad \text{whith} \quad \frac{1}{\sqrt{\lambda}} = 2\log(3.71 \cdot \frac{2d}{s})$$

where: h ... loss of energy head [m]
L .. length of joint in the flow direction [mm]
d ... joint width [mm]
v ... mean flow rate [m/s]
s ... absolute roughness [mm]

Assuming an idealised rectangle with width b and length and a constant joint width d in m, the overall flow in l/s results from:

$$Q = d.b.v = 4b \cdot \sqrt{\frac{g.h}{L}} \cdot d^{3/2} \cdot \log(3.71 \frac{2d}{s})$$

If this relation is adapted to the measured values and extended to n equally long, superimposed joints, on which the measured strain is equally distributed,

$$Q = 0.66 \cdot n^{3/2} \cdot \sqrt{h} \cdot d^{3/2} \cdot \log(1.48 \cdot d \cdot n)$$

results.

where n ... Number of joints in the measured zone

This function is practically identical with the measured variation. If n = 1, i.e. with only one joint, and if n = 5, i.e. with a flow through 5 joints of equal width, the values listed below in Table 8/2 result for the absolute roughness s, joint length b and flow rate $v^2/2g$ as manifested in the "spraying width" of the exiting water jets.

Table 8.2: Characteristic values for the flow through joints for Fig. 8.54

	s [mm]	b [m]	$v^2/2g$ [m]
n = 1	5.0	5.25	0.75
n = 5	1.0	11.70	0.15

The flow rates correspond to Reynolds numbers of up to $\Re$ = 35.000, confirming the assumption of a turbulent flow. Since, in addition, the variation for several storage periods with varying joint widths and water inflows at equal reservoir level is very low, this flow model represents the actual flow conditions with sufficient exactness.

Even though there was no danger of erosion in the rock due to seepage, rehabilitation measures were carried out. One obvious measure, i.e. injection underneath the upstream dam base at a high reservoir level, was not considered effective, since this would hinder recovery upon lowering the reservoir level by approximately 100 m and cause additional tensile stresses at the downstream dam base.

Due to the restriction of the joint openings to a depth of only 3 m, it was sufficient to sink an only 5 m deep elastic diaphragm wall from the bottom gallery in 1980/81 while the dam remained in operation

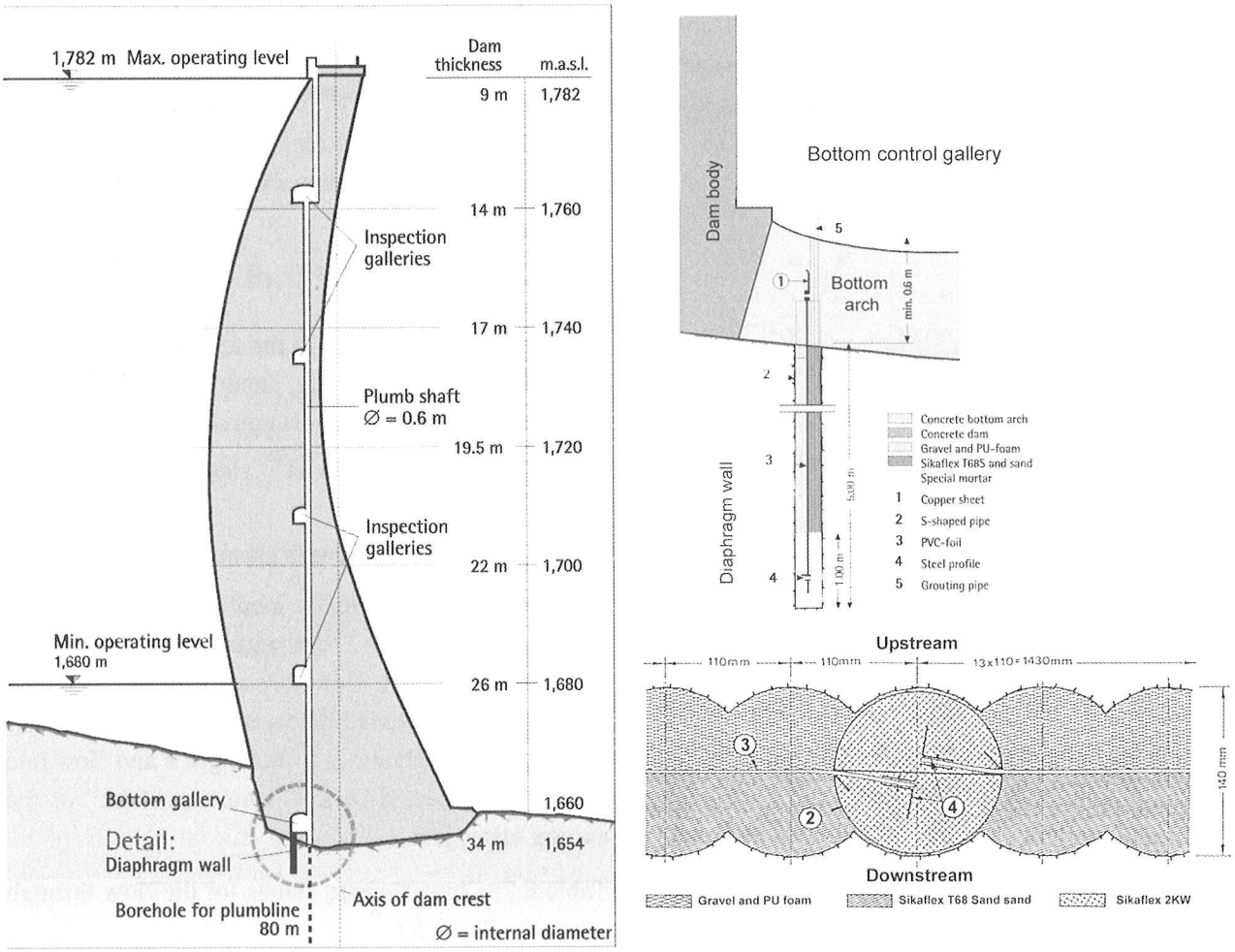

Fig. 8.58 Schlegeis diaphragm wall, standard sections (Stäuble 1994).

(Fig. 8.58); thereby, the seepage around the diaphragm wall could be decreased from maximally 200 l/s to approximately 4 l/s. At all three measurement levels, the results of the piezometer measurements (Fig. 8.59) show upstream of the grout curtain a high dependency, immediately behind the grout curtain only a slight dependency and underneath the downstream dam base no dependency at all on the storage level.

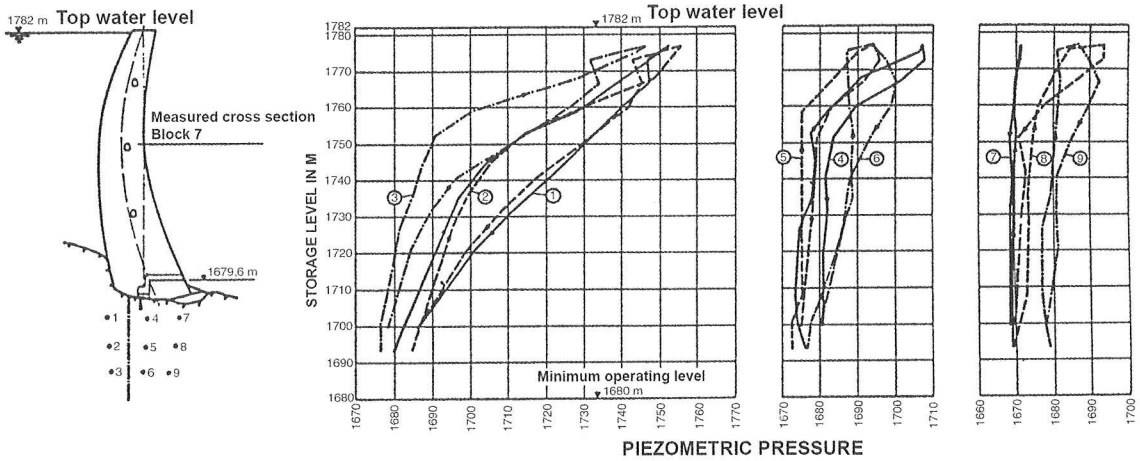

Fig. 8.59: Results of the piezometer measurements as a function of the storage level after installation of the diaphragm wall [61].

8.8 RESERVOIR SLOPES

The Durlassboden reservoir, created in 1964/66 by the construction of a 85 m high earth dam with a central core shall serve to illustrate the surveillance of reservoir slopes. Due to the geological and morphological situation, the stability of the reservoir slopes was a major concern, so that an extensive geodetic monitoring network was set up in order to facilitate an early discovery of a potential increase in movements (Fig. 8.60). In the location drawing, the areas with the largest displacements are clearly discernable.

The time-dependent variation of the displacements of several representative points (Fig. 8.61) indicates a quite uniform behaviour with a slow decrease in movements. The variation in the gradients can be correlated to years of high or low precipitation. Point RH6 represents an interesting exception in an area which was subjected to additional water influx due to a water ditch at the mountain side of a recently constructed forest road. Immediately after the water ditch was sealed, the movements decreased to the previous amount.

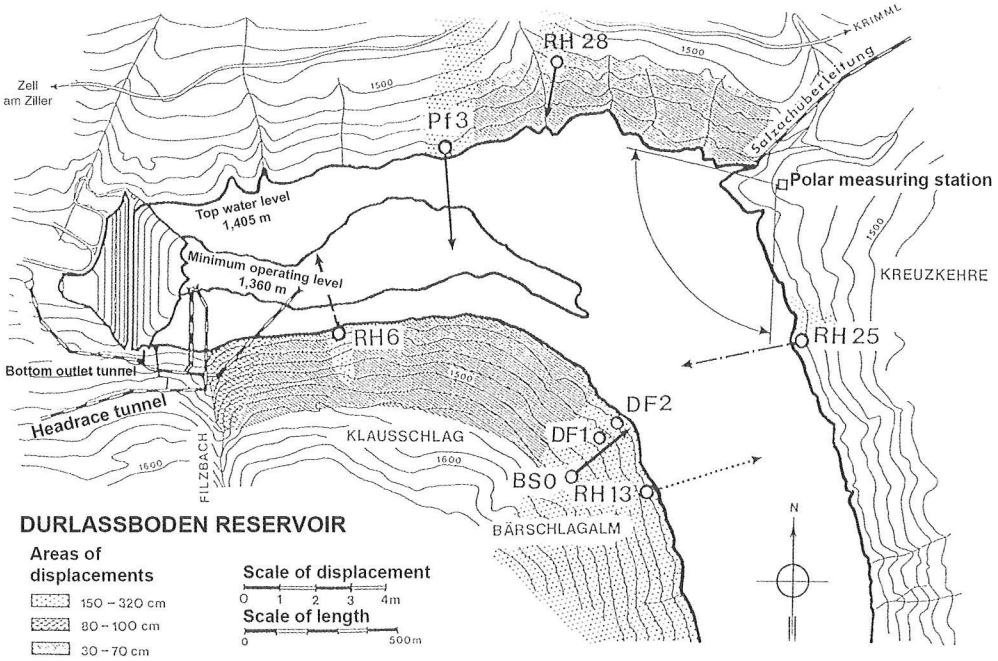

Fig. 8.60: Location drawing of the Durlassboden reservoir including the displacement vectors of several selected points 1965-1997.

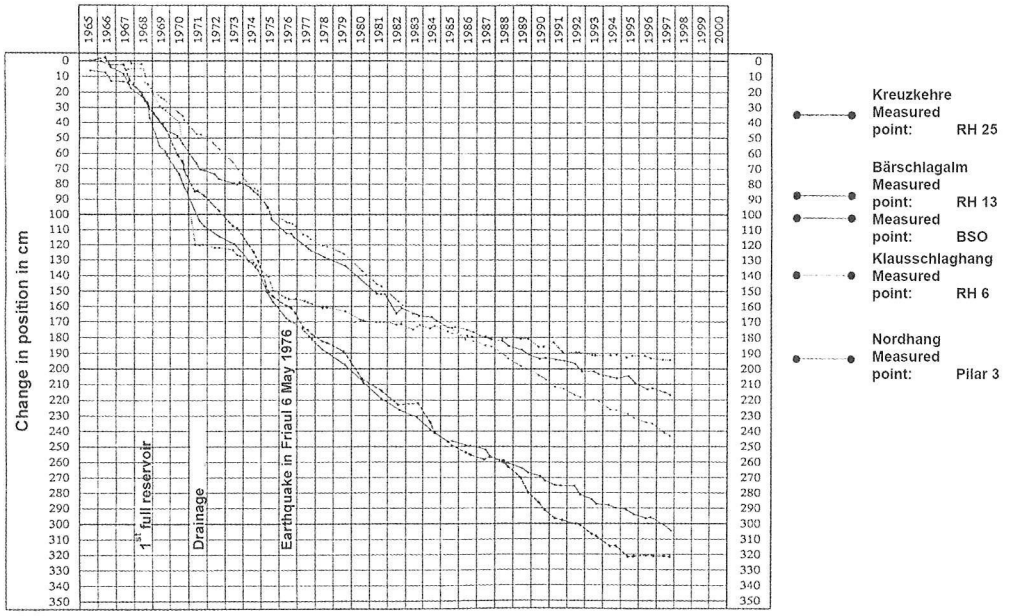

Fig. 8.61: Durlassboden reservoir, time-dependent displacement of several slope points [64], (Leobacher 1998).

8.9 SUMMARY

For a general verification of constant dam safety, it is sufficient to verify that the deformations remain constant under constant external influences. A quantitative verification of safety can, however, only be achieved using a hybrid model, i.e. by calibration of a static model based on the measurement results.

In this chapter, various aspects that must be taken into consideration for calibration have been specified by discussing the measurements taken at the highest Austrian arch dams:

1) All deformation measurements on the prototype confirm the time-dependent deformation behaviour of concrete and rock known from laboratory tests, such as:

– All deformations are dependent on time and the load history; only after 15 - 20 operating years (load cycles) can a purely elastic behaviour be expected;

– The residual deformations can attain 25% or more of the overall deformation; their increase decreases only slowly;

– The elastic deformations decrease by 25% or more; they are however still dependent on the load history (hysteresis cycle).

Only if these influences are taken into consideration in the calculation methods and the measured values correspond sufficiently to the calculated values, can the static model be considered reliable. Only by using hybrid models can the justification of the simplifications on which all static and dynamic calculations are based be checked and the theoretical foundations be improved, if required.

2) The relation between the storage-dependent behaviour of the underground and the seepage quantities has been proven; this makes it possible to deduce a safety factor against inadmissible seepage already at the initial top storage period. This safety factor includes of course the stress field along the dam base.

REFERENCES

Kansai Electric Power Company: Static and dynamic behaviour of Kurobe dam. 1988

Ludescher H.: Die Sanierung der Kölnbreinsperre. ÖIAZ 1990, Heft 1.

Ludescher H.: Felsmechanische Untersuchungen anlässlich der Verstärkung der Kölnbreinsperre. Felsbau 1991, Heft 2.

Lombardi G.: Les Tassements exceptionels au Barrage de Zeuzier. Publications de la Societé de Mécanique des Soles et des Roches, N° 18, 1988.

Stäuble H.: The behaviour of the Schlegeis arch dam and the measures taken to improve it. Proceedings of the Int. Conf. on Safety of dams in Coimbra. A.A. Balkema 1984

Stäuble H., Wagner E.: Comments on the Arrangement of grout curtains with special regard to uplift pressures in the case of large dams. Proceedings of the Int. Workshop on dam safety evaluation. Grindelwald, Schweiz, 1993

Zenz G. : Sperre Zillergründl, 3-D-Berechnung. Interner Bericht der Tauernkraft 1991.

Interne technische Berichte von ÖDK und TKW (unveröffentlicht).

9. CONCLUSIONS

By the end of the 21st century, world population will have increased five fold since the early 1900s; the usable land area and the usable water resources available without technical interventions, however, will essentially remain the same. It is, therefore, to be expected that the retention of surplus run-off for flood protection as well as for use during dry periods, and the thus resulting need to create reservoirs through the construction of dams will gain in importance. In future decades, project engineers will have to face the difficult task of finding optimal solutions capable of reconciling the to a certain extent conflicting demands for safety, economic efficiency and environmental compatibility.

Determination of safety factors must be based both on load as well as calculation assumptions. To enable comparability of the static safety of arch dams, a standard determination method should be defined. For this purpose, the ultimate load method is recommended. To receive comparable safety factors for various arch dams, it is of primary importance to determine the manner of load increase: the load should be increased by increasing the specific weight of the water. This would produce the lowest safety factor that will then have the same magnitude as for embankment dams.

More sophisticated calculation methods often result in a more uniform stress curve and thus in a decrease in stress peaks. Constant safety factors can cause a decrease in until then "hidden reserves". 'The true risk of any engineering system design or the true reliability of any model of a natural system will never be known exactly' (Yen 1986).

A new safety definition has been proposed based on the safety against flow over, through and under the dam:

– The safety against flow over the dam is dependent not only on the hydrological definition of the design flood, but also on the hydraulic-constructive design (e.g. for energy conversion) and ensured functional reliability (e.g. obstructions, mechanical gates) of the spillways. The design flood should be deduced from a theoretically still admissible extrapolation of the observation period, in combination with a multiplication factor taking the local conditions into consideration.

– The safety against flow through the dam is dependent not only on the water tightness of the concrete, but also on the crack resistance, particularly at the upstream face and in the underground. The tensile strength must be compared to the relevant principal tensile stress comprising the in most cases negligible secondary stresses as well. The length of unavoidable initial cracks must remain below the critical crack length, which can be determined as a function of the water pressure using fracture-mechanical methods.

– The safety against flow under the dam presupposes a sufficient water tightness and depth of the grout curtain. The impermeability of the underground is, however, dependent on the stress state as well, which in turn is decisively influenced by the storage level. The grout curtain must, therefore, be installed in an area in which the stress state during impounding will not be more unfavourable than during construction.

The hydrological safety can be checked during operation, the safety against inadmissible seepage can be deduced during the initial full storage period. This definition underlines the importance of measuring the water quantities during operation, whether due to inflowing flood waves or seepage flows through or under the dam.

The demand for optimal economic efficiency will be a central concern and will in many cases conflict to some degree with the self-evident demand for maximal security. Optimal economical efficiency can be achieved by rationalizing design and construction; often, however, it is attempted to achieve improved economic efficiency through increased material utilization, i.e. higher allowable stresses. Thereby, however, hidden safety reserves are often unintentionally abandoned decreasing the actual safety of the structure. Rationalization of the design should, therefore, rather aim at simpler construction methods. An increased material utilization is only justifiable, if the actual properties of the materials used are known with sufficient exactness and realistic calculation methods as well as representative design criteria are used.

The principle of strictly preserving nature will have to yield to the more creative approach of forming nature to achieve new, yet still satisfactory and sustainable ecological conditions.

Natural sciences, and therefore construction engineering, can be subdivided into two fields:

- descriptive natural sciences that are interested in the description of conditions, from the universe down to the single cell; and
- explanatory natural sciences that attempt to explain nature, such as the big bang, relativity or evolution theories.

One important question in regard to all explanatory natural sciences is whether they truly represent the actual conditions; this, however, is not necessary and in most cases not even possible in the humanities. Scientific thinking requires, therefore, that the observation of the actual conditions in nature correspond to the relevant theories, in case of civil engineering to the results of static calculations. This principle underlines the necessity of extensive monitoring the dam behaviour.

Therefore the appropriateness of the theories on which static calculations are based must be examined as well, e.g. whether they describe all deformations of a structure with sufficient exactness. This requires that the structure's reactions to external influences be measured and compared to the calculation results. Many examples in the field of arch dams have shown that these obvious requirements are hardly met:

– The calculated compressive strength does not correspond to the fracture stress in the fracture areas, not even in regard to the algebraic sign. In the tests to determine the compressive strength, fracture occurs along different areas, depending on the manner of loading as well as the geometry and size of the test specimen. Therefore, different compressive strengths result.

– The deformation behaviour of concrete and rock is dependent on time and the load history; this is reflected in all deformation measurements but ignored in the calculations.

– Checking of earthquake calculations on the prototype is hardly possible due to the measurement techniques available; it could however be done by comparing the crack pattern to the tensile stresses resulting from dynamic calculations in cases in which concrete dams were subjected to strong earthquakes.

85% of all existing dams were constructed in the 2nd half of the 20th century. Almost every 200th dam has failed, every 10th dam was damaged, approximately two thirds of these during construction or in the initial 10 years of operation; this indicates design or construction defects.

Future developments to improve safety should be based on past experience. The most important indicators of needed developments can be discovered by analysing damage causes. Only the study of damage cases will provide the necessary information, reveal weaknesses in design or construction or verify that the required safety was not achieved.

If the experiences, observations and ideas presented in this paper invite discussion, encourage a more detailed treatment of some special questions and lead to improved evaluation criteria in the future, it will have served its purpose.

Yen B. C. et al.: First order reliability analysis. Proc. of stochastic and risk analysis in hydraulic engineering. Water resources Publications, Littleton, Colorado, USA, 1986.

ANNEX

ANNEX A - 1

Geometric characteristics of arch dams

See figures 5.2 - 5.6

1	2	3	4	5	6	7	8	9	10	11	12	13
DAM (Country)	Geometric data								λ_D	d_k/H	V/H^3	V/W
	H	S_1	S_2	d_A	C	V_{USBR}	V	W				
	m					1000m³		1000t				
Almendra (E)	197	468	124	33,0	8,10	1509,2	2186	3852	3,157	0,168	0,286	0,567
Cancano (I)	136	327	70	25,9	9,00	377,0	552	1162	2,872	0,190	0,219	0,475
Contra (CH)	220	337	65	25,0	13,68	896,0	658	2999	1,737	0,114	0,062	0,219
Curnera (CH)	158	300	124	25,0	10,92	739,0	670	2024	3,152	0,158	0,170	0,331
Dobra (A)	52	175	82	20,0	16,50	39,4	90	138	5,948	0,385	0,640	0,652
Drossen (A)	112	305	71	24,6	15,60	250,5	335	763	3,392	0,220	0,238	0,439
El Cayon (Ho)	226	345	185	48,0	12,91	3128,0	1470	5610	2,886	0,212	0,127	0,262
Emosson (CH)	180	365	145	48,5	13,21	1248,0	933	3121	3,300	0,269	0,160	0,299
Gebidem (CH)	120	236	60	18,0	13,00	198,0	325	707	2,560	0,150	0,188	0,460
Gigerwald (CH)	127	340	95	19,0	16,90	408,0	460	1194	3,654	0,150	0,225	0,385
Hierzmann (A)	58	143	36	17,0	12,10	25,1	43	100	3,194	0,293	0,220	0,430
Inguri (USR)	272	545	185	50,0	10,45	4744,0	3882	9729	3,014	0,184	0,193	0,399
Klaus (A)	55	180	60	9,5	22,30	37,4	40	130	4,879	0,173	0,240	0,308
Kölnbrein (A)	200	515	167	36,0	16,86	2114,0	1550	4848	3,786	0,180	0,194	0,320
Kops (A)	120	360	100	34,0	18,26	402,0	450	1126	4,082	0,283	0,260	0,400
Laparan (F)	106	260	93	16,5	13,90	224,7	200	726	3,788	0,156	0,168	0,275
Les Toules (CH)	86	375	100	20,5	41,60	243,2	240	590	5,814	0,238	0,377	0,407
Limberg (A)	120	300	90	37,0	9,50	314,5	443	976	3,536	0,308	0,256	0,454
Limmern (CH)	146	323	83	25,0	12,10	466,2	550	1439	2,896	0,171	0,177	0,382
Luzzone (CH)	208	410	90	36,0	10,38	1220,0	1350	3447	2,385	0,173	0,150	0,392
Maina die Sauris (I)	136	122	40	15,0	9,20	135,0	100	534	1,326	0,110	0,040	0,187
Mauvoisin (CH)	237	468	115	53,5	6,99	2100,0	2030	5378	2,527	0,226	0,152	0,377
Möll (A)	56	120	23	7,5	16,80	16,7	26,5	69	2,422	0,134	0,151	0,384
Mratinje (Yu)	220	265	85	45,0	10,45	1071,0	731	3001	1,761	0,205	0,069	0,244
Naguilhes (F)	55	138	18	2,0	14,10	18,0	26	66,5	2,340	0,036	0,156	0,391
Nalps (CH)	127	405	105	23,0	14,80	518,4	592	1371	4,192	0,181	0,289	0,432
Ottenstein (A)	69	200	103	24,0	19,80	89,5	124	295	5,371	0,348	0,377	0,420
Place Moulin (I)	154	485	200	40,0	18,90	1413,0	1500	3104	5,222	0,260	0,411	0,483
Pra da Stua (I)	43	143	43	15,0	9,20	16,7	31	60	4,709	0,349	0,390	0,517
Punt dal Gal (CH)	130	463	155	24,5	16,40	788,3	740	1874	5,321	0,188	0,337	0,395
Ranna (A)	45	110	36	18,0	7,10	11,9	32	53	3,611	0,400	0,351	0,604
Ridracoli (I)	104	350	142	36,5	12,20	382,9	650	1012	5,535	0,351	0,578	0,642
Roggiasca (CH)	68	146	50	7,5	21,30	38,9	32	164	3,244	0,110	0,102	0,195
Salza (A)	52	100	46	12,0	13,40	16,1	23	78	3,368	0,231	0,164	0,295
Schlegeis (A)	131	565	143	34,0	20,10	946,0	980	2012	5,602	0,260	0,436	0,487
St. Croix (F)	95	125	27	7,0	15,20	46,3	50	217,6	1,579	0,074	0,058	0,230
Sta. Maria (CH)	117	490	185	21,0	22,79	783,0	625	1719	6,644	0,179	0,390	0,364
Takane (JP)	133	250	105	28,0	12,10	396,0	335	1207	3,145	0,211	0,142	0,278
Tolla (F)	90	102	12	2,4	22,80	25,5	17	128	1,004	0,027	0,023	0,133
Vajont (I)	262	175	51	23,0	7,25	990,0	353	2673	0,931	0,088	0,020	0,132
Val di Lei (CH)	143	538	100	28,0	18,80	877,4	834	1993	4,188	0,196	0,285	0,418
Vouglans (F)	130	390	92	25,0	10,10	483,8	670	1323	3,762	0,192	0,305	0,506
Zervreila (CH)	151	423	90	35,0	14,40	682,7	650	1849	3,336	0,232	0,189	0,352
Zeuzier (CH)	156	230	35	25,6	7,69	243,0	300	940	1,485	0,164	0,079	0,319
Zillergründl (A)	186	445	155	40,0	14,03	1557,0	1325	3768	3,646	0,215	0,206	0,352

LEGENDE

H ... Largest dam height above foundation
S_1 .. Chord length at the crest
S_2 .. Chord length at 0,15 H above foundation
C ... Slenderness coefficient (Lombardi)

$$\lambda_D = \sqrt{\frac{S_1 + S_2}{0.15H^2}}$$ ... Reservoir characteristic

V_{USBR} Dam volume after USBR
V ..... Actual dam volume
d_a ..... Thickness of the base of the highest dam section
W ..... Water load parallel to the valley, related to the valley cross section

ANHANG A - 2

STATIC CHARACTERISTS – HEEL STRESSES

to Fig. 5.37

Name	σ_r N/mm²	Höhe m	Name	σ_r N/mm²	Height m	Name	σ_r N/mm²	Height m
Vajont	5,7	262	Sa.Giustina	3,7	152	Drossen	4,7	107
Mauvoisin	6,2	237	Zervreila	5,4	151	Cavagnoli	4,0	105
Contra	7,7	218	Moiry	5,0	150	Torogh	3,3	80
Glen Canyon	6,9	214	Limmern	4,0	149	Rossens	3,8	80
Kölnbrein	9,3	197	Curnera	3,8	148	Gusana	5,3	75
Kurobe	5,9	188	Valle di Lei	6,2	138	Ottenstein	3,4	65
Zillergründl	6,6	186	Gigerwald	5,8	131	Solis	1,6	58
Oymapinar	4,4	185	Schlegeis	6,4	130	Möll	2,8	56
Tignes	4,9	180	Nalps	4,3	128	Klaus	2,5	49
Emosson	7,8	180	Kops	5,5	121	Ranna	1,2	45
Lienne	4,4	158	Santa Maria	7,3	117	Sölk	1,7	38

ANHANG A - 3

Estimation of the lowest Eigenfrequency according to GEIGER

$$\omega_1 = 5{,}5/\sqrt{\delta_w}$$

Fig. 5.23

NAME	Height m	δ_w cm	ω_1 in Hz		
			measured	calculated	according to Geiger
Schlegeis	131	6,0	2,15	2,14	2,1
Kölnbrein	198	16,5*	1,21	1,20	1,2
Klaus	55	0,7	6,0		6,0
Möll	56	0,7	6,1	6,0	6,0
Kops	122	5,2	2,27	2,26	2,2
Emosson	180	8,0	1,9		2,0

* The vibration tests were performed in the first year reaching the top water level

ANNEX A - 4

DYNAMIC CHARACTERISTICS
Measured Eigenfrequencies

see Fig.5.24

Name of the dam	Type	Height m	Eigenfrequency in Hz ω_1	ω_2	ω_3	Storage-level
Widerschwing	VA	25	8,6	8,9	12,6	top
Grandiazzo	PG	37	11,3	13,8	18,4	high
Corfino	VA	38	11,4	12,1	15,1	
Furlo	VA	43	16,2	21,9	25,6	
Barcis	VA	50	7,6	10,1	15,3	top
Grotta	VA	50	8,4	11,9	16,8	
Val d'Auna	AG	53	5,7	6,6	7,3	
Klaus	VA	55	6,0			
Möll	VA	56	6,1	6,2	7,0	high
Morasco	PG	57	6,5	7,9	8,1	top
Ambiesta	VA	59	4.1	4,7	7,1	high
Stramentizzo	VA	64	4,3	6,1	9,2	high
Passante	PG	71	5,6	6,3	8,6	empty
Talvacchia	AG	77	3,7	3,8	5,4	high
Fiastra	VA	87	4,3	5,6	7,3	low
Campo Moro	PG	96	6,2	8,8	12,0	low
Vagli	PG	96	8,7	11,9	14,8	low
Suviana	PG	97	6,0	8,7	10,6	low
Campo Moro	PG	97	6,2	8,7	11,7	low
Pieve di Cadore	AG	112	4,0	4,3	4,6	
Kops	VA	122	2,3	2,5	3,2	
Schlegeis	VA	131	2,1	2,3	2,8	high
Lumiei	VA	136	4,0	5,9	8,9	high
Place Moulin	AG	155	2,0	2,1	2,9	
Nagawado	VA	155	3,3	3,6	4,7	
Alpe Gera	PG	174	3,5	4,7	6,2	empty
Emosson	VA	180	1,9	3.0	4,1	
Zillergründl	VA	186				
Kurobe	VA	188	1,8	2,1	3,2	top
Kölnbrein	VA	198	1,2	1,4	1,7	high
Contra	VA	218	1,8	2,1	2,6	

[1] [47]

[2] ENEL - ISMES: An Overview of in situ Dynamic Tests on Concrete Dams
Int. Symp. on Earthquakes and Dams, Beijing, May 1987.

[3] Kansai Electric Power Company: Static and Dynamic Behaviour of Kurobe Dam. 1988

[4] Severn R.T. et al.: Vibration tests on Emosson arch dam, Switzerland.
Earthquake engineering and structure dynamics, Vol. 10, 1982.

[5] Brownjohn J.M.W. et al.:Ambient Vibration Survey of Contra Dam. University of Bristol,
Department of Civil Engineering.

ANNEX B - 1

DAMS AFFECTED BY EARTHQUAKES

TYPE
VA Arch dam
PG .. Gravity dam
TE .. Rock fill dam
ER .. Earth fill dam
CB .. Buttress dam

FOUNDATION
R .. Rock
A .. Alluvions

ACCELERATION
1 gal .. 1 cm/s²
1 g ..... 9,81 m/s²
100 gal ≈ 1 g

DAMAGE
0 ....no
I .... negligible
II ... moderate
III .. severe
IV .. failure

See Fig. 2.9, 2.10

DAM					EARTHQUAKE						
					Distance in km		max. acceleration g				
							bottom				crest
							esti-mated	measured			
NAME	Type	Height in m	Foundation	Completion	Epicentre	Fault	horizontal	horizontal	vertical	horizontal	Damage
San Francisco, USA, Apr.18, 1906, 8,3 (Richter Scale)											
Bear Gulch	TE	15,0			3						0
Belvedere	TE	16			8						0
Chabot	TE	41,0		1892	30		0.35				0
Cowell	TE	15,0		1890	19		0.45				0
Crocker	TE	15,0			2						0
Emerald Lake	TE	17,0		1885	2		0.75				0
Estates	TE	28,0		1903	29		0.35				0
Forrest Lake	TE	18,0		1890	45		0.25				0
Lagunitas	TE	16			8						0
Lake Chabot	TE	15,0		1870	47		0.25				0
Lake Frey	TE	25,0		1894	60		0.20				0
Lake Herman	TE	15,0		1905	52		0.25				0
Lake Temescal	TE	32,0	DD	1869	29		0.35				I
Lower Chrystal Springs	VA	38,7		1890	0						0
Lower St. Helena	TE	15,0		1878	52		0.25				0
Notre Dame	TE	15,0	R		3		0.75				0
Piedmont	TE	16,0	A	1905	29		0.35				II
Pilarcitos	TE	31,0		1866	3		0.75				0
Port Costa	TE	15			45						0
San Andreas	TE	30,0	D	1870	0		0.8				III
Upper Crystal Springs	TE	23,0	D	1878	0		0.8				III
Upper San Leandro	TE	38,0			37						0
Upper St. Helena	TE	15,0	R	1900	52		0.25				0
W. San Andreas	TE	32,0			0						I
Kanto, Japan, September 1, 1923, 7,9 (Richter Scale)											
Upper Murayama	TE	24,0	A	1923			0.25				III
Tokyo W.S.	TE	24,0				24,0					I
Ono	TE	49,3	D	1913		30,0	0.3				III
Lower Murayama	TE	16,2	A	1927			0.25				III
Santa Monica, USA, August 1930, 6,3 (Richter Scale)											
Chatsworth Dam	TE	13,4		1918	19						III
Peru, October 10, 1938											
Malpaso	ER	70,0		1936							I

DAM					EARTHQUAKE						
NAME	Type	Height in m	Foundation	Completion	distance in km		max. acceleration g				Damage
							bottom			crest	
							esti-mated	measured			
					Epicentre	Fault	Horizontal	Horizontal	Vertical	Horizontal	
El Centro, USA, May 18, 1940, 7,1 (Richter Scale)											
Laguna	TE	15,0			67						I
Illapel, Chile, Apr. 6, 1943, 7,9 (Richter Scale)											
Recoleta	TE	46,5	D	1934		83,0	0.21			0.38	I
La Laguna	TE	41,0				186,0					0
Culimo	TE	37,0	D			161,0					0
Cogoti	ER	82,7	R	1940		89,0	0.15				III
Tottori, Japan, 1943, 7,4 Richter Scale											
Mitani	PG	27,0			8						I
USSR, 1944, 5,7 (Richter Scale)											
Boz ´Suiskaya	TE	27,4	D	1943			0.17				II
Nankai, Japan, December 21, 1946, 8,1 Richter Scale)											
Otani-ike	TE	27,0	R	1920							III
Honen-ike	MV	29,7		1930							II
Kern County, USA, July 21, 1952, 7,7 (Richter Scale)											
South Haiwee	TE	27,7	A	1913		153,0	0.04				I
Isabella	TE	57,0				86,0					0
Fairmont	TE	37,0		1912		58,0	0.18				0
Dry Canyon	TE	20,0	A	1912		72,0	0.12				III
Drinkwater	TE	32,0		1923		67,0	0.13				0
Bouquet Canyon	TE	58,0		1934		74,0	0.12				0
Fallon, USA; 23 - 08 - 54; 6,7 (Richter Scale)											
Lahontan	TE	41			48						0
Australia, 1954, 5,5 (Richter Scale)											
Barossa	VA	36,0		1902	45						II
Orleansville, Algeria, September 1954, 7,7 (Richter Scale)											
Ponteba Dam	PG(M)	18,0	R	1870	4						II
Eureka, USA, December 21, 1954, 6,6 (Richter Scale)											
Arcata	TE	17,0			8						II
San Francisco Bay east, USA, October 23, 1955, 5,4 (Richter Scale)											
Saint Mary	TE	16,8	A	1937	3						II
Great Britain, February 11, 1957, 6,5 (Richter Scale)											
Blackbrook Dam	PG	30,0	R	1906	6		0.35				II
Mexico, 28 - 07 - 57; 7,5 (Richter Scale)											
Pinzanes	TR	73									0
India, December 11, 1957, 6,5 (Richter Scale)											
Koyna	PG	103,0	R?	1962	3			**0.6**		**0.7**	III
USA, August 17, 1959, 7,6 (Richter Scale)											
Hebgen	TE	37,5	DD	1915	0		0.7				III
Kitamino, Japan, Aug. 19, 1961, 7,2 (Richter Scale)											
Miboro	ER	131,0	R	1960		17,0				0.25	II

NAME	DAM: Type	DAM: Height in m	DAM: Foundation	DAM: Completion	EARTHQUAKE: distance in km: Epicentre	EARTHQUAKE: distance in km: Fault	EARTHQUAKE: max. acceleration g: bottom: estimated: Horizontal	EARTHQUAKE: max. acceleration g: bottom: measured: Horizontal	EARTHQUAKE: max. acceleration g: bottom: measured: Vertical	EARTHQUAKE: max. acceleration g: crest: measured: Horizontal	Damage
Papudo Zapallar, Chile, July 8, 1971, 7,5 (Richter Scale)											
Rungue	TE	21,0	D	1962	94		0.11			0.19	II
Pitama	TE	16,5	D	1932	93		0.11			0.17	I
Paloma	TE	82,0	R		196						0
Orozco	TE	15,5			93						0
Lo Ovalle	TE	13,0	D	1932	96		0.11			0.17	II
LLiu-Lliu	TE	20,0	D	1917	87		0.12			0.23	III
Huechun	TE	15,4	D	1932	112		0.09			0.14	II
Culimo	TE	37,0	D	1933	56		0.18			0.35	II
Cogoti	ER	82,7	R	1940	168		0.05				II
Catapilco	TE	14,0	D	1910	40		0.21			0.38	III
Haicheng, China, February 4,1975, 7,3 (R. S.)											
Shimenling	TE	46,0			33		0.17			0.25	III
Shenwao	PG	52,6			75						I
Sandaoling	TE	17,0									III
Oroville, USA, 1. August,1975, 5,7 (Richter Scale)											
Oroville	ER	267			3						0
Mexico, 11. 10. 1975, 5.9 (Richter Scale)											
La Villita	ER	66			40						0
El Infiernillo	ER	162			79						0
Mexico, 15. 11. 1975, 7,2 (Richter Scale)											
La Villita	ER	66			27						0
El Infiernillo	ER	162			23						0
Friaul, Italien, May 1976, 6,5 (Richter Scale)											
Sta. Lucia		58			47						0
Lumiei		136			34						0
Ambiesta	VA	59	R	1957	15			0,37	0,2		0
Ca'Zul		74	R	1965	34						0
Ca'Selva		109	R	1965	35						0
Lago di Tramonti		75			31						0
Barcis	VA	50	R	1954	46						0
Comelico	VA	67	R	1931	55						0
S. Caterina	PG	59	R	1931	56						0
Pieve di Cadore		112	R	1949	56						0
Valle di Cadose	VA	61	R	1950	57						0
Vajont	VA	262	R	1961	60						0
Gallina		92			61						0
Tangshan, China, July 28, 1976, 7,8 (Richter Scale)											
Touho	TE	22,0									III
Siathinze	VA(M)	20,5									II
Douhe	TE	22,0					0.40				III
Bahie	TE	66,0	A	1960	100-150		0.10			0.16	IV

NAME	DAM				EARTHQUAKE						
					distance in km		max. acceleration g bottom esti-mated	max. acceleration g bottom measured		max. acceleration g crest measured	
	Type	Height in m	Foundation	Completion	Epicentre	Fault	Horizontal	Horizontal	Vertical	Horizontal	Damage
Vrancea, Romania, March 4, 1977, 7,2 (Richter Scale)											
Izvorul Muntelui	PG	125,0	D	1961	100		0.05				I
Poiana Uzului	CB	80	R	1972	52						0
Paltinul Doftana	VA	108	R	1971	90						0
Vidraru Arges	VA	166	R	1965	160						0
Negovanu	VA	62	R	1960	185						0
Miyagiken, Japan, 6.12.1978, 7,4 (R.S.)											
Tarumizu	ER	47			100						0
Mexico, March 14, 1979, 7,6 (Richter Scale)											
La Villita	ER	60,0	A	1967	108			**0.15**		**0.39**	II
El Infiernillo	ER	147,5		1963	87			**0.13**		**0.36**	II
Mammoth Lakes, USA, May 27, 1980, 6,1 (Richter Scale)											
Vermilion	ER	50			21						0
Long Valley	ER	42	R	1941	near			**0.2**		**0.5**	0
Morgan Hill, USA, April 24, 1984, 6,2 (Richter Scale)											
Leroy Anderson	ER	72,0		1950	16			**0.41**		**0.63**	II
Coyote	ER	36			24						II
Japan, September 14, 1984, 6,8 (Richter Scale)											
Makio	ER	106,0	D	1961	5		0.6				I
Chile, 3. 3. 1985, 7,7 (Richter Scale)											
Rapel	VA	120									II
Mexico, September 19, 1985, 8,1 (Richter Scale)											
La Villita	ER	60,0	A	1967	60			**0.3**		**0.7**	II
El Infiernillo	ER	147,5		1963	68			**0.2**		**0.4**	II
Spitak, Armenia, December 7/8, 1989, 7,0 (Richter Scale)											
Gumush	ER	17,3			60						II
Dzoraget	PG	15,0			40						II
New Zealand, March 2, 1987, 6,3 (Richter Scale)											
Matahina	ER	70,0		1965	40						II
Algeria, October 31, 1988, 5,4 (Richter Scale)											
Bouroumi	ER	100,0	D	1986	15		0.15			0.3	II
Loma Prieta, USA, October 17, 1989, 7,1 (Richter Scale)											
Uvas	TE	36,0				20,0					0v
Stevens Creek	TE	37,0				30,0					0
Newell	TE	66,0		1960	18						II
Lexington	TE	65,0		1953	16		0.45			0.45	II
Leroy Anderson	ER	72,0		1950	18			**0.23**		**0.43**	II
Guadalupe	TE	47,0		1935	18		0.45				II
Elmer J. Chesbro	TE	29,0			19						II
Coyote	TE	43,0			30						0
Austrian	TE	62,0		1950	8		0.5				III
Almaden	TE	34,0		1936	16						I

DAM					EARTHQUAKE						
					distance in km		max. acceleration g				
							bottom			crest	
							esti-mated	measured			
NAME	Type	Height in m	Foundation	Completion	Epicentre	Fault	Horizontal	Horizontal	Vertical	Horizontal	Damage
Pomona Valley, USA, February 28, 1990, 5,5 (Richter Scale)											
San Antonio	TE	49,0			3						I
Iran, June 21, 1990, 7,6 (Richter Scale)											
Sefid Rud	CB	106,0		1963		< 1.0					III
Hyogoken-Nanbu, Japan, Jan. 1, 1995, 7,2 (Richter Scale)											
Tokiwa	TE	33,6		1975		0,7					II
Tachigahata	PG	33,3				1,0					I
Taniyama	TE	28,2				1,5					I
Tanno	PG	33,8				3,0					I
Maruyama	PG	31,0				7,0					I
Hitokura	PG	75,0		1982	47	10,0		**0,183**	0,064		I
Sengari	PG	42,4		1931		10,0					I
Minoogawa	ER	47,0		1983	48	11,0		**0,128**	0,075		I
Dondo	PG	71,5		1985		12,0		**0,111**	---		I
Aono	PG	29,0				19,0					I
Ookawaso	PG	50,8				25,0					I
Takahara	PG	34,0				25,0					I
Kamogawa	PG	43,5		1951		26,0					I
Hatauogawa	PG	30,4				26,0					I
Inohana	PG	27,8				28,0					I
Haiso	ER/PG	26,0				28,0					I
Ayuyagawa	PG	46,2		1969		27,0					I
Anagawa	PG	23,5				27,0					I
Gongen	ER	32,6		1982		28,0		**0,103**	0,067		I
Yuzuruha	PG	42,0		1975		32,0					I
Dainichgawa	PG	43,5		1964		35,0					I
Amagase	VA	72,0		1964	78	45,0		**0,095**	0,024		I
Kisenyama	ER	91,0		1969	80	46,0		**0,09**	0,044		I
Oono	PG	61,4			82	49,0		**0,029**	0,024		I
Shirakawa	TE	30,0			73	50,0		**0,05**	0,048		I
Gohormatau	PG	33,3				1,0					I
Dotani	TE	16,6				1,0					II
Kitayama	TE	24,5				2,0					II
Showaike	TE	18,3				8,0					II
Nunomo	PG	72,0			86	59,0		**0,029**	0,016		?*
Takayama	PG	67,0		1969	90	60,0		**0,013**	0,013		?
Ikuno	PG	56,5		1973	67	61,0		**0,013**	0,016		?
Hase	PG	102,0			65	63,0		**0,03**	0,022		?
Kurokawa	ER	98,0		1984	71	63,0		**0,085**	0,053		?
Senzoku	PG	41,4			75	64,0		**0,032**	0,016		?
Oota 1	ER	55,5		1974	65	64,0		**0,028**	0,020		?
Tataragi	ER	64,5			72	65,0		**0,065**	0,020		?
Muroo	PG	63,5		1974	88	67,0		**0,021**	0,021		?
Yasumuro	PG	50,0			76	70,0		**0,038**	0,031		?
Shorenji	VA	82,0		1970	98	74,0		**0,018**	0,014		?

DAM					EARTHQUAKE						
					distance in km		max. acceleration g				
							bottom			crest	
							esti-mated	measured			
NAME	Type	Height in m	Foundation	Completion	Epicentre	Fault	Horizontal	Horizontal	Vertical	Horizontal	Damage
Sarutani	PG	74,0		1957	79	77,0		**0,018**	0,013		?
Masaki	PG	67,0		1977	95	85,0		**0,033**	0,033		?
Fukui	PG	42,5			96	86,0		**0,032**	0,015		?
Asahi	VA	85,1		1977	91	86,0		**0,014**	0,014		?
Ishidagawa	ER	43,5			124	87,0		**0,012**	0,007		?
Seto	ER	110,5		1978	92	87,0		**0,035**	0,012		?
Oozuchi	ER	43,5			121	88,0		**0,022**	0,011		?
Zao	ER	56,0			122	88,0		**0,049**	0,025		?
Hachisu	PG	78,0		1986	109	93,0		**0,026**	0,019		?
Yokoyama	CB	80,8		1963	168	131,0		**0,023**	0,017		?
Tsugawa	PG	76,0			105	102,0		**0,028**	0,019		?
Shingu	PG	42,0		1975	148	138,0		**0,01**	0,012		?
Sameura	PG	106,0		1974	166	155,0		**0,009**	0,006		?
Nishidaira	PG	34,0		1926	168	131,0		**0,038**	0,025		?
Kamioosu	ER	98,0			192	155,0		**0,009**	0,005		?
Ikohara	VA	111,0			108	102,0		**0,012**	0,010		?
Eigenji	PG/TE	68,0		1969	129	93,0		**0,029**	0,014		?
Iwaya	ER	127,5		1976	230	195,0		**0,012**	0,003		?
Oys	ER	56,5			362	328,0		**0,003**			?

*The figures 2.13 and 2.14 these dams are classified with none or negligible damages; moderate or severe damages would be known.

REFERENCES

Yamazumi A.: Influence of the Hyogoken-Nanbu Earthquake on Japanese Dams. Felsbau 1996/5

Serafim J.L.: Effects caused by Earthquakes on Dams. Proc. Int. Symposium On Earthquakes on Dams, Vol. 2, Beijing , China 1992.

USCOLD: Observed Performance of Dams during Earthquakes. 1984, 1992

ANNEX B - 2

INDUCED EARTHQUAKES

With a Magnitude > 4,0 after Richter-Scale

DAM	COUNTRY	DAM HEIGHT m	STORAGE VOLUME mil. m³	START OF FILLING	MAXIMUM EARTHQUAKE	MAGNI-TUDE
Koyna	India	103	2,780	1962	1967	6.3
Kariba	Zambia	128	175,000	1958	1963	6.2
Kremasta	Greece	160	4,750	1965	1966	6.2
Xinfengjiang	China	105	14,000	1959	1962	6.1
Srinakharin[1]	Thailand	140	17,745	1977	1983	5.9
Marathon	Greece	67	41	1929	1938	5.7
Oroville	USA	236	4,400	1967	1975	5.7
Aswan	Egypt	111	164,000	1964	1981	5.6
Benmore	New Zealand	110	2,040	1964	1966	5.0
Eucumbene	Australia	116	4,761	1957	1959	5.0
Hoover	USA	221	36,703	1935	1939	5.0
Bajina Basta	Yugoslavia	90	340	1966	1967	5.0
Bhatsa	India	88	947	1981	1983	4.9
Kerr	USA	60	1,505	1958	1971	4.9
Kurobe	Japan	186	149	1960	1961	4.9
Monteynard	France	155	275	1962	1963	4.9
Shenwo	China	50	540	1972	1974	4.8
Akosombo[2]	Ghana	134	148,000	1964	1964	4.7
Canelles	Spain	150	678	1960	1962	4.7
Danjiangkou	China	97	16,000	1967	1973	4.7
Grandval	France	88	292	1959	1963	4.7
Kastraki	Greece	96	1,000	1968	1969	4.6
Lake Pukaki	New Zealand	106	9,000	1976	1978	4.6
Nurek	Tadjikistan	317	1,500	1972	1972	4.6
Fuziling	China	74	470	1954	1973	4.5
Khao Laem[3]	Thailand	130	8,860	1984	1985	4.5
Piastra	Italy	93	13	1965	1966	4.4
Vouglans	France	130	605	1968	1971	4.4
Clark Hill	USA	60	3,517	1952	1974	4.3
P. Colombia	Brazil	40	1,500	1973	1974	4.2
Volta Grande		56	2,300	1974		
Camarillas	Spain	49	37	1960	1964	4.1
Manicouagan 3	Canada	108	10,423	1975	1975	4.1

References:

(1) Klaipongpan S.: Geological and seismicity evaluation of Srinagarind Dam. In S. Prakash (ed.), Proc. of 2. Int. Conf. on Recent Advances in Geotechnical Earthquake Engineering and oil Dynamics, University of Missouri-Rolla, 1991.

(2) Vladut T.: Environmental Aspects of Reservoir induced Seismicity. Water Power and Dam Construction, May 1973.

(3) Hetrakul N.: Post Evaluation on Reservoir Triggered Seismicity of Khao Laem Dam. In S. Prakash, Proc. 1991.

All others: Gupta H.K.: Reservoir induced Earthquakes, Elsevier, Amsterdam 1992.

ANNEX C

PAPERS OF THE AUTHOR

1959

1. Der Parabelbogen im Talsperrenbau. Dissertation an der Techn. Hochschule Wien
2. Die baulichen Anlagen des Kraftwerkes Schwarzach. Mit E. Tremmel. ÖZE 1959/Heft 2

1961

3. Der Parabelbogen im Talsperrenbau. (Kurzfassung der Diss.) Der Bauingenieur 1961, Heft 4.
4. Zur Berechnung und wirtschaftlichen Formgebung von Bogengewichtsmauern. ÖIAZ 1961/8.
5. Landschaft und Kraftwerksbau. Universum-Natur-Technik, 1961/Heft 19/20.

1964

6. Die Talsperren der Kraftwerksgruppe Glockner Kaprun, Beobachtungsergebnisse und deren statische Deutung. Schriftenreihe „Die Talsperren Österreichs" 1964, Heft 14.
7. Zur Überwachung von Staumauern. ÖZE 1964, Heft 11.

1965

8. Zum derzeitigen Stand der Theorie von Gewölbemauern (Zusammenfassung vom Symp. on Arch Dams, Southampton 1964). ÖIAZ 1965, Heft 1.
9. The Interaction between Waterhammer and Surge Tank Oscillation. Int. Symp, Waterhammer in Pumped Storage Schemes, Chicago, Nov. 1965; ASME New York.

1966

10. Die Auswertung von Messungen an Betontalsperren und deren dynamisches Verhalten. ICOLD 1964, Bericht über Q. 29. Schriftenreihe „Die Talsperren Österreichs" 1964, Heft 15.

1967

11. Evaluation of Deformation Measurements at Concrete Dams. ICOLD 1967, Q. 34, R. 38.
12. Die Sperre Schlegeis. ÖZE 1967, Heft 8.

1968

13. Symposium für die Berechnung von Gewölbemauern (Bericht). ÖIAZ 1968, Heft 7.
14. Einige statische Probleme des Dammes Durlaßboden. ÖZE 1968/Heft 8

1969

15. Die Sicherheit von Staumauern in Hinblick auf deren Gründung (Zusammenfassung ICOLD 1967, Q. 32. Schriftenreihe „Die Talsperren Österreichs" 1968, Heft 17.

1970

16. Instrumentation and Interpretation Procedures on Large Dams in Austria.
    Mit H. Petzny. ICOLD 1970, G.P. 5.
    Deutsche Fassung: Messeinrichtungen und Methoden der Auswertung an österreichischen Talsperren. Schriftenreihe „Die Talsperren Österreichs" 1970, Heft 18.

17. Concrete Design for Schlegeis Arch Dam. Mit A. Wogrin. ICOLD 1970, Q. 39, R. 9.
Deutsche Fassung: Die Betonentwicklung für die Sperre Schlegeis.
Schriftenreihe „Die Talsperren Österreichs“ 1970, Heft 18.
18. Festigkeitseigenschaften des Gneises. Mit M. Eiselmayer, H. Huber, K. Mignon,
ISRM 1970, Thema 3 - 41.
19. Das Verformungsverhalten von Gneis. Mit E. Tremmel. ISRM 1970, 2-40.
20. The Dams of the Zemm Hydroelectric Scheme. World Dams Today, 1970; Japan Dam Ass.

1971

21. Die Talsperren der Tauernkraftwerke. Mit R. Mühlfellner u. K. Rienößl;.
Energie aus Gletscherwasser, Verlag Koska 1971.
22. Projekte für den weiteren Wasserkraftausbau. Energie aus Gletscherwasser, Verlag Koska 1971.
23. Hydraulic Problems encountered during design of the Zemm Power Scheme;
Water Power, July 1971.
24. Die Zemmkraftwerke. Techn. Rundschau, Nr. 52, 10. 12. 1971.

1972

25. Die Bogengewichtsmauer Schlegeis. Mit J.Schlosser, H.Stäuble. ÖZE 1972, Heft 10.
26. Meßtechnische Überwachung bei der Inbetriebnahme der baulichen Anlagen des KW Mayrhofen.
ÖZE 1972, Heft 10.

1973

27. Bogengewichtsmauer Schlegeis: Das Verhalten des Felsuntergrundes während der
ersten beiden Teilstauperioden. Rock Mechanics, 1973, Supp. Nr. 2.
28. Reservoirs and environment in the High Mountains. Mit E. Stefko. ICOLD 1973, Q 40, R 45.
Deutsche Fassung: Hochgebirgsspeicher und Umwelt.
Schriftenreihe „Die Talsperren Österreichs“ 1974/Heft 21
29. Bottom outlets and stilling caverns at high Dams. ICOLD 1973, Q 41, R 40.
Deutsche Fassung: Grundablässe mit Toskammern bei hohen Talsperren.
Schriftenreihe „Die Talsperren Österreichs“ 1974/Heft 21
29a: Contribution to the Discussion of Q 41: Design flood.
30. Optimization of Dam Concreting by Cable Cranes. Mit W. Jurecka. ICOLD 1973, Q. 43, R. 12.
Deutsche Fassung: Optimierung des Betoniervorganges bei Staumauern mit Kabelkränen.
Schriftenreihe „Die Talsperren Österreichs“ 1974/Heft 21

1974

31. Die Zemmkraftwerke. ÖIAZ 1974/Heft 2.
32. Gründungsprobleme der Gewölbemauer Kölnbrein. Mit E. Magnet.ISRM 1974, Vol. 2B.
33. Standsicherheit von Staumauern. Seminar Concrete Structures, Bergamo 1974.
34. Erfahrungen mit Hochwasserentlastungsanlagen österreichischer Talsperren. ÖWW 1974,Heft 5/6.

1975

35. Analysis of an Arch Dam Taking Account of the Cracked Tension Zone at the Dam Base.
Mit M. Eiselmayer. Int. Symp. on Criteria and Assumptions for Numerical Analysis of Dams.
Swansea 1975.

1976

36. Untersuchungen über Sickerwasser und Dränagen für Talsperren und deren Untergrund. ICOLD 1976, Bericht über die Frage 45, Öst. Wasserwirtschaft 1976, Heft 11/12.
37. Rock Deformations and Seepage Flow in the Foundation of the Schlegeis Arch Dam. Mit G. Heigerth. ICOLD 1976, Q. 45, R. 30.
    Deutsche Fassung: Felsverformungen und Sickerströmungen im Untergrund der Sperre Schlegeis. Schriftenreihe „Die Talsperren Österreichs" 1975/Heft 22
38. The Development of the Kölnbrein Arch Dam Projekt. Mit W. Finger, Rainer, H. Stäuble. ICOLD 1976, Q. 46, R. 27.
    Deutsche Fassung: Entwicklung des Projektes der Gewölbemauer Kölnbrein. Schriftenreihe „Die Talsperren Österreichs" 1975/Heft 22.

1977

39. Entwicklungen beim Bau österreichischer Staumauern. Öst. Wasserwirtschaft 1977, Heft 9/10 (mit englischer Übersetzung).
40. The Mass Concrete of Kölnbrein Arch Dam. World Dams Today, 1977, Japan Dam Association
41. Massenbetonprobleme beim Bau der Gewölbemauer Kölnbrein. Deutscher Talsperrentag 1977.
42. Die Entwicklung des Speicherkraftwerksprojektes in Osttirol. ÖWW 1977/Heft 6.

1978

43. Die Sperren der Kraftwerksgruppe Malta. Mit. R. Mußnig. Energie aus Schwarz und Weiß, Verlag Koska 1978.

1979

44. Die Gewölbemauer Kölnbrein. Mit J. Schlosser, H. Stäuble, K. Klemen u..H. Gatti. ÖZE 1979, Heft 1/2.
45. The Dynamic Behaviour of Arch Dams; Investigations by Means of Calculations and Measurements. ICOLD 1979, Q. 51, R. 9.
46. Developments in Austrian Concrete Dam Construction. ICOLD 1979, GP 1.
47. Zum Schwingungsverhalten von Gewölbemauern. Mit M. Eiselmayer. Öst. Wasserwirtschaft 1979, Heft 5/6.

1980

48. Die Überwachung der Talsperren des Tauernkraftwerkes Glockner Kaprun. ÖZE 1980/H. 9.
49. Speichereinfluss auf Hochwässer. mit P. Ganahl; Interprävent 1980, Bd. 2.
50. Ein Werk widerlegt seine Gegner (Kraftwerksgruppe Glockner-Kaprun). Kontakt 1980/11

1981

51. Erdbebenprobleme bei Bogenstaumauern. Deutscher Talsperrentag, Berlin 1981. Zusammenfassung in Wasserwirtschaft 1981/Heft 4.

1982

52. Interpretation of Data obtained from Deformation Measurements in the Foundation. Mit H. Stäuble. ICOLD 1982, Q.52, R.11.
    Deutsche Fassung: Auswertung von Messungen der Felsverformungen bei der Gewölbemauer Schlegeis. Schriftenreihe „Die Talsperren Österreichs", 1983 , Heft 26.

1983

53. Die Kraftwerksgruppe Zemm-Ziller. ÖWW 1983/Heft 5/6.
54. Gründungsprobleme bei der Gewölbemauer Zillergründl. Felsbau 1983, Heft 3/4.

1984

55. Grundlagen für den Entwurf der Bogenstaumauer Zillergründl. Wasserwirtschaft 1984/Heft 3.
56. Possibilities Improving the Safety of Large Dams. Proc. Int. Conf. on Safety of Dams, Coimbra 1984. A.A. Balkema.
57. Messungen von Spannungen und Verformungen im Bereich der Aufstandsfläche an der Bogenmauer Schlegeis. 6. Nat. Symp. f. Felsmechanik, Aachen 1984.
58. Gedanken zur Automatisierung der Talsperren-Überwachung. Schriftenreihe „Die Talsperren Österreichs" 1984, Heft 27.
59. Zum Stand der Fernüberwachung der Österreichischen Talsperren. Schriftenreihe „Die Talsperren Österreichs", 1984, Heft 27.

1985

60. Die Sanierung einer Leckstelle in der Dichtwand des Erddammes Eberlaste. Festschrift anlässlich des 60. Geburtstages von Prof. Dr. W. Schober.
61. Das Verhalten des Untergrundes der Bogenmauer Schlegeis. Mit H. Stäuble. Felsbau 1985/3.
62. 35 Jahre Planung, Bau und Betrieb von Pumpspeicheranlagen der Tauernkraftwerke AG. ÖWW 1985/Heft1/2.
63. 30 Jahre Tauernkraftwerk Glockner Kaprun. ÖZE 1985/Heft 10.
64. Das Langzeitverhalten österreichischer Talsperren: Gerlos, Limberg, Margaritze, Möll, Drossensperre, Mosersperre, Schlegeis, Durlaßboden, Eberlaste. Schriftenreihe „Die Talsperren Österreichs", 1985, Heft 28.
65. Die Verlandung von Speicherräumen österreichischer Talsperren. Schriftenreihe „Die Talsperren Österreichs", 1985, Heft 28.
66. Zur hydrologischen Sicherheit der Hochwasserentlastungsanlagen österreichischer Talsperren. Schriftenreihe „Die Talsperren Österreichs", 1985, Heft 28.
67. How to Avoid Thermal Cracking of Mass Concrete. ICOLD 1985, Q. 57, R. 15. Deutsche Fassung: Betontechnologische Möglichkeiten zur Vermeidung von Rissen in Massenbeton. Schriftenreihe „Die Talsperren Österreichs", 1986, Heft 30.
68. How can the structural significance of cracks be evaluated and how can cracks be repaired if necessary? ICOLD 1985, C., Q. 57 - 12. Deutsche Fassung: Risse in Betonsperren, ein altes immer gegenwärtiges Problem. Schriftenreihe „Die Talsperren Österreichs", 1986, Heft 30.
69. Safety Control of the Dams of the Glockner-Kaprun Development. Mit F. Breitenstein und W. Köhler. ICOLD 1985, Q. 56, R. 59. Deutsche Fassung: Die Überwachung der Sicherheit der Talsperren der Kraftwerksgruppe Glockner Kaprun. Schriftenreihe „Die Talsperren Österreichs", Heft 30, 1986.
70. The Behaviour of the Kölnbrein Arch Dam. Mit K. Baustädter. ICOLD 1985, Q. 57, R. 37. Deutsche Fassung: Das Verhalten der Bogenmauer Kölnbrein. Schriftenreihe „Die Talsperren Österreichs", 1986, Heft 30.

1987

71. Influence of the Foundation on the stresses acting near the base of arch dams. Mit R. Promper. ISRM 1987. Deutsche Fassung:. Einfluss des Untergrundes auf die Spannungen und Verformungen an der Aufstandsfläche. Mit R. Promper. ISRM 1987
72. Die Sperre Zillergründl. ÖIAZ 1987, Heft 11/12.
73. Dynamic Calculations and Tests on Arch Dams. ICOLD Executive Meeting 1987.
74. Zur Gewährleistung der Sicherheit von Talsperren - Erfahrungen und Folgerungen. Symp. Sicherheit und Kontrolle von Wasserbauten. Graz 1987.
75. Some Aspects of Arch Dam Design. Workshop on Arch Dams, Coimbra 1987.
76. Die Kraftwerksgruppe Glockner - Kaprun; Die Kraftwerksgruppe Salzach; Die Kraftwerksgruppe Zillertal; Die Tauernkraftwerke als Ingenieurbureau. Vertrauen in die Kraft des Wassers. Verlag Koska, 1987.

1988

77. Monitoring of Austrian Dams, 1988. ICOLD Bulletin 68.
78. Influence of Alpine Reservoirs on Flood Discharge. ICOLD 1988, Q. 63, R. 85
79. Gedanken zur Sicherheit von Talsperren. ÖIAZ 1988, Heft 4.

1990

80. Aspects on Safety of Dams. Proc. Symp. Geotechnical Aspects. A.A. Balkema 1990.
81. Fracture Mechanics and its Limits of Application in the Field of Dam Design. Eng. Fract. Mech., 1990/Heft 1/2/3.

82a. Umweltbeziehungen der Wasserkraftnutzung im Gebirge. Teil 1, (als Vorsitzender des gleichnamigen Arbeitskreises der EVU). Schriftenreihe des ÖWAV, Heft 80/1990

1991

83. Grenzen der Kontinuumstheorie in der Felsmechanik. ISRM 1991, Workshop W 3.
84. Cracks around the Abutment of Concrete Dams. Int. Conf. on Dam Fracture. Denver, 1991.
85. Injektionen in Fels und Beton. Felsbau 1991/Heft 3.
86. Concrete Dams in Austria - Developments and Experiences. ICOLD 1991, Dams in Austria, Öst. Nat. Komm. f. Talsperren.
87. Environmental aspects of hydropower development in Austria. ICOLD 1991, Dams in Austria, Öst. Nat. Komm. f. Talsperren.
88. Umweltbeziehungen der Wasserkraftnutzung im Gebirge. ÖIAZ 1991/Heft 5/6.

82b. Umweltbeziehungen der Wasserkraftnutzung im Gebirge. Teil 2, (als Vorsitzender des gleichnamigen Arbeitskreises der EVU). Schriftenreihe des ÖWAV, Heft 87/1991

1992

89. Design Considerations on High Arch Dams. Symp. on High Arch Dams, Nanjing 1992.
90. Zur Energiebilanz von Stromversorgungsproblemen. ÖIAZ 1992/Heft 10

1993

91. Grouting - From Experience to Theory. ISRM News Journal, March 1993 (Vol. 1, Nr. 2)
92. Aspects on a Theory of Grouting. EUROCK 1993, Workshop W 5.
93. Grouting in Rock and Concrete; Proceedings of th Int. Conf. in Salzburg. Herausgeber. A.A. Balkema, Rotterdam 1993
94. Gewölbemauern - Analyse von Verformungsmessungen an der Aufstandsfläche. Felsbau 1993/Heft 5.

1994

95. Erneuerbare Energieen zur Deckung des Energiebedarfes. ÖIAZ 1994, Heft 6.
96. Injektionen in Fels. Mit G. Kühling. Felsmechanik - Symposium Aachen 1994.

1995

97. Injektionen - Von der Empirik zur Theorie. Vortrag anlässlich des Seminars 'Injektionen mit Feinstbindemitteln' an der Techn. Akademie Esslingen, Feb. 1995
98. Offene Fragen einer Theorie der Injektionen. ISRM 1995, Vol. 2.
99. Questions of a Theory on Grouting. Proceedings 'Il Miglioramento e il Rinforzo dei Terreni e delle Rocco. XIX Convegno Nazionale di geotecnica, Pavia. Associazione Geotecnica Italiana, Vol. II.
100. Anchors in Theory and Practice. Proceeddings of the Int. Conf. in Salzburg. Herausgeber. A.A. Balkema 1995

1996

101. Gemeinsame Optimierung notwendig. Einige Überlegungen zur Deckung des künftigen Energiebedarfes. Umwelt-Journal 1996/2
102. Rock Grouting. Final Report, Chairman of the ISRM Commission. Int. Journal of Rock Mechanics and Mining Sciences, 1996, No.8.
103. Stabilität von Hängen und Böschungen bei Erdbeben. Felsbau 1996/Heft 5

1997

104. Zur Gründung von Staumauern aus felsmechanischer Sicht. Felsbau 1997/Heft 1.
105. Gedanken zur Prüfung des Betons aus der Sicht des Statikers, ÖIAZ 1997/Heft 3
106. Recent aspects on the design of high arch dams. Dam Engineering 1996, Volume 7, Issue 4, Nachtrag 1997, Volume VIII, Issue 1.
    The mathematics of dam safety. Int. Water Power & Dam Construction, May 1997.
107. Wasserwirtschaft und Wasserbau - Rückblick und Ausblick. TU Innsbruck, Institut für Wasserbau, Festschrift anläßlich des 60. Geburtstages von Prof. Scheuerlein. Sept. 1997.
108. Tunnels for Hydropower schemes. ÖIAZ 1997, Heft 4.

1998

109. Stresses and strains around the abutment of high arch dams. Proceedings of the Symposium on Dam Safety, Barcelona. A.A. Balkema 1998.
110. Einführung in die Problematik einer Theorie der Injektionen im geklüfteten Fels. Mitteilungen des Inst. f. Ingenieurgeologie der TU Wien, 1998, Bd. 1.

1999

111. Zur Überwachung von Talsperren. ÖIAZ 1999/11.
112. Gewölbemauern, Erfahrungen, Probleme, Entwicklungen. Schriftenreihe „Die Talsperren Österreichs", Band 33.

2001

113. Gedanken zur Beurteilung der Sicherheit von Talsperren. Wasser, Energie, Luft 2001, Heft 7/8
114. 50 Jahre Salzburger Kolloquium. Felsbau 2001, Heft 5

Published in series

„Die Talsperren Österreichs“ (Large Dams in Austria)

Volume 1: A.W. REITZ: Beobachtungseinrichtungen an den Talsperren Salza, Hierzmann, Ranna und Wiederschwing (1954)

Volume 2: H. FLÖGL: Der Einfluß des Kriechens und der Elastizitätsänderung des Betons auf den Spannungszustand von Gewölbesperren (1954)

Volume 3: A.W. REITZ, R. KREMSER und E. PROKOP: Beobachtungen an der Ranna-Talsperre 1950 bis 1952 mit besonderer Berücksichtigung der betrieblichen Erfordernisse (1954)

Volume 4: K. STUNDL: Hydrochemische Untersuchungen an Stauseen (1955)

Volume 5: J. STINI: Die baugeologischen Verhältnisse der österreichischen Talsperren (1955)

Volume 6: H. PETZNY: Meßeinrichtungen und Messungen an der Gewölbesperre Dobra (1957)

Volume 7: E. TREMMEL: Limbergsperre, statische Auswertung der Pendelmessungen (1958)

Volume 8: R. KETTNER: Zur Formgebung und Berechnung der Bogenlamellen von Gewölbemauern (1959)

Volume 9: H. TSCHADA: Sohlwasserdruckmessungen an der Silvrettasperre (1959)

Volume 10: W. STEINBÖCK: Die Staumauern am Großen Mühldorfersee (1959)

Volume 11: E. FISCHER: Beobachtungen an der Hierzmannsperre (1960)

Volume 12: H. GRENGG: Statistik 1961 (1962) Ausgabe in englischer Sprache (1962)

Volume 13: A. OREL: Gesteuerte Dichtungsarbeiten beim Erddamm des Freibachkraftwerkes, Kärnten 1964

Volume 15: Sammel-Ergebnisse des 8. Talsperren-Kongresses in Edingburgh 1964 (1966)

Volume 16: O. GANSER: Die Meßeinrichtungen der Staumauer Kops 1968

Volume 17: 9. Talsperren-Kongress in Istanbul 1967 (1969)

Volume 18: Österreichische Beiträge zum Talsperrenkongress Montreal (1970)

Volume 19: H. GRENGG: Statistik 1971 der Talsperren, Kunstspeicher und Flußstauwerke (1971)

Volume 20: J. KORBER: Die Entlastungsanlagen der österreichischen Talsperren (1973)

Volume 21: Österreichische Beiträge zum Talsperrenkongreß in Madrid 1973 (1974)

Volume 22: Österreichische Beiträge zum 12. Talsperrenkongreß in Mexico 1976 (1975)

Volume 23: H. PETZNY, W. SCHOBER, R. WIDMANN: Messungen an österreichischen Talsperren (1977)

Volume 24: R. PARTL: Statistik 1977 (Ausgabe auch in Englisch)

Volume 25: Österreichische Beiträge zum 13. Talsperrenkongreß 1979 in New Delhi

Volume 26: Österreichische Beiträge zum 14. Talsperrenkongreß 1982 in Rio de Janeiro

Volume 27: Fernüberwachung österreichischer Talsperren

Volume 28: Langzeitverhalten österreichischer Talsperren und Flußstauwerke

Volume 29: Hydro power schemes and large dams in Austria

Volume 30: Österreichische Beiträge zum 15. Talsperren-Kongreß 1985 in Lausanne

Volume 31: Österreichische Beiträge zum 16. Talsperren-Kongreß 1988 in San Francisco

Volume 32: Dams in Austria (1991)

Volume 33: R. WIDMANN, Gewölbemauern (Erfahrungen – Probleme – Entwicklungen), with abridged version in English (1999)

Volume 34: W. SCHOBER, Embankment Dams (Research and development, construction and operation) (2003)

Kufferath

Austrian National Committee on Large Dams
Elisabethstrasse 59/4, A-8010 Graz, Phone ++43/316/354708, Fax ++43/316/354706, secretary@atcold.at, www.atcold.at